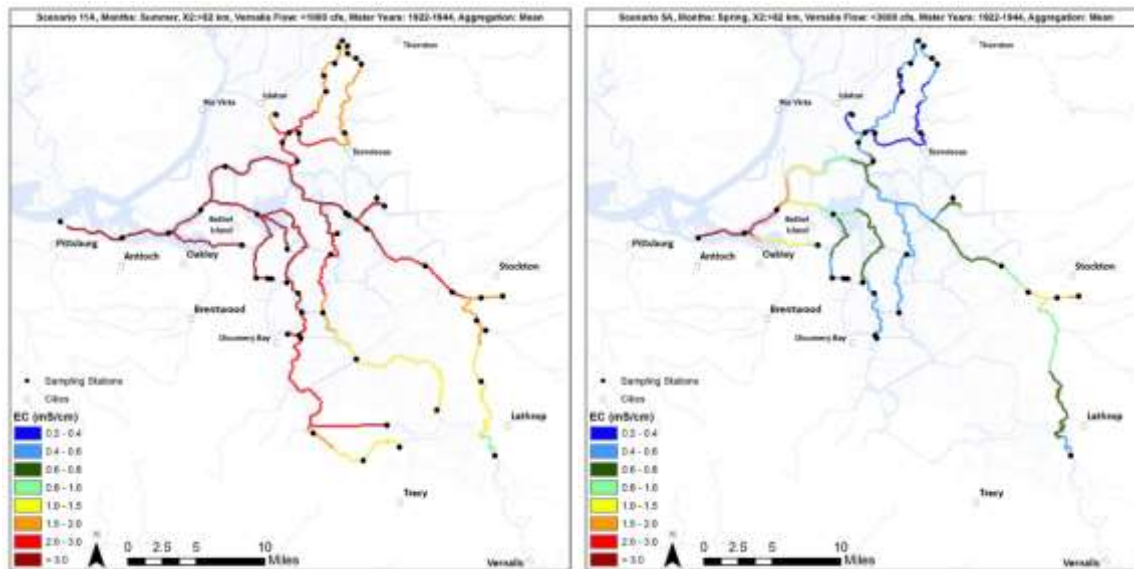


MAPPING AND TREND EVALUATION OF INTERIOR DELTA SALINITY



Prepared for:

Paul Hutton, Ph.D., P.E.

Metropolitan Water District of Southern California

1121 L Street, Suite 900

Sacramento CA 95814-3974

Prepared by:

John Rath, Carrie Munill and Sujoy Roy

Tetra Tech, Inc.

3746 Mt. Diablo Blvd, Suite 300, Lafayette, CA 94549

March 2015

TABLE OF CONTENTS

1. Introduction	1-1
2. Data Sources and Cleaning	2-1
2.1. Historical “Bulletin 23” Data.....	2-1
2.2. Modern Data Stations	2-1
2.3. Data Cleaning	2-2
3. Mapping of Salinity Data	3-1
3.1. Grouping of Data.....	3-1
3.2. Interpolation and Mapping.....	3-2
4. Trend Analysis	4-1
5. Conclusions.....	5-1
6. References.....	6-1
Appendix A. Maps of Mean Salinity.....	A-1
Appendix B. Maps of 25 th Percentile Salinity.....	B-1
Appendix C. Maps of 50 th Percentile (Median) Salinity.....	C-1
Appendix D. Maps of 75 th Percentile Salinity.....	D-1
Appendix E. Trend Plots.....	E-1

LIST OF TABLES

Table 2-1 Station-level data sources used for this analysis.....	2-3
Table 3-1 Summary of information presented in maps.....	3-3
Table 4-1 Mann-Kendall test results of salinity.....	4-4
Table 4-2 Mann-Kendall test results for salinity over 1922-1967.	4-4
Table 4-3 Mann-Kendall test results for salinity over 1968-2012.....	4-5

LIST OF FIGURES

Figure 4-1	Grouping of stations for trend analysis.....	4-6
Figure E-1	Time series plots of group A by month.....	E-2
Figure E-2	Time series plots of group B by month.....	E-3
Figure E-3	Time series plots of group C by month.	E-4
Figure E-4	Time series plots of group D by month.	E-5
Figure E-5	Time series plots of group E by month.....	E-6
Figure E-6	Time series plots of group F by month.....	E-7
Figure E-7	Time series plots of group G by month.	E-8
Figure E-8	Time series plots of group H by month.	E-9
Figure E-9	Time series plots of group I by month.....	E-10
Figure E-10	Time series plots of group J by month.	E-11
Figure E-11	Box plots (when $n > 5$) and scatter plots of monthly average EC data for group A	E-12
Figure E-12	Box plots (when $n > 5$) and scatter plots of monthly average EC data for group B	E-13
Figure E-13	Box plots (when $n > 5$) and scatter plots of monthly average EC data for group C	E-14
Figure E-14	Box plots (when $n > 5$) and scatter plots of monthly average EC data for group D	E-15
Figure E-15	Box plots (when $n > 5$) and scatter plots of monthly average EC data for group E	E-16
Figure E-16	Box plots (when $n > 5$) and scatter plots of monthly average EC data for group F	E-17
Figure E-17	Box plots (when $n > 5$) and scatter plots of monthly average EC data for group G.....	E-18
Figure E-18	Box plots (when $n > 5$) and scatter plots of monthly average EC data for group H.....	E-19

Figure E-19 Box plots (when $n > 5$) and scatter plots of monthly average EC data for group IE-20

Figure E-20 Box plots (when $n > 5$) and scatter plots of monthly average EC data for group J.....E-21

EXECUTIVE SUMMARY

This document presents an overview of salinity at stations in the interior of the Sacramento-San Joaquin River Delta, using data from a variety of sources representing water years 1922 to 2012. The data are presented as maps over different time intervals (1922-1944; 1945-1967; and 1968-2012), given similar ranges in the position of the X2 isohaline and San Joaquin River flows. Maps are presented for salinity aggregated as the mean, 25th percentile, median (50th percentile), and the 75th percentile. In general the maps show the intrusion of salinity into the central and southern Delta when X2 values are high and especially when San Joaquin River flows are low. For the cases where salinity intrusion occurs, and given similar hydrology, the 1922-1944 salinities are often different from 1945-1967 and 1968-2012 periods.

In addition, trends on the data are evaluated across the entire period of record at stations where the record was sufficiently complete, and a statistical comparison of the salinity levels over different periods was performed with data being grouped by the X2 range, San Joaquin River inflows, and season. Over the entire period of record (1922-2012), the statistically significant trends are typically negative, i.e., salinities declining, with the exception of the San Joaquin River stations where they are typically positive. This pattern is also seen in the first part of the record (1922-1967): the statistically significant trends are typically negative, with the exception of the San Joaquin River stations, where they are typically positive. For the latter part of the record (1968-2012), the statistically significant trends are more likely to be positive than negative (i.e., increasing salinity).

Box plots were used to summarize the data shown in maps. As expected, summer specific conductance values are higher than spring values, although the magnitude of the difference varies by region. There are also differences of specific conductance over the time intervals considered: areas typically in the western portion of the study domain show decreases over the period, and in the south, show small increases.

This work provides an overview of salinity in the interior Delta with the data being interpreted through maps and statistical analyses. However, in future these data may also be used for calibration of models, such as the DSM2 model, to represent the range of salinity variation over the nine-decade period of record.

1. INTRODUCTION

This work builds on a recently completed analysis of salinity trends in the western Delta which was based on all available salinity data from 1922-2012, collected by various state and federal entities (Tetra Tech, 2014). This analysis is herein referred to as the 2014 report. In this work we evaluate, through maps and statistical analysis, the changing patterns of salinity in the interior Delta, particularly the southern Delta, over the same period. Salinity in the southern Delta relates to the beneficial uses of water in the Delta, and the State Water Resources Control Board is currently in the process of reviewing water quality objectives for the protection of southern Delta agricultural beneficial uses.

As part of the 2014 report, salinity data in scanned paper reports from the California Department of Water Resources (and its predecessor entity, Department of Public Works) were digitized and integrated with modern data from the California Data Exchange Center (CDEC) into a single database. Because the focus of the original report was on the western Delta, CDEC data were compiled only from relevant stations. Here, we incorporated modern salinity data reported by CDEC from relevant interior Delta stations. Appropriate data cleaning methodologies were applied to the historical data to develop a monthly data set to evaluate salinity changes in the interior Delta stations over the past nine decades. Maps were developed for specific hydrologic conditions and time periods, by developing averages and other statistical metrics of the available data, and by interpolating across the Delta channels. Statistical analyses of trends at key locations were performed to support interpretation of the maps.

The methods used are further described in the following chapters. Chapter 2 of this report describes data sources and the cleaning methodology employed. This chapter is related to an electronic database of all relevant data that may be used for future analysis. Chapter 3 describes the approach and the grouping of data for the maps, as well as key observations from the maps. The actual maps are presented in Appendix A through D. Chapter 4 presents a summary of the statistical analysis of the data, grouped in a manner similar to that shown in the maps, and Appendix E contains a set of supporting plots evaluating trends and changes over time. Chapter 5 presents the key conclusions of this analysis.

2. DATA SOURCES AND CLEANING

This work combined historical grab sample salinity data from across the Delta, typically reported as chlorinity or chloride concentrations, with more recent continuous salinity sensor data, measured as electrical conductivity (EC), and reported as specific conductance, which is the EC corrected to 25 °C.

2.1. HISTORICAL “BULLETIN 23” DATA

Data for the early part of the record come from the previously assembled dataset for the 2014 report and are referred to as the Bulletin 23 data. The data were extracted right after the processing step of converting chloride concentrations to specific conductance. In particular, this is before the tidal correction and neighbor cleaning or filling steps that were used for analysis of the western Delta salinity gradient. We used all stations in the region of interest that had more than five observations and then excluded those with “drain” in the name, as salinity in those measurements may be more representative of agricultural runoff than seawater intrusion.

2.2. MODERN DATA STATIONS

We have based the modern dataset for this work on the Interagency Ecological Program (IEP) water quality dataset (<http://www.water.ca.gov/iep/products/data/dssnotice.cfm>) and what was publicly available on CDEC’s website (<http://cdec.water.ca.gov/cgi-progs/queryCSV>). A dialog with DWR produced no additional sources of post-1972 salinity data for use in the study.

The IEP water quality data stations are designated using River Kilometer Indices (RKI). We used a schematic of DSM2 that was also annotated with RKIs to visually identify the IEP stations with specific conductance data that are relevant to the interior Delta. Certain IEP locations appear to correspond precisely to CDEC locations and these were relabeled with the CDEC station names during the processing.¹

The CDEC website gives the coordinates of its water quality stations, and we visually identified interior Delta stations and downloaded their data. Stations with non-event, surface electrical conductivity datasets were selected for further processing. For consistency, stations that specifically referenced bottom salinity were excluded. The list of stations we found to be relevant to the interior Delta and its western boundary conditions are listed in Table 1.

A Microsoft Access database accompanying this report contains the data at various stages of its processing, and references to the relevant tables are made in the following descriptions. The Metadata table holds information about the individual sources of salinity data (IEP/CDEC/B23 origin, time resolution/duration of the measurements, sensor/variable

¹ This applied to stations with the codes HLL (Holland Tract), ANH (Antioch), JER (Jersey Point), SAL (San Andreas Landing), and VER (Vernalis).

names, etc.). The stations table is the eventual unique list of stations with monthly average data. The tables containing the salinity data itself reference these two tables for easier querying and to save space (see the database relationships for details).

2.3. DATA CLEANING

The Bulletin 23 data were previously screened for gross outliers as part of the processing for the 2014 report, so these data are present in both the Original Data and Cleaned Data tables in the database.

The IEP/CDEC data had several cleaning procedures applied to it. The data after download from CDEC or export from IEP quality.dss are in the Original Data table in the database.

- Physically implausible values (greater than 50,000 or less than 10 $\mu\text{S}/\text{cm}$) were removed.
- The data came with measurement unit annotations, and all units were converted to $\mu\text{S}/\text{cm}$.
- Certain sections of data appeared to have mislabeled units. If making a correction of mS to/from μS resulted in the data falling in a range consistent with the rest of the record, that correction was done; otherwise, the inconsistent section was removed.
- Otherwise, the data were plotted and points or entire sections of data were manually identified for removal.

The primary focus was on removing suspect data that would also affect eventual averaging to the monthly time step. The general rules for identifying data as suspect were:

- Isolated points very much above or below its neighbors, particularly for sub-daily data
- Long runs of flat line data
- Runs of very wild data, particularly for time durations above 15 minutes
- The threshold of suspicion was lower immediately before or after periods of missing values in the uncleaned data.
- Some IEP stations had redundant data from different sources at the same RKI. We generally just used the source that appeared cleanest.

The data following these cleaning procedures are in the Cleaned Data table of the accompanying Access database.

**Table 2-1
Station-level data sources used for this analysis.**

Station ID	Source	Name
SLTRM004	IEP	Three Mile Slough @ San Joaquin River
RSMKL008	IEP	Mokelumne River @ Terminous
SLPPR000	IEP	Piper Slough @ Bethel Tract
RSAN072	IEP	San Joaquin River @ Brandt Bridge
CHCCC006	IEP	Contra Costa Canal @ Pumping Plant #1
CHGRL009	IEP	Grant Line Canal (East Position)
RMID015	IEP	Middle River @ Middle River (west channel)
RMID027	IEP	Middle River at Tracy Blvd
RMID023	IEP	Middle River @ Borden Hwy
RMID041	IEP	Middle River near Old River
ROLD014	IEP	Old River at Holland Cut
ROLD024	IEP	Old River at Bacon Island
ROLD046	IEP	Old River
ROLD047	IEP	Old River
ROLD059	IEP	Old River at Tracy Road
RSAN087	IEP	San Joaquin River @ Mossdale
RSAN018	IEP	San Joaquin River @ Jersey Point
RSAN014	IEP	San Joaquin River at Blind Point
RSAN007	IEP	San Joaquin River @ Antioch
RSAN058	IEP	San Joaquin River @ Rough and Ready Island (also called San Joaquin River @ Stockton Ship Channel)
RSAN037	IEP	San Joaquin River @ Prisoners Point
RSAN032	IEP	San Joaquin River at San Andreas Landing
RSAN112	IEP	San Joaquin River @ Vernalis
RMKL019	IEP	North Fork Mokelumne River
SLPPR003	IEP	Piper Slough @ Bethel Island
SLRCK005	IEP	Rock Slough (CCC)
ANH	CDEC	San Joaquin at Antioch
BET	CDEC	Bethel Island
BLP	CDEC	Blind Point
DSJ	CDEC	Dutch Slough at Jersey Isle
FAL	CDEC	False River
FRP	CDEC	Farrar Park
HLL	CDEC	Holland Tract
HLT	CDEC	Middle River Near Holt
HOL	CDEC	Hollard Cut
JER	CDEC	Jersey Point

Station ID	Source	Name
LPS	CDEC	Little Potato Slough
MOK	CDEC	Mokelumne R at San Joaquin R
NMR	CDEC	North Mokelumne R @ W Walnut Grove Rd
ORQ	CDEC	Old River at Quimbey
OSJ	CDEC	Old River at Frank's Tract
PPT	CDEC	Prisoner's Point
PRI	CDEC	Prisoner's Point near Terminous
PTS	CDEC	Pittsburg
SAL	CDEC	San Andrea's Landing
SJJ	CDEC	San Joaquin R at Jersey Point
SMR	CDEC	South Mokelumne R @ W Walnut Grove Rd
STI	CDEC	Staten Island
TSL	CDEC	Threemile Slough at San Joaquin R
VER	CDEC	Vernalis

3. MAPPING OF SALINITY DATA

Observed salinity data were averaged in preparation for presentation on maps and were classified into different groups that were characteristic of the season and hydrology.

3.1. GROUPING OF DATA

A monthly average specific conductance was calculated for each station and month. For the grab sample-based Bulletin 23 data, this was simply the average of all the observations in a given month. For the continuous CDEC data, we first averaged the hourly and 15-minute data to the daily level. In this averaging process, if at least 50% of the possible values in a day (12 observations for hourly data or 48 observations for 15-minute data) were missing, the daily average was also identified as missing.

On each date the non-missing value with the largest original time resolution (daily > hourly > 15 minute) is kept for monthly averaging. The monthly average is also undefined if more than 50% of the days in the month (varying by calendar month) are missing. The data after the monthly averaging process are in the MonthlyEC database table in the accompanying Access database.

Once the monthly averages were calculated, they were split into subsets based on four categories:

1. **Monthly San Joaquin River X2 position:** The X2 categories are (1) < 54 km (approximately Martinez), (2) between 54 km and 82 km, and (3) > 82km. Gaps in the time series, as calculated in the 2014 report, were filled through linear interpolation (except for the large gap between August 1941 and December 1943). This data filling exercise is justified because the accuracy needed to split the X2 data into three broad categories is less than required for the trend evaluation provided in the 2014 report, so additional interpolation allowed more of the south Delta grab sample salinity to be placed into an X2 category. The filled and unfilled X2 time series are in the SanJoaquinX2 table in the database.
2. **Season:** (1) April-June is classified as “Spring” and (2) July-September is classified as “Summer”.
3. **Vernalis flow:** The time series was taken from DAYFLOW (Water year or WY 1930-2012) and was supplemented by DWR Bay-Delta Office data for the early part of the record (WY 1922-1929). Vernalis flow was described as: (1) above or (2) below the median flow (to the nearest 1,000 cfs) within each season. The combined Vernalis flow data are in the VernalisFlow table in the database.
4. **Time period:** The data were split into three periods defined by water years: (1) 1922-1944, (2) 1945-1967, and (3) 1968-2012.

The mean as well as the 25th, 50th, and 75th percentiles of the monthly averages were evaluated for each subset. The results of these sub-setting procedures are in the AveragedEC table in the Access database.

3.2. INTERPOLATION AND MAPPING

Classical interpolation approaches used to interpolate spatial data are commonly based around the straight-line (Euclidean) distance between the observations. However, salinity transport occurs only along the stream network in the Delta. In going from station-based salinity measurements to maps with interpolated values of salinity, we need a method that incorporates the stream network structure of the Delta. Ver Hoef and Peterson (2010) describe a “flexible framework for modelling spatially continuous data from stream networks.” We applied this framework (hereafter referred to as SSN after the name of the R software package the authors wrote to implement it) to each of the categories to create a corresponding map with interpolated values along the major channels of the Delta. We constructed a network representation of the interior Delta and the locations of the stations in the salinity datasets. One limitation of the SSN method is that the network representation cannot have closed loops; therefore some approximations had to be made in the representation.

In this SSN framework, the interpolated value at any particular location is based on the observed data from nearby stations in the sense of distance along the stream network, with the closest stations’ data having the most weight. There are various details about this spatial relationship that can be adjusted in a particular SSN model. The goal here was to simply visualize the spatial structure of the salinity data rather than try to explore relationships with other variables or make detailed predictions. Therefore we chose to use a simple interpolation model for specific conductance on the log scale with a spatial relationship that extends both upstream and downstream. This latter choice is important in this application because the salinity in this region is due to both seawater intrusion and watershed runoff-based processes.

The resulting maps are shown by method of data aggregation (mean, 25th percentile, 50th percentile, and 75th percentile) in Appendices A through D. The different scenarios that are mapped are summarized in Table 3-1. The scenarios are numbered 1 through 12 for different X2 and Vernalis flow conditions, and A, B, or C representing the three time intervals. Note that some combinations of X2 and Vernalis flow are associated with no data and are left blank. Table 3-1 also contains a brief narrative summary of the maps presented in the Appendices. In general the maps show the intrusion of salinity into the central and southern Delta when X2 values are high and especially when San Joaquin River flows are low. For the cases where salinity intrusion occurs, the scenario that is most different is typically Scenario A, i.e., for similar hydrology, Scenario B (1945-1967) and C (1968-2012) are often similar.

Table 3-1
Summary of information presented in maps.

Season	Scenario	X2 Range (km)	Vernalis Flow Range (cfs)	Comparison across time periods: 1922-44 (A), 1945-67 (B), 1968-2012 (C)
Spring	1	<54	< 3000	No data.
	2	<54	≥ 3000	Overall, little difference across the three time periods. Mean salinity was between 0.2-0.4 mS/cm at all stations. This was consistent with other data aggregation approaches as well (25 th percentile, median, and 75 th percentile).
	3	54-82	< 3000	Scenario 3A and 3C are similar, with slightly lower concentrations in the south Delta for Scenario 3B. Mean salinity was between 0.2-0.4 mS/cm in the Central Delta, and slightly higher in the south,
	4	54-82	≥ 3000	Patterns were similar across Scenarios 4A, 4B, and 4C. Mean salinity was between 0.2-0.4 mS/cm at most stations.
	5	>82	< 3000	Similar patterns over three periods. Higher south Delta concentration than above scenarios, ranging from 0.6-1 mS/cm; concentrations lower in central Delta (0.2-0.8).
	6	>82	≥ 3000	No data.
Summer	7	<54	< 1000	No data.
	8	<54	≥ 1000	No data.
	9	54-82	< 1000	Mean salinity was between 0.2-1.0 mS/cm in the south Delta in Scenario 9B, and marginally lower in Scenario 9C. No data for 9A.
	10	54-82	≥ 1000	Mean salinity was between 0.2-0.4 mS/cm in the central Delta, and 0.4-0.6 mS/cm in the south, with similar patterns seen across the three periods.
	11	>82	< 1000	Overall, Scenario 11B and 11C are similar, with much higher salinities for Scenario 11A. In 11A, often greater than 3.0 mS/cm in the central Delta, 0.8-2.0 mS/cm in the south. In 11B and 11C, 0.6-1.0 mS/cm in the central Delta, and slightly higher concentrations in the south.
	12	>82	≥ 1000	Scenario 12B and 12C are similar, with much higher salinities for Scenario 12A. In 12B and 12C, between 0.2-0.8 mS/cm in the central and south Delta; in 12A between 0.6 and 1.5 mS/cm.

4. TREND ANALYSIS

Stations in the interior Delta were grouped to evaluate trends and/or changes over time. Because the data from the Bulletin 23 stations are generally less frequently measured, nearby stations were grouped to provide meaningful data sets for analysis. To begin with, Bulletin 23 and CDEC stations were mapped to identify groups of stations that were on the same channel and/or close to one another. The stations considered are shown in Figure 4-1, and the groups we identified are labeled A through J. In identifying the groups the presence of CDEC and Bulletin 23 data in each group was considered such that trends could be computed over the longest possible period.

For each of the 10 groups of selected stations, we created a single monthly time series by averaging all the monthly average specific conductance values from the dataset used to create the interpolated maps. Figures E1–E10 in Appendix E show the plots of these time series. Only groups A, C, D, and J were deemed sufficiently complete to run a meaningful trend analysis over the entire period of record. Group B data are incomplete in the early part of the record and only shown for 1968-2012. The test of trend we used is the same Mann-Kendall test used in the 2014 Salinity Trends Report: a normal Mann-Kendall test on each of the seasonal subseries (all the January values together, all February values together, etc.) and a seasonal Mann-Kendall test on the entire record.

The Mann-Kendall test results are shown in the table below in Table 4-1 through Table 4-3, for 1922-2012, 1922-1967, and 1968-2012. Over the entire period of record (Table 4-1), the statistically significant trends are typically negative, i.e., salinities declining, with the exception of Group J (San Joaquin River stations) where they are typically positive. The westernmost of the station groups evaluated (Group A) shows relatively large negative slopes in July, August and September. These patterns are also seen in the first part of the record (1922-1967) (Table 4-2): the statistically significant trends are typically negative, with the exception of Group J, where they are typically positive. There are large declines in salinity in August through December for groups A, C, and D. For the latter part of the record (Table 4-3), the statistically significant trends are more likely to be positive than negative (i.e., increasing salinity). There are increases in salinity in Groups A and D, and decreases in Group J.

For all the groups, we examined the distribution of the monthly EC specific conductance values under each scenario used to create the interpolated maps (scenario labels in Table 3-1). Not all groups have an abundance of data for all scenarios, due both to the sparseness of data for some groups, as illustrated in the time series plots, and to some scenarios representing less common conditions (e.g., lower Vernalis flow combined with less salinity intrusion represented by a seaward X2). The monthly data are displayed as discrete points in all cases, and for scenarios with at least 6 observations, boxplots overlay the data to give a summary of the distribution. Ten sets of plots, each categorized by summer and fall, and are

shown in Appendix E in Figures E-11 to E-20. The following is a narrative summary for each of the groups.

Group A (Figure E-11). Boxplots for **spring** showed that scenario 5 had the highest monthly averages of specific conductance. The median for the time period 1922-1944 has the highest average specific conductance which was around 2.5 mS/cm. The plots show that the average salinity continues to decrease to the end of three time periods to 2012. Boxplots for **summer** showed scenario 11 had the highest monthly averages of specific conductance. The median for time period 1922-1944 displayed the highest numbers with the median being over 10 mS/cm. The plots illustrate that the average salinity continues to decrease over the three periods to 2012.

Group B (Figure E-12). Boxplots for **spring** indicated scenario 5 had the highest monthly averages of specific conductance. The median for time period 1968-2012 shows the highest average of EC, which was around 0.3 mS/cm. There has been a slight increase in salinity from 1945-1967 to 1968-2012. Each of the boxplots had very little or no data from 1922-1944. Boxplots for **summer** indicated scenario 12 had the highest monthly average of specific conductance. The highest average came from time period 1922-1944 which was over 1.0 mS/cm. In scenario 12 the specific conductance decreased over each time period.

Group C (Figure E-13). Boxplots for **spring** displayed low salinities throughout, although scenario 5 was marginally higher. The median for the time period 1922-1944 has the highest average specific conductance which was around 0.4 mS/cm. The plots show the average salinity continues to decrease to the end of three time periods to 2012. Boxplots for **summer** showed much higher salinities, with scenario 11 displaying the highest monthly averages of specific conductance. The median for time period 1922-1944 displayed the highest numbers with the median being around 1.0 mS/cm. The EC averages from 1922-1944 also showed that the highest to lowest points varied by a factor of 10. The plots illustrate the average specific conductance continues to decrease over the three periods to 1968-2012.

Group D (Figure E-14). Boxplots for group D scenarios for **spring** displayed low concentrations for scenarios 2, 3, and 4, with scenario 5 displaying the highest monthly values of EC. The median for the time period 1922-1944 has the highest average specific conductance which was around 0.4 mS/cm. There was very little data for the other time periods (1922-1944 & 1945-1967). Boxplots for **summer** showed scenario 11 had the highest monthly averages of specific conductance. The median for time period 1922-1944 displayed the highest numbers, about 7.0 mS/cm. The plots illustrate the specific conductance decreased by a factor of 10 in the time period 1945-1967, but there was a slight increase to 1968-2012.

Group E (Figure E-15). Boxplots for group E scenarios for **spring** displayed scenario 5 had the highest monthly averages of specific conductance. The plots show the average specific conductance slightly decreases to the end of three time periods to 2012 over all the scenarios. Boxplots for group E scenarios for **summer** showed scenario 11 had the highest monthly averages of EC. The median for time period 1922-1944 displayed the highest numbers with the average being around 1.0 mS/cm. The EC from 1922-1944 also showed a difference of an interval of 10 from the highest to lowest points. The plots show that the

average specific conductance continues to decrease into time period 1945-1967 but there is a slight increase from then to 1968-2012.

Group F (Figure E-16). Data were limited for this group. Boxplots for group F scenarios for **spring** indicated scenario 3 had the highest monthly averages of EC. The median for time period 1968-2012 shows the highest average of specific conductance, which was around 0.7 mS/cm. There has been a slight increase in specific conductance from time period 1945-1967 to 1968-2012. Boxplots for **summer** indicated scenario 10 and 12 were very similar having the highest specific conductance averages out of the four scenarios.

Group G (Figure E-17). Boxplots for group G scenarios for **spring** indicated scenario 3 and 5 had the highest monthly averages of specific conductance. The median for time period 1968-2012 shows the highest average of specific conductance, which was around 0.9 mS/cm. There has been an increase in salinity from time period 1945-1967 to 1968-2012. Each of the scenarios had very little data and none from 1922-1944. Boxplots for **summer** showed scenario 11 had the highest monthly averages of specific conductance. The median for time period 1968-2012 displayed the highest numbers with the average being around 2 mS/cm. The plots illustrate the average specific conductance from 1922-1944 decreased over 1945-1967 then increased in 1968-2012.

Group H (Figure E-18). Boxplots for group H scenarios for **spring** all had similar results. Boxplots for group H scenarios for **summer** showed scenario 11 had the highest averages of EC. The median for time period 1922-1944 displayed the highest numbers with the average being around 0.7 mS/cm. The plots illustrate the average specific conductance decrease into time period 1945-1967 but then there was minimal increase from 1968-2012. In summer, there have been declines over all the time intervals.

Group I (Figure E-19). Boxplots for group I scenarios for **summer** indicated scenario 3 and 5 were very similar having the highest EC averages out of the four scenarios. Boxplots for group I scenarios for summer showed scenario 11 had the highest averages of specific conductance. The median for time period 1922-1944 displayed the highest numbers with the average being approximately 1 mS/cm. The plots illustrate the average specific conductance decrease into time period 1945-1967 but then there was a small increase from 1968-2012.

Group J (Figure E-20). Boxplots for group J scenarios for **spring** indicated scenario 5 had the highest monthly averages of specific conductance. The median for time period 1945-1967 shows the highest average of specific conductance, which was approximately 1 mS/cm. There has been a slight decrease in specific conductance from 1967 to 2012. There was little data from 1922-1944. Boxplots for **summer** showed scenario 11 had the highest averages of EC, although scenario 12 was similar. The median for time period 1968-2012 displayed the highest numbers with the average of about 1 mS/cm. The specific conductance averages from 1922-1944 increased slightly over each of the time intervals.

In summary, the box plots succinctly show that the summer EC values are higher than spring values, although the magnitude of the difference varies by region. There are also differences of EC over the time intervals considered: areas typically in the western portion of the study domain show decreases over the period, and in the south, show small increases.

Table 4-1

Mann-Kendall test results of salinity. Values are the Sen's slope estimate in $\mu\text{S}/\text{cm}/\text{year}$. An asterisk indicates significance of the Mann-Kendall test at the 5% level. The period of trend evaluation was 1922-2012.

Season	Group A	Group C	Group D	Group J
Jan	0.87	-1.01*	0.13	5.62*
Feb	-1.16	-0.73*	-1.23*	5.51*
Mar	-0.99*	-0.83*	-0.72	4.85*
Apr	-0.62	-1.07*	-0.52	1.37
May	-0.44	-1.46*	0.05	0.47
Jun	-0.74	-1.53*	-0.66	2.82*
Jul	-6.79*	-2.53*	-1.83	0.90
Aug	-26.55*	-3.03*	-4.31*	-0.29
Sep	-17.07*	-3.25*	-5.18*	0.36
Oct	-2.45	-2.61*	-1.93	0.08
Nov	5.01	-2.12*	-0.38	3.18*
Dec	6.18	-1.16*	2.89	5.16*
All	-1.32*	-1.73*	-0.88*	2.29*

Table 4-2

Mann-Kendall test results for salinity over 1922-1967. Values are the Sen's slope estimate in $\mu\text{S}/\text{cm}/\text{year}$. An asterisk indicates significance of the Mann-Kendall test at the 5% level.

Season	Group A	Group C	Group D	Group J
Jan	-2.21	-4.17*	-3.20	7.75*
Feb	-1.52	-3.63*	-1.29	6.90*
Mar	-0.78	-3.62*	-0.43	8.27*
Apr	-1.47	-4.15*	-3.14*	7.60
May	-3.62	-5.03*	-4.15*	3.89
Jun	-2.90	-5.30*	-5.31*	3.79
Jul	-6.37	-8.83*	-9.37*	13.17*
Aug	-59.74*	-9.89*	-15.98*	8.71*
Sep	-110.82*	-12.30*	-34.81*	8.32*
Oct	-34.66*	-7.99*	-15.28*	6.62*
Nov	-11.13*	-8.16*	-9.91*	4.60*
Dec	-6.77*	6.46*	-0.83*	3.66*
All	-6.66*	-6.57*	-7.35*	6.63*

Table 4-3
Mann-Kendall test results for salinity over 1968-2012. Values are the Sen's slope estimate in $\mu\text{S}/\text{cm}/\text{year}$. An asterisk indicates significance of the Mann-Kendall test at the 5% level.

Season	Group A	Group B	Group C	Group D	Group J
Jan	4.61	2.67*	0.80	0.64	6.67*
Feb	0.46	1.43	1.04	-1.42	4.61
Mar	0.19	1.33*	0.36	-0.49	4.60
Apr	0.26	1.60*	-0.16	0.55	-5.53*
May	-0.54	1.71*	-0.97*	1.58	-10.69*
Jun	-1.21	0.08	-0.66	0.45	-6.20
Jul	-2.72	-0.77	-0.75*	-0.58	-9.79*
Aug	4.27	0.32	-0.34	2.47	-8.96*
Sep	16.43*	1.61	-0.24	9.23*	-4.35
Oct	16.40*	2.37*	-0.16	9.60*	-1.97
Nov	22.70*	3.41*	0.31	9.78*	1.09
Dec	26.44*	4.55*	0.71	10.89*	5.17
All	0.90*	1.51*	-0.06	1.74*	-2.73*

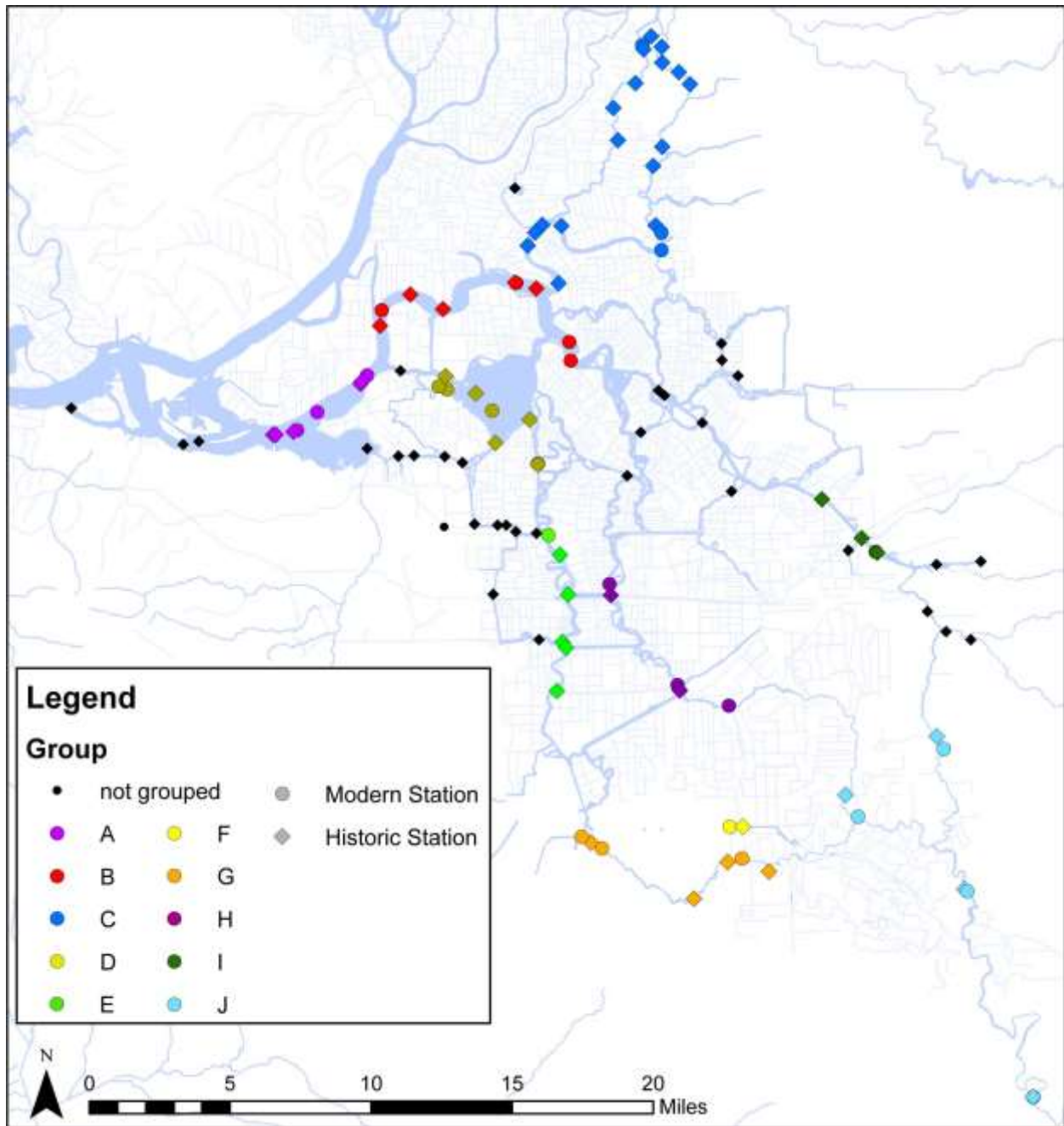


Figure 4-1 Grouping of stations for trend analysis.

5. CONCLUSIONS

This work is an effort to compile and collect interior Delta salinity data, paralleling the effort for the western Delta presented in the 2014 Tetra Tech report. This work used maps and statistical analysis over similar hydrologic conditions, to show changes over time. For example, the different presentations in this work clearly show how the distribution of interior Delta salinity in the summer months has changed following 1944, when Shasta Dam was completed.

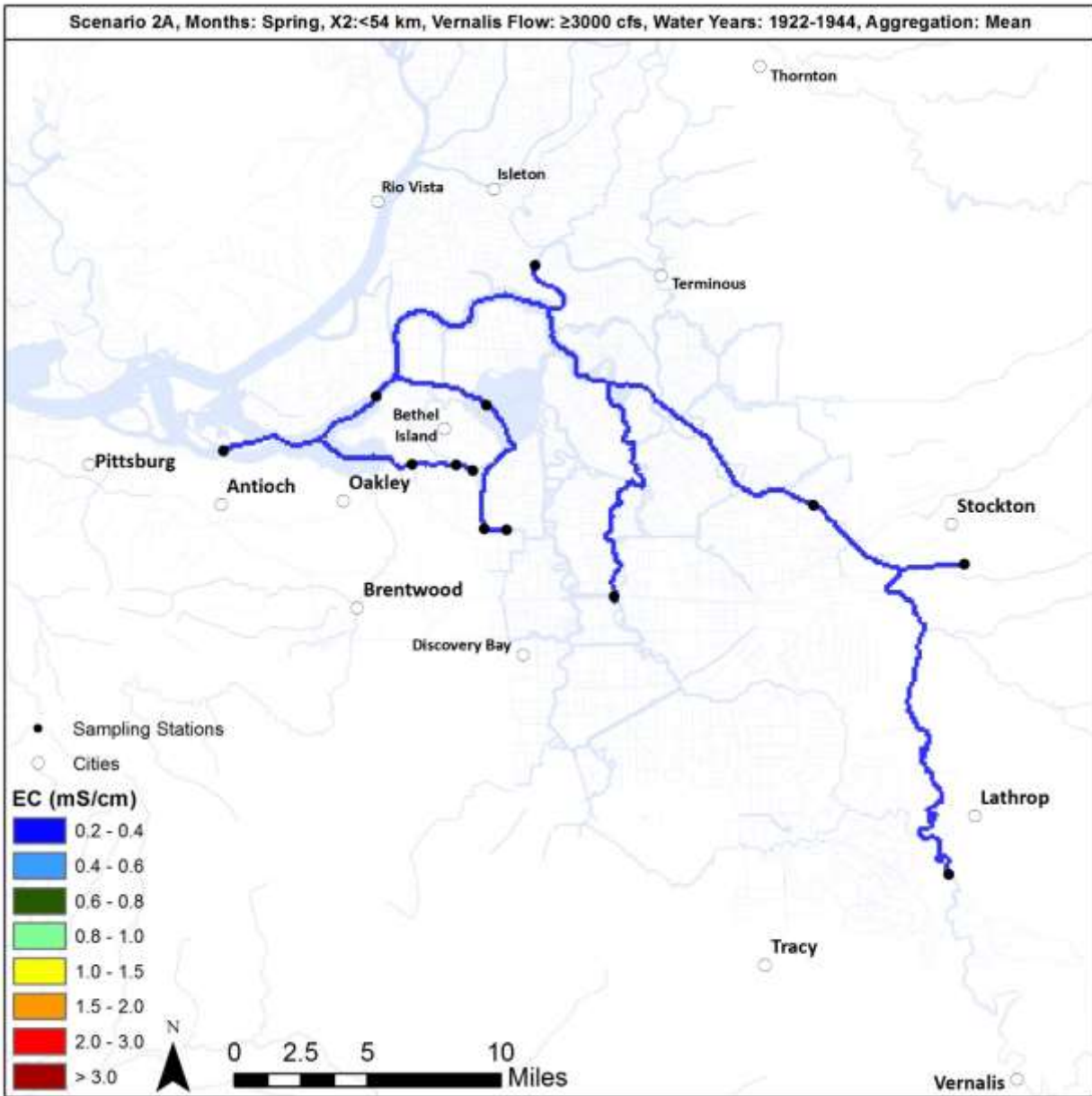
In the 2014 report, the data were also subject to a modeling analysis along the estuarine salinity gradient (using, for example, the Kimmerer-Monismith model and the Delta Salinity Gradient model). The modeling was used to evaluate changes in salinity under hydrologic conditions beyond those typically used in the western Delta (i.e., modeling from 1922-present, as compared to 1967-present as previously done). The modeling of interior Delta salinity is considerably more complex requires models such as the DSM2 model or more complex tools. It is conceivable that these data will provide the basis for model evaluation over the full time horizon, although such an effort was beyond the scope of the present work.

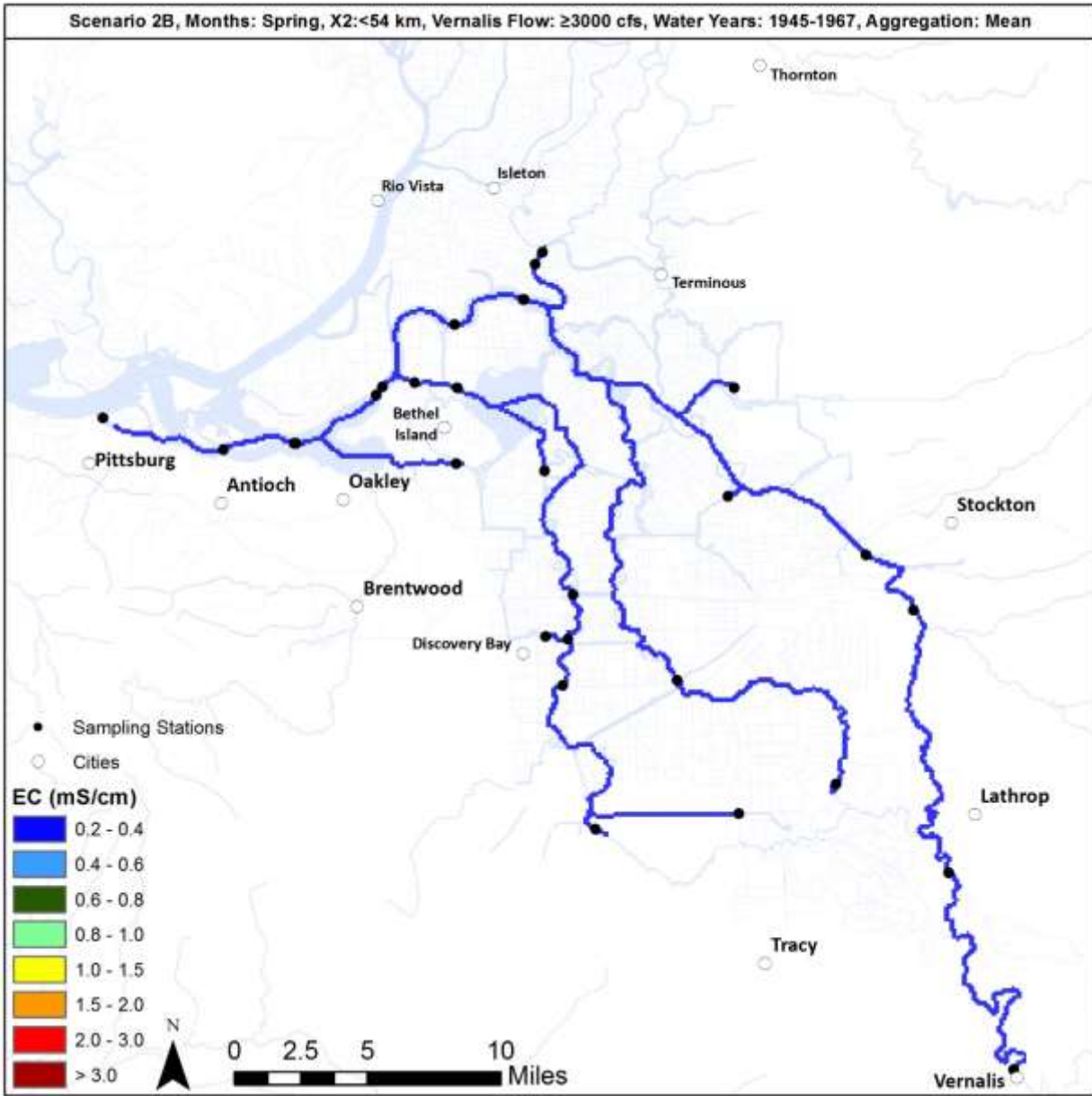
6. REFERENCES

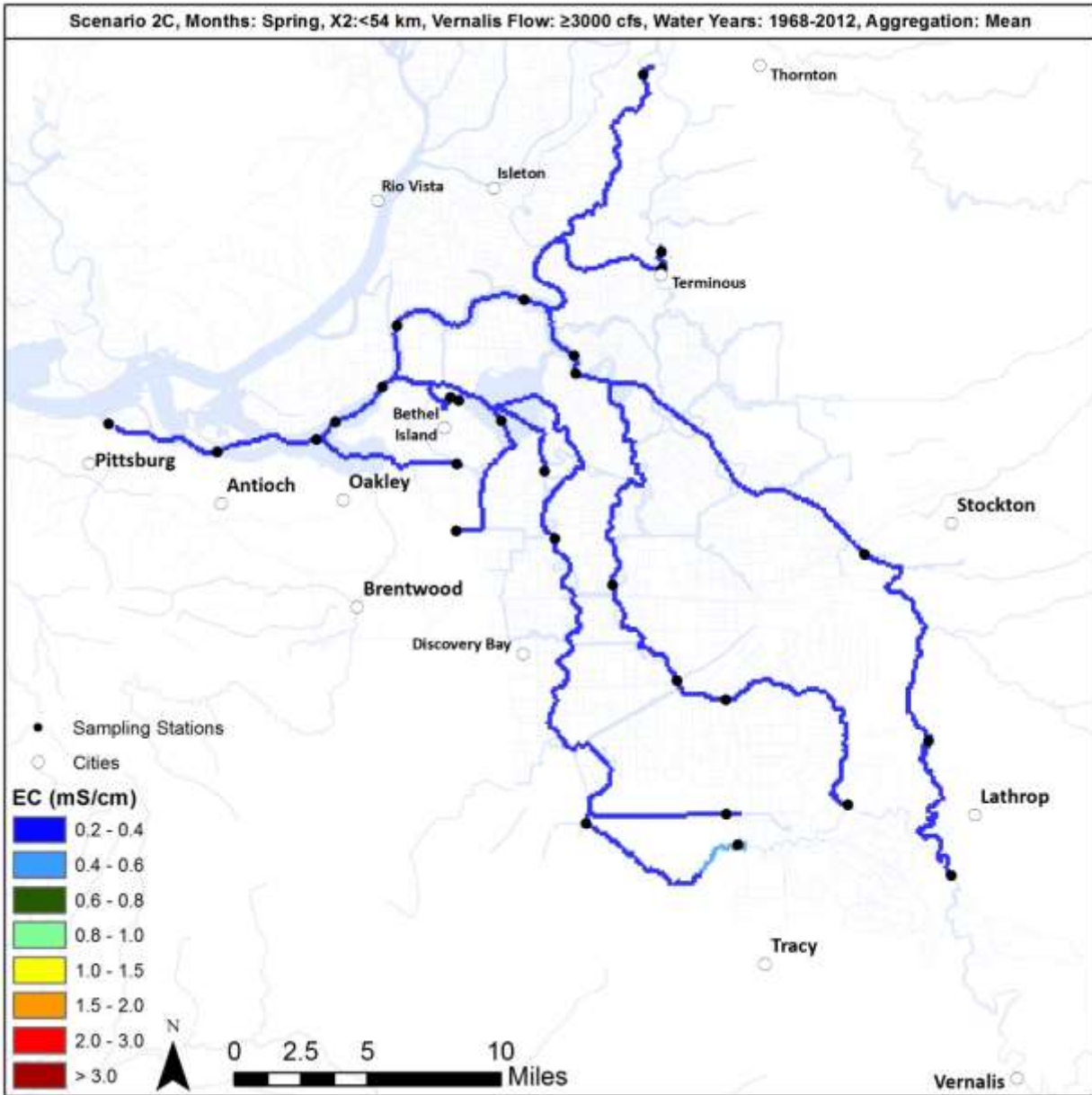
Tetra Tech (2014). Salinity Trends in Suisun Bay and the Western Delta (October 1921 – September 2012), Prepared for the San Luis and Delta Mendota Water Authority and State Water Contractors, January 16, 2014.

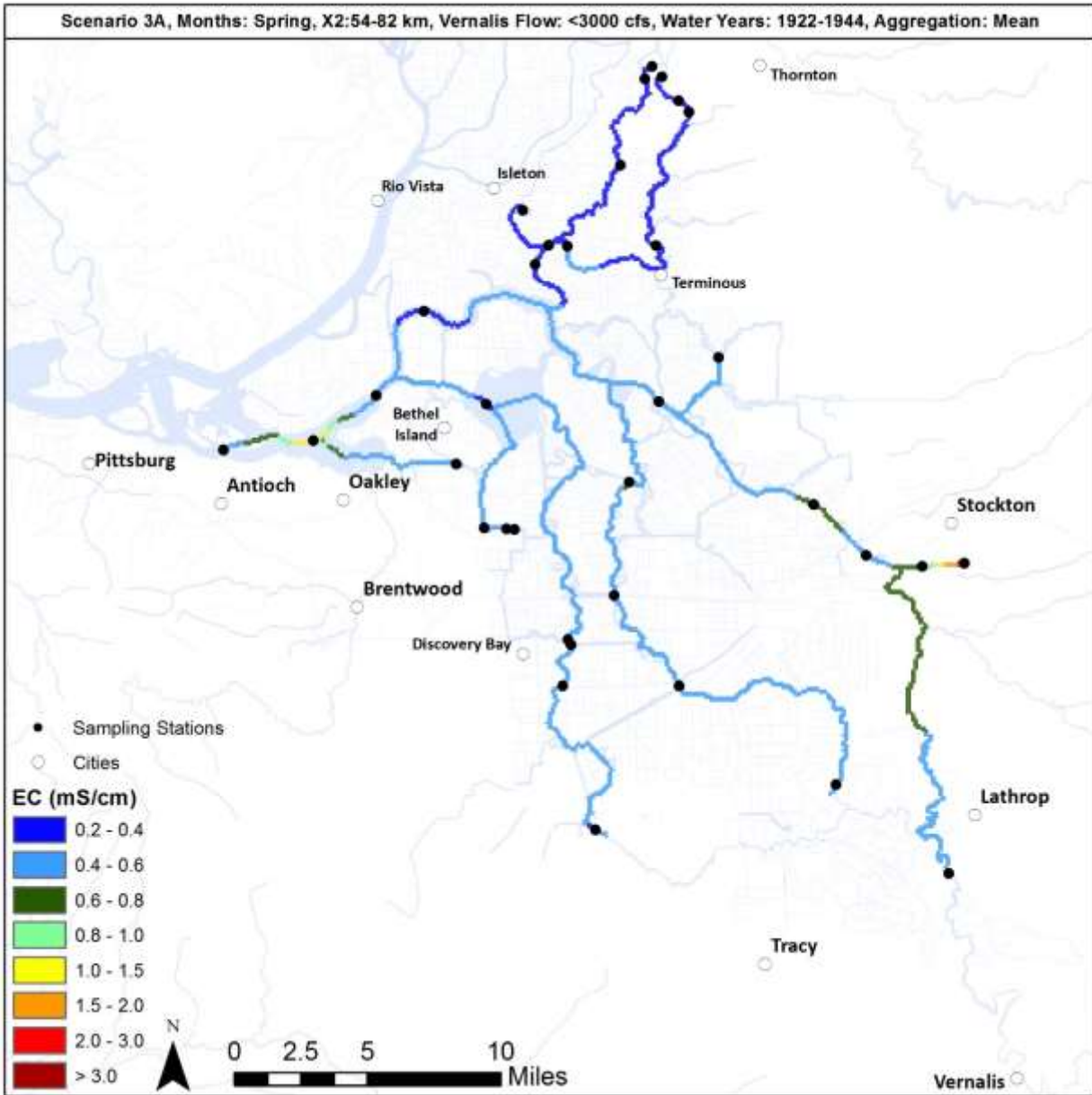
Ver Hoef, Jay M., and Erin E. Peterson. "A moving average approach for spatial statistical models of stream networks." *Journal of the American Statistical Association* 105.489 (2010).

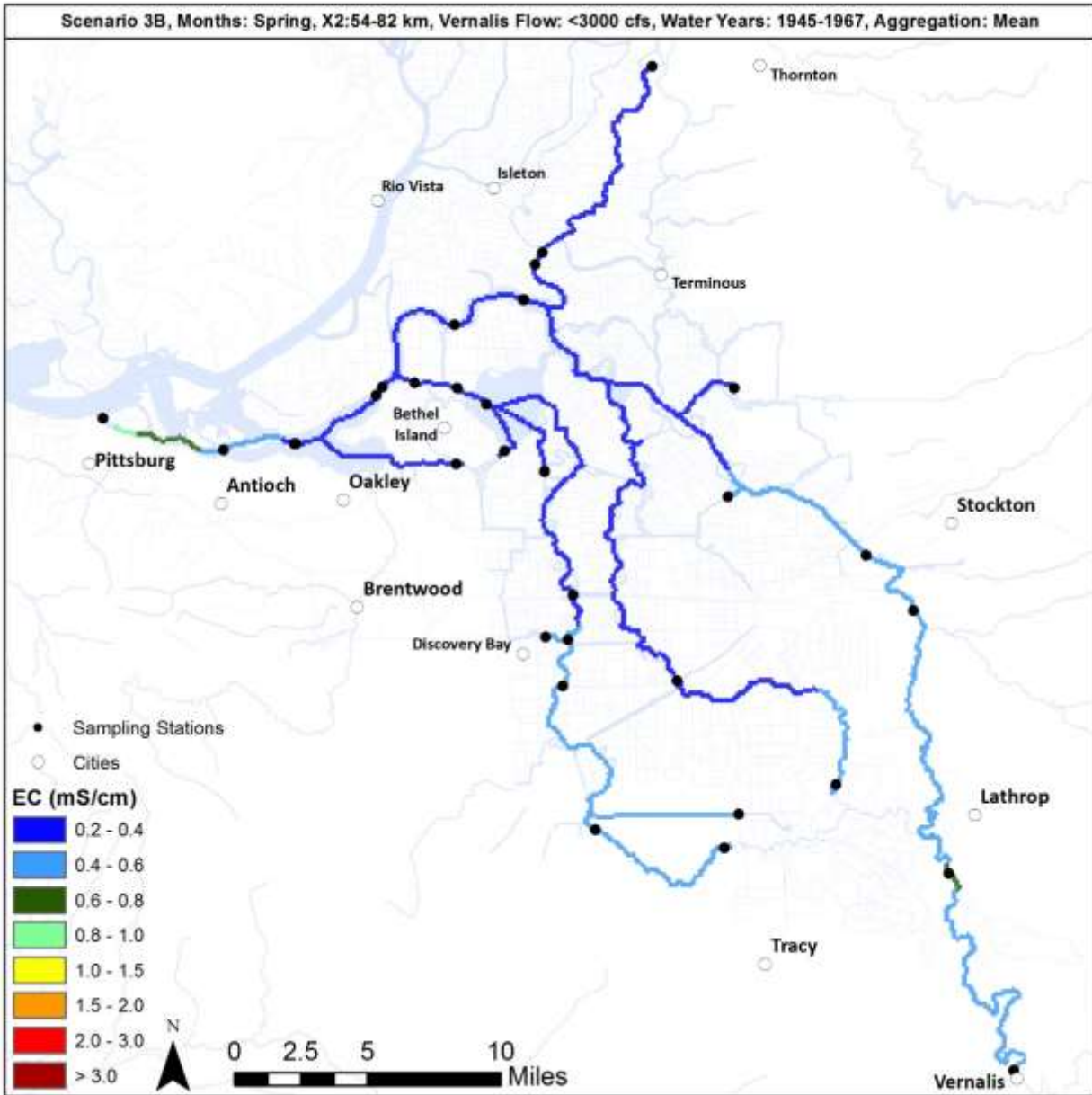
Appendix A. MAPS OF MEAN SALINITY

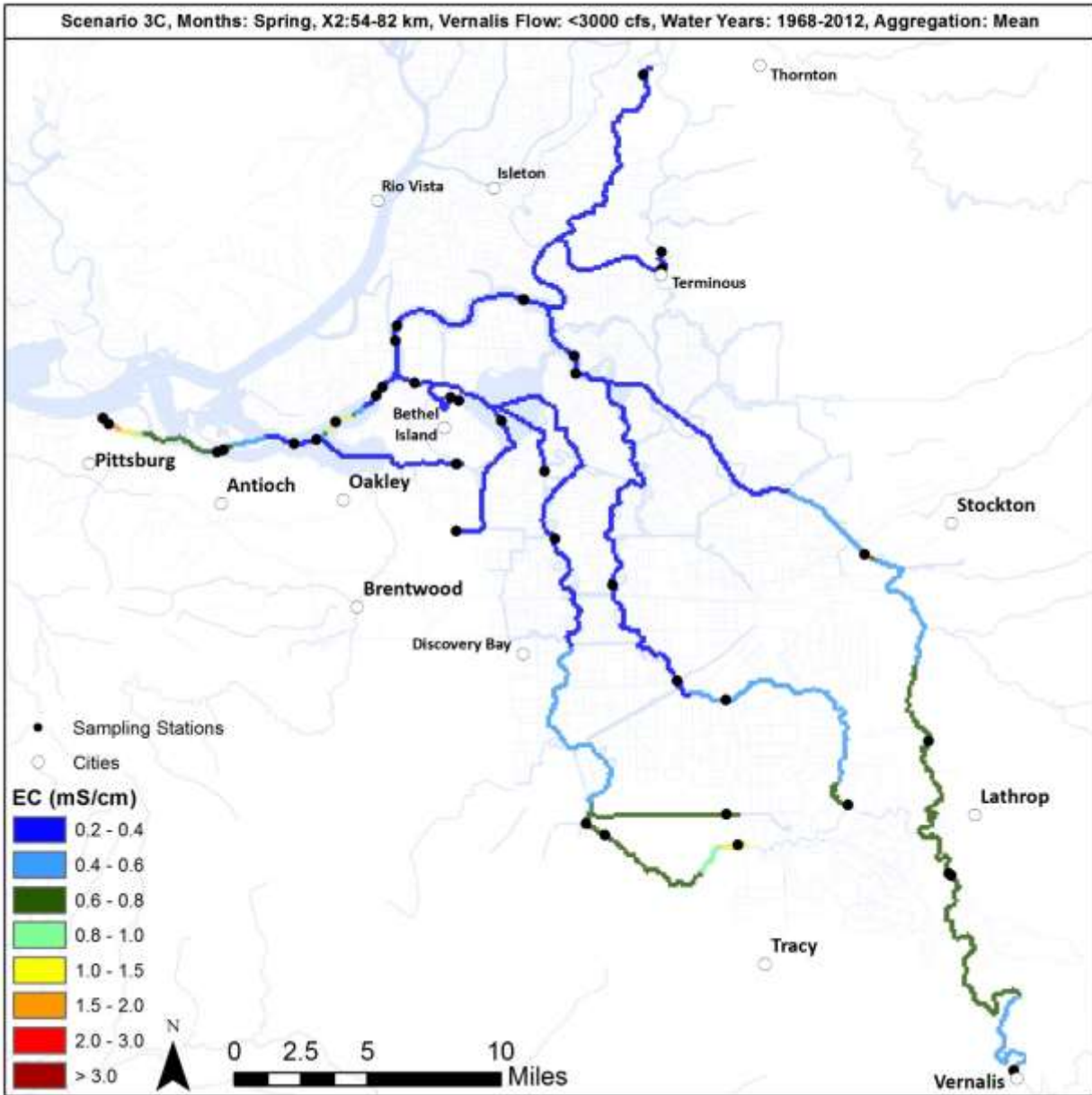


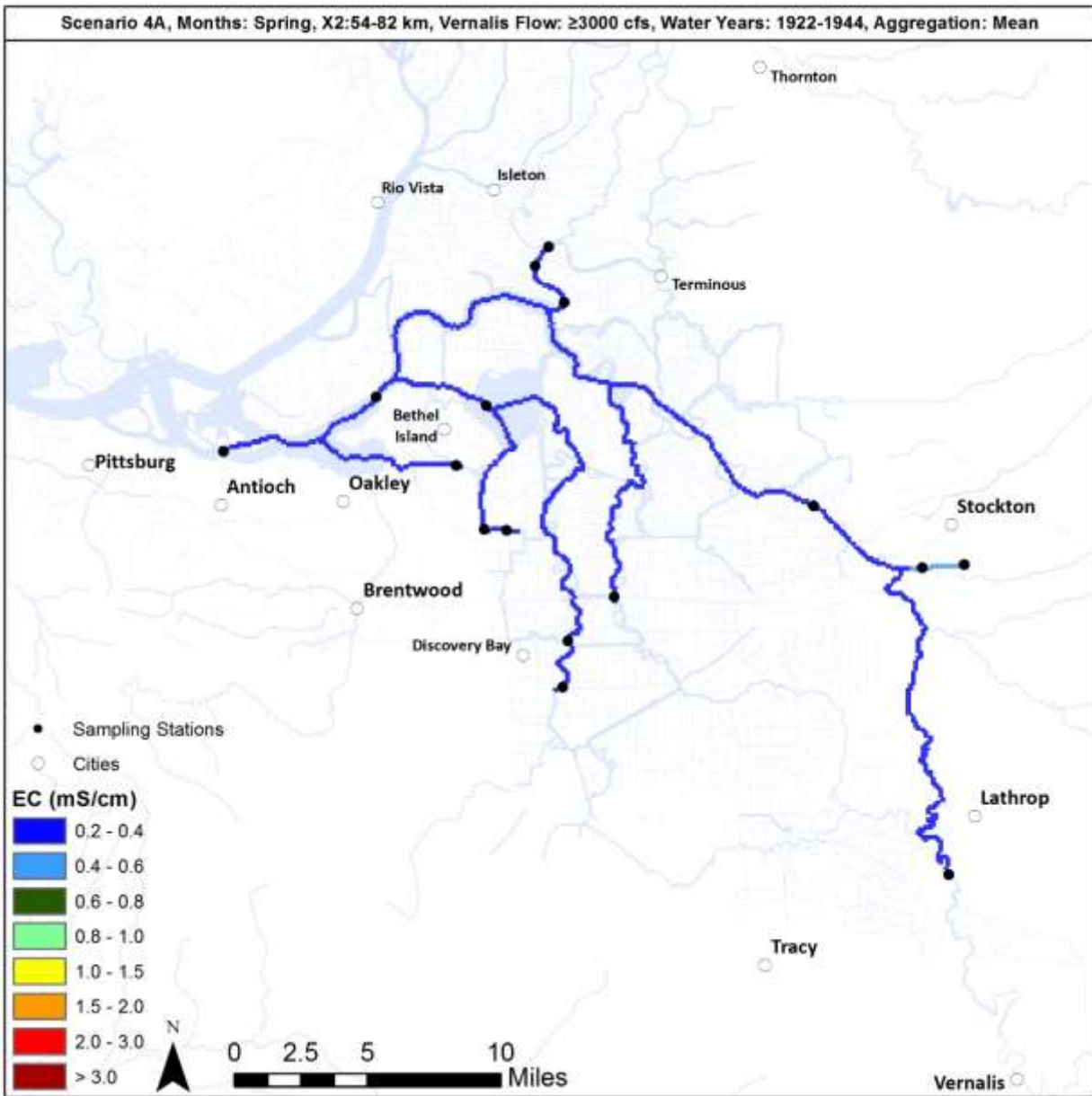


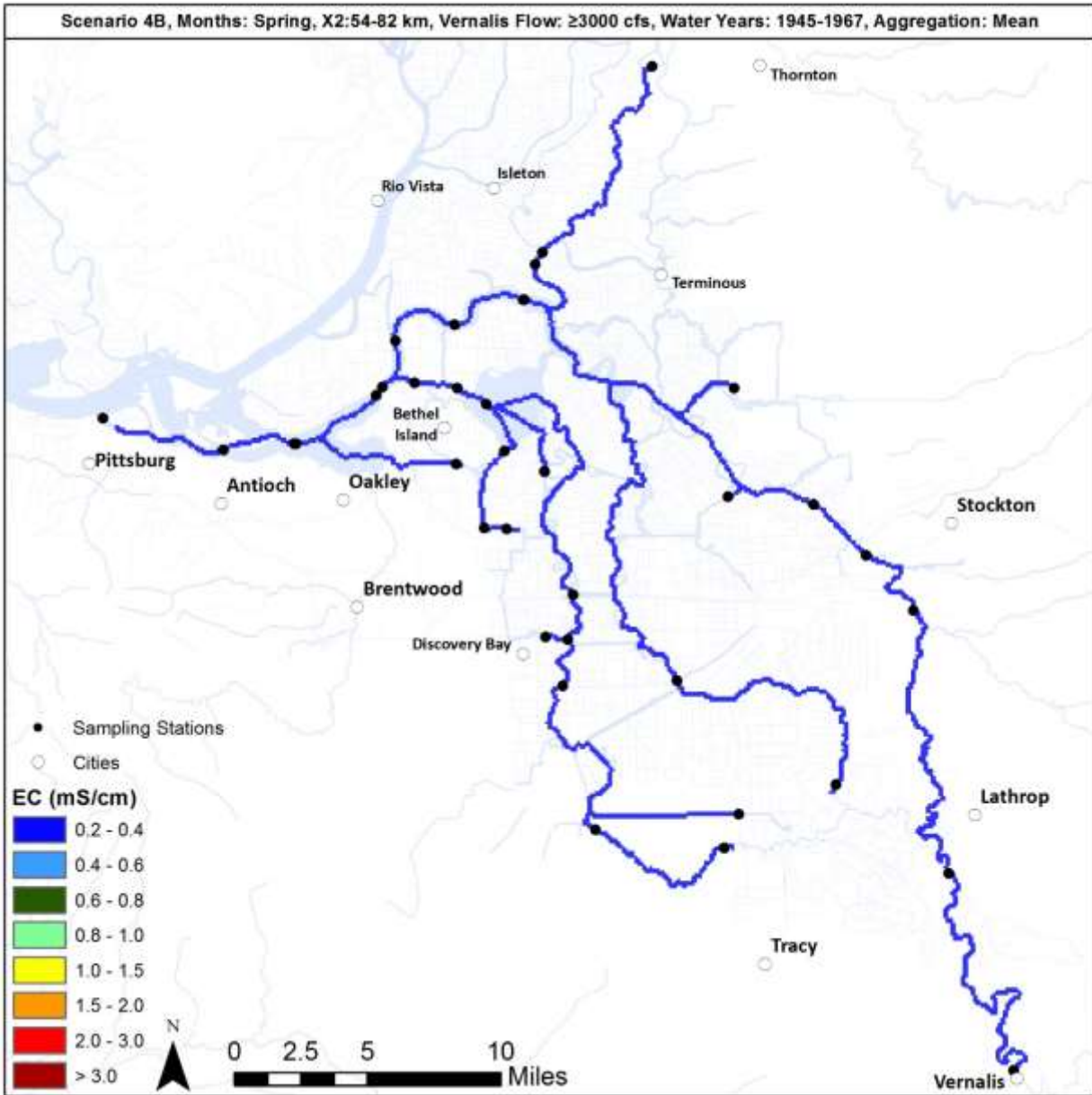


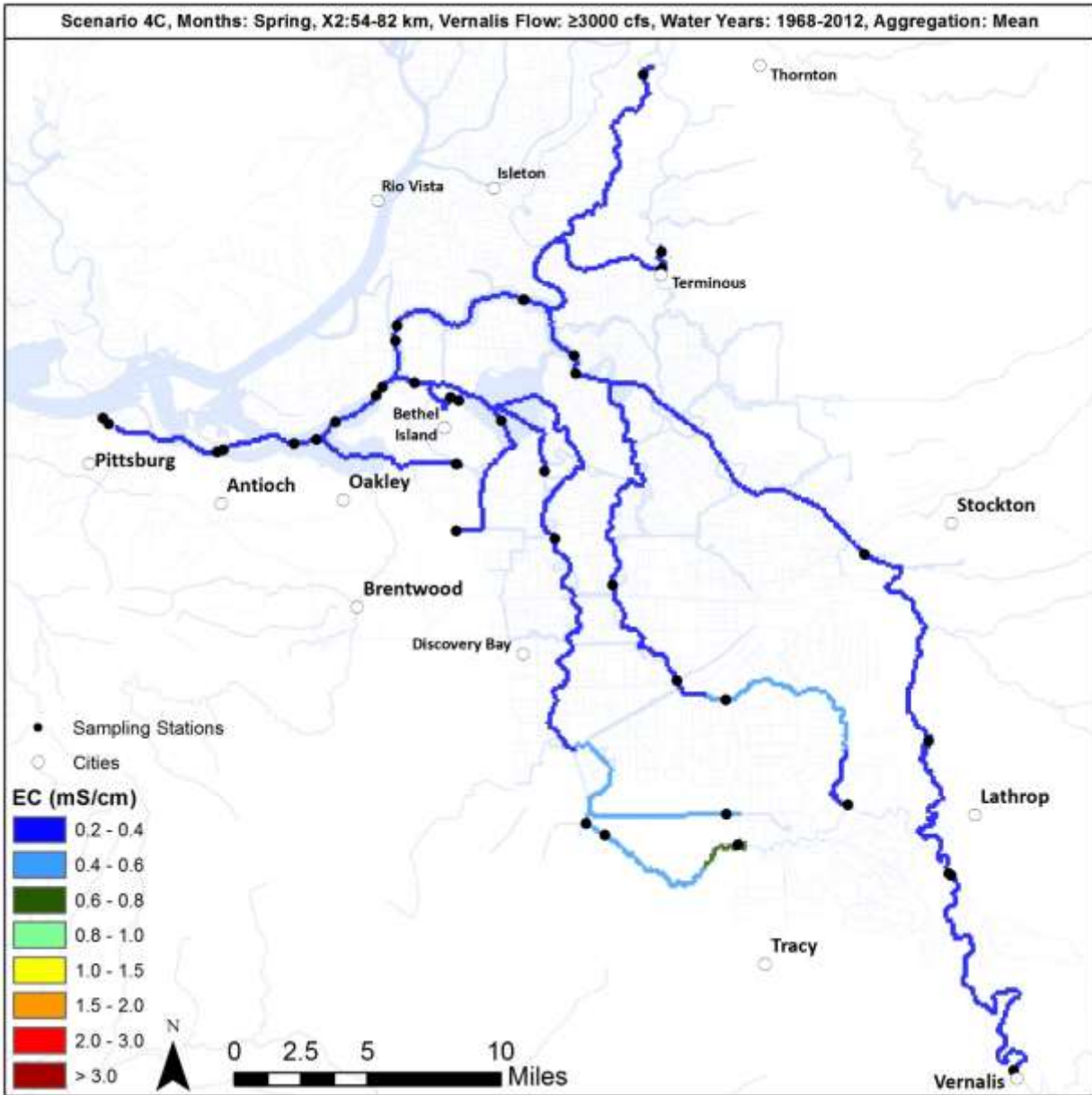


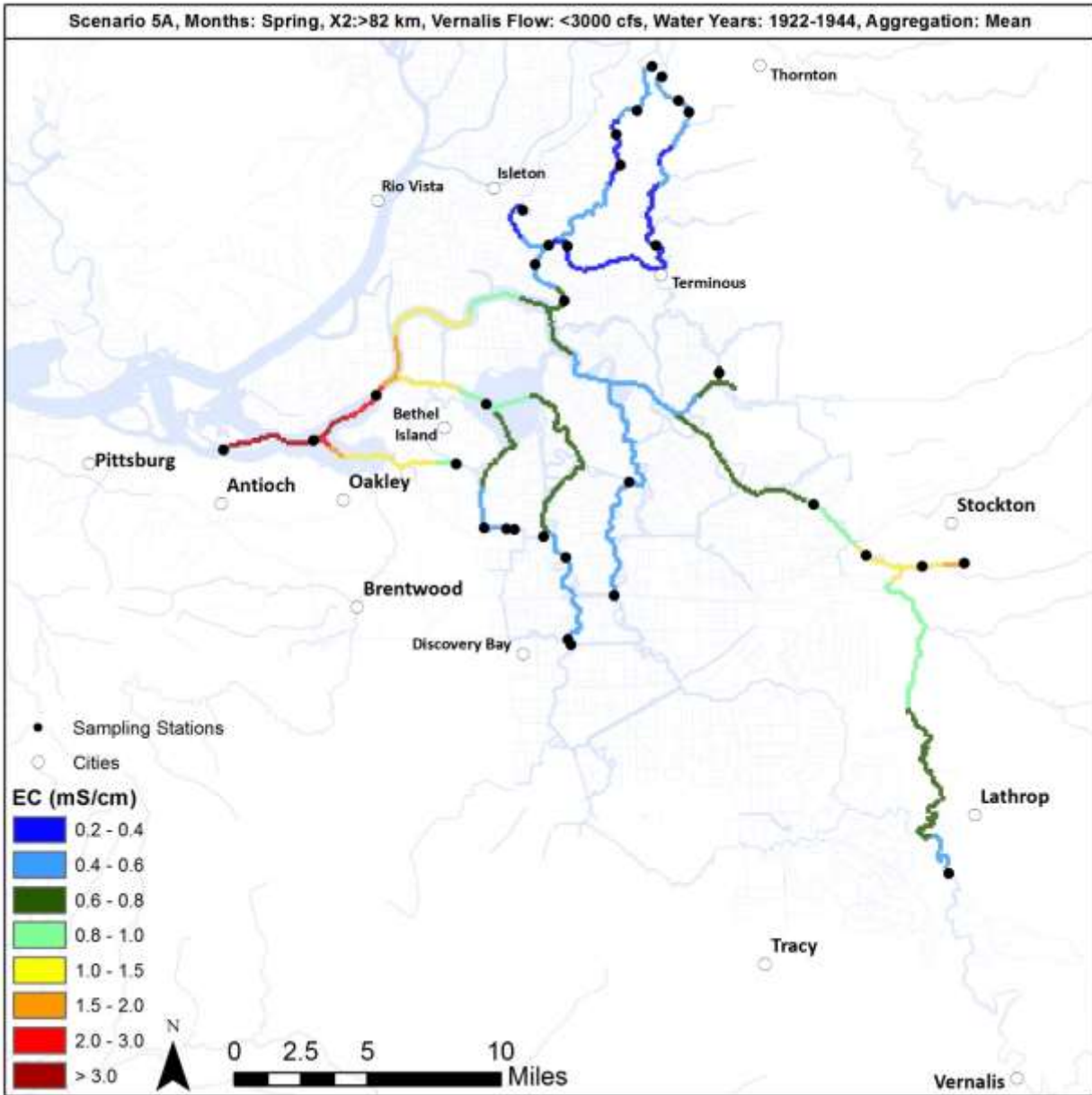


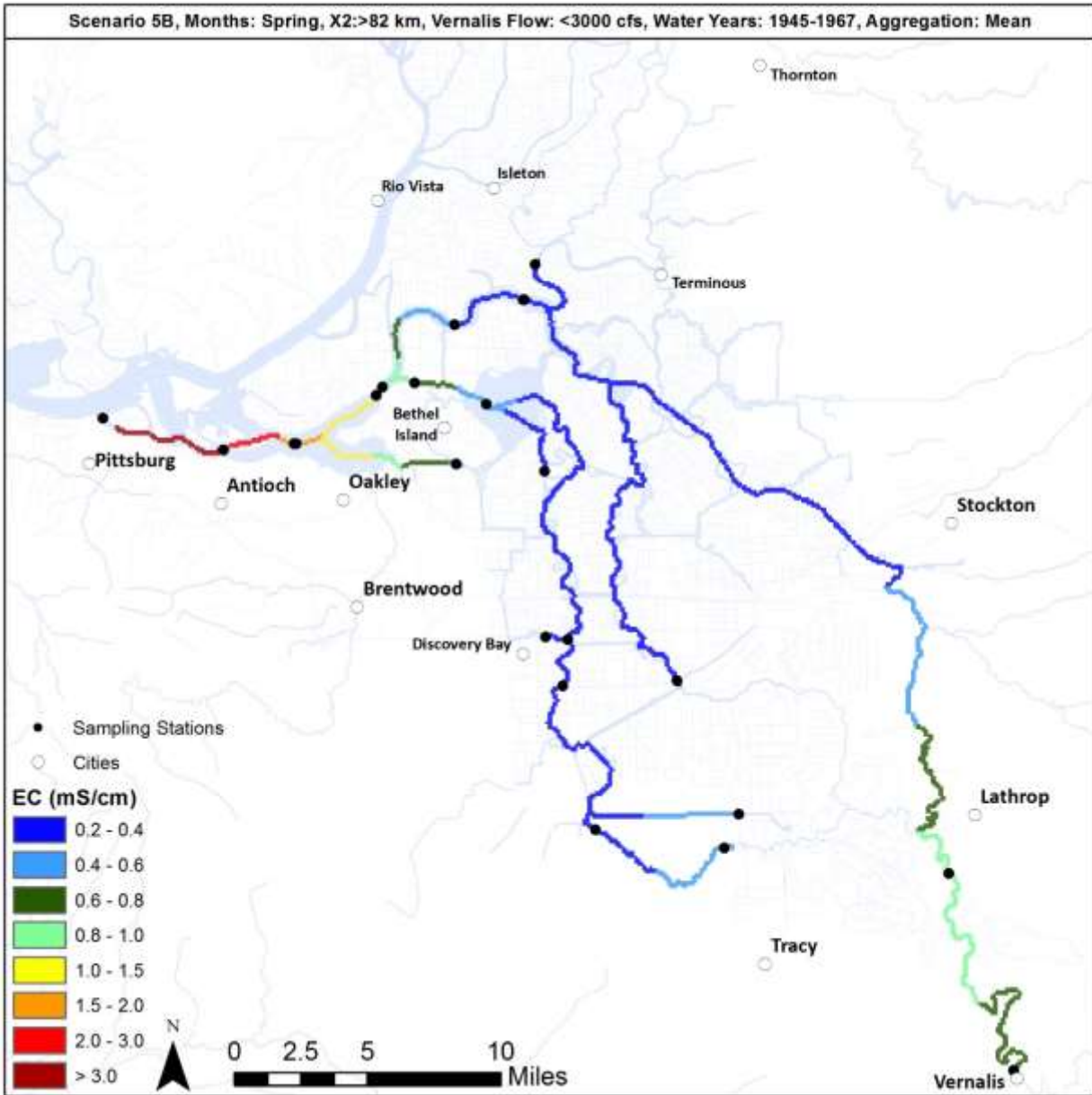


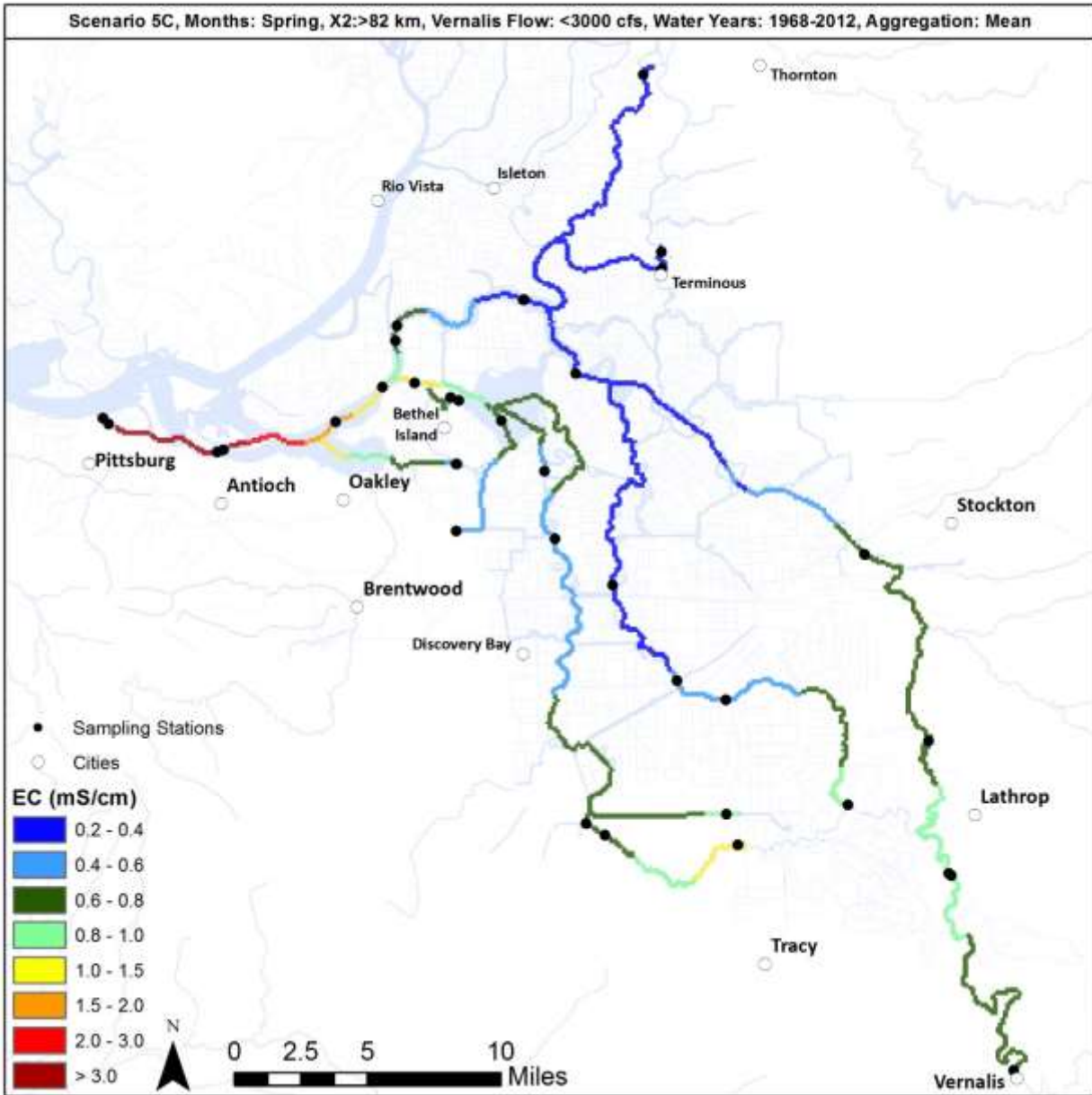


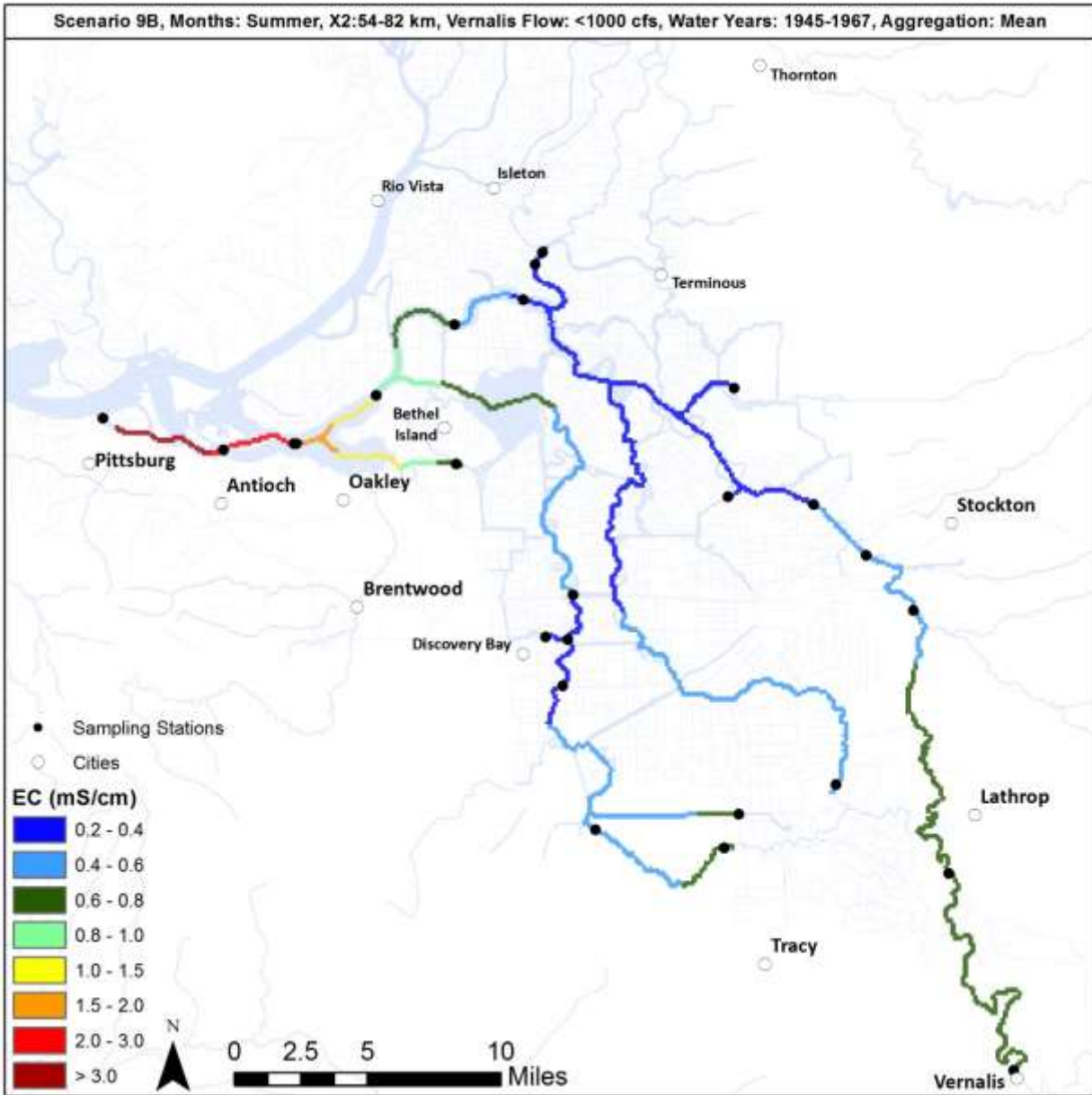


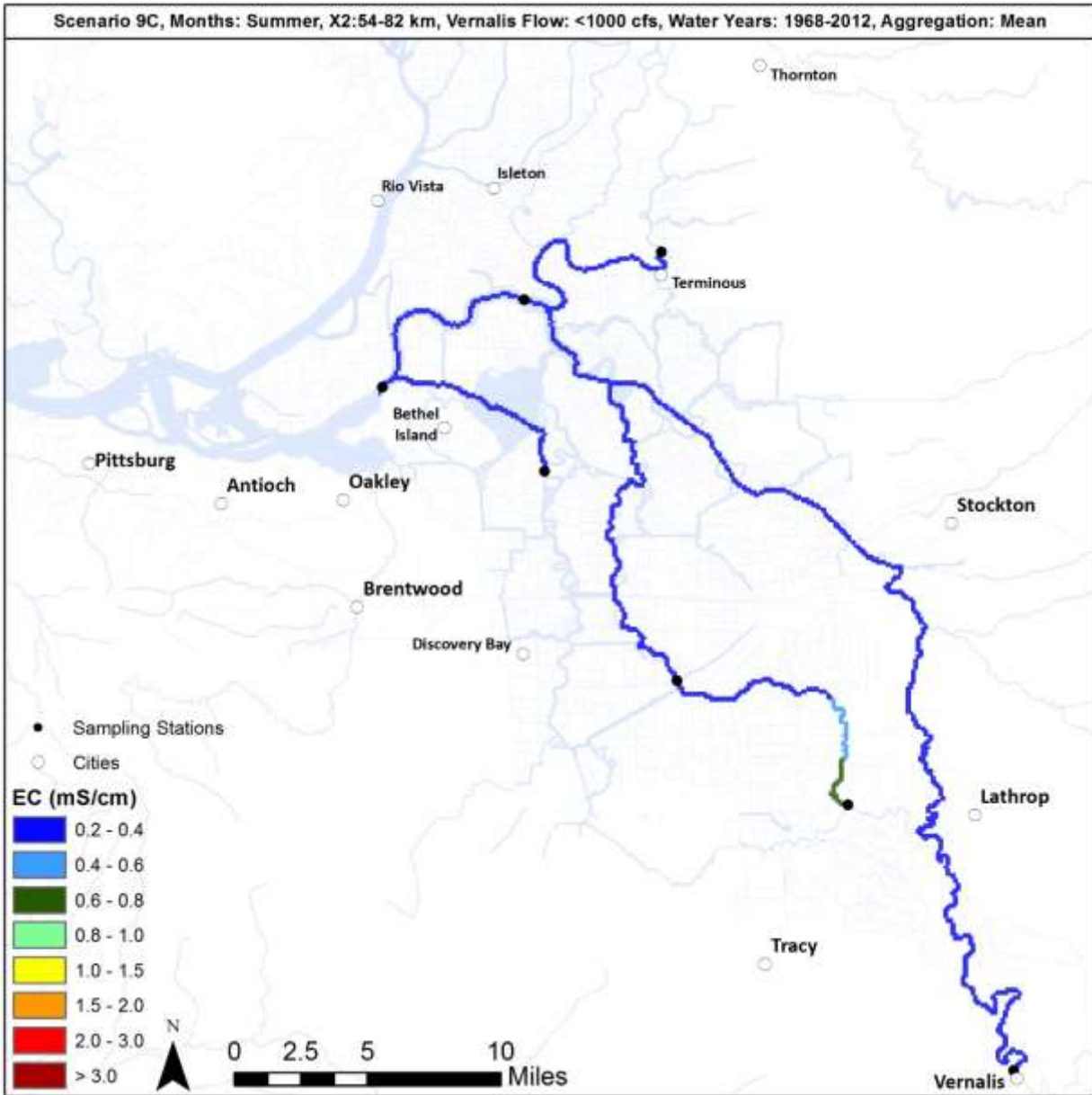


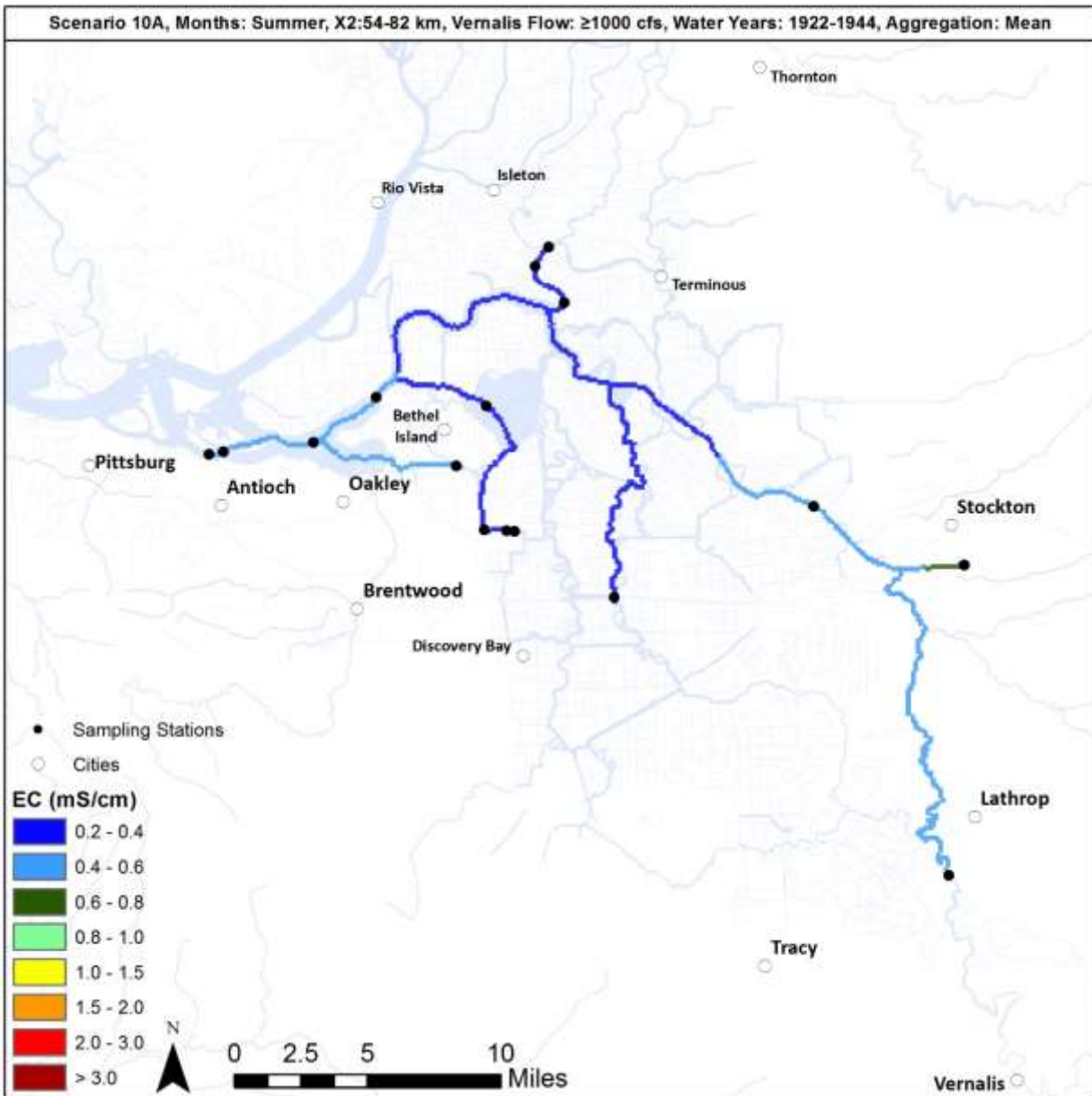


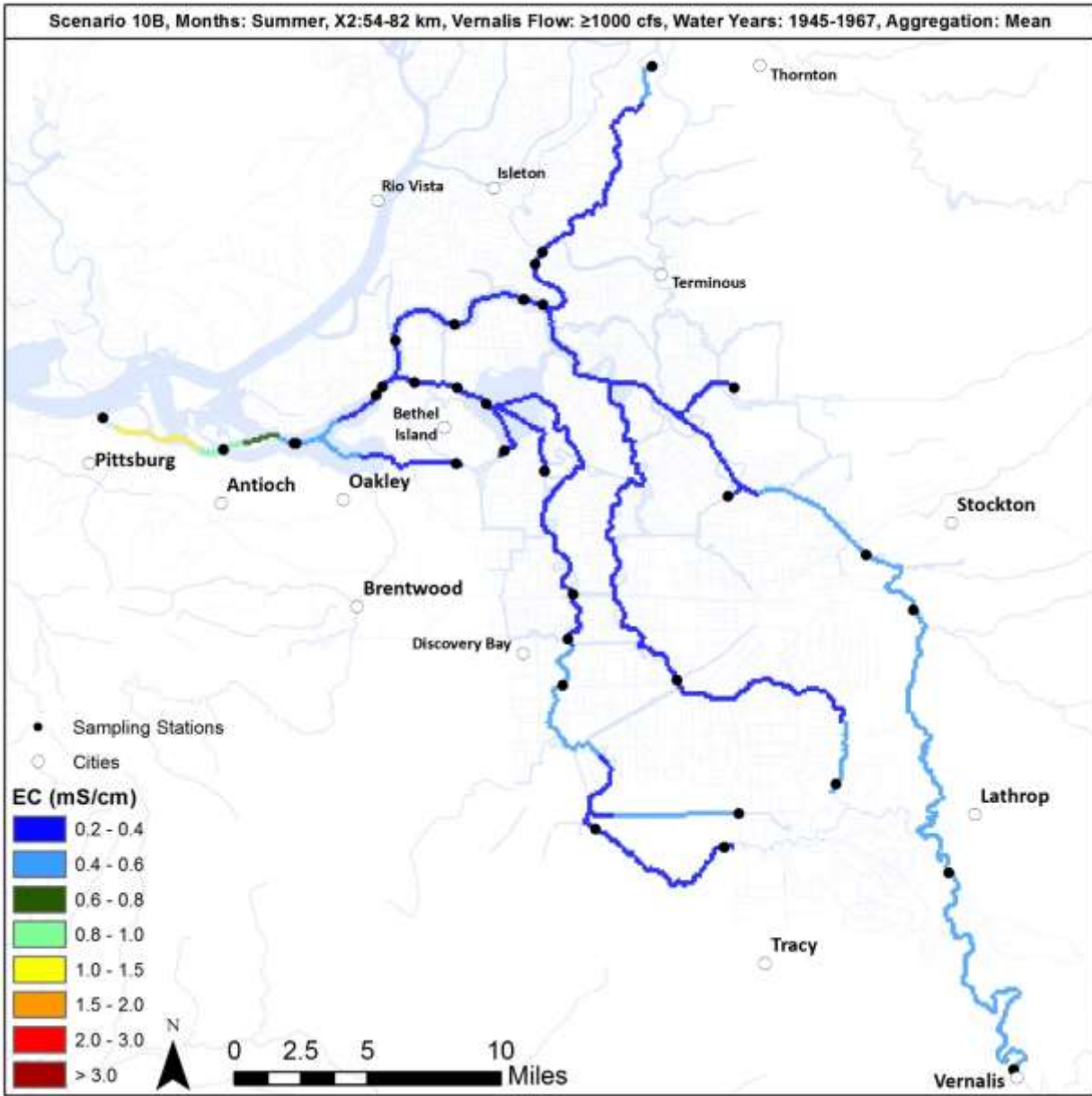


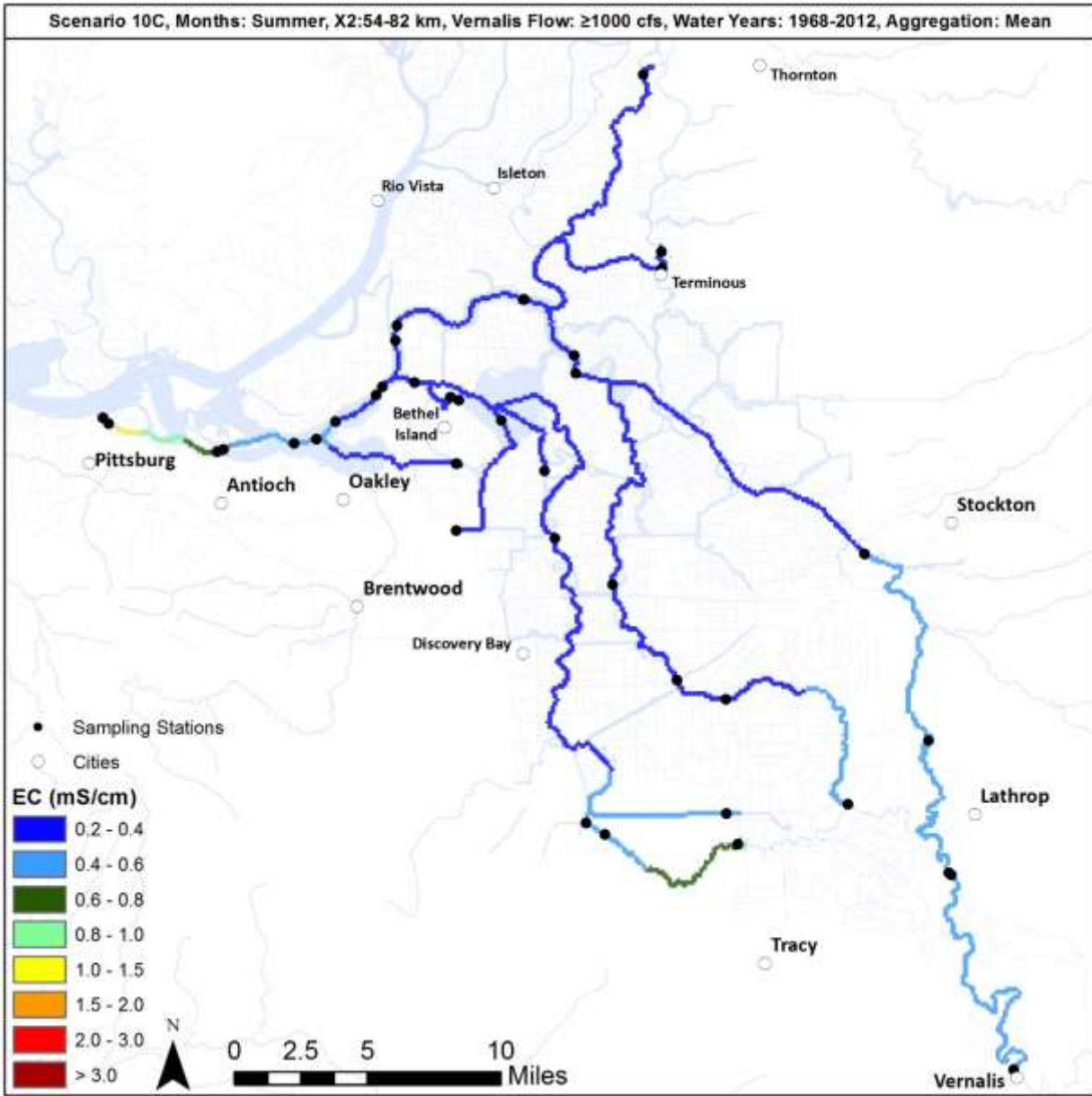


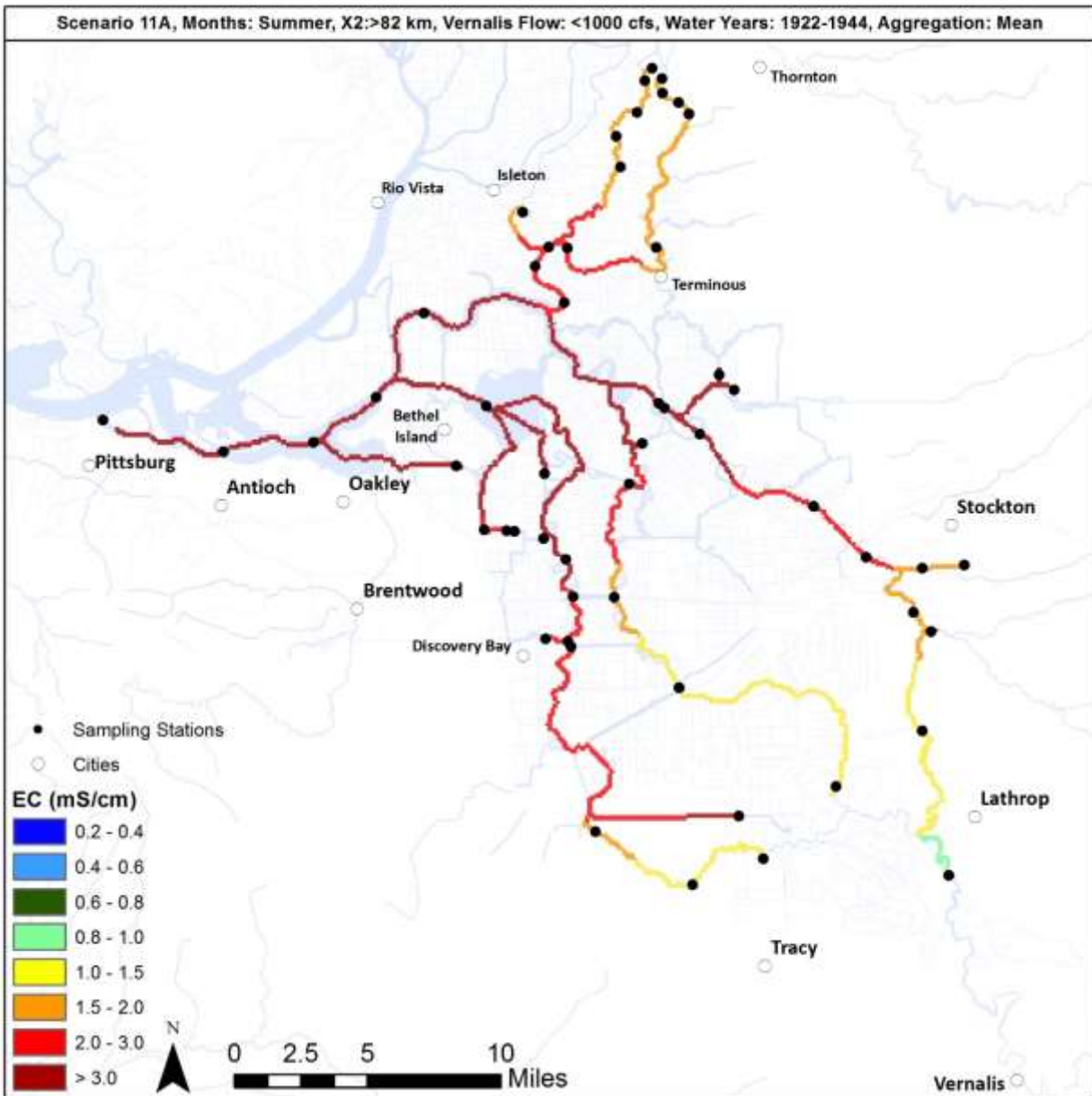


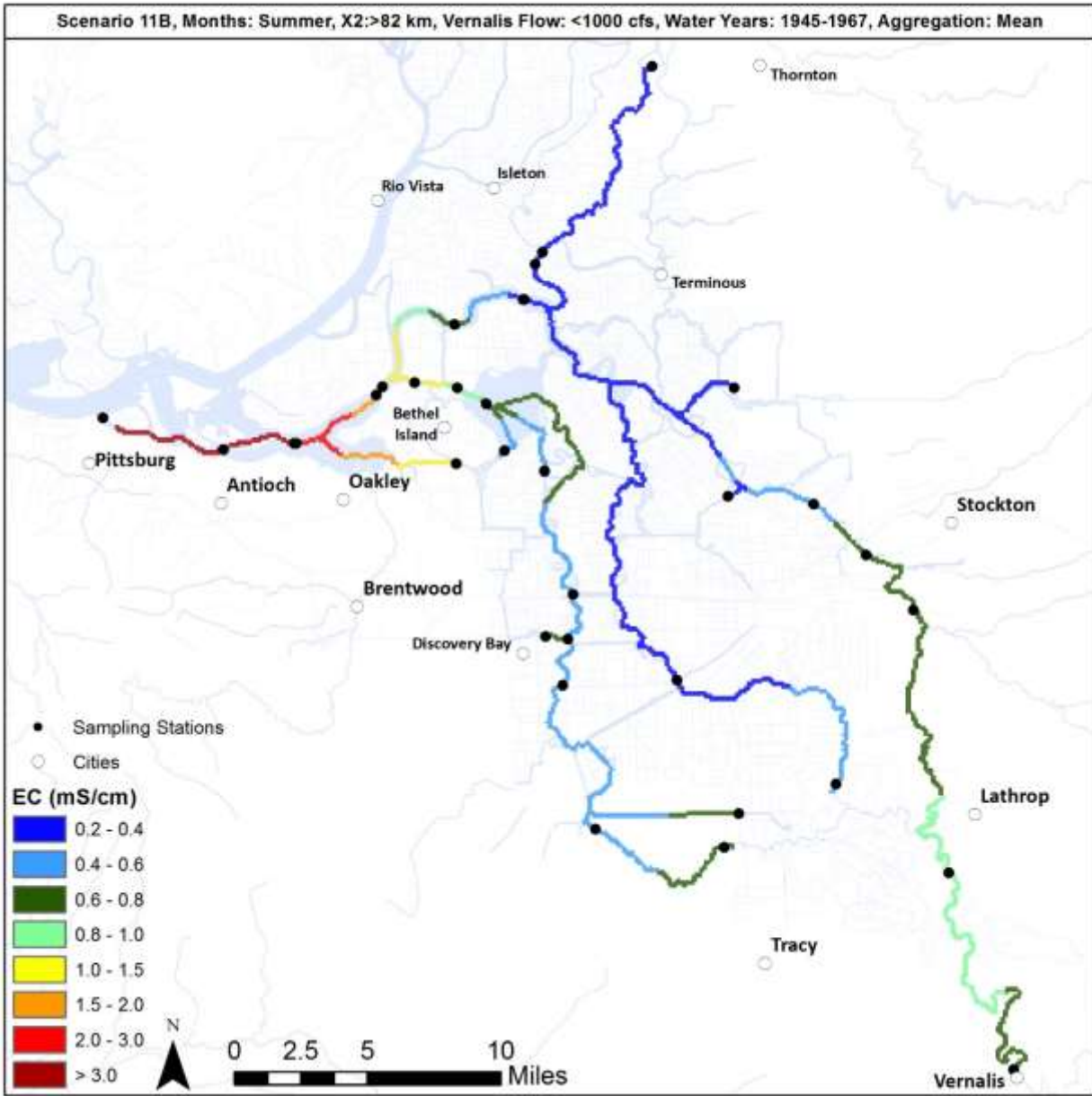


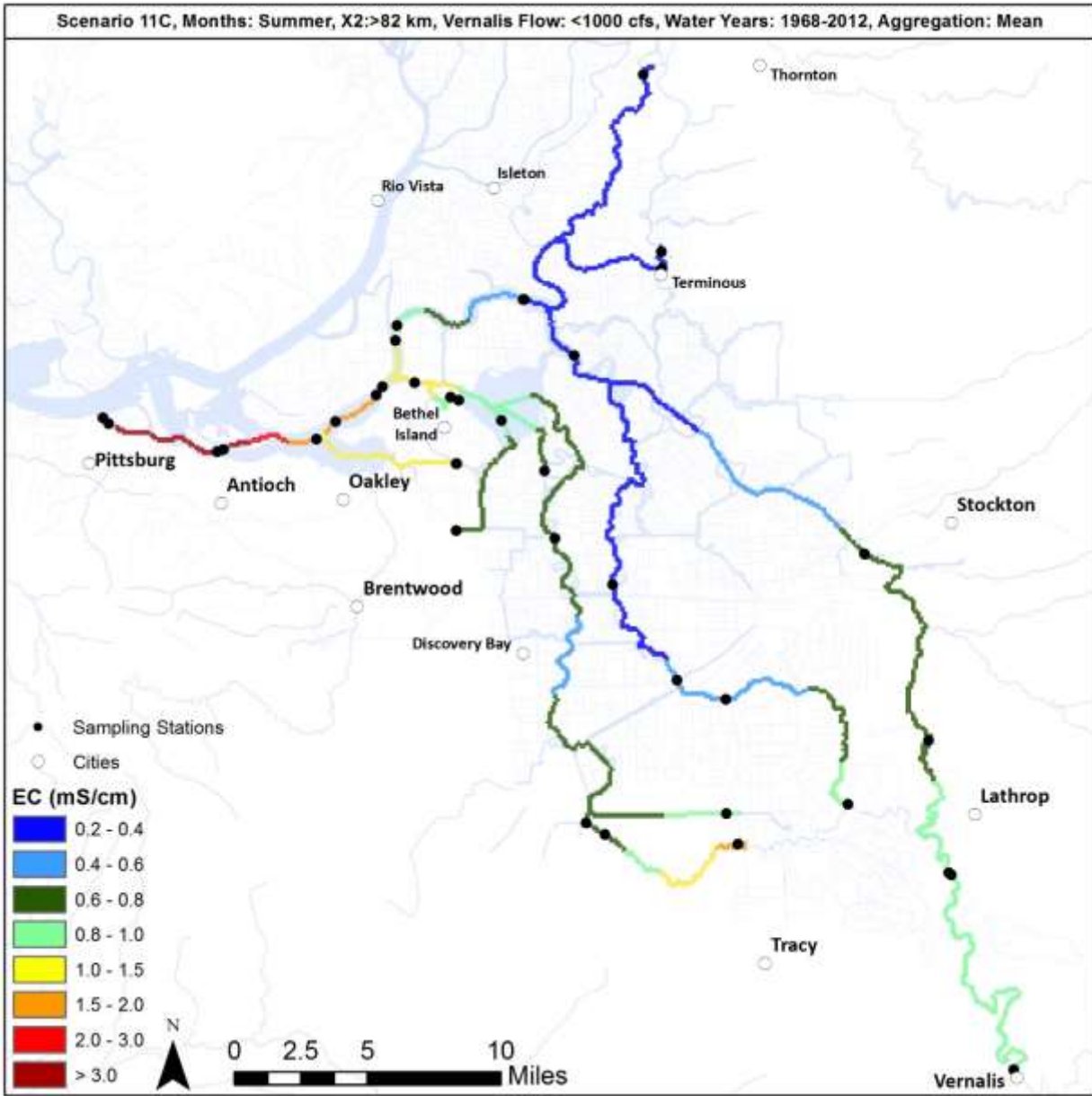


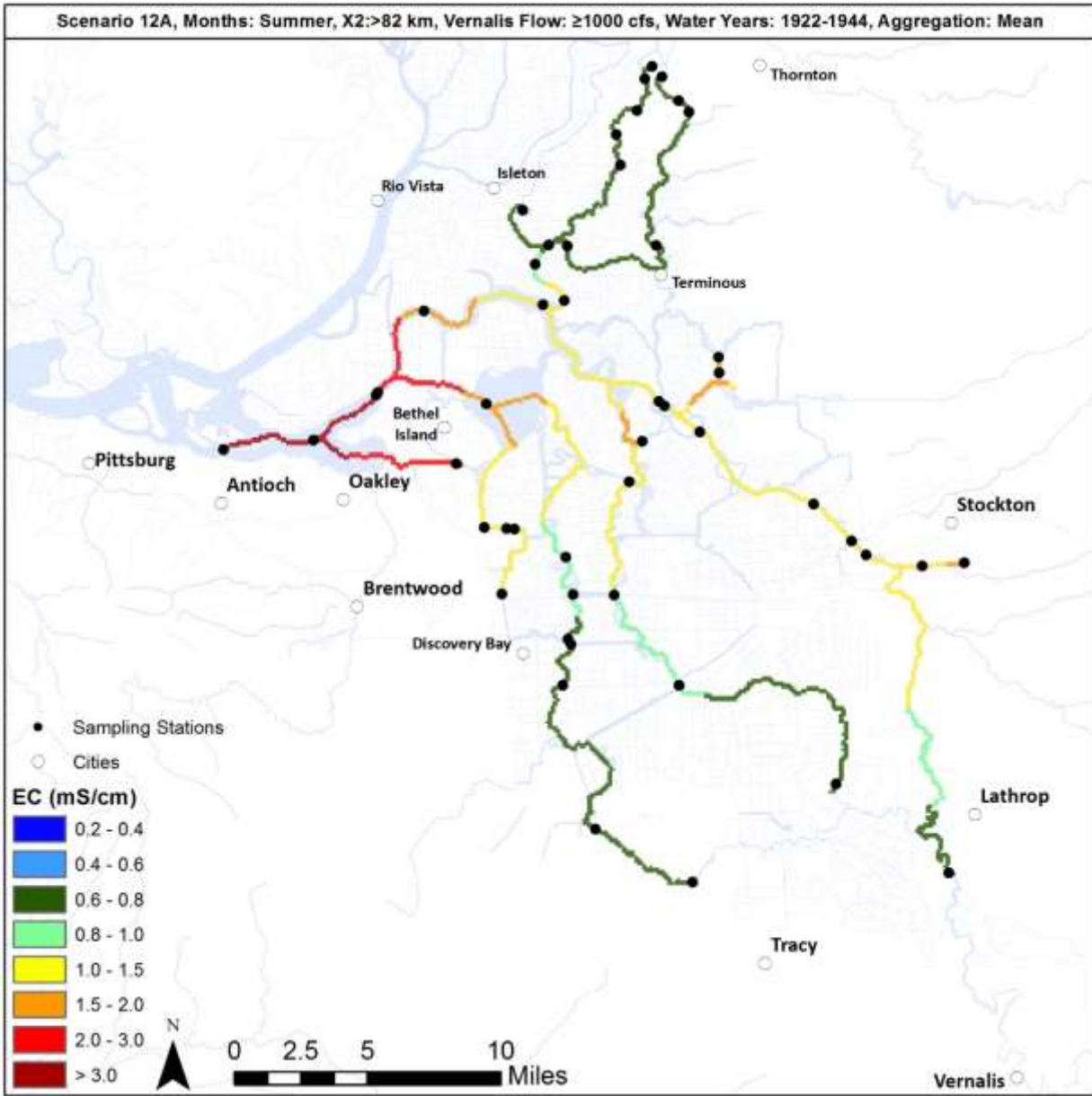


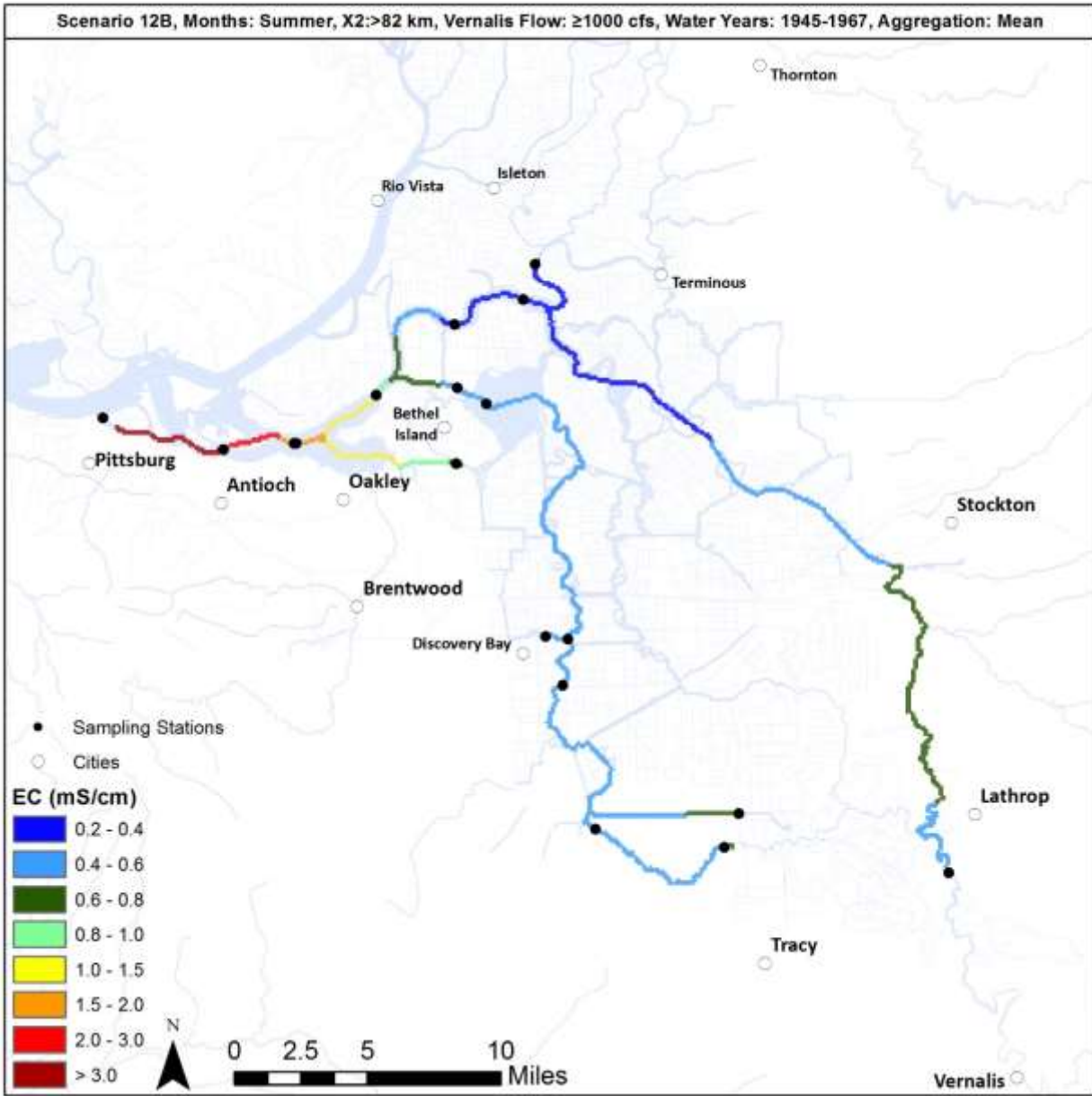


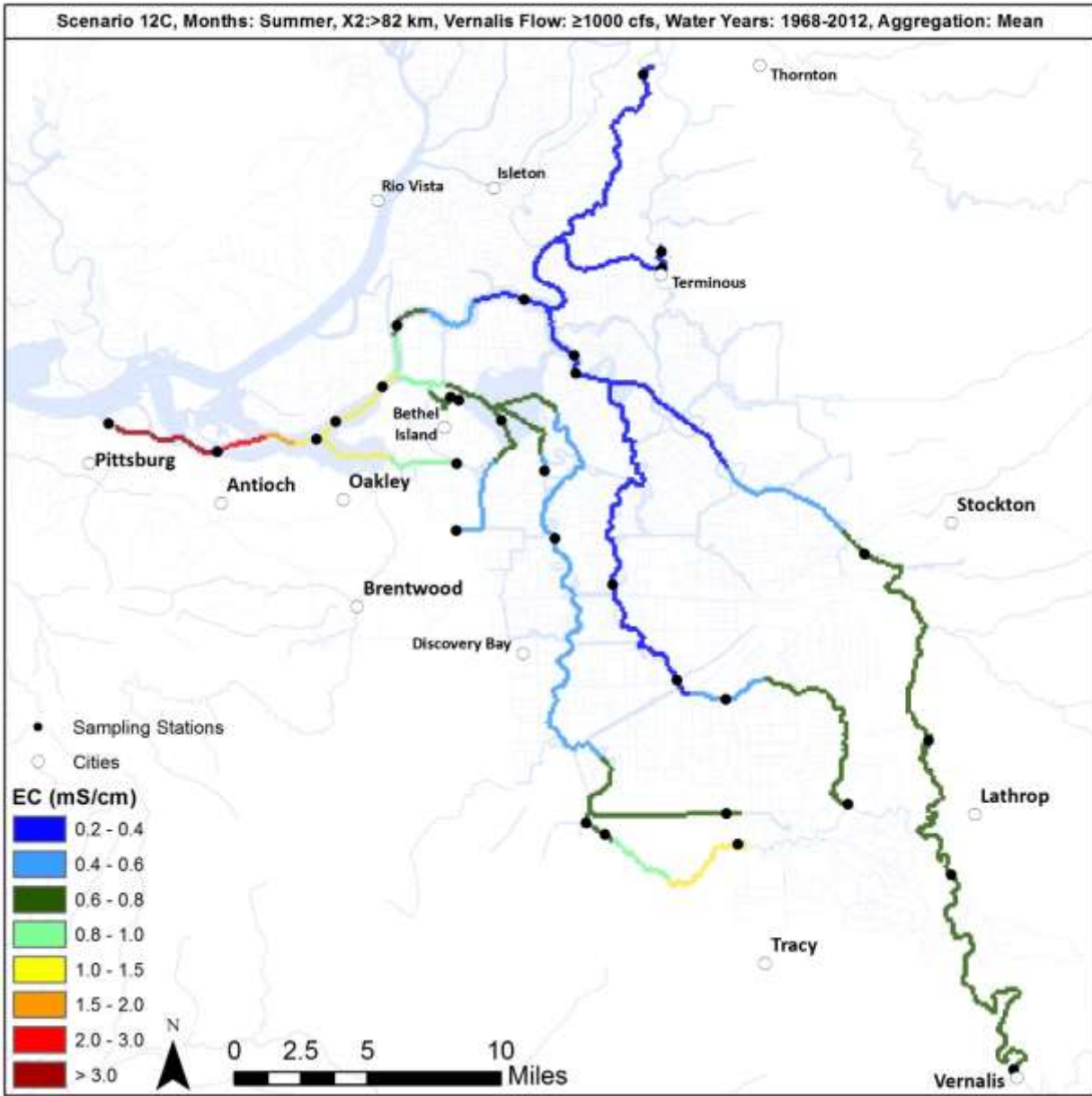




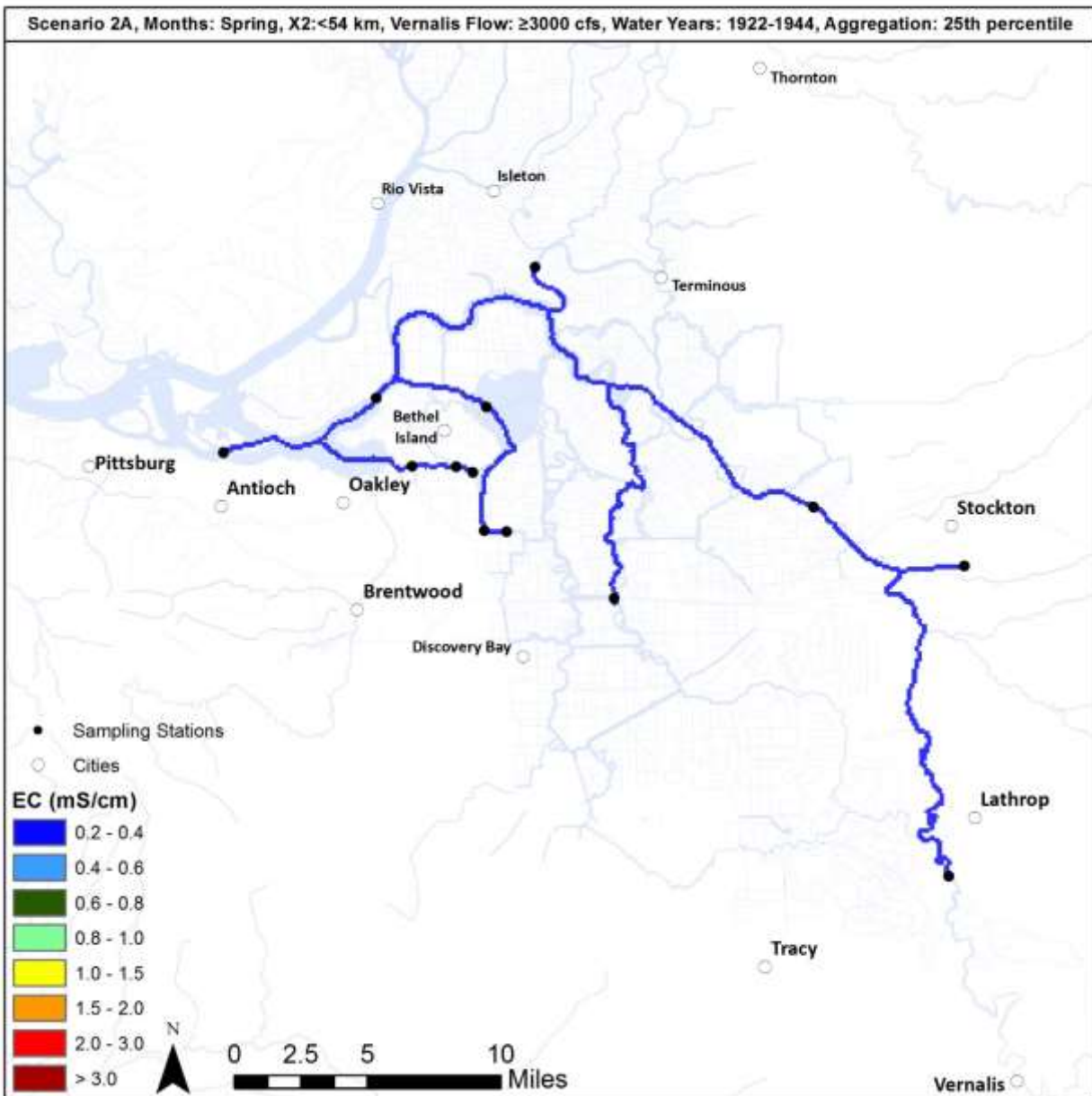


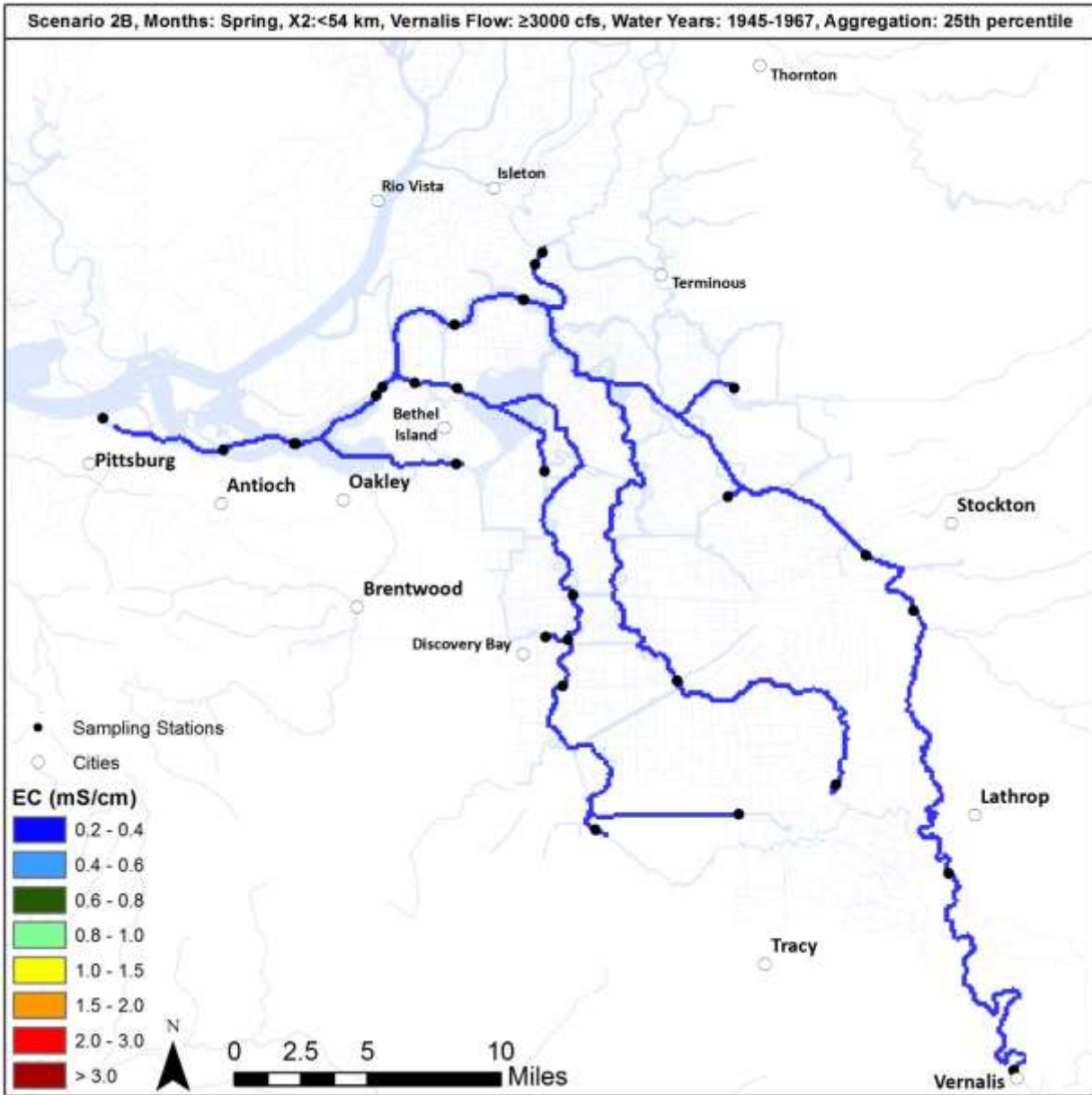


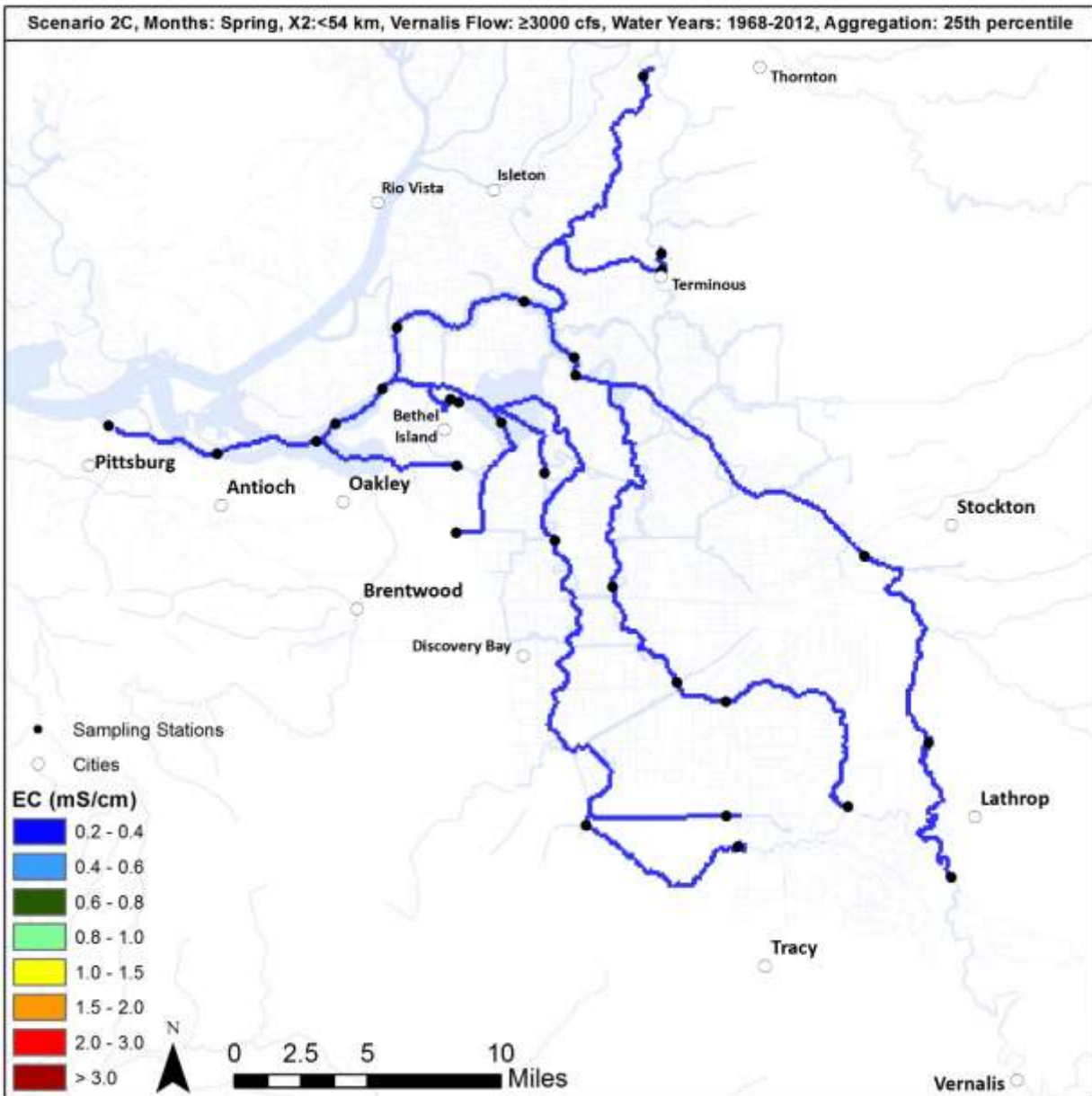


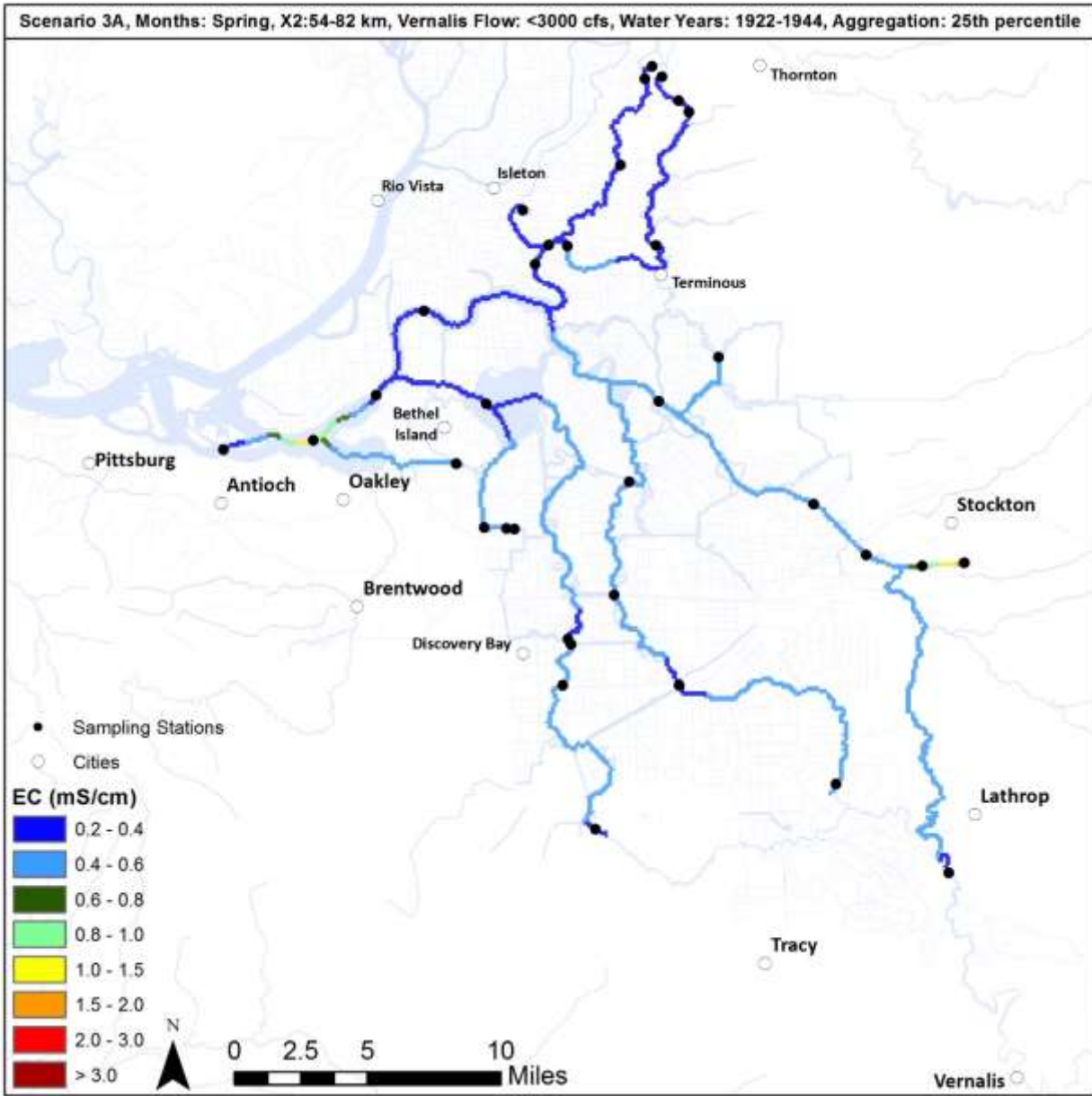


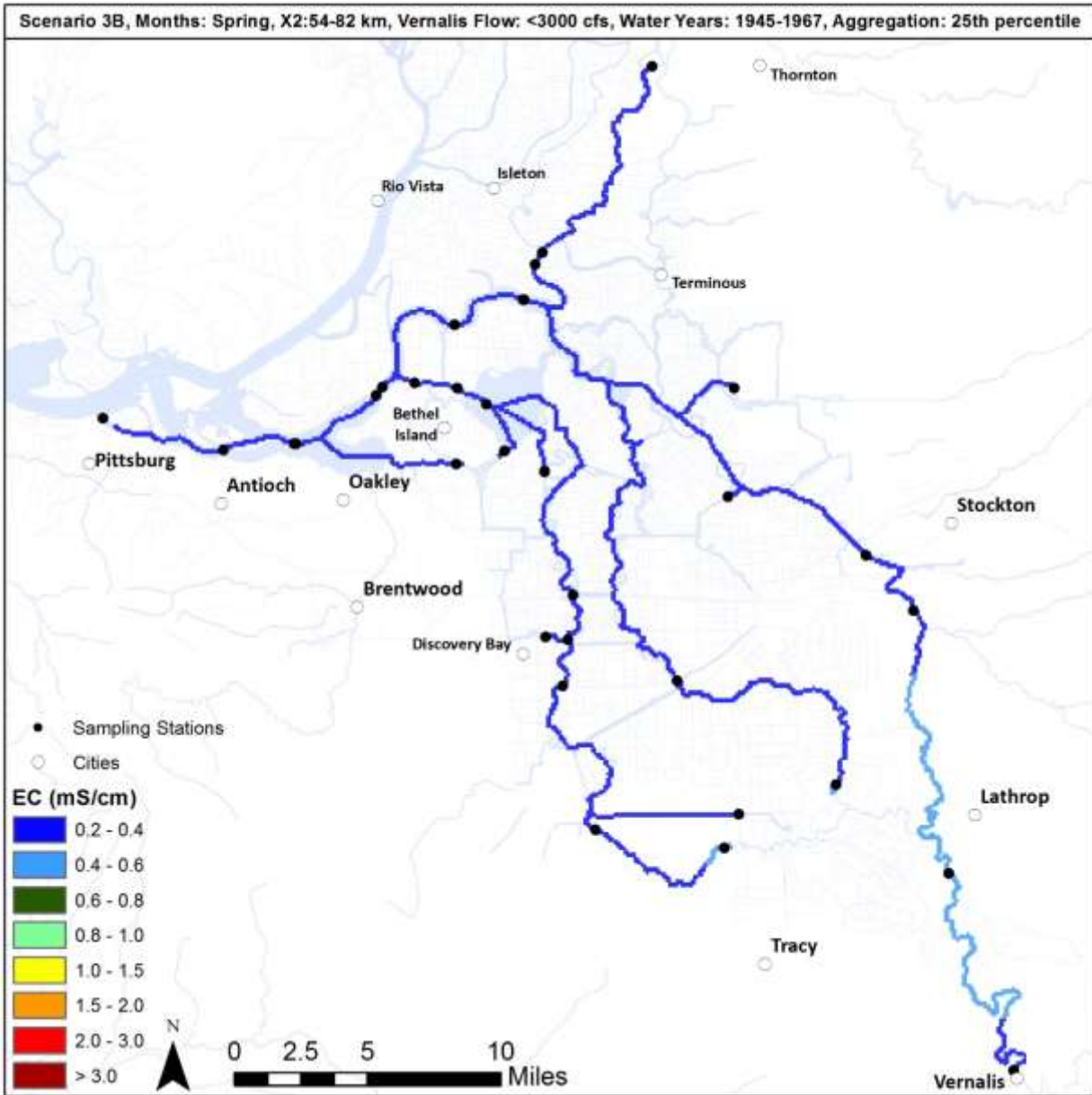
Appendix B. MAPS OF 25TH PERCENTILE SALINITY

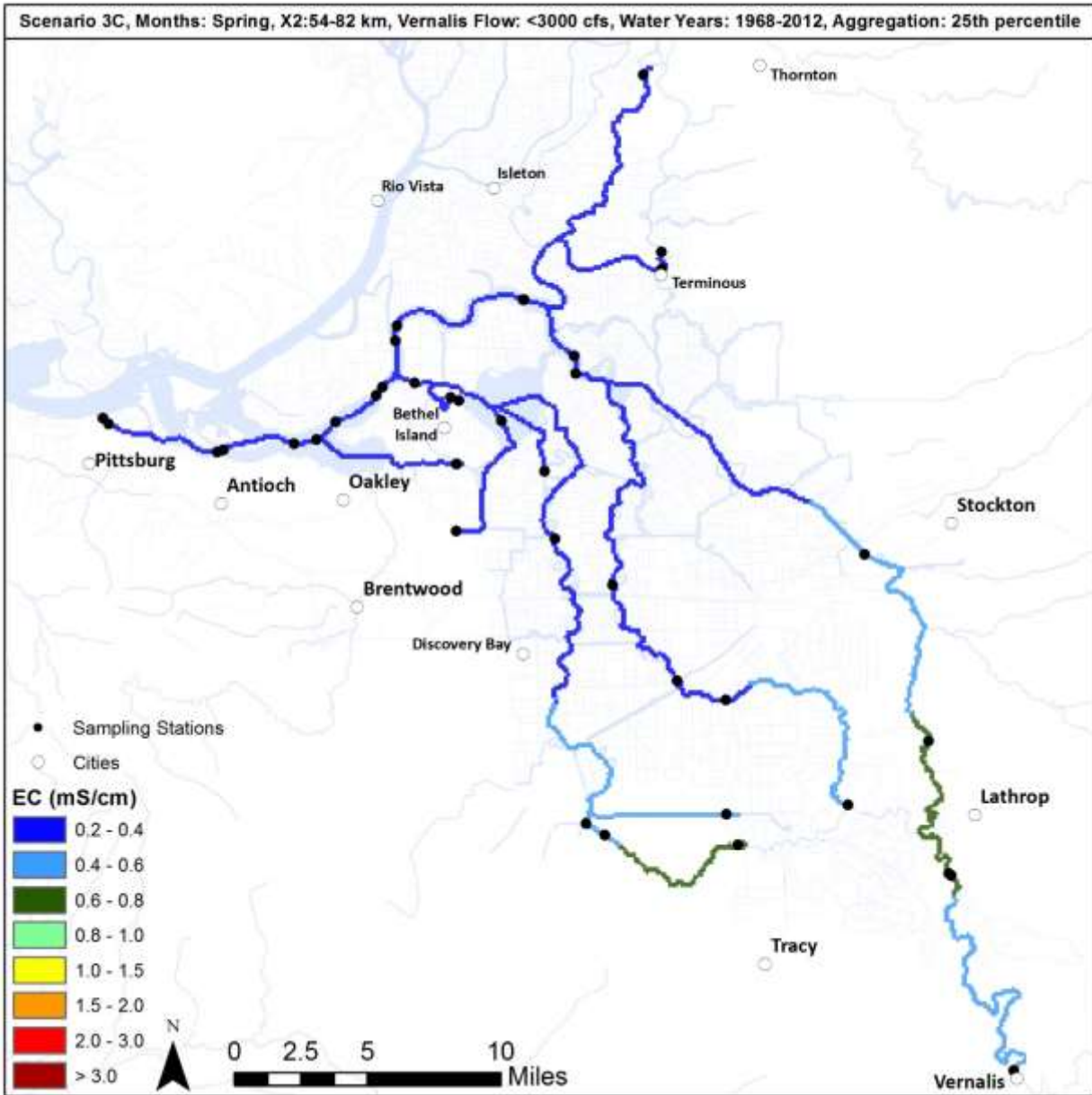


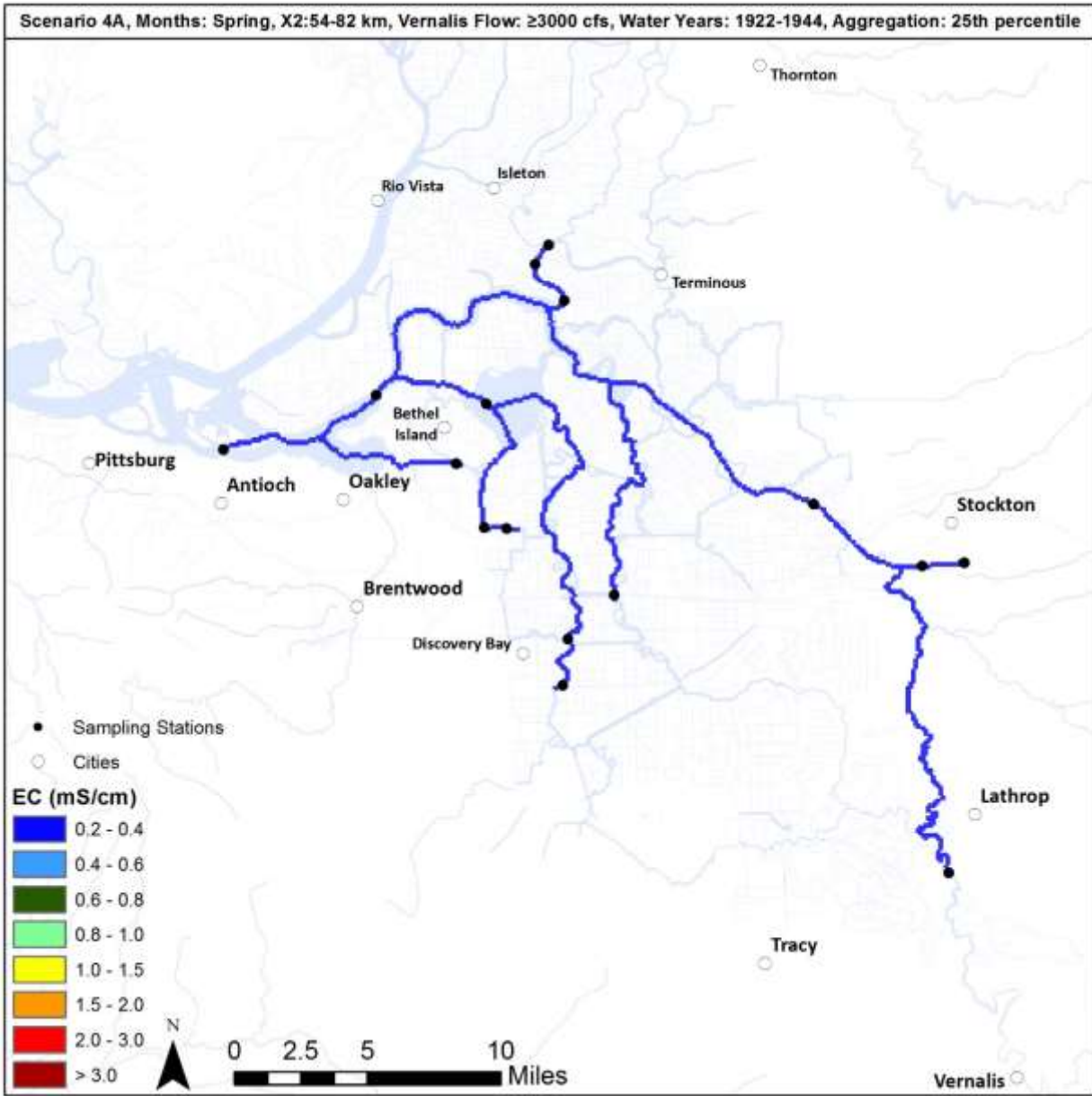


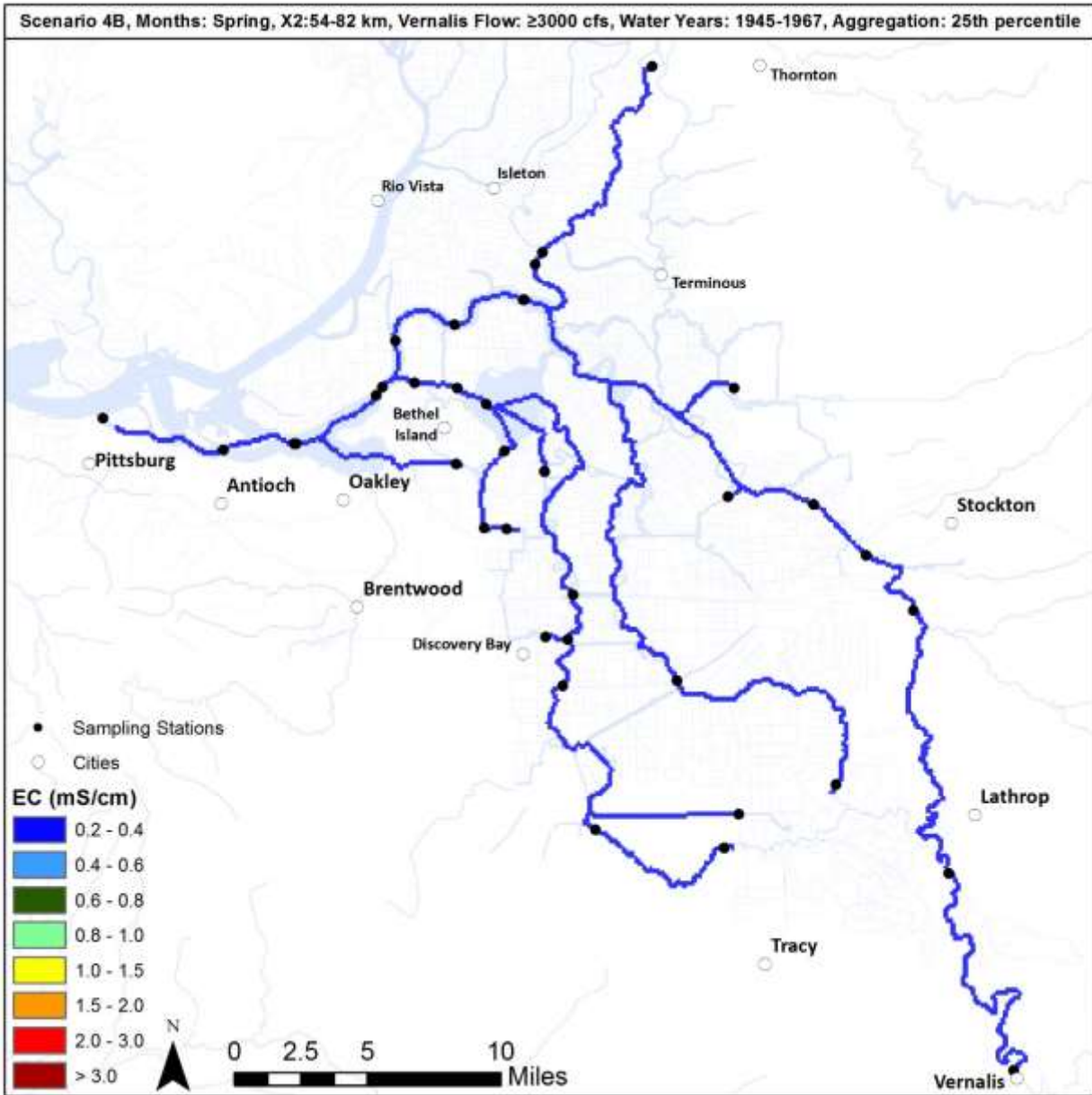


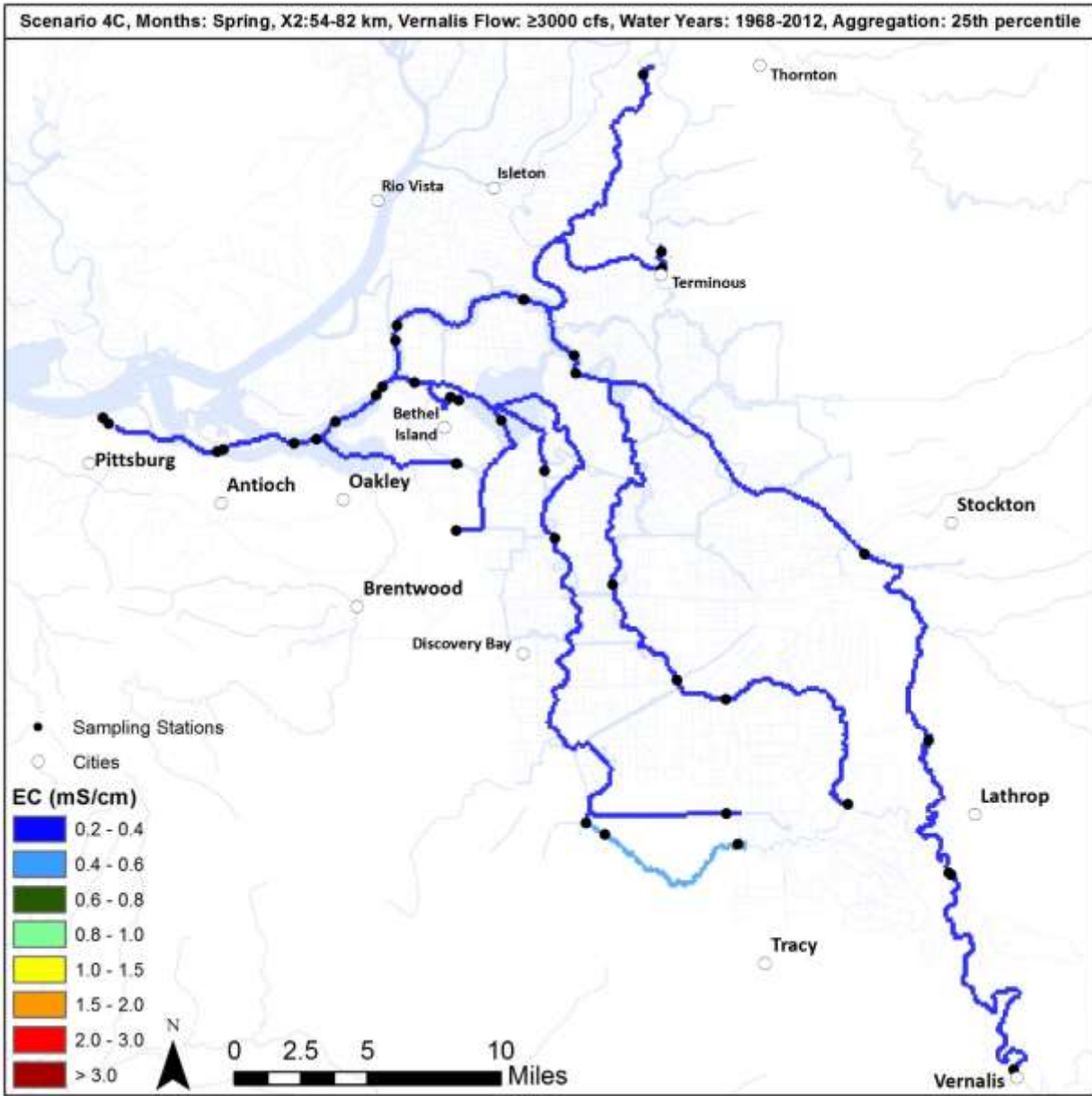


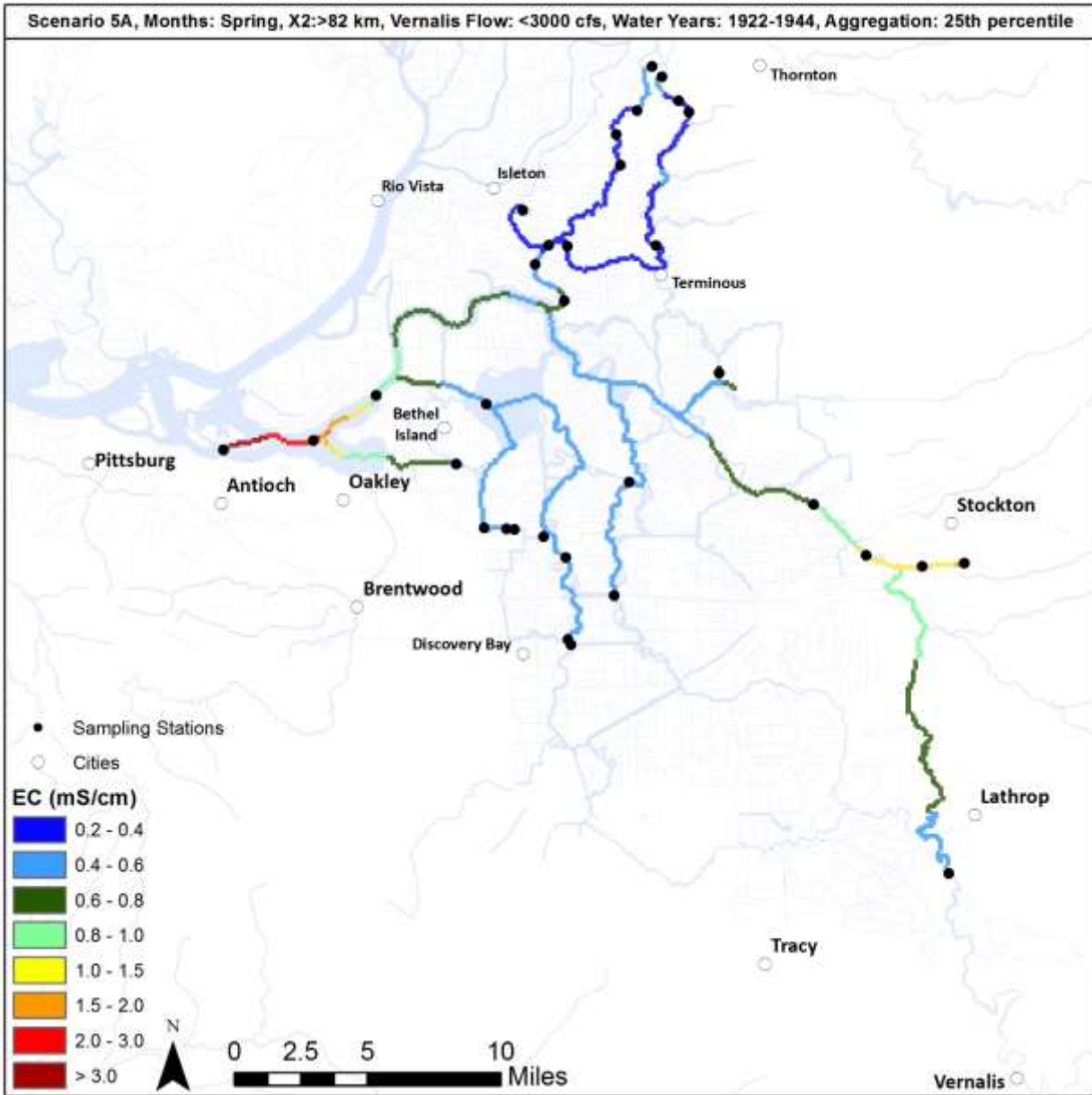


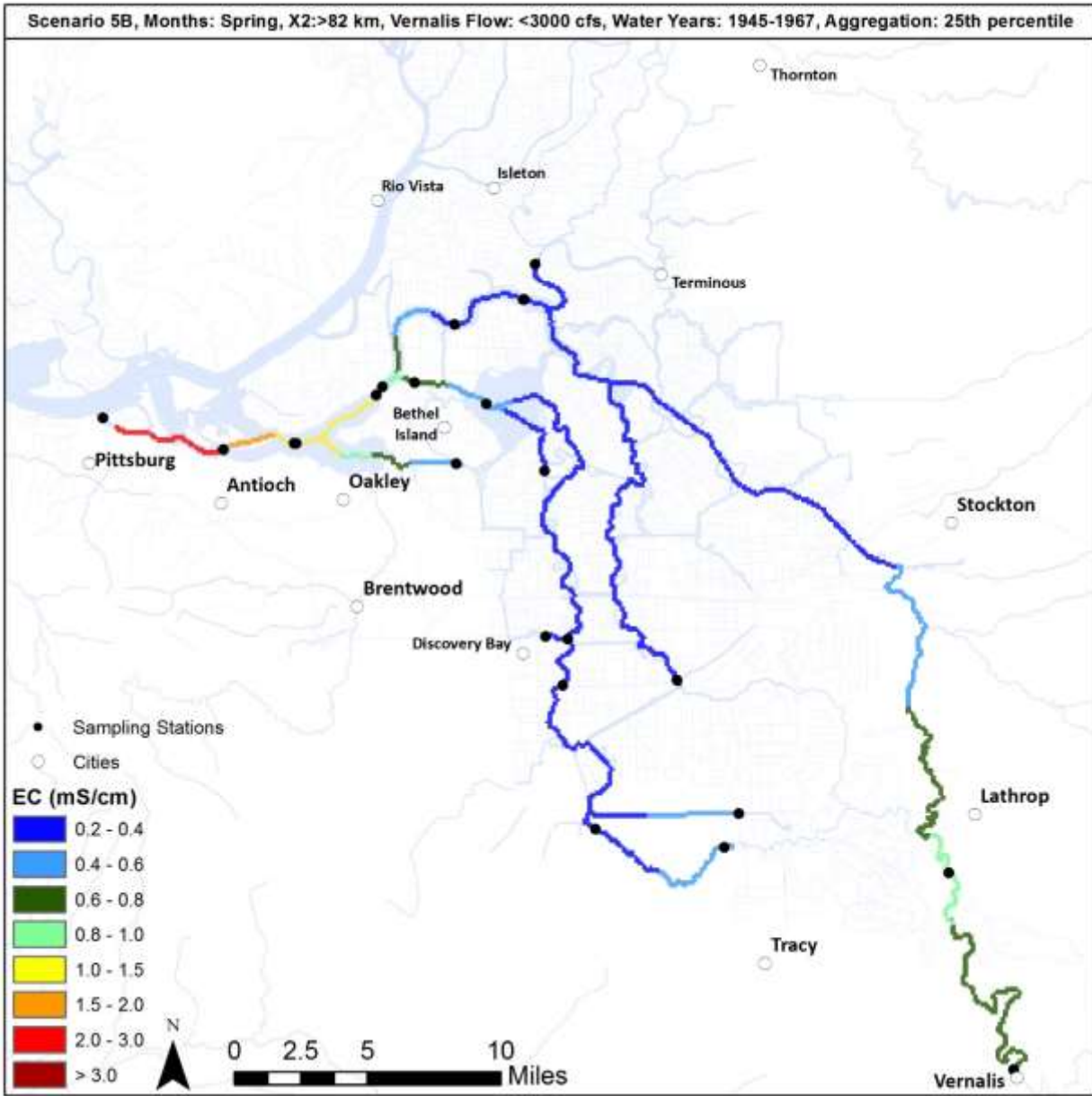


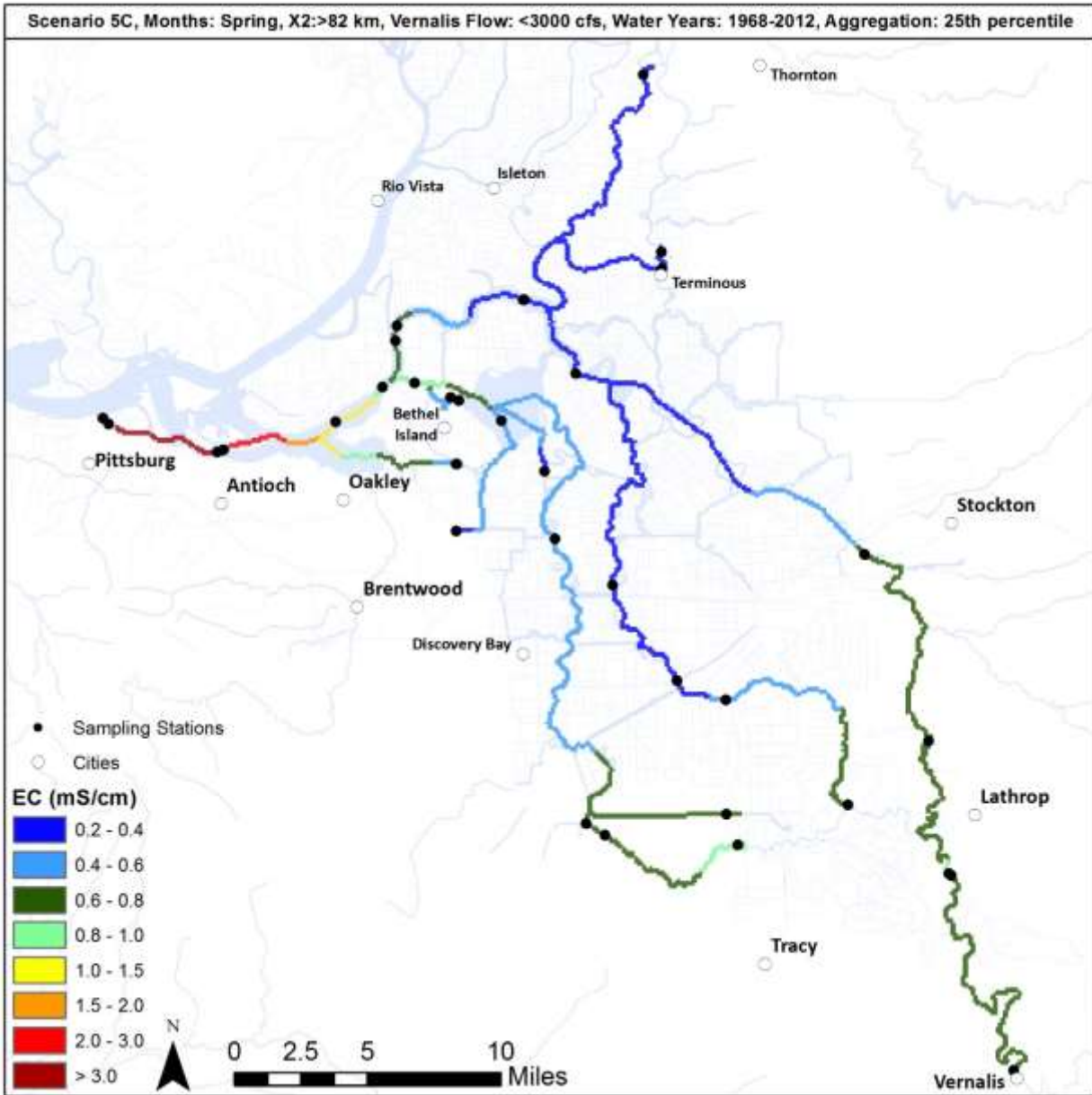


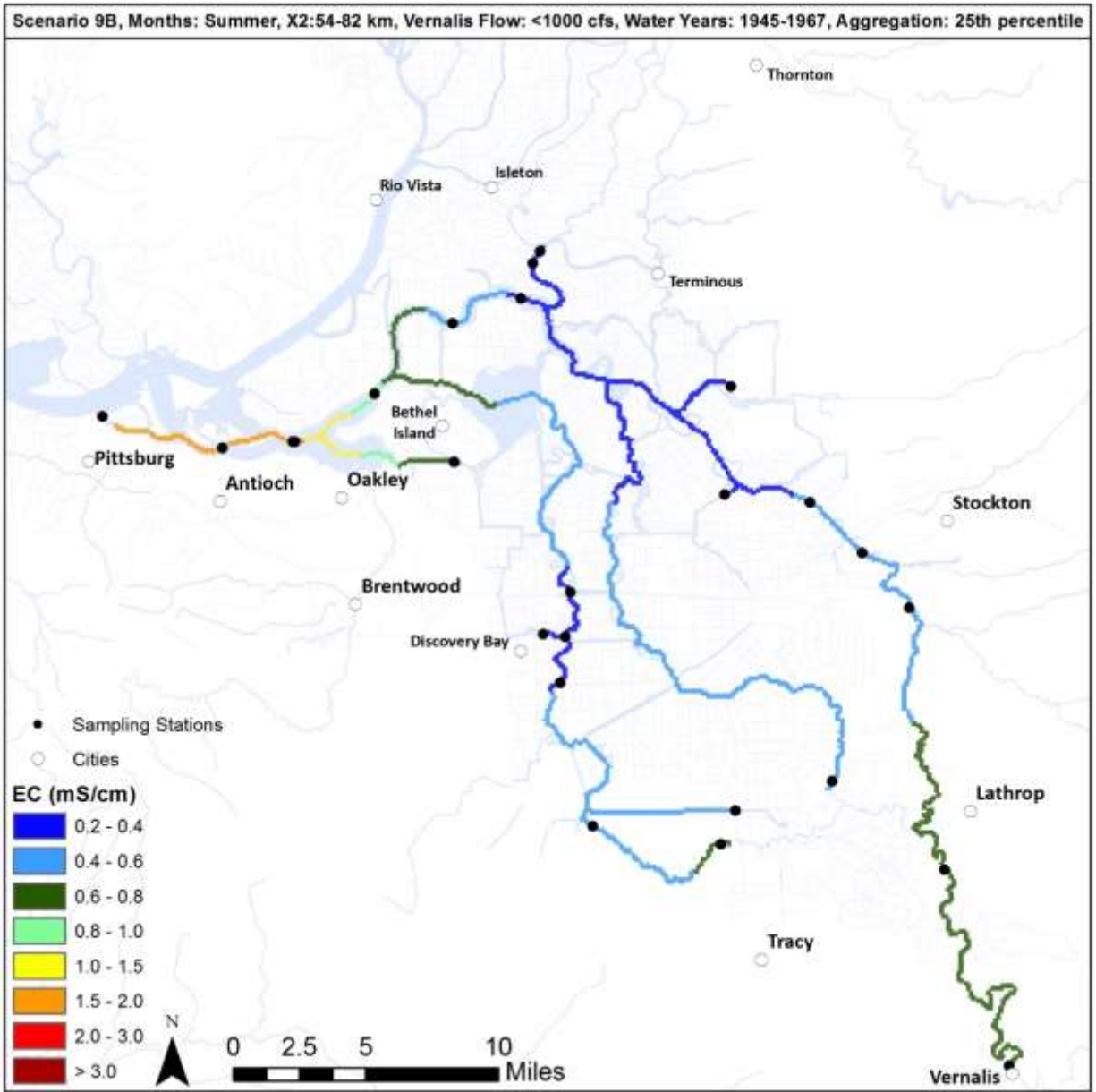


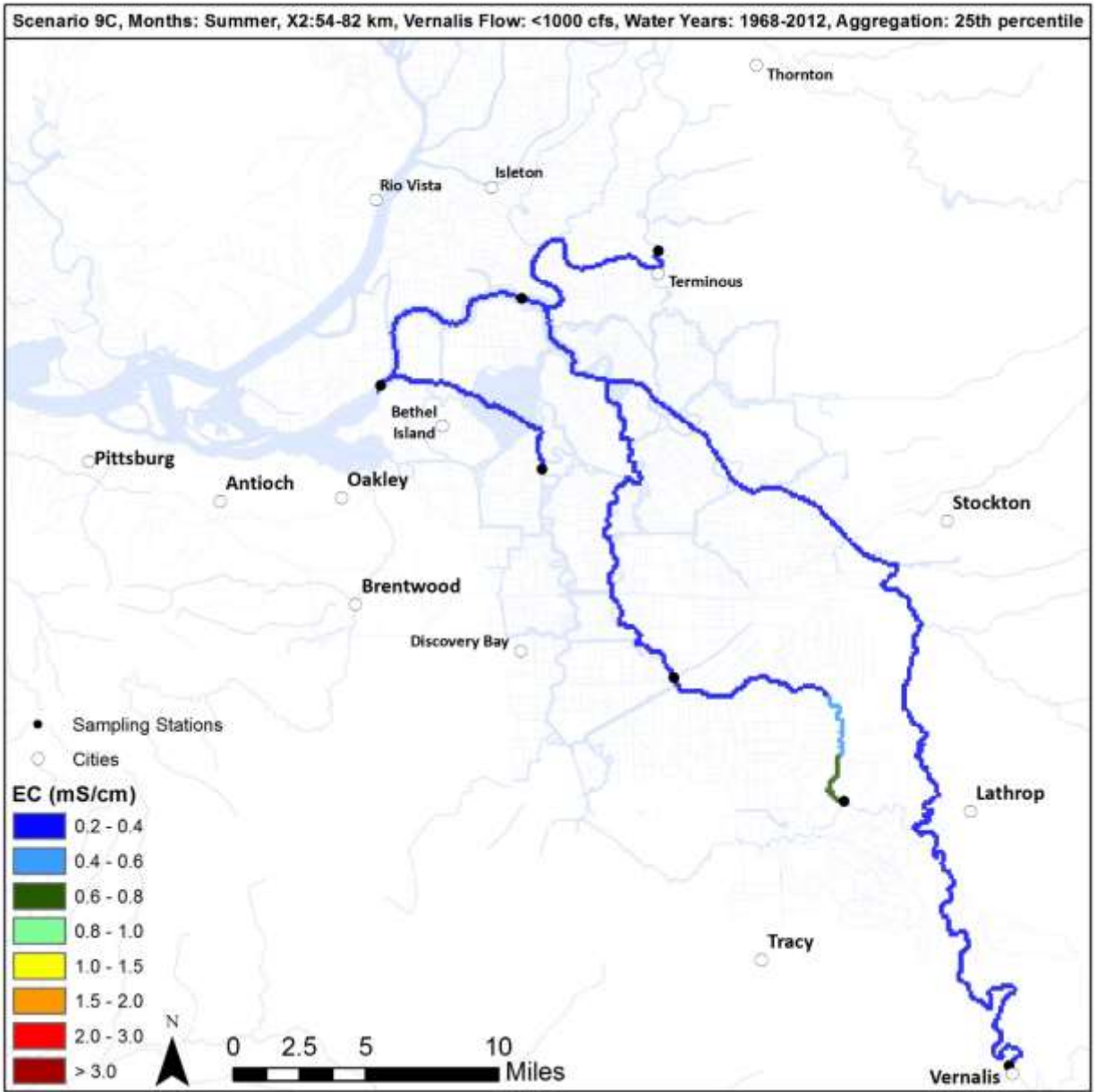


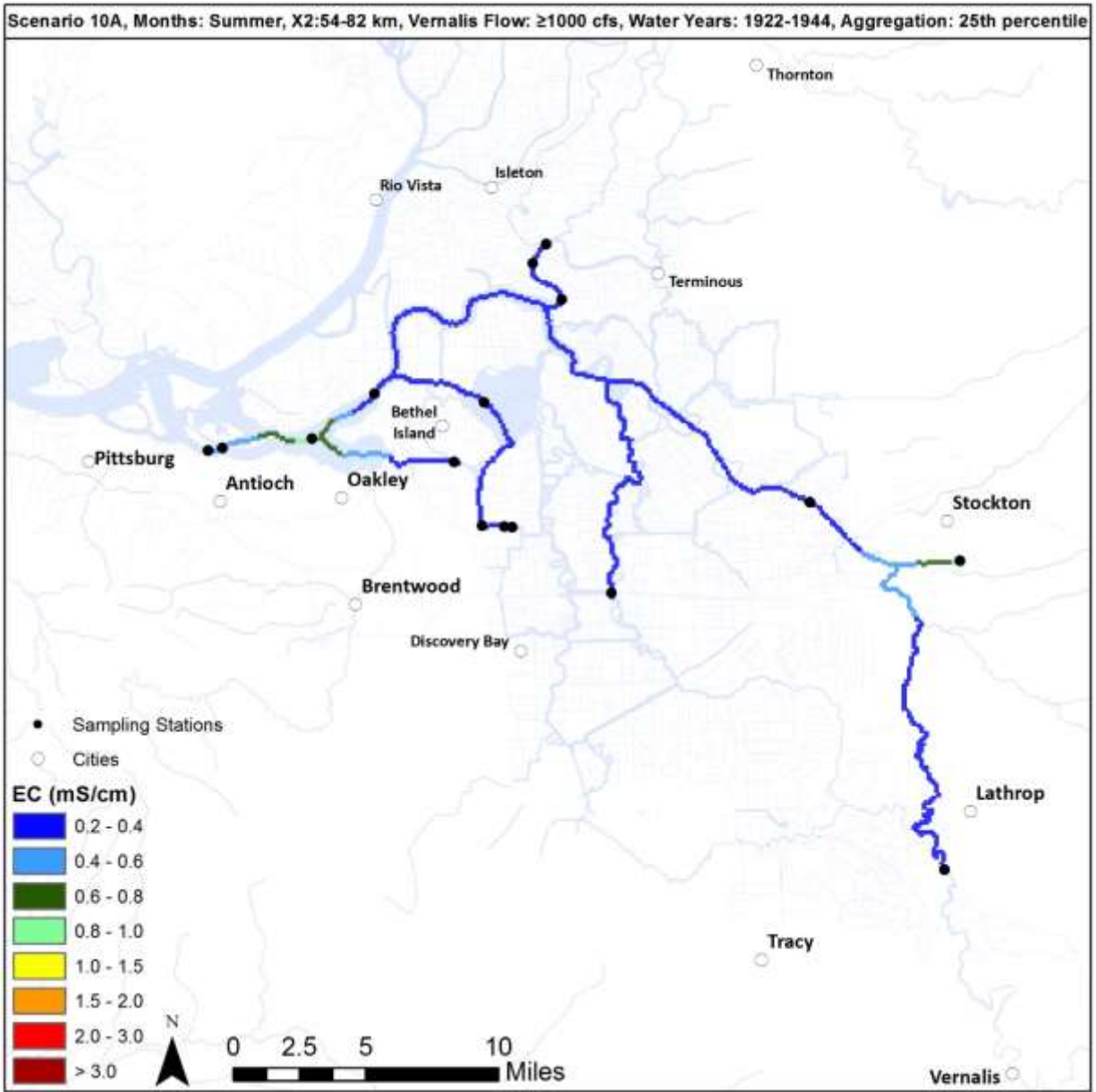


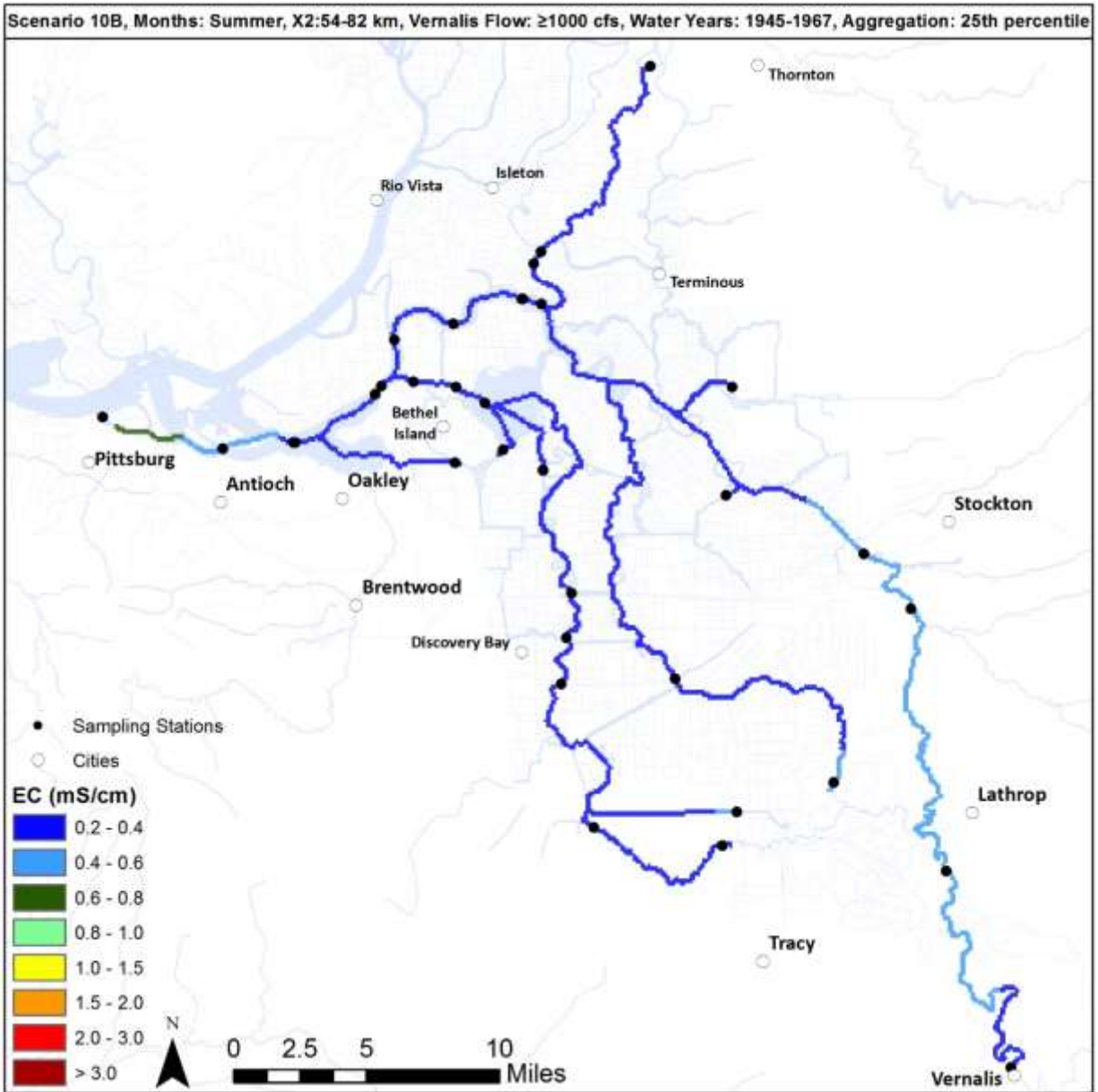


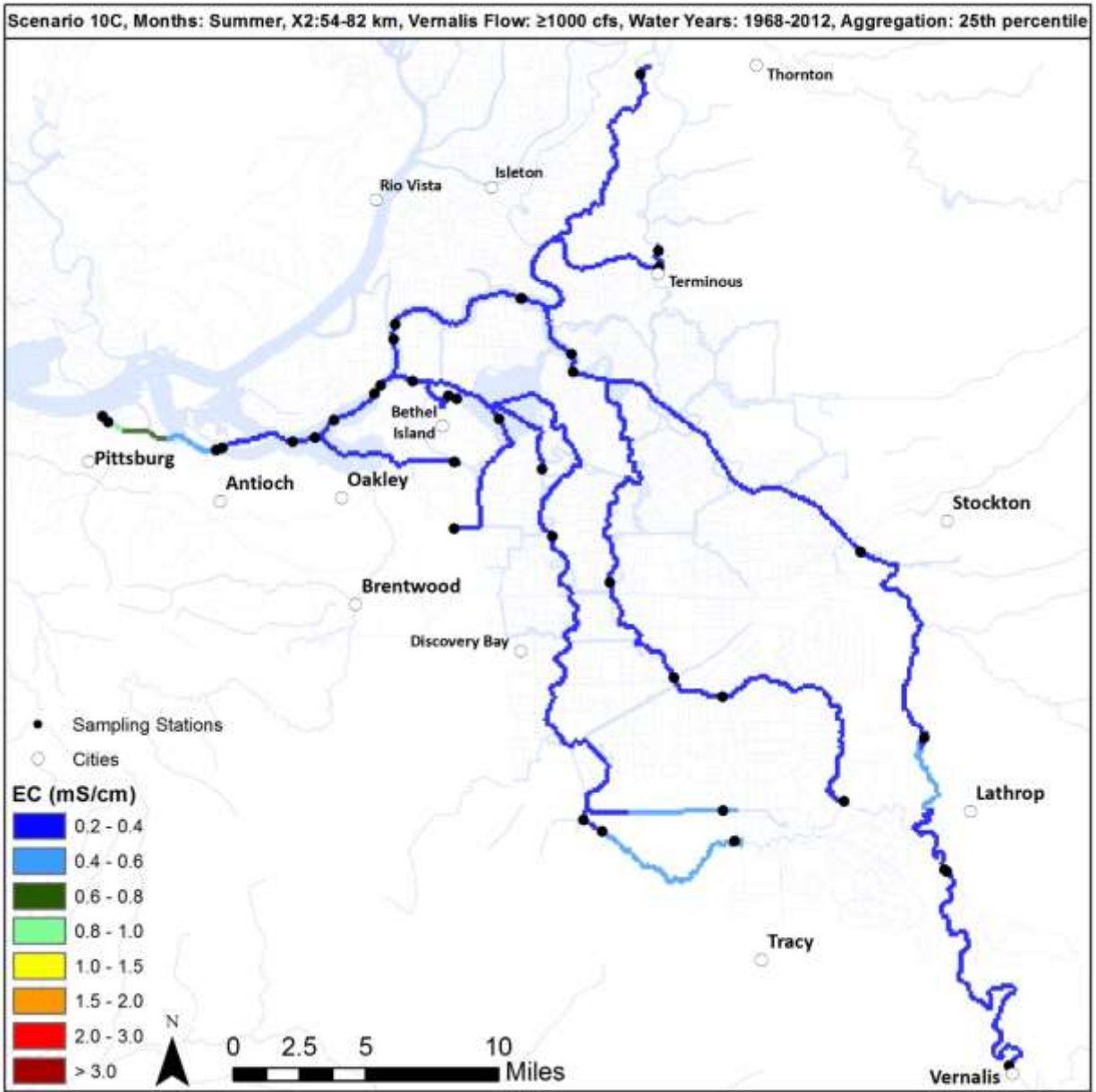


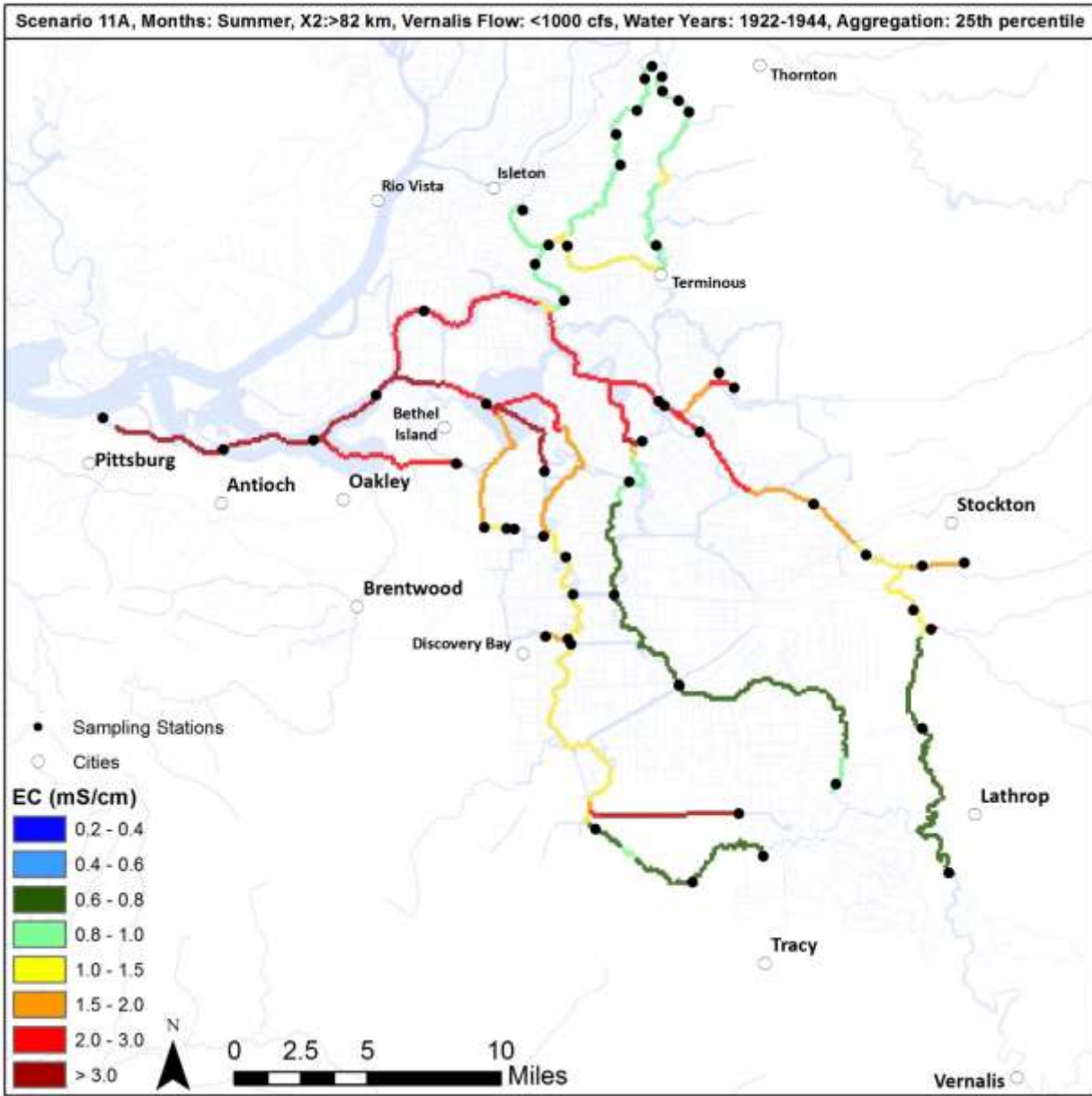


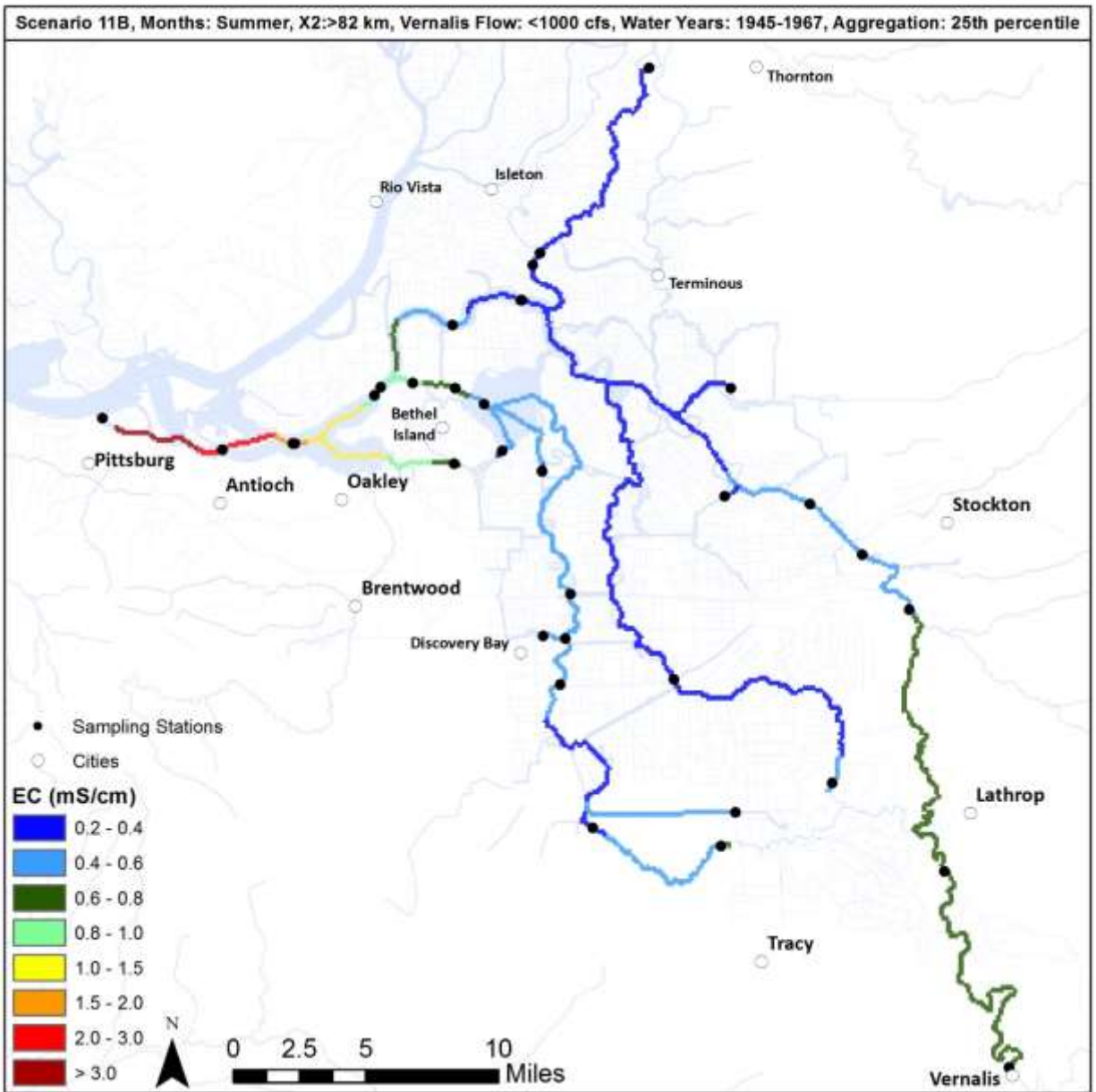


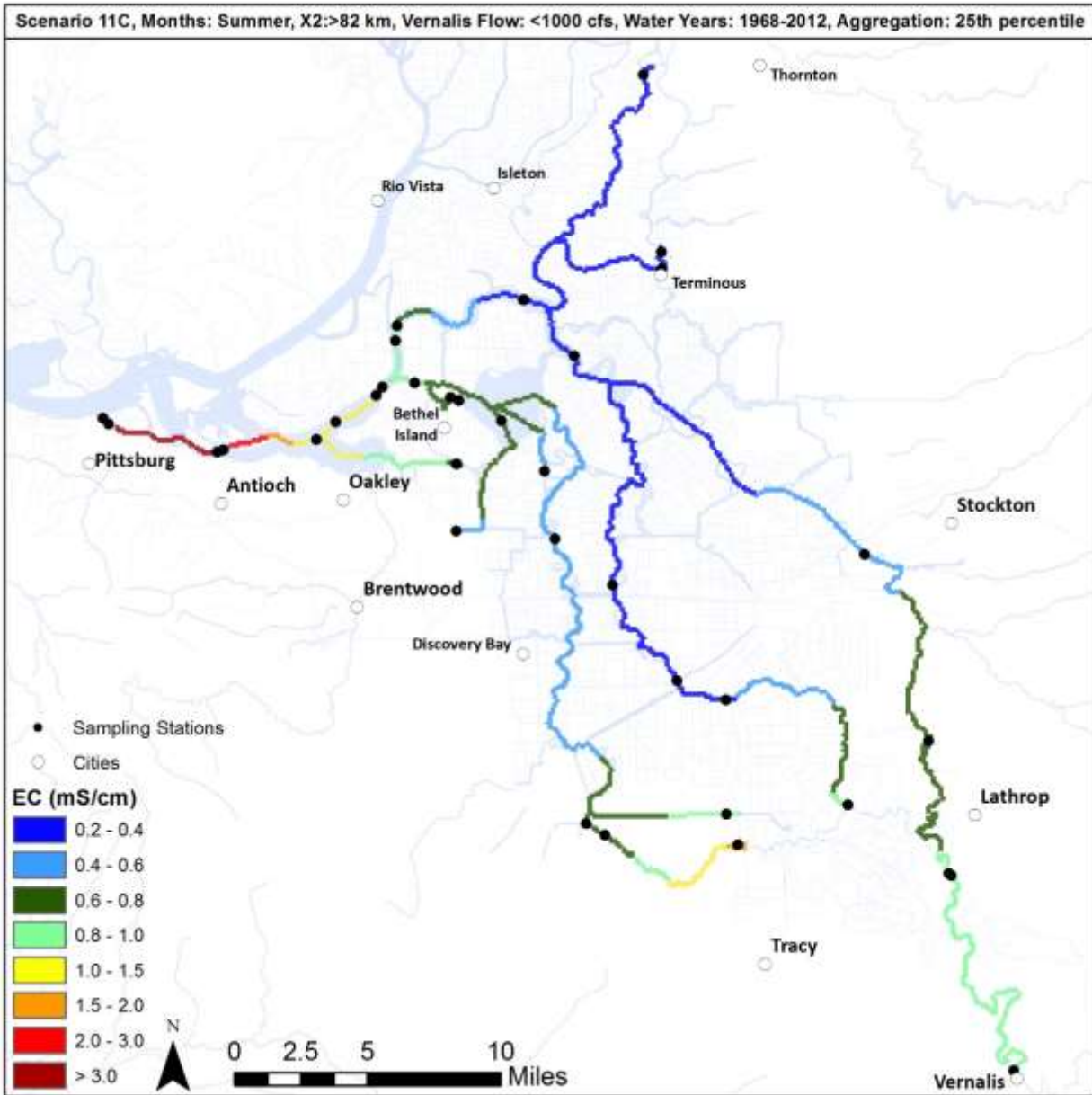


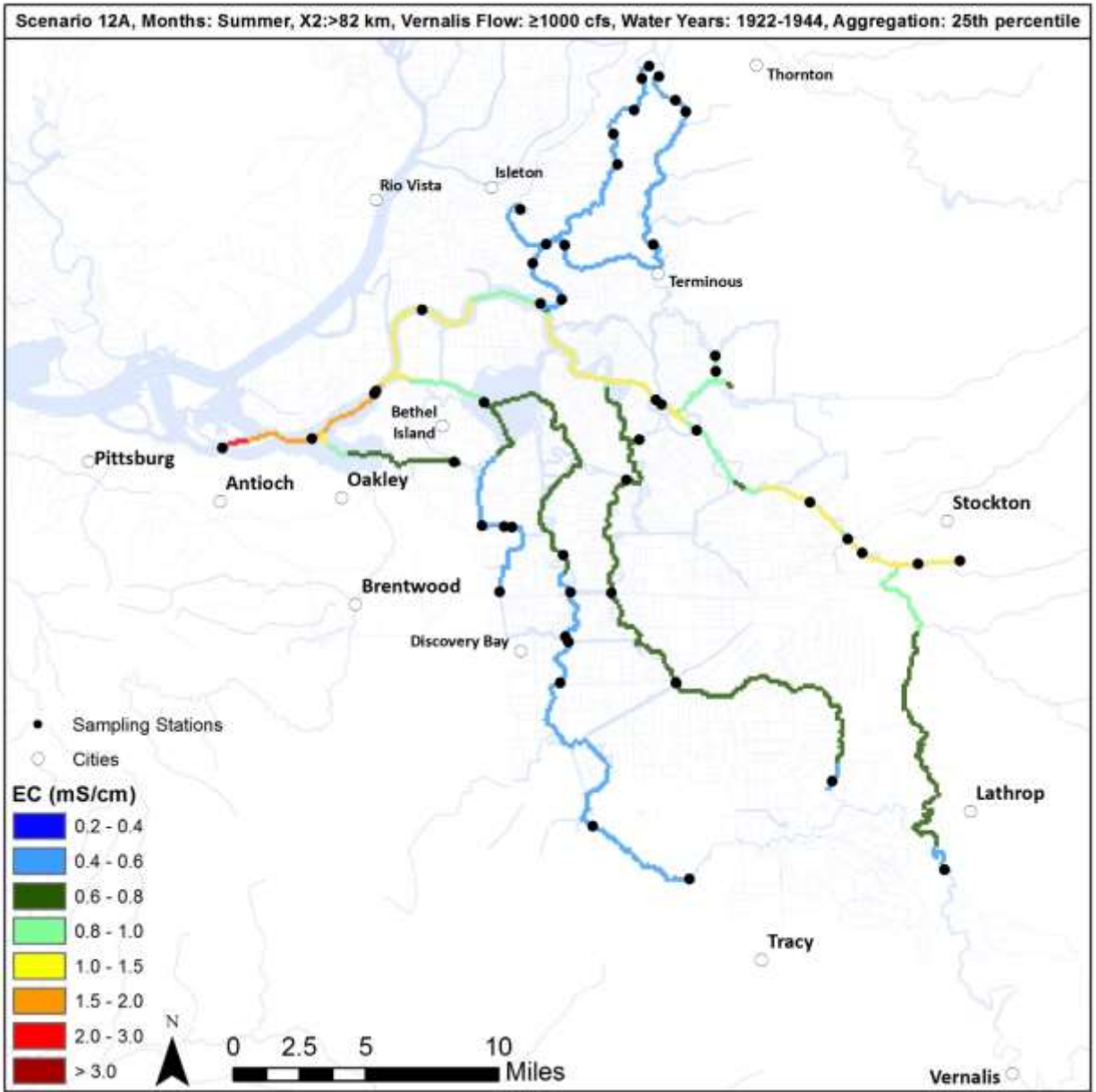


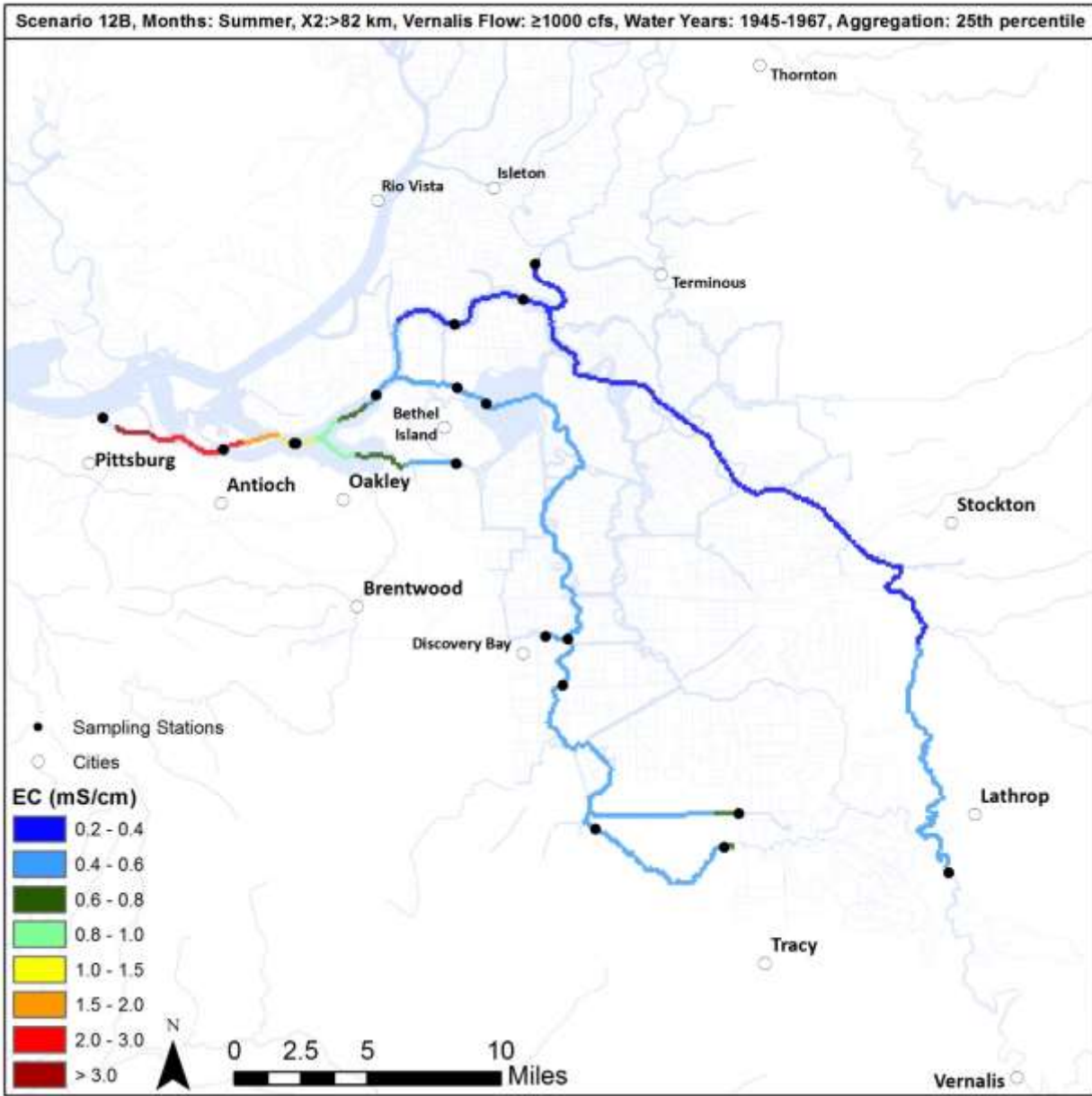


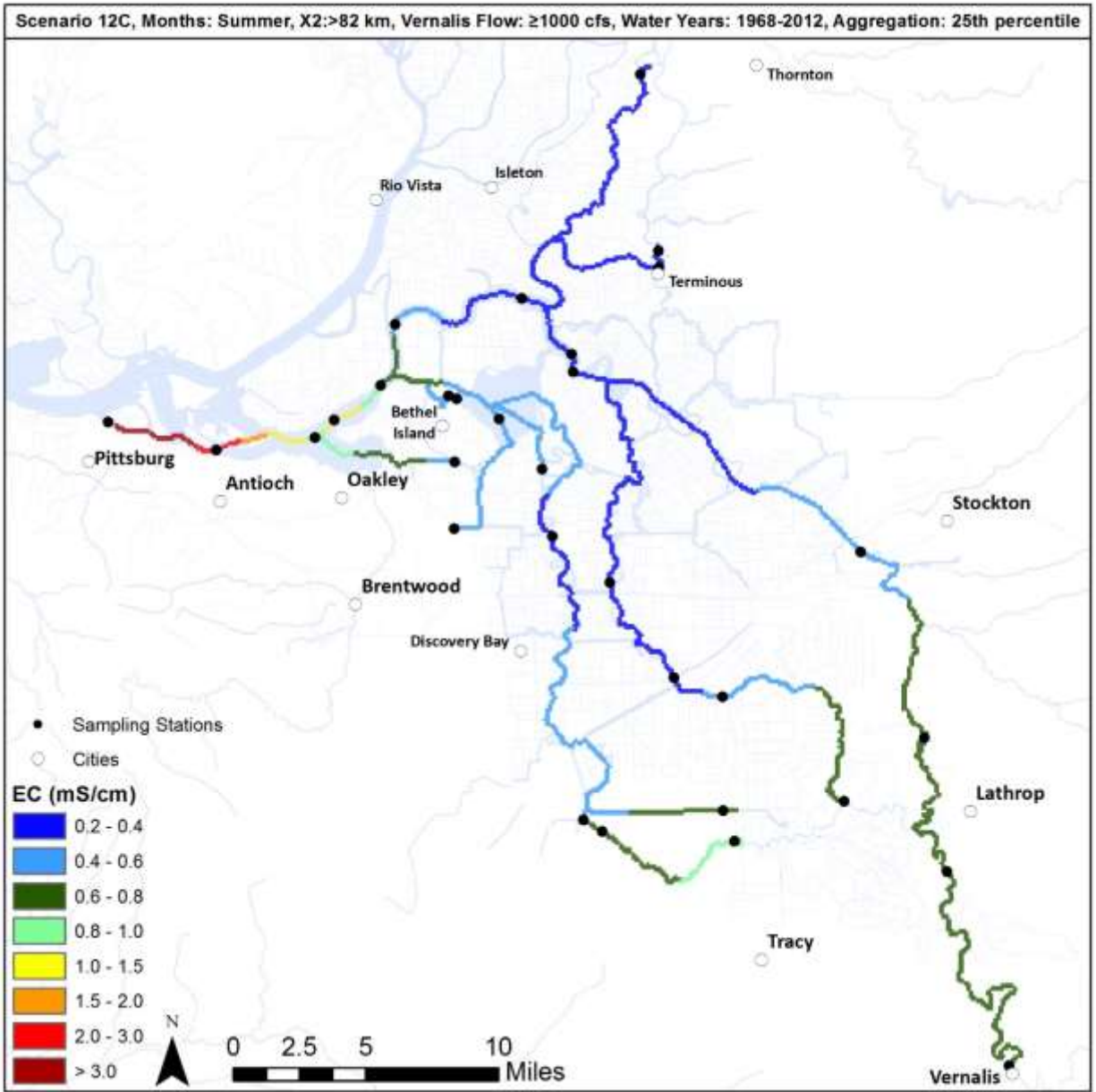




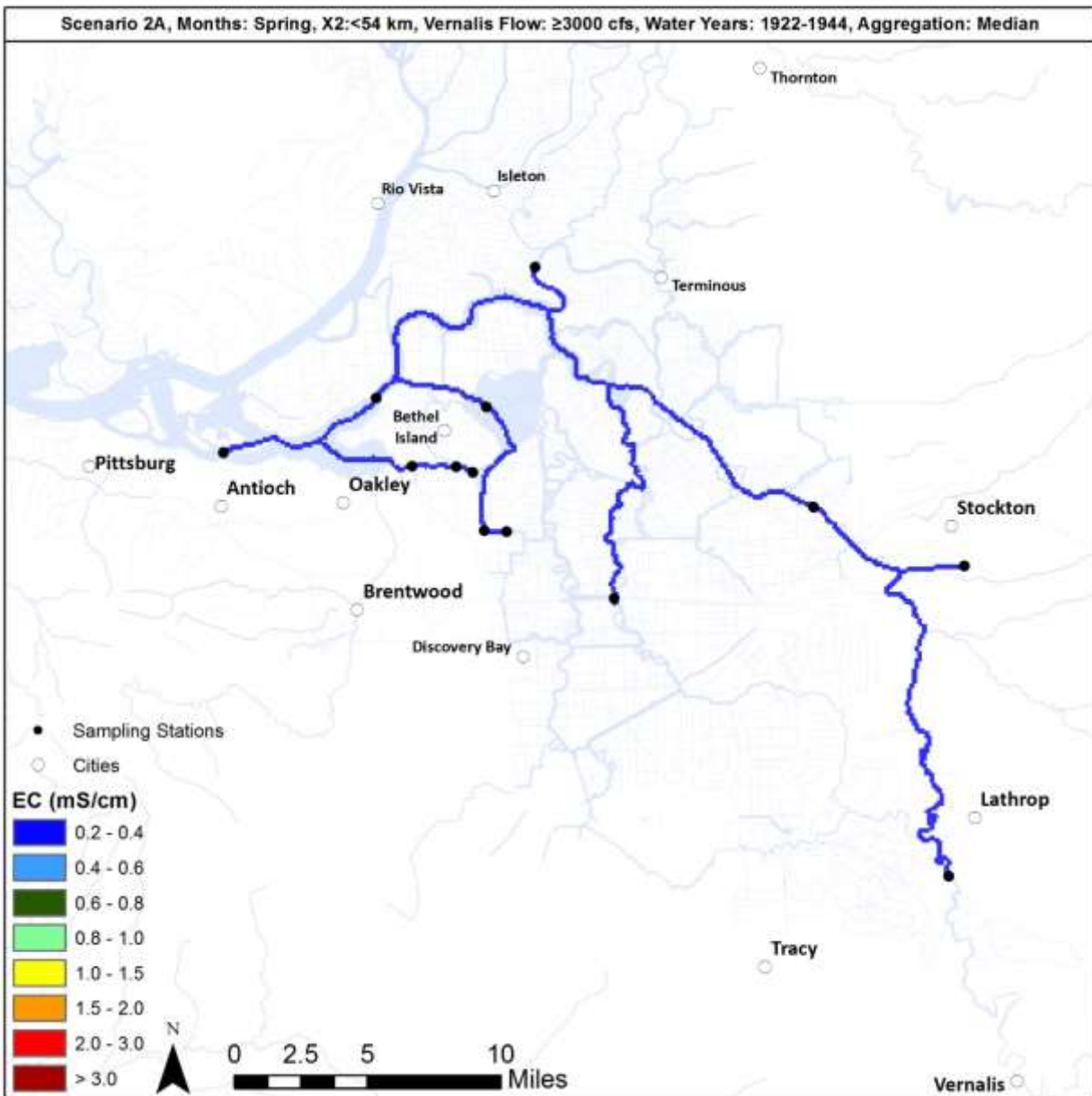


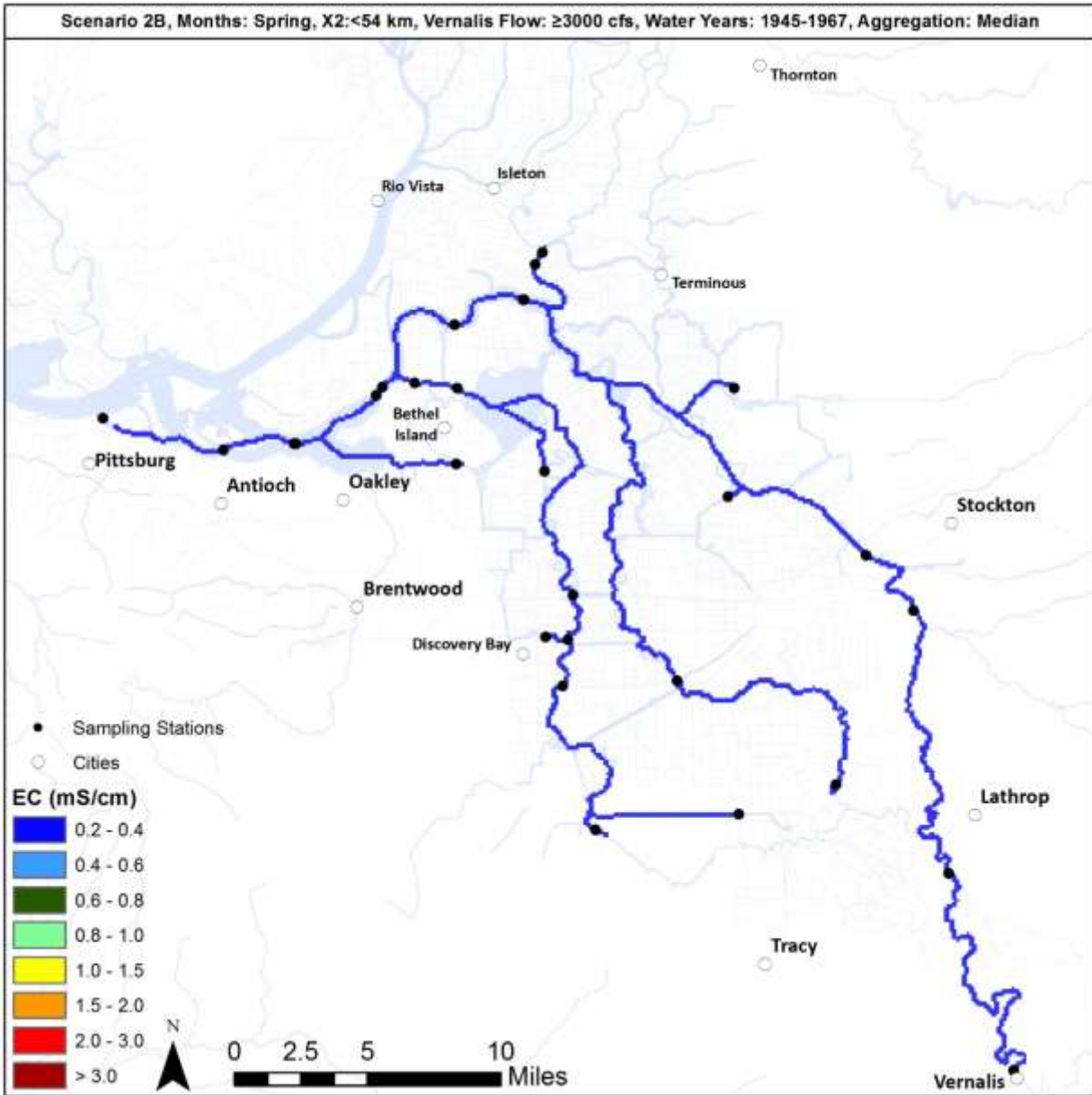


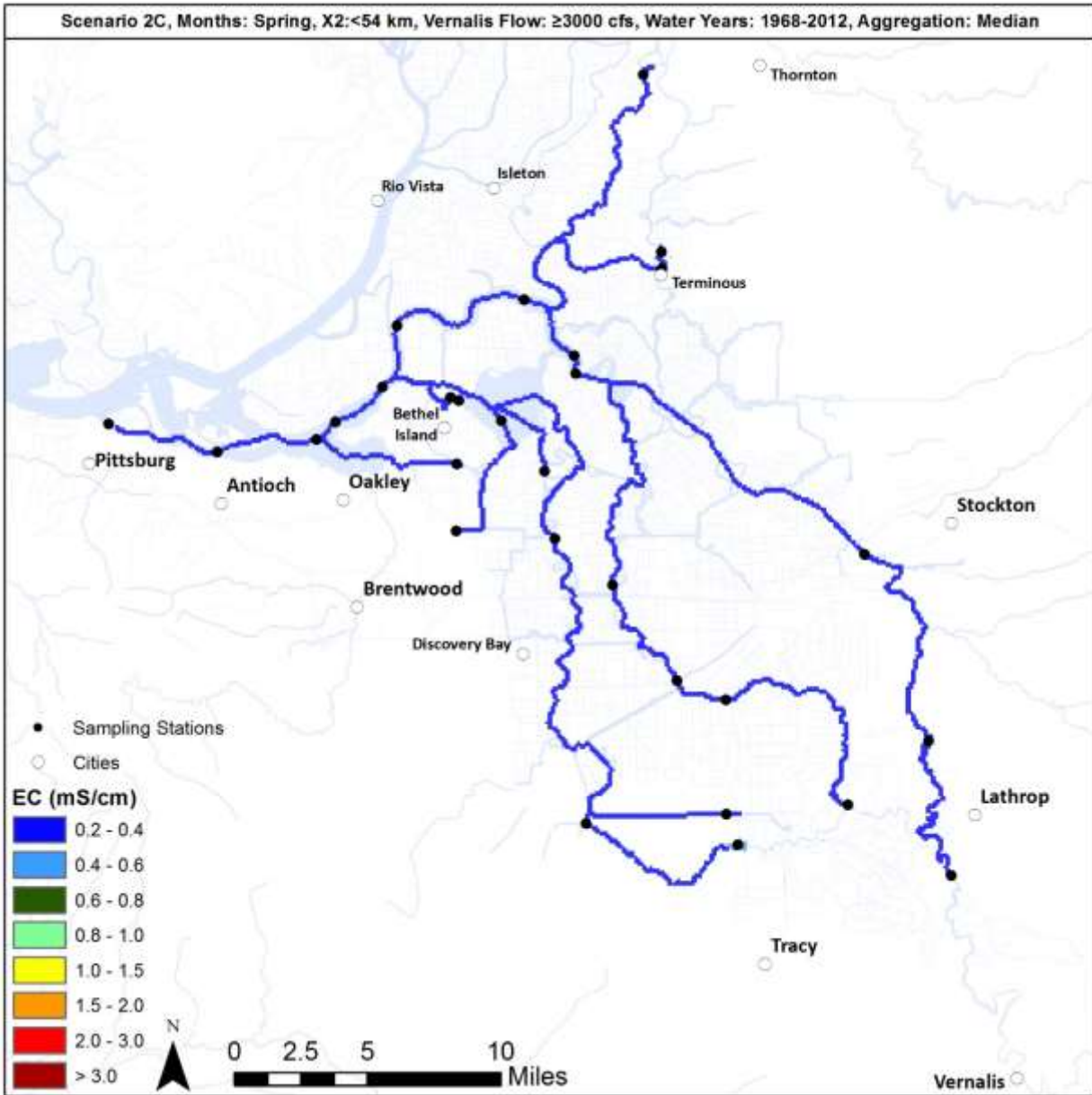


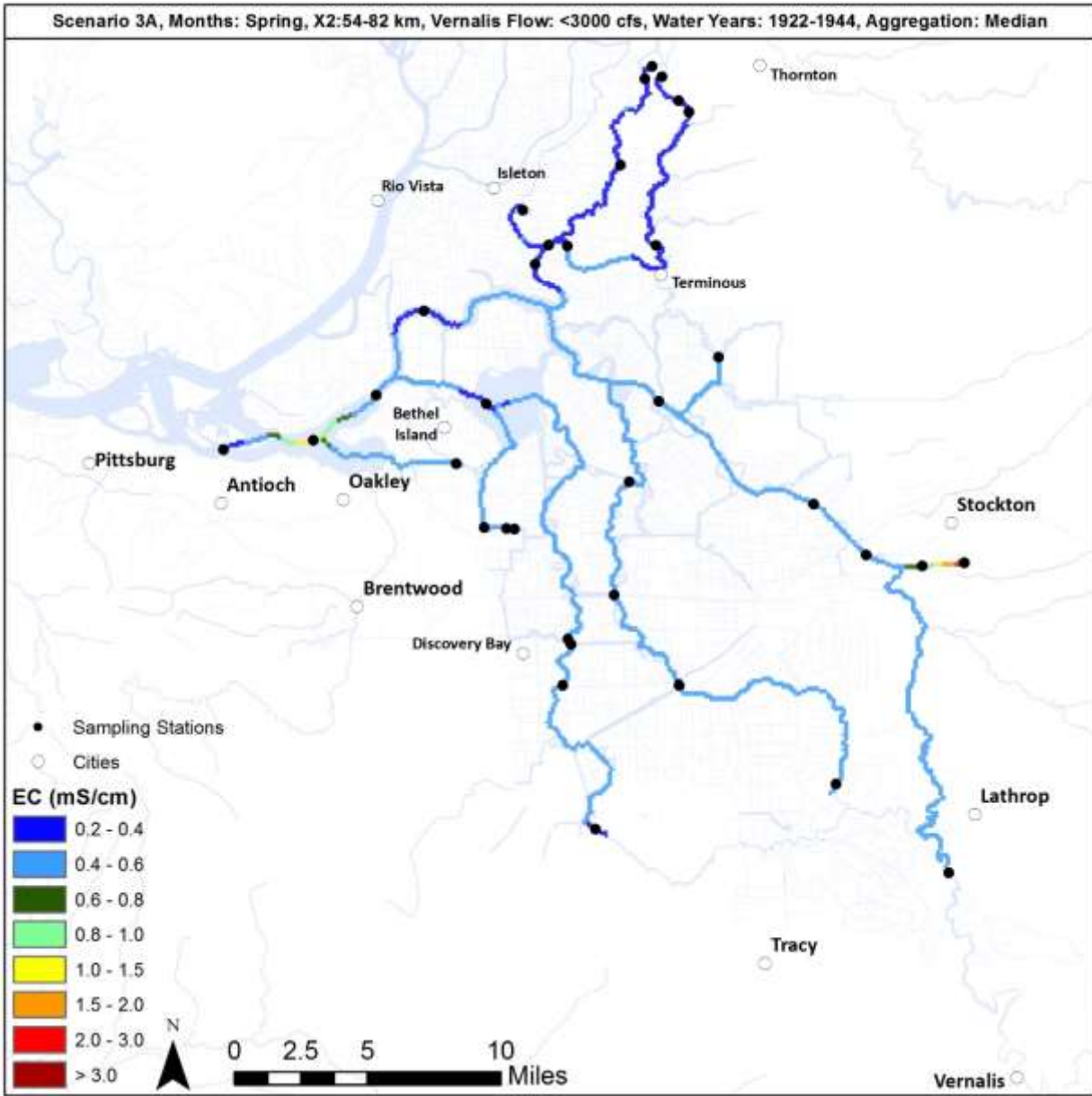


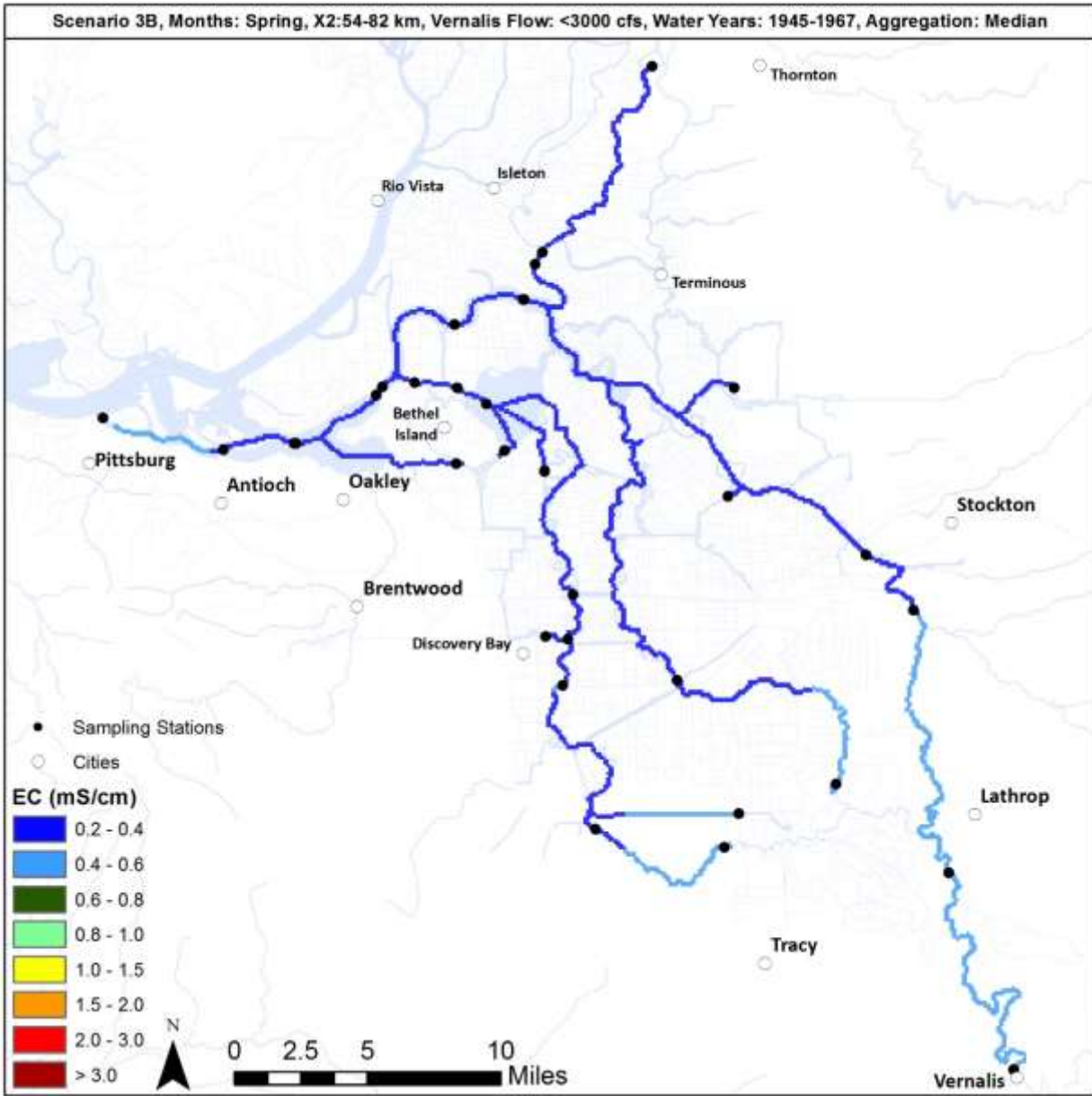
Appendix C. MAPS OF 50TH PERCENTILE (MEDIAN) SALINITY

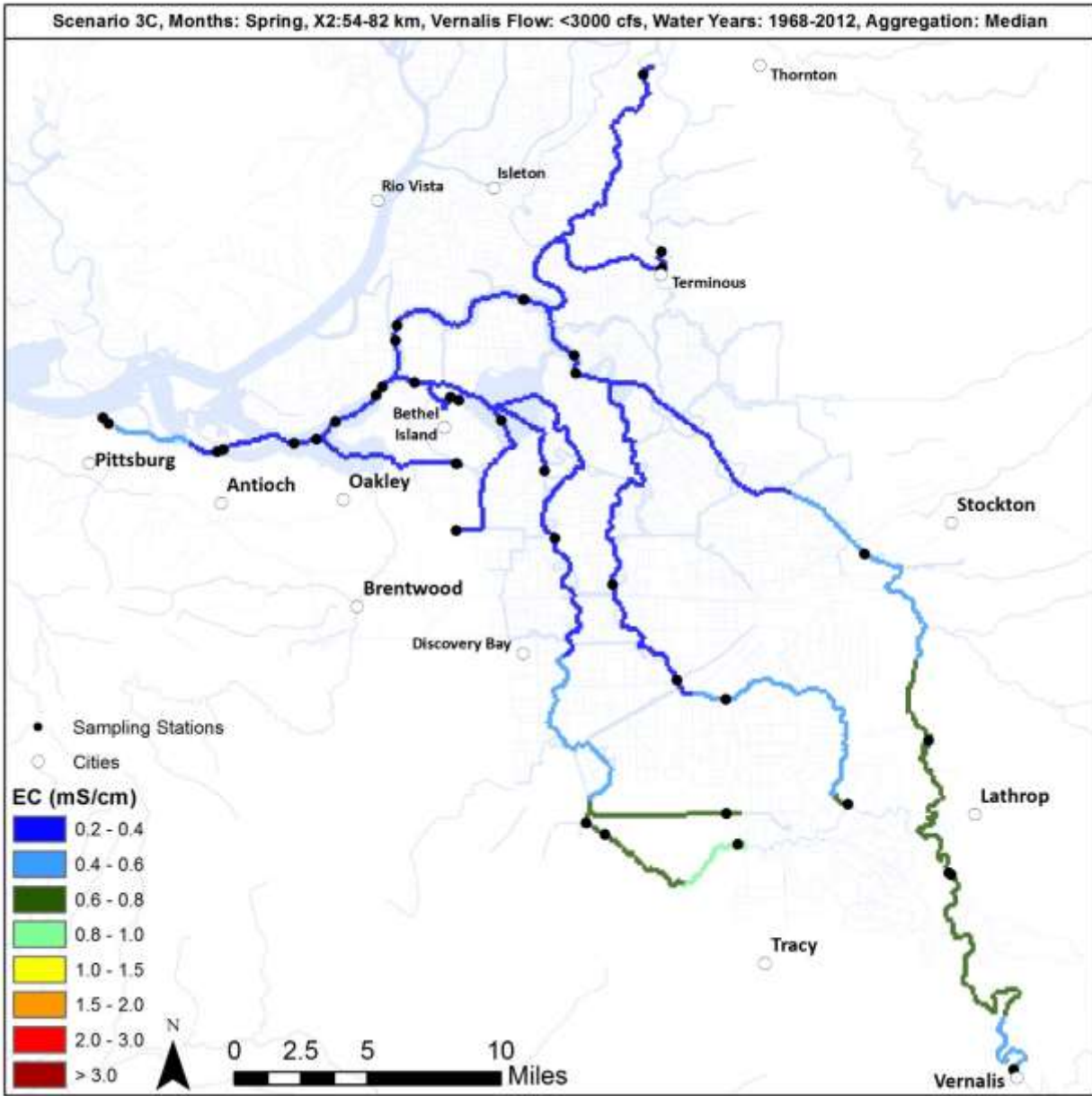


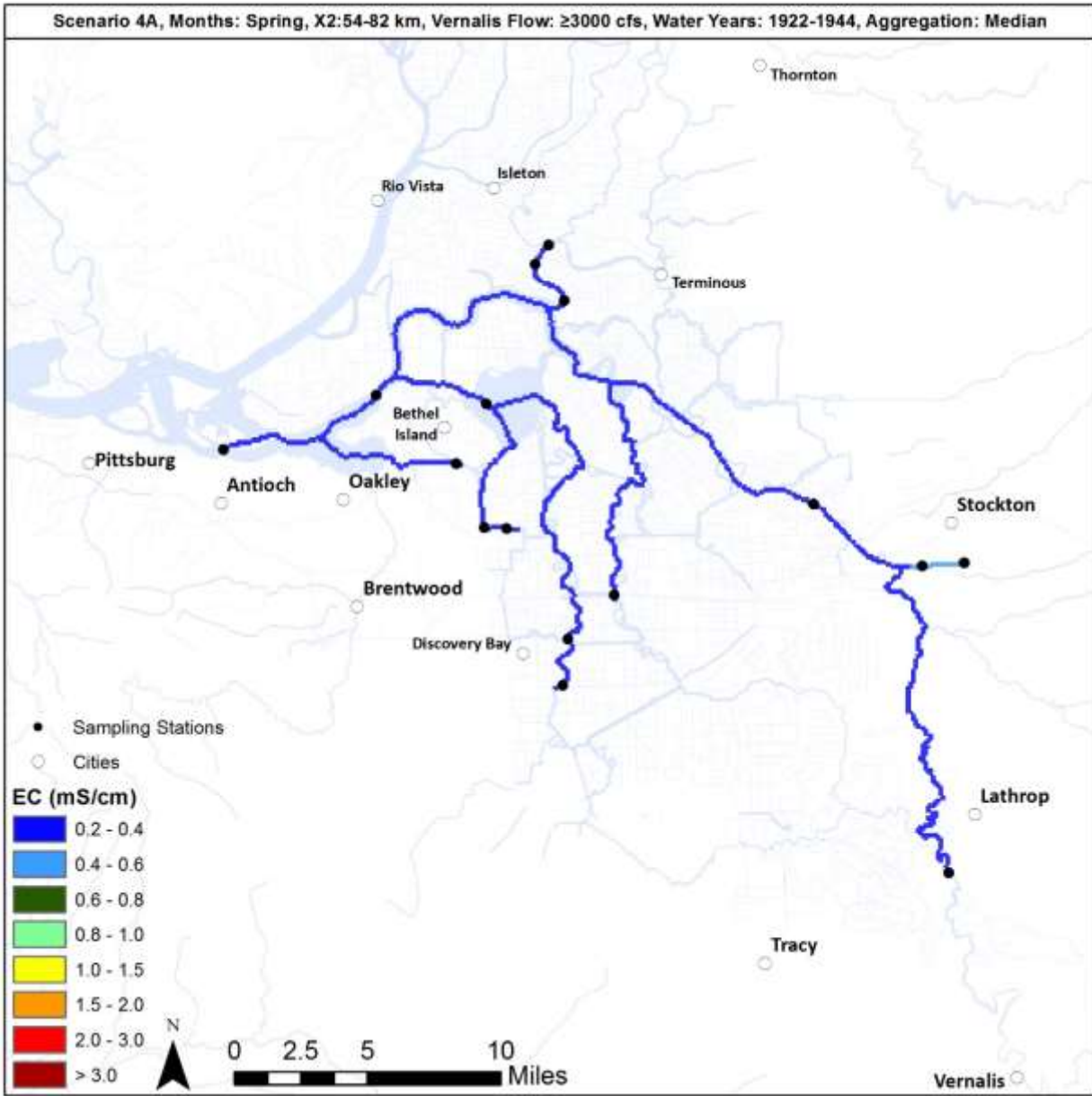


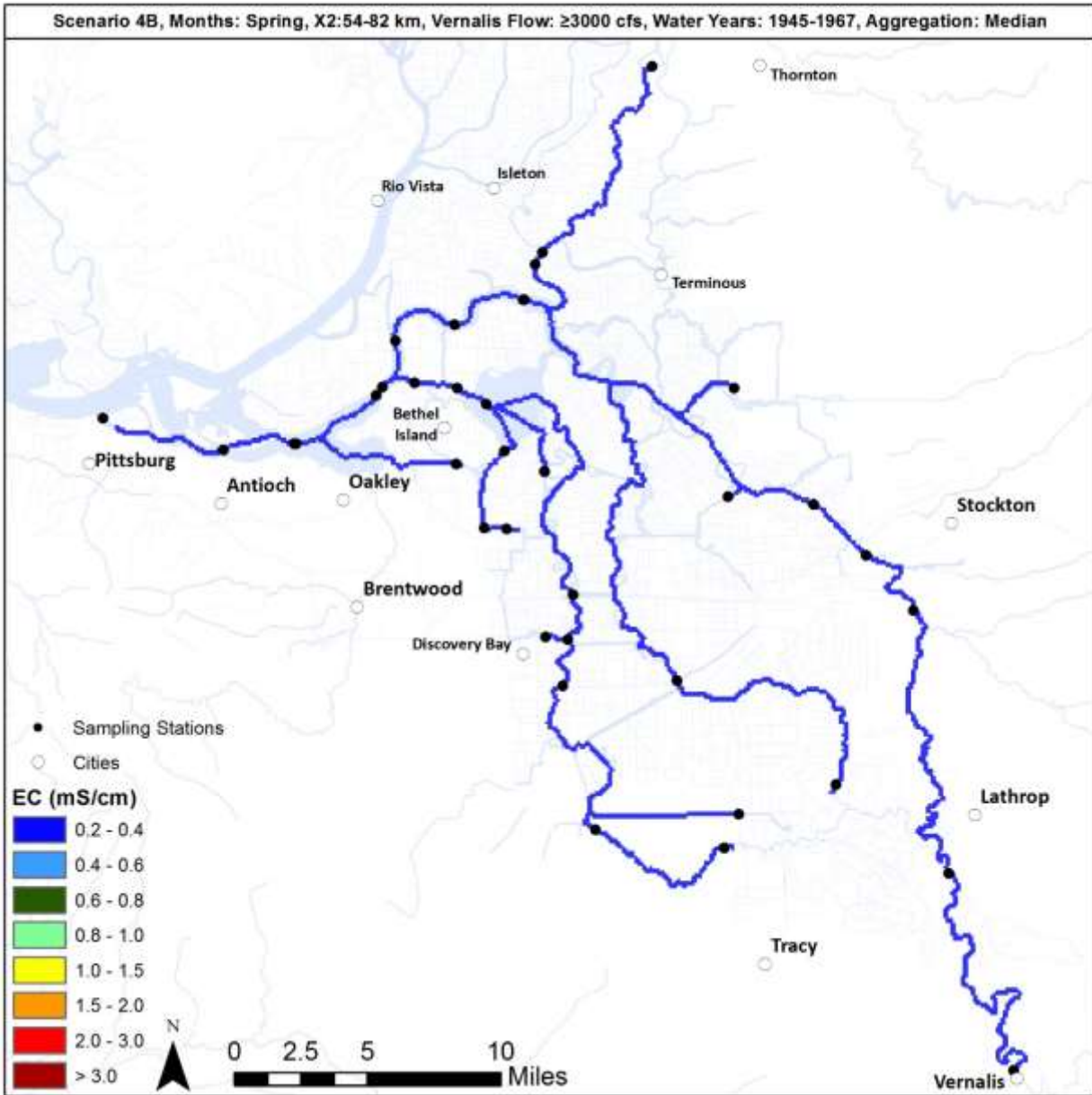


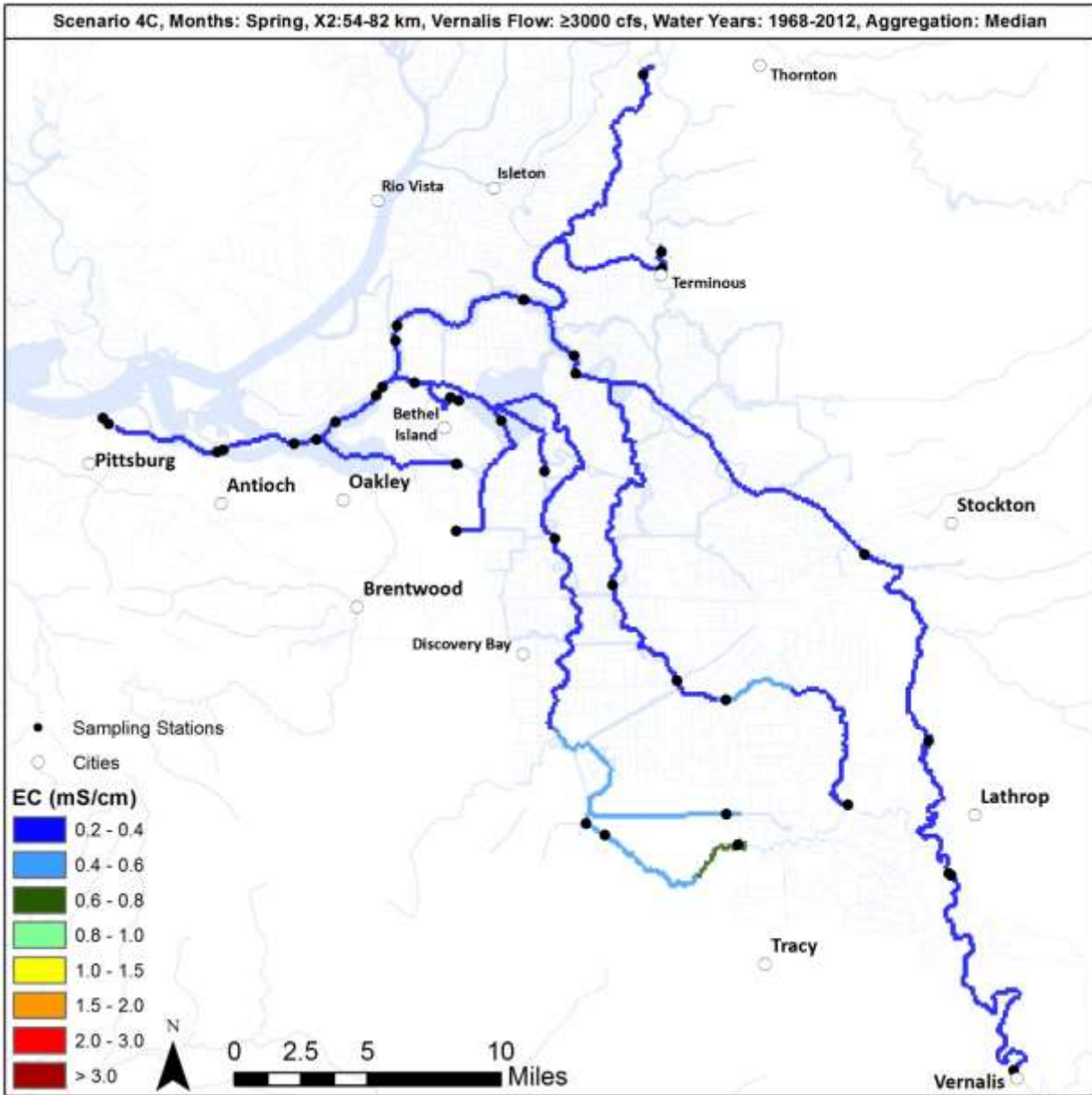


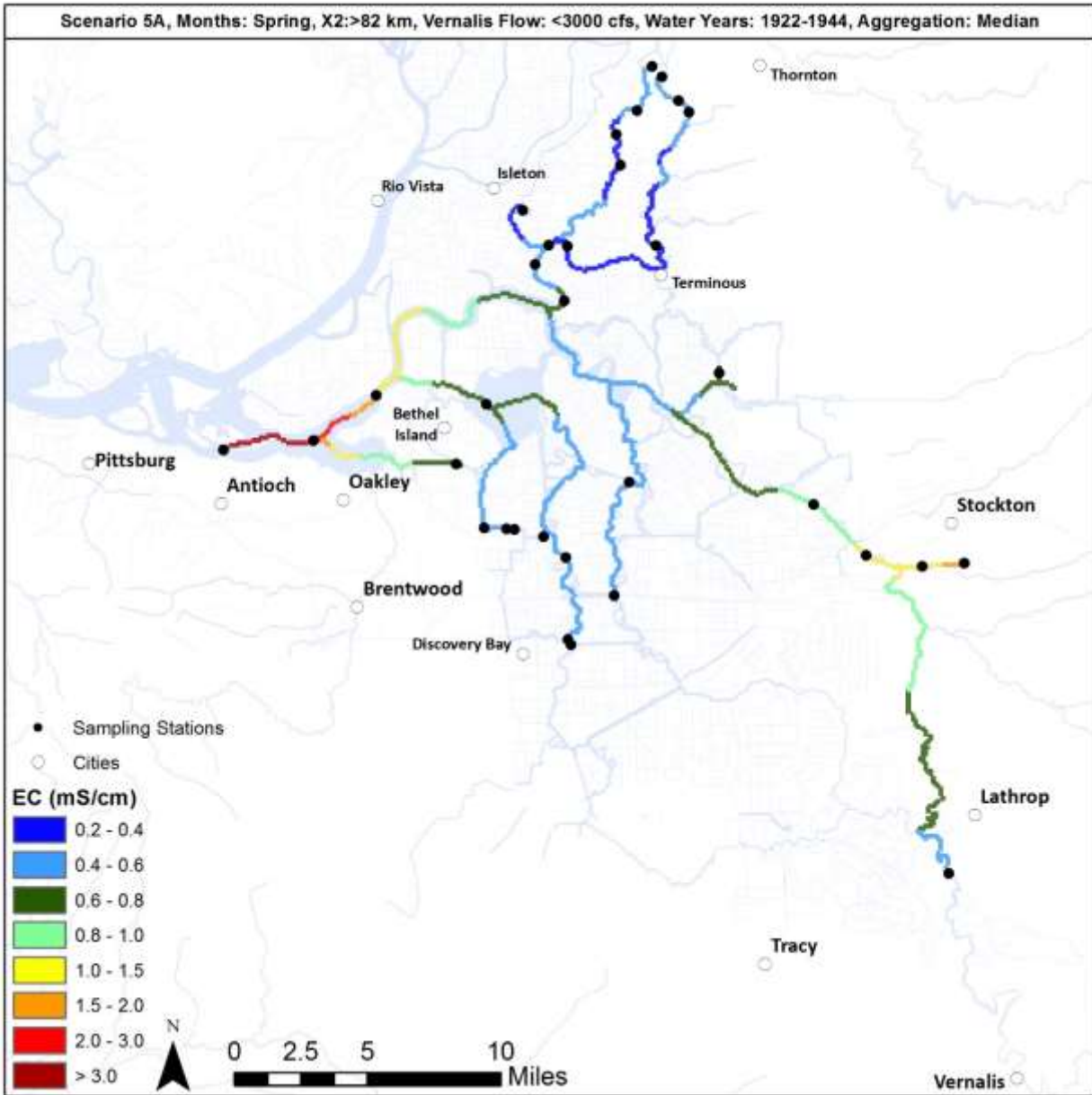


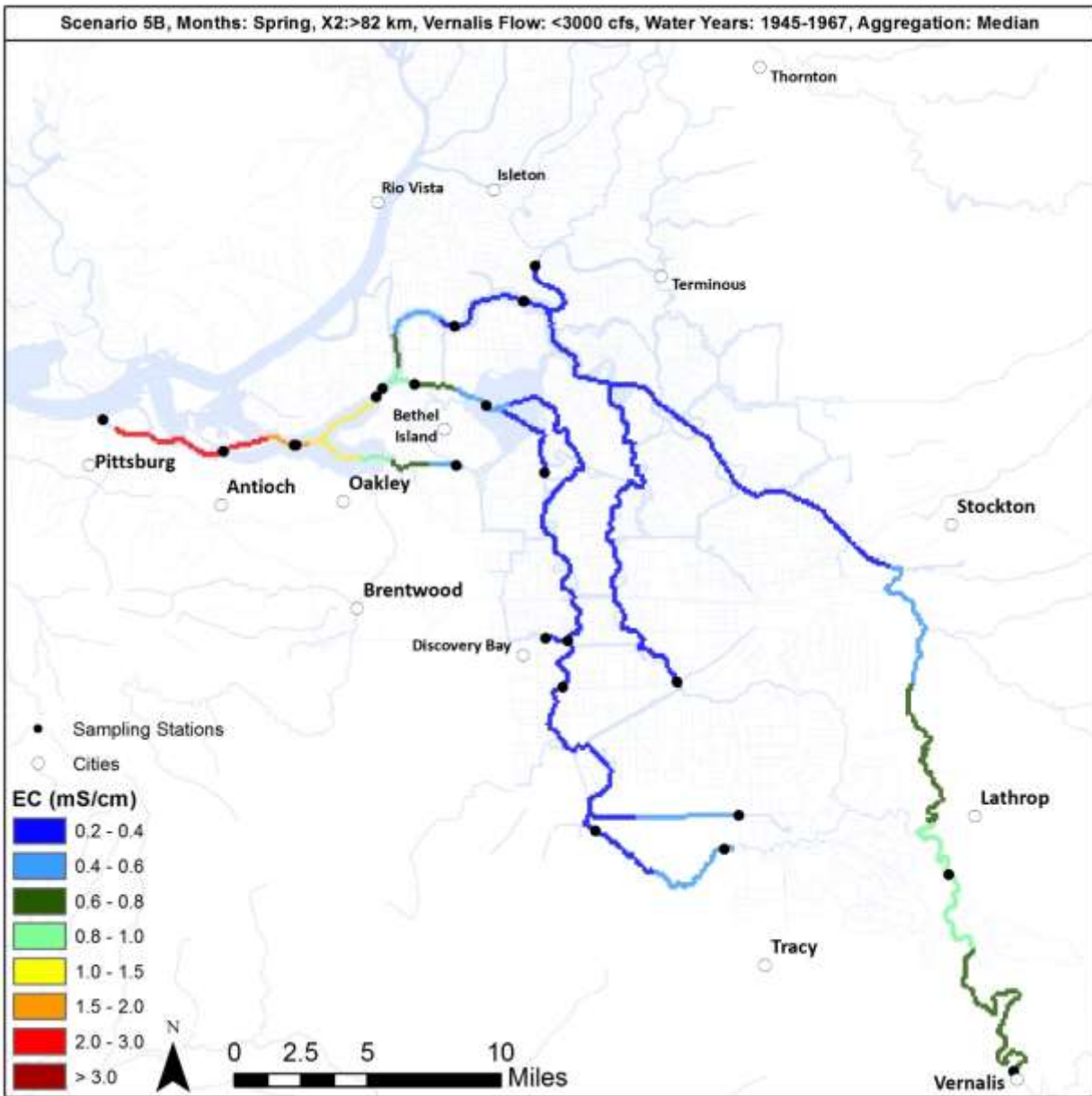


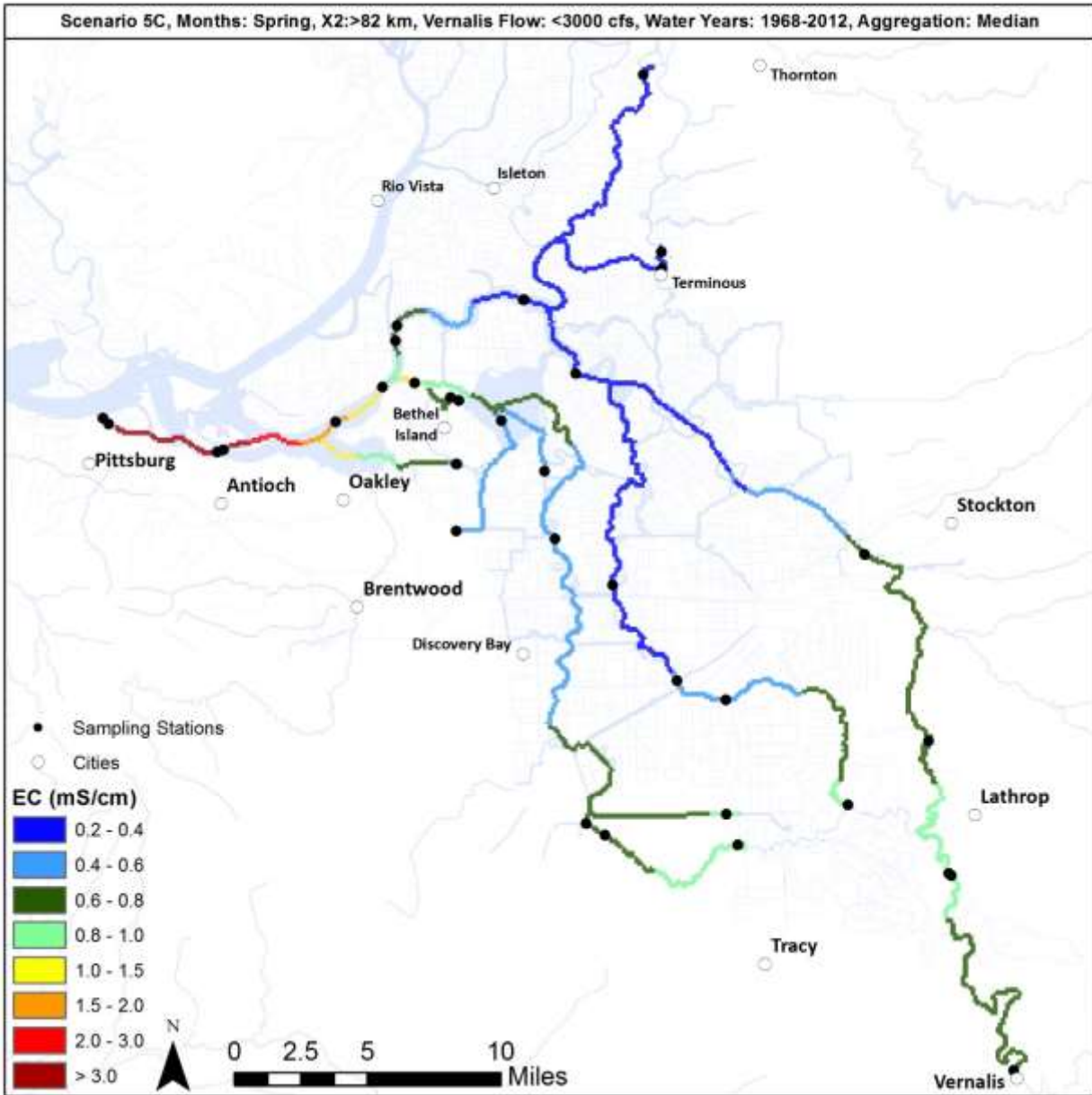


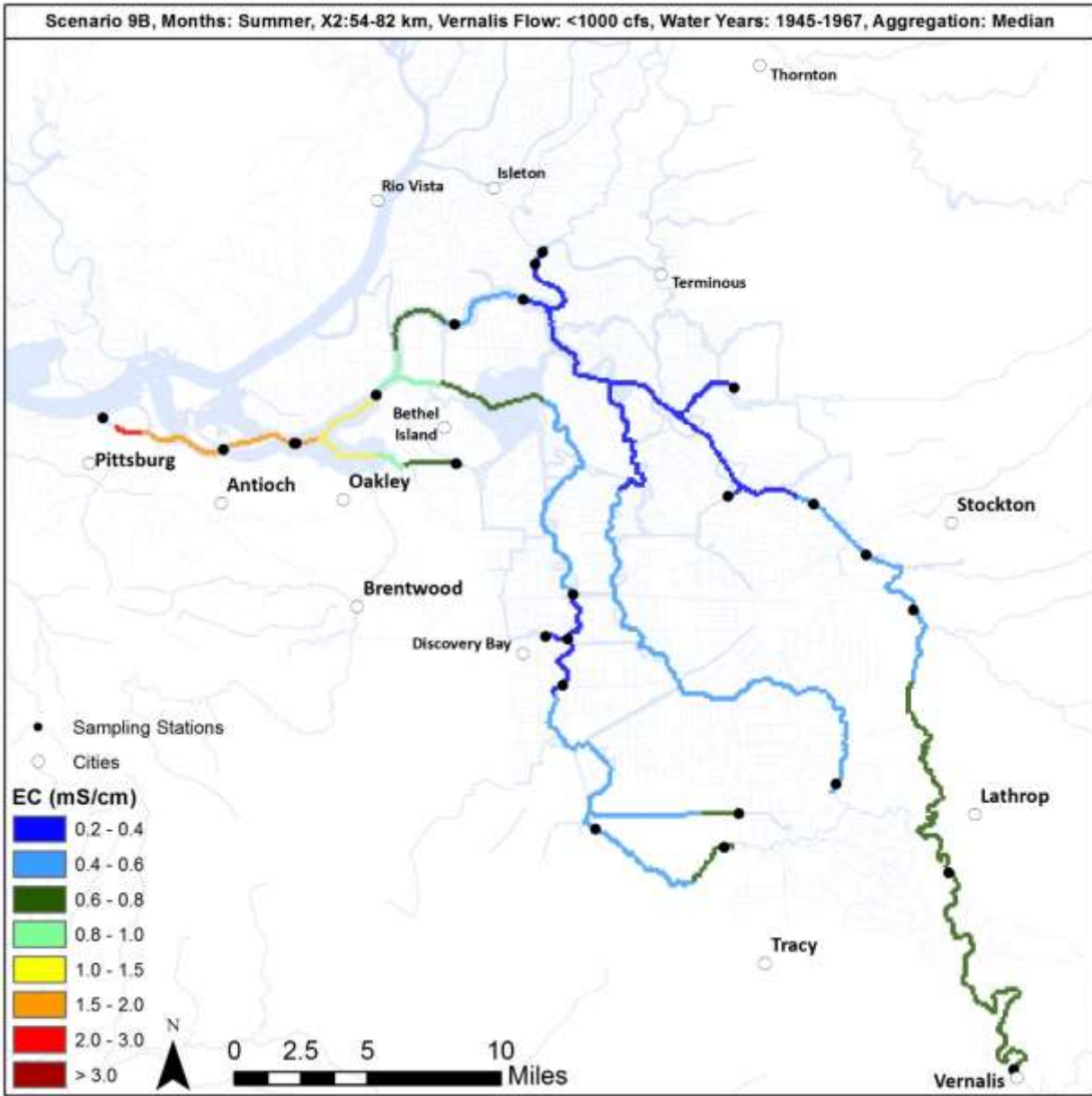


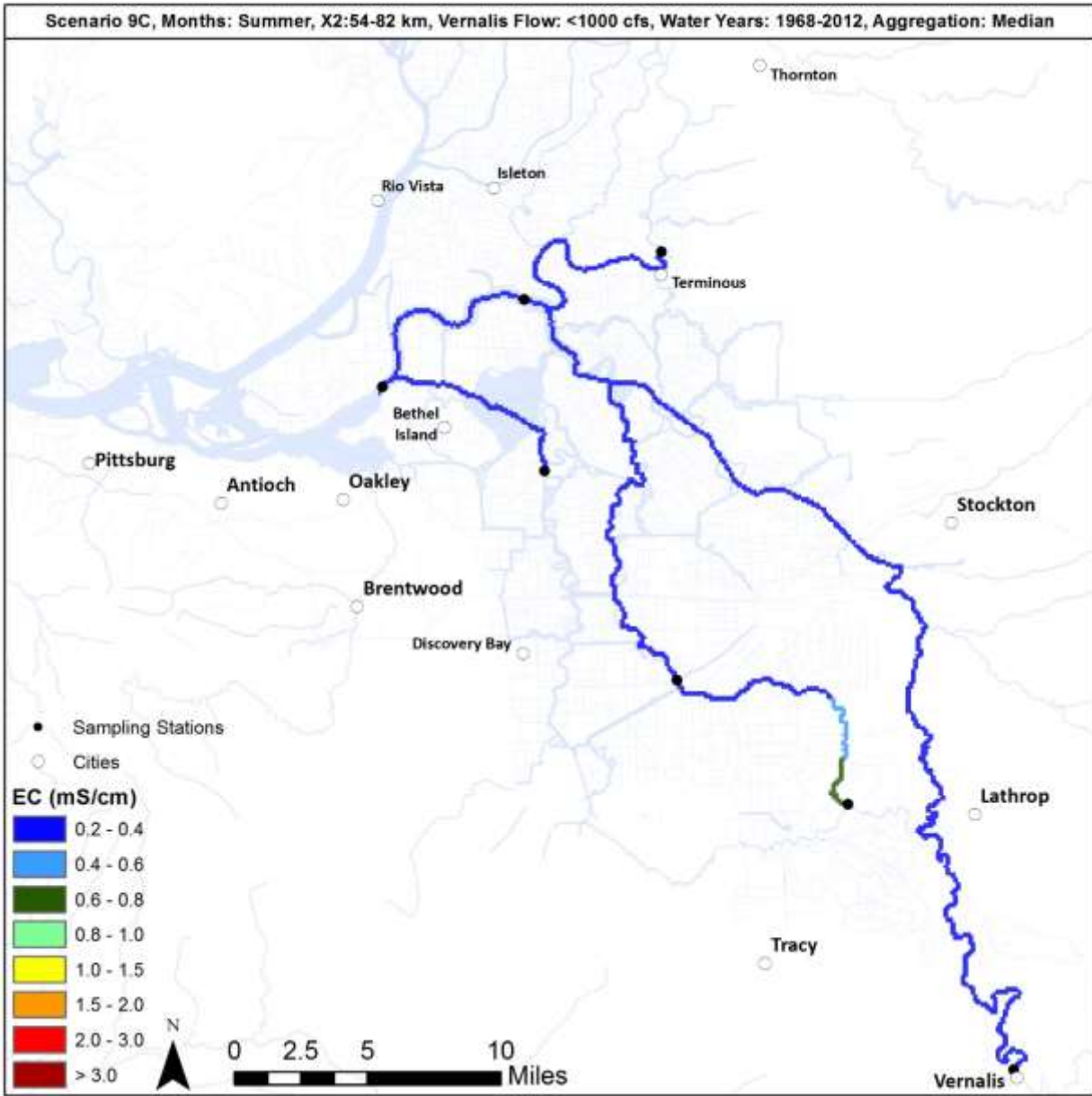


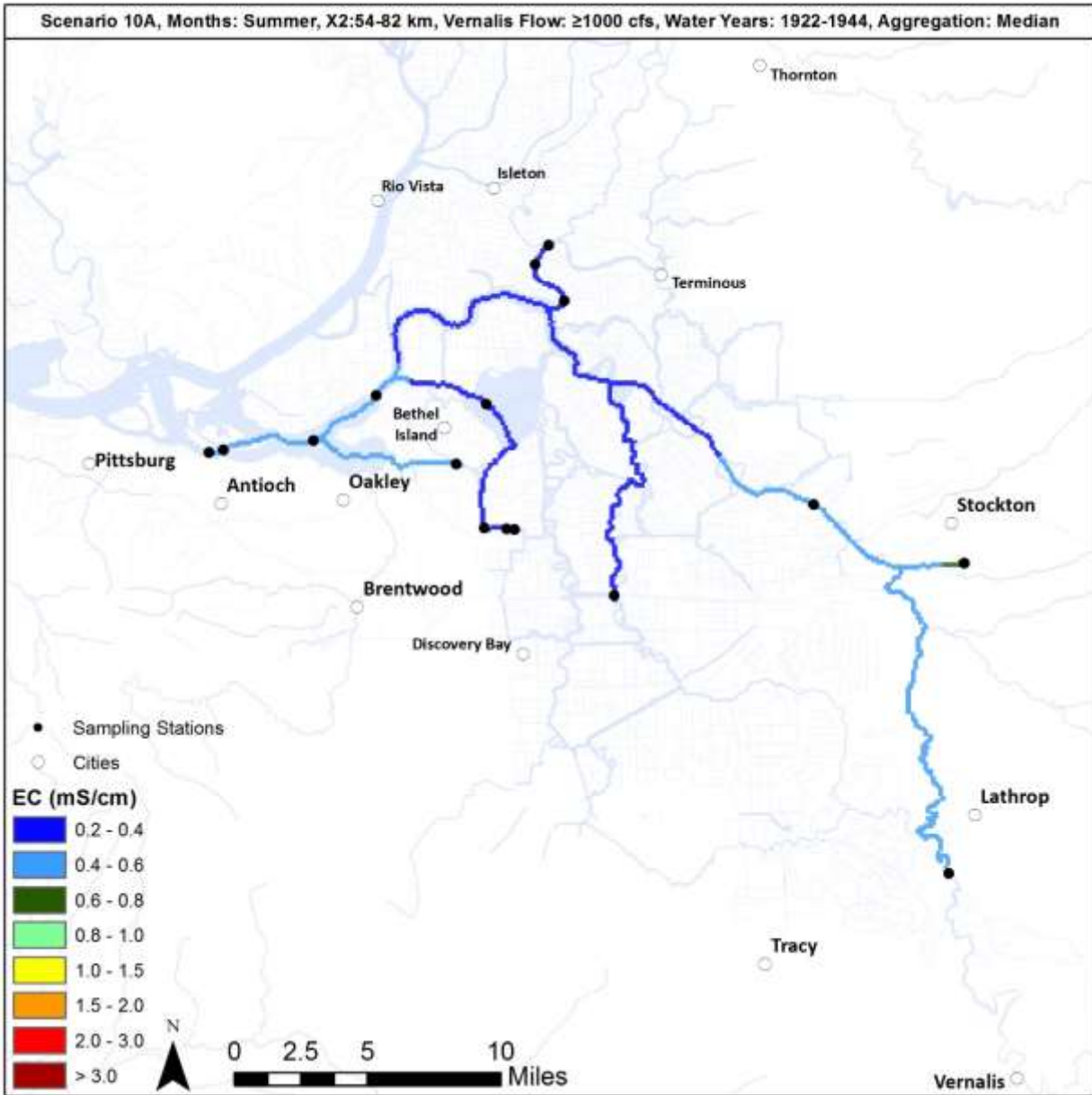


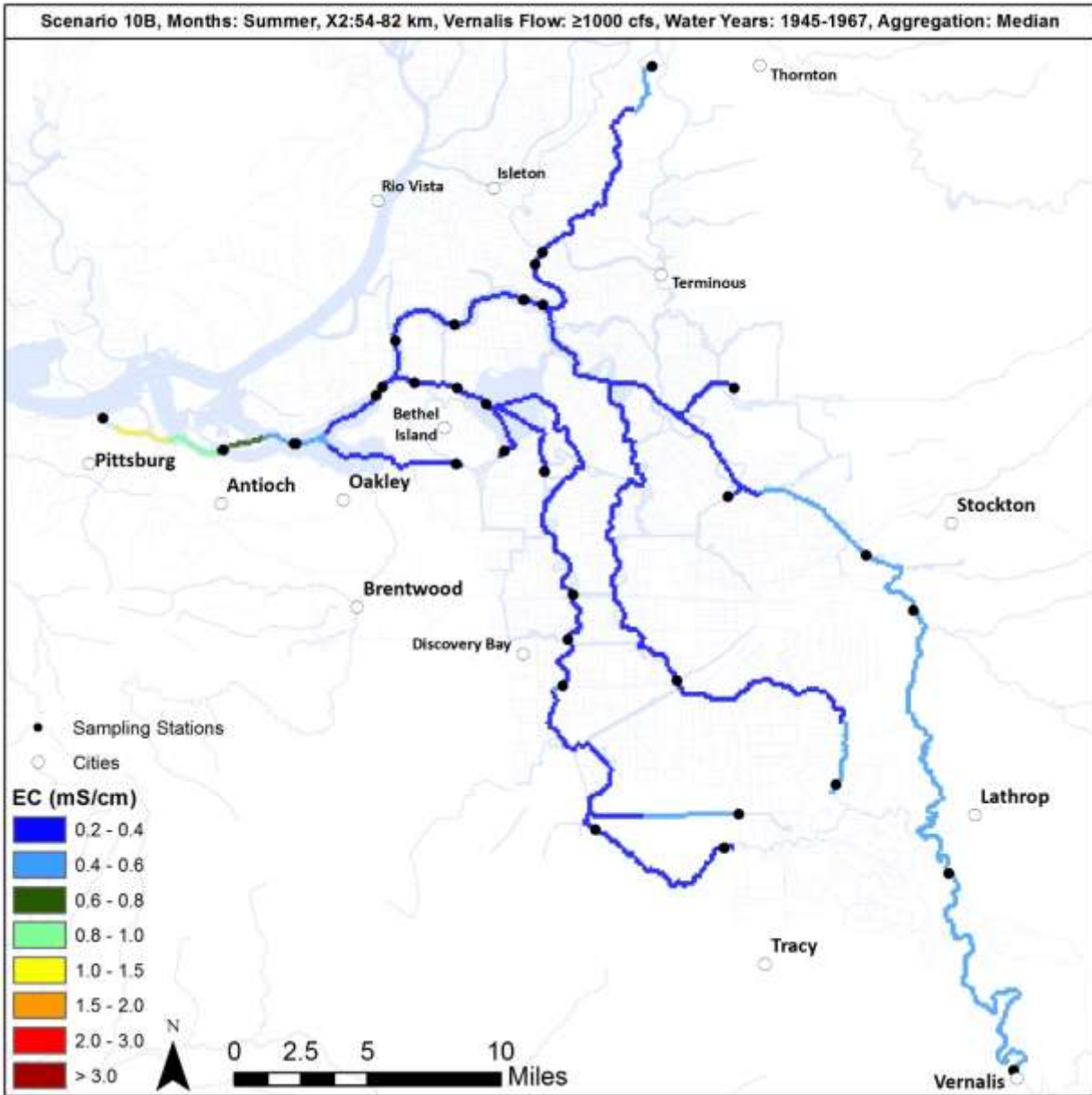


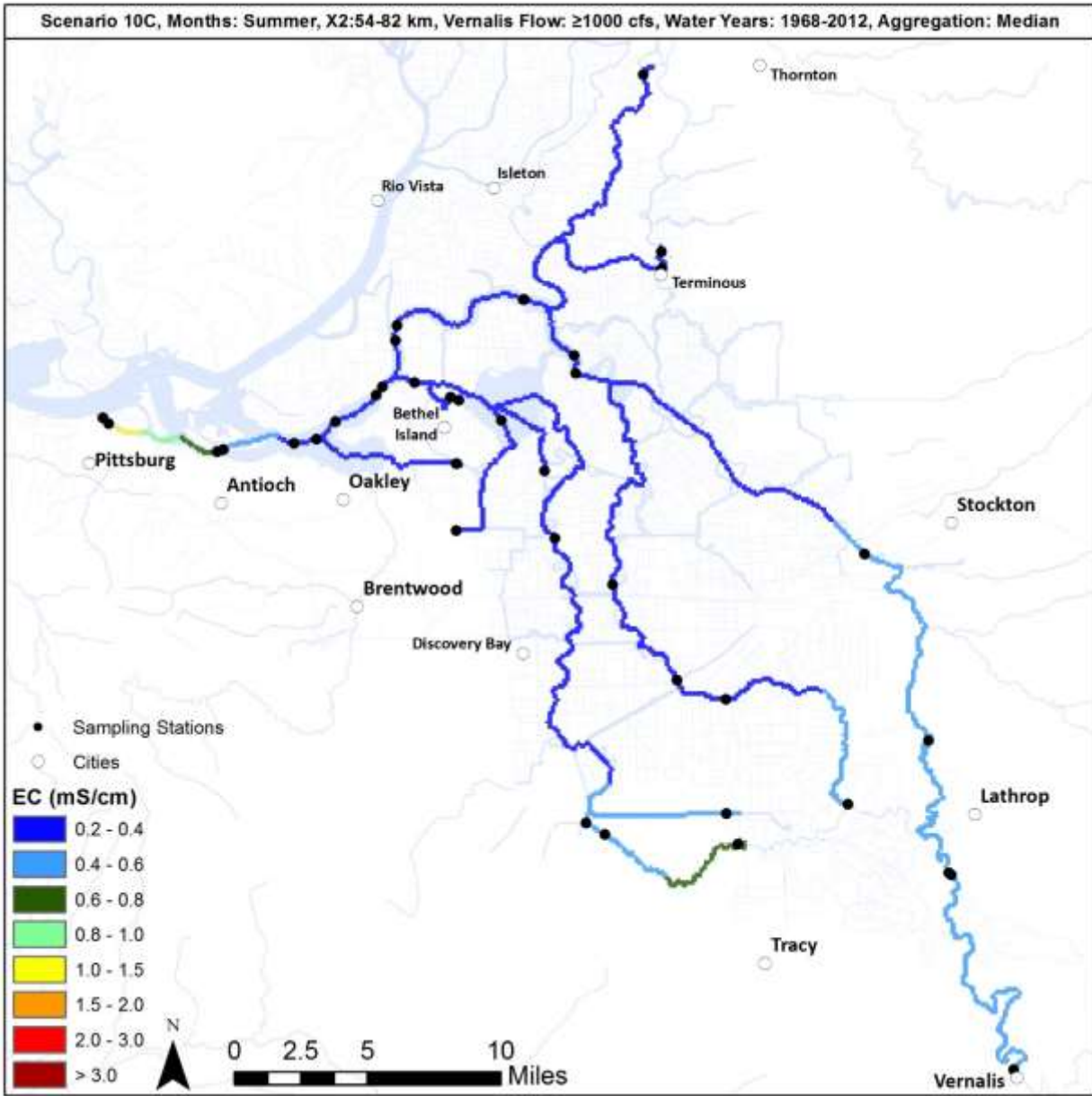


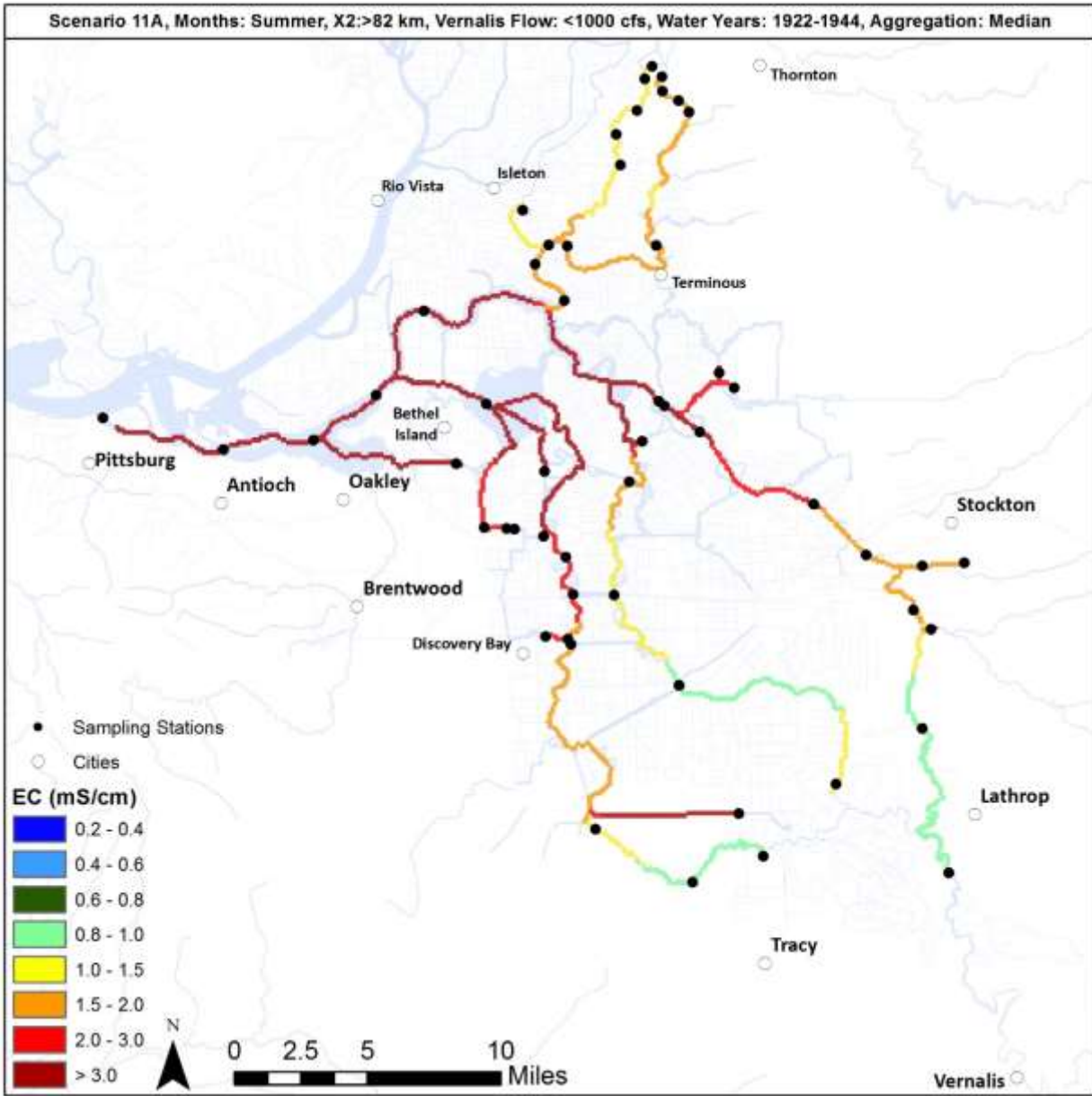


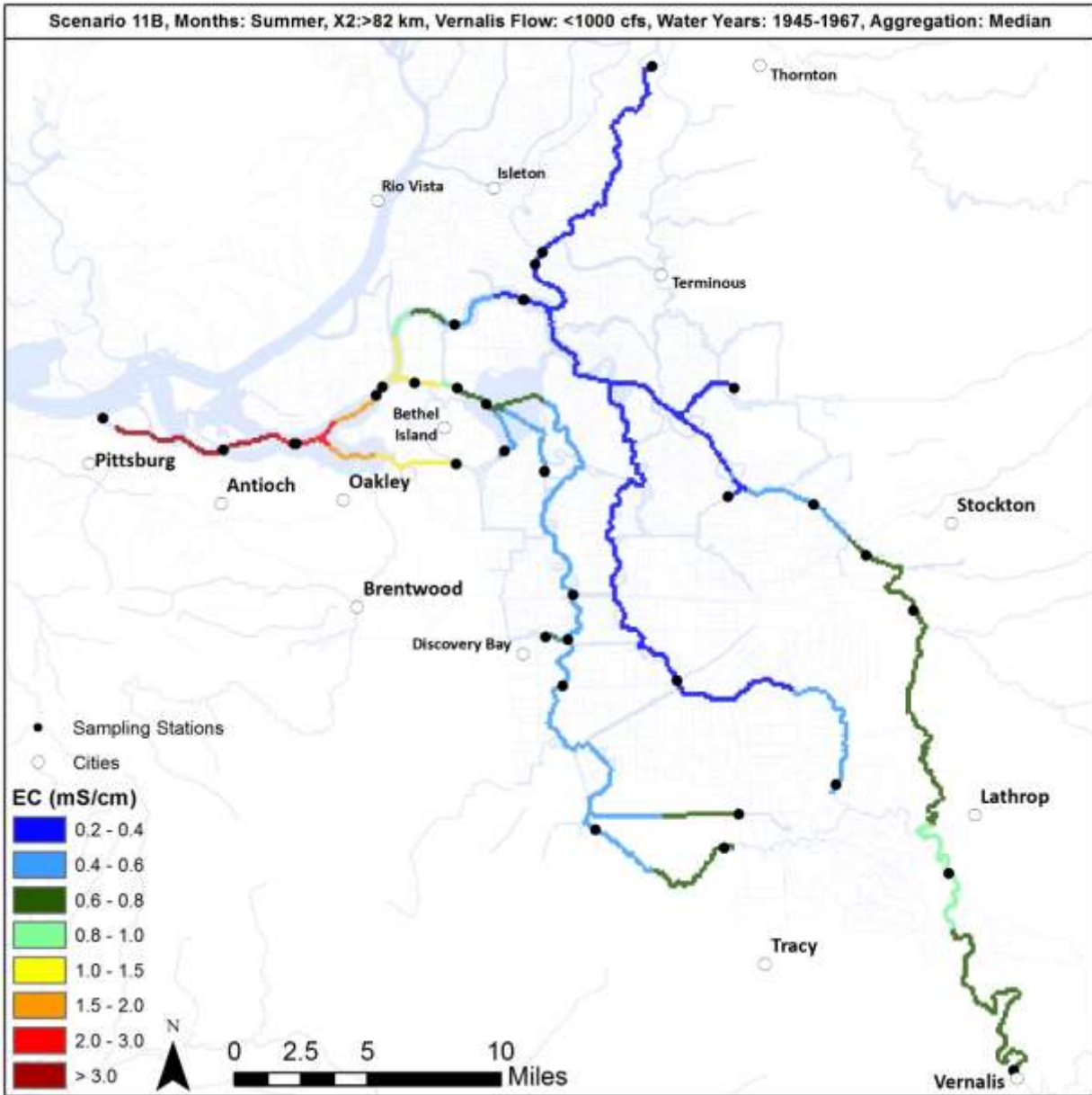


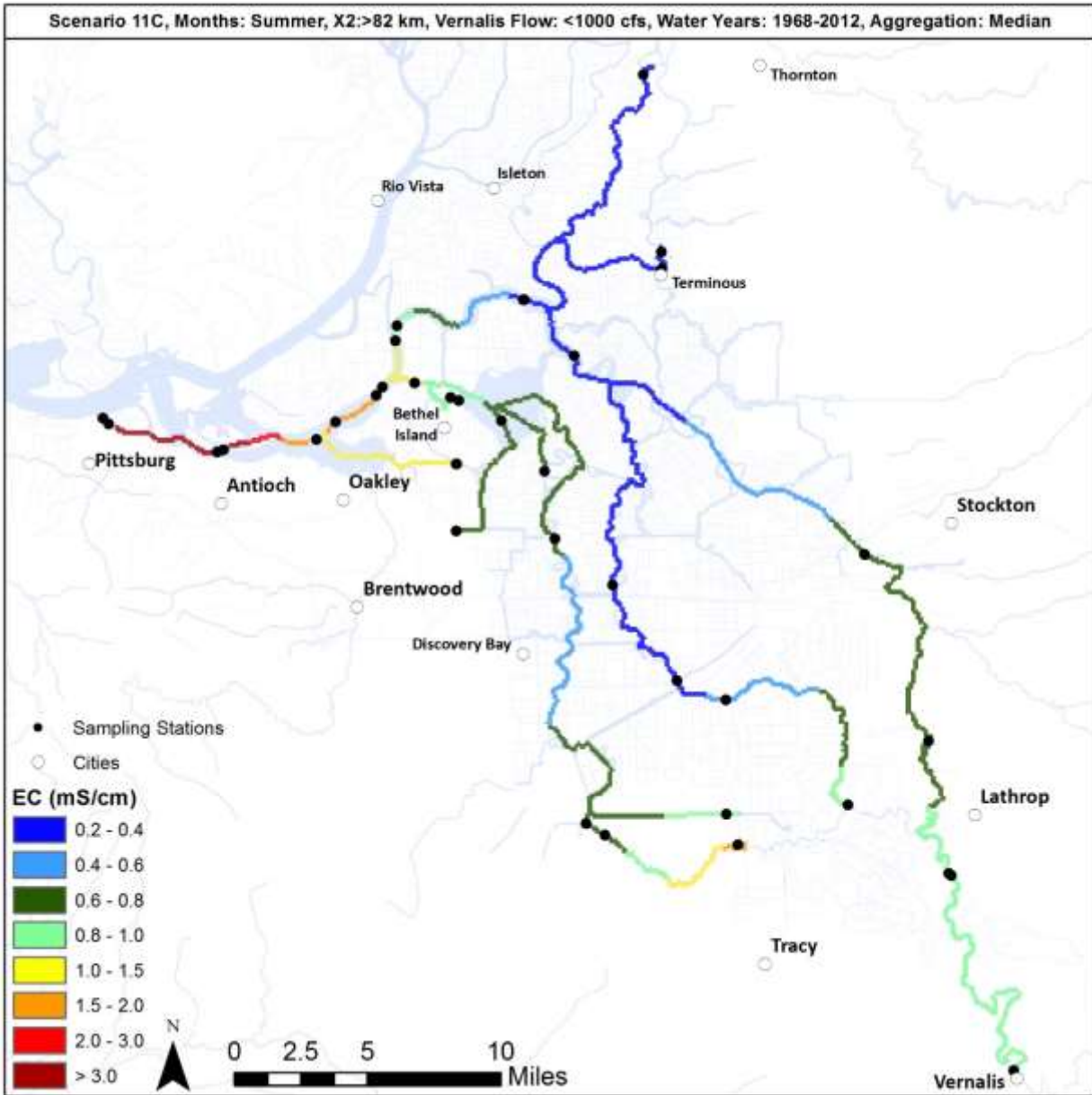


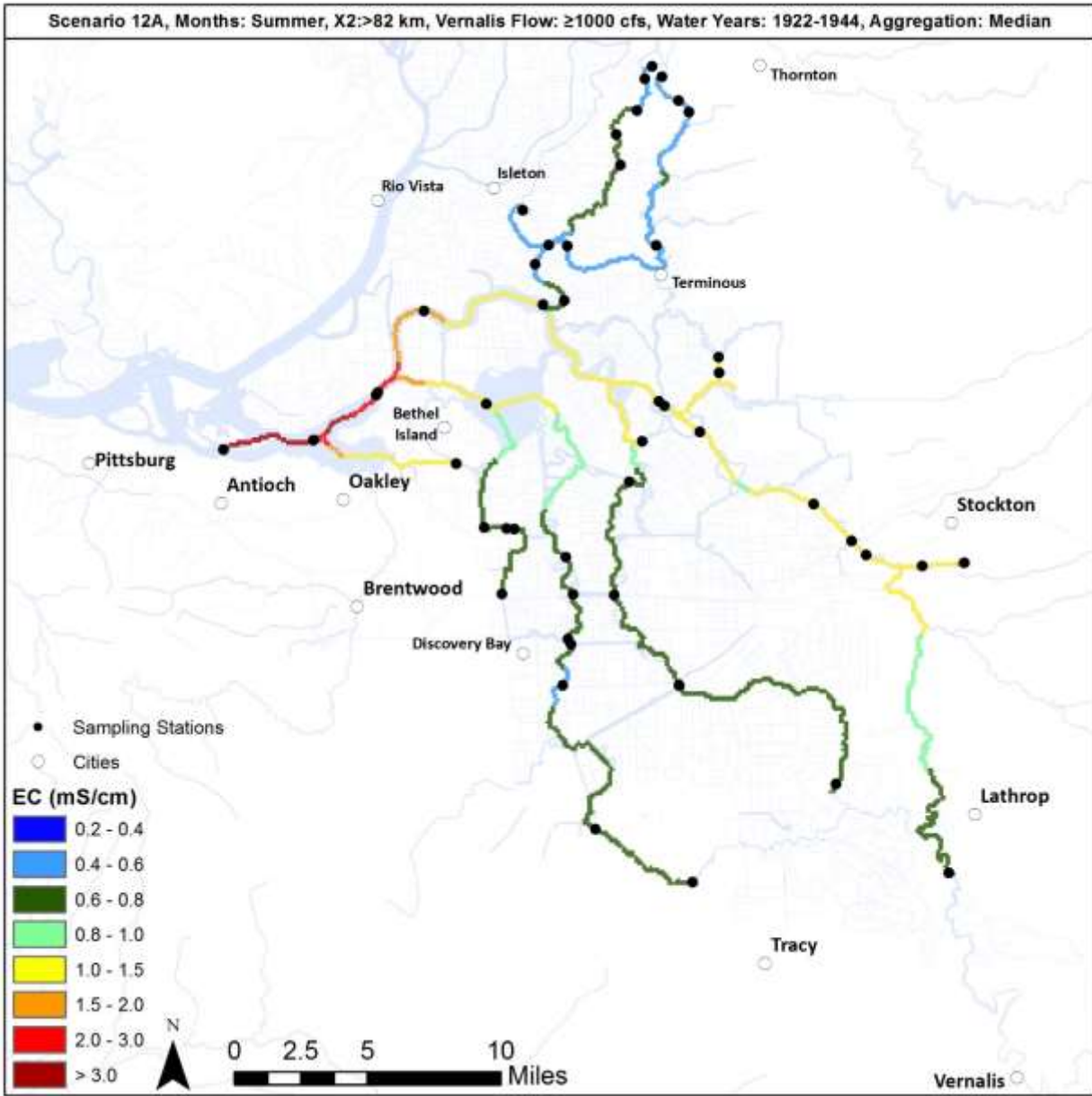


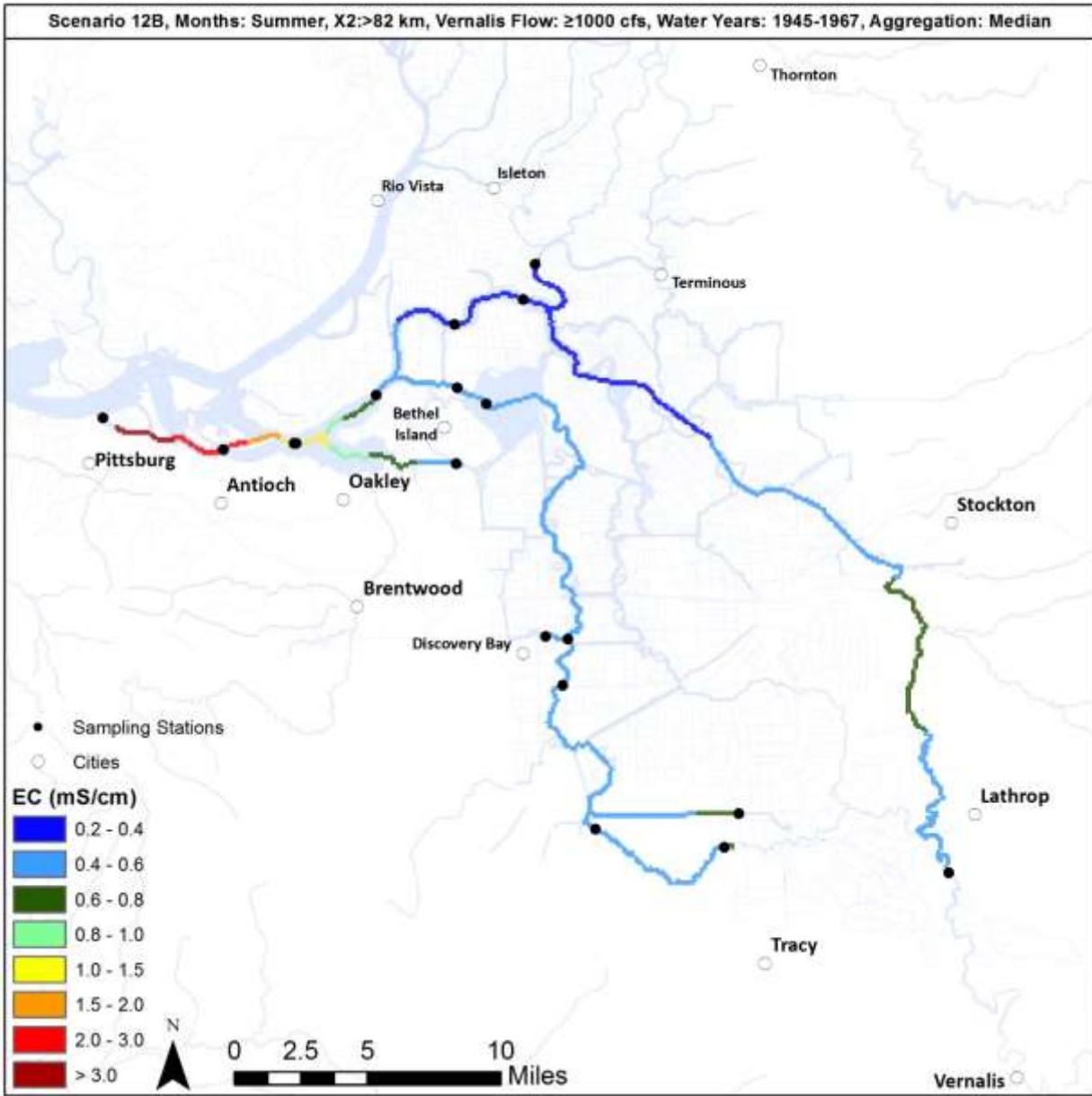


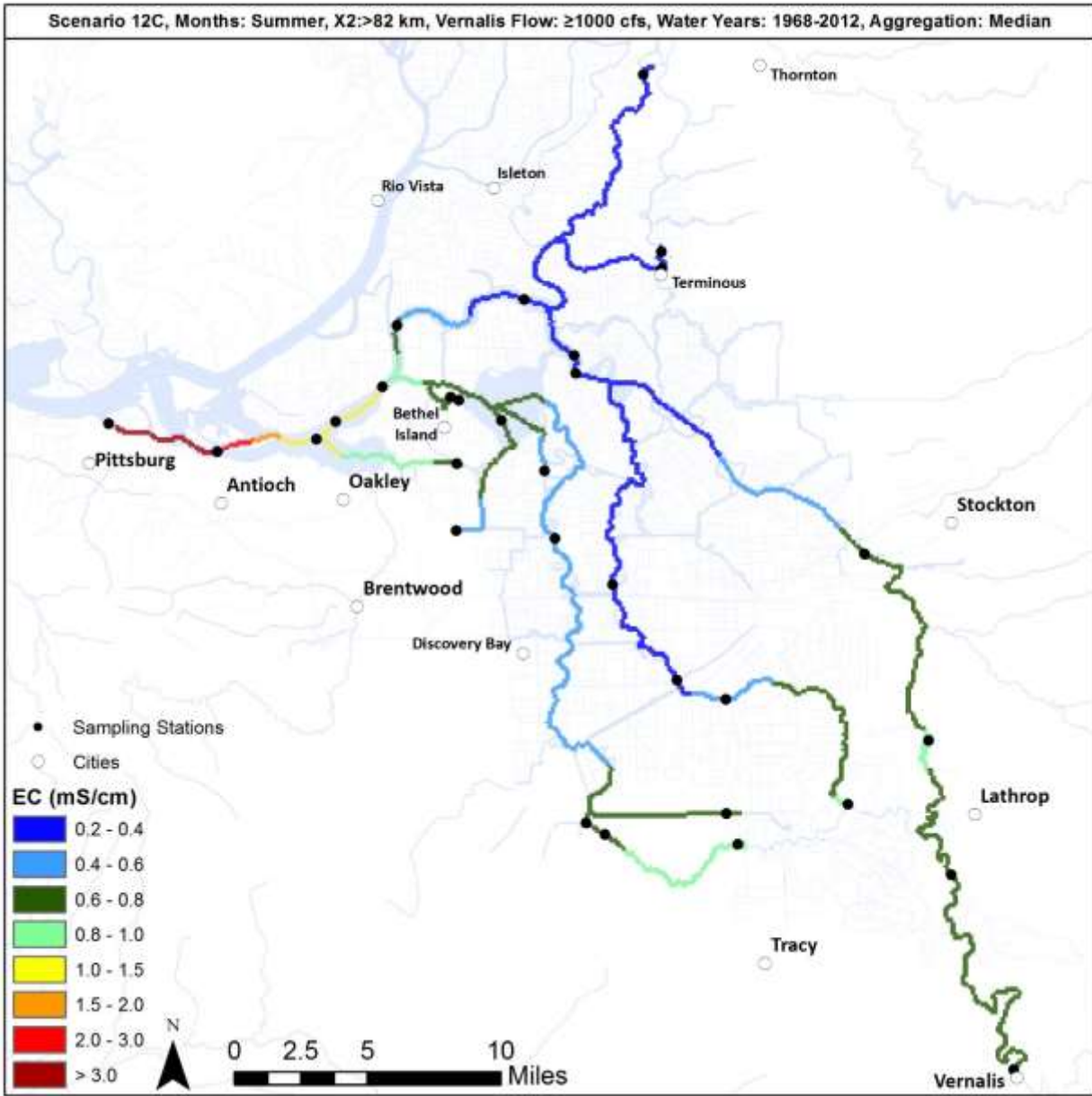




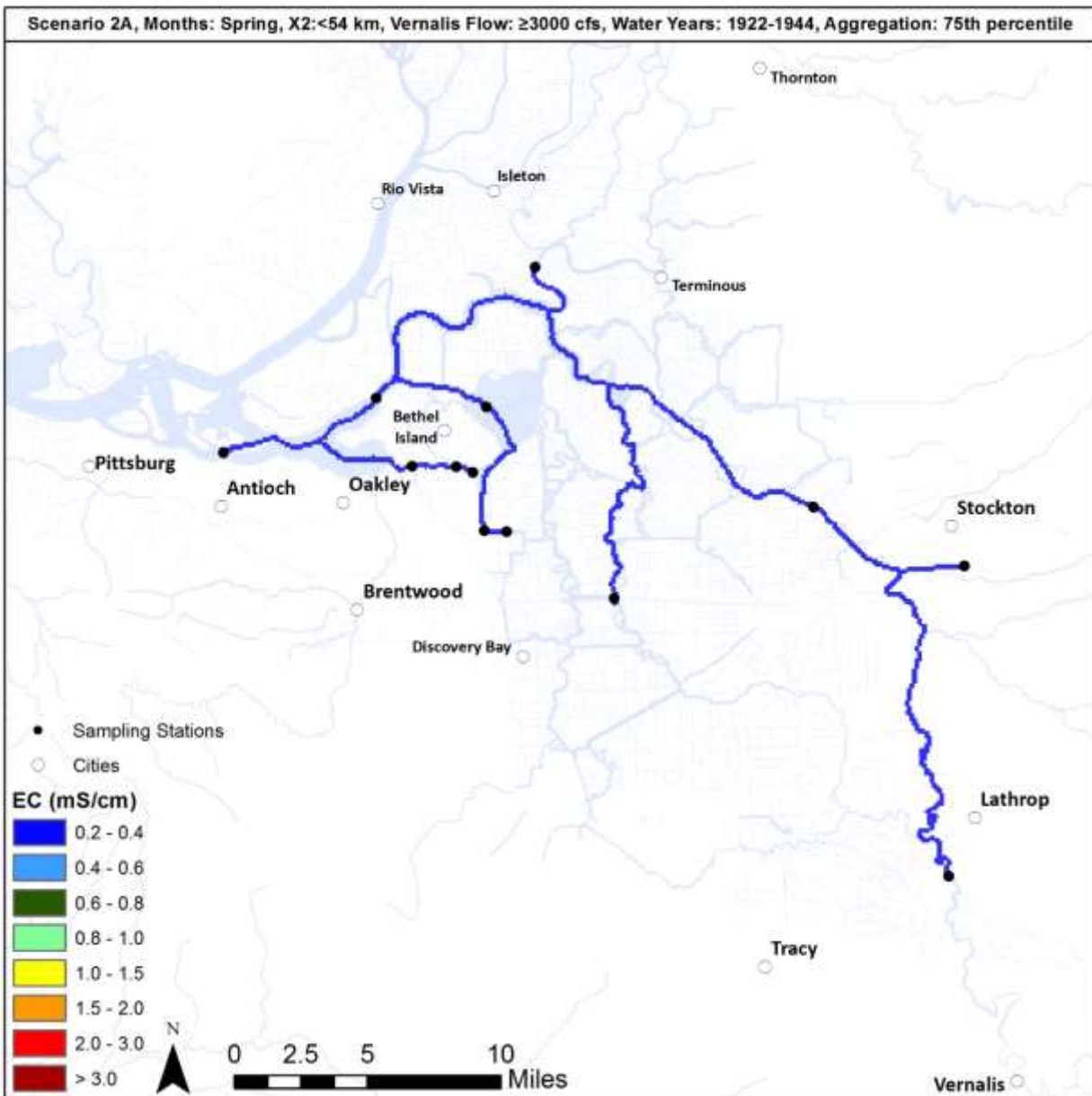


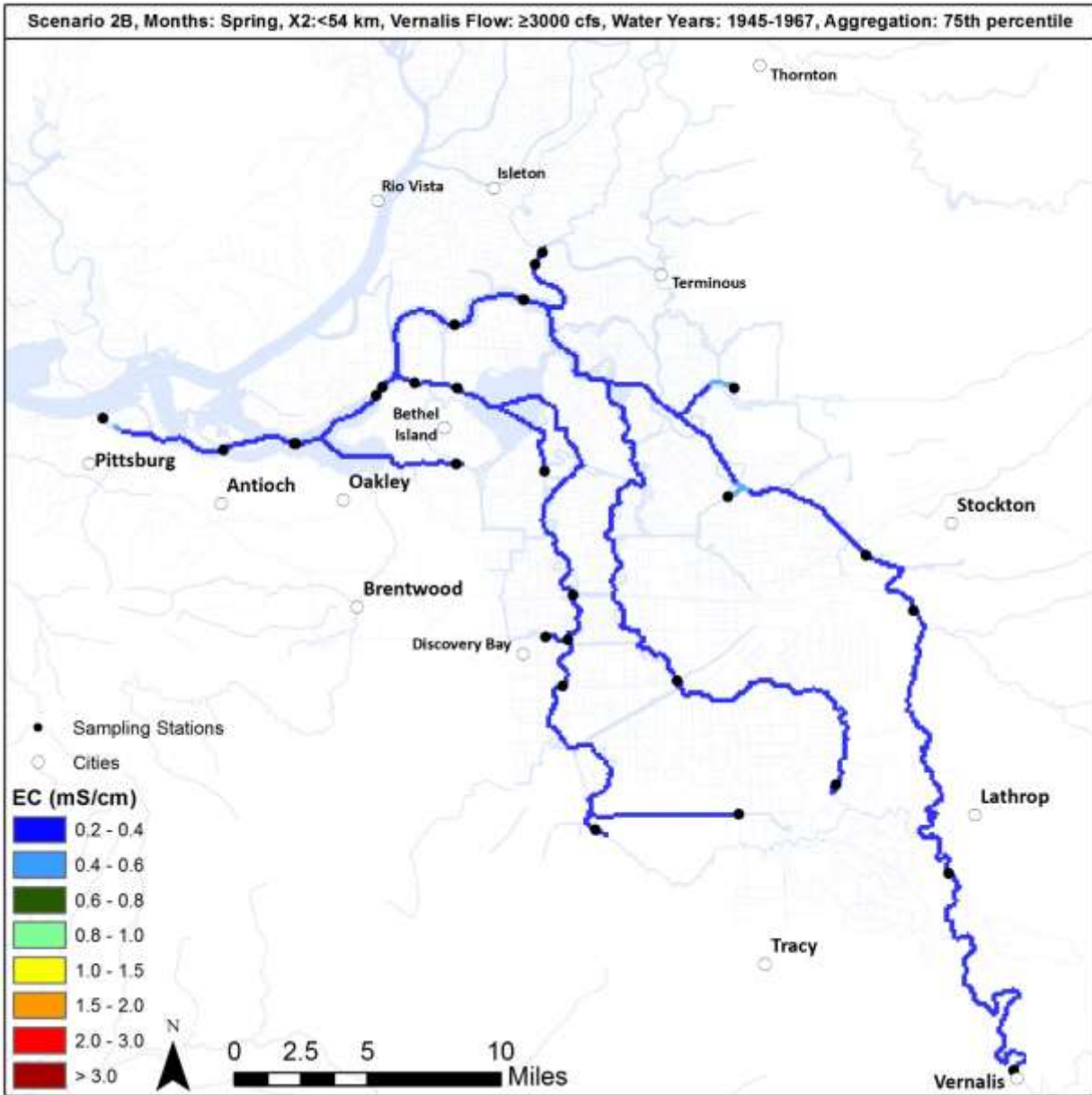


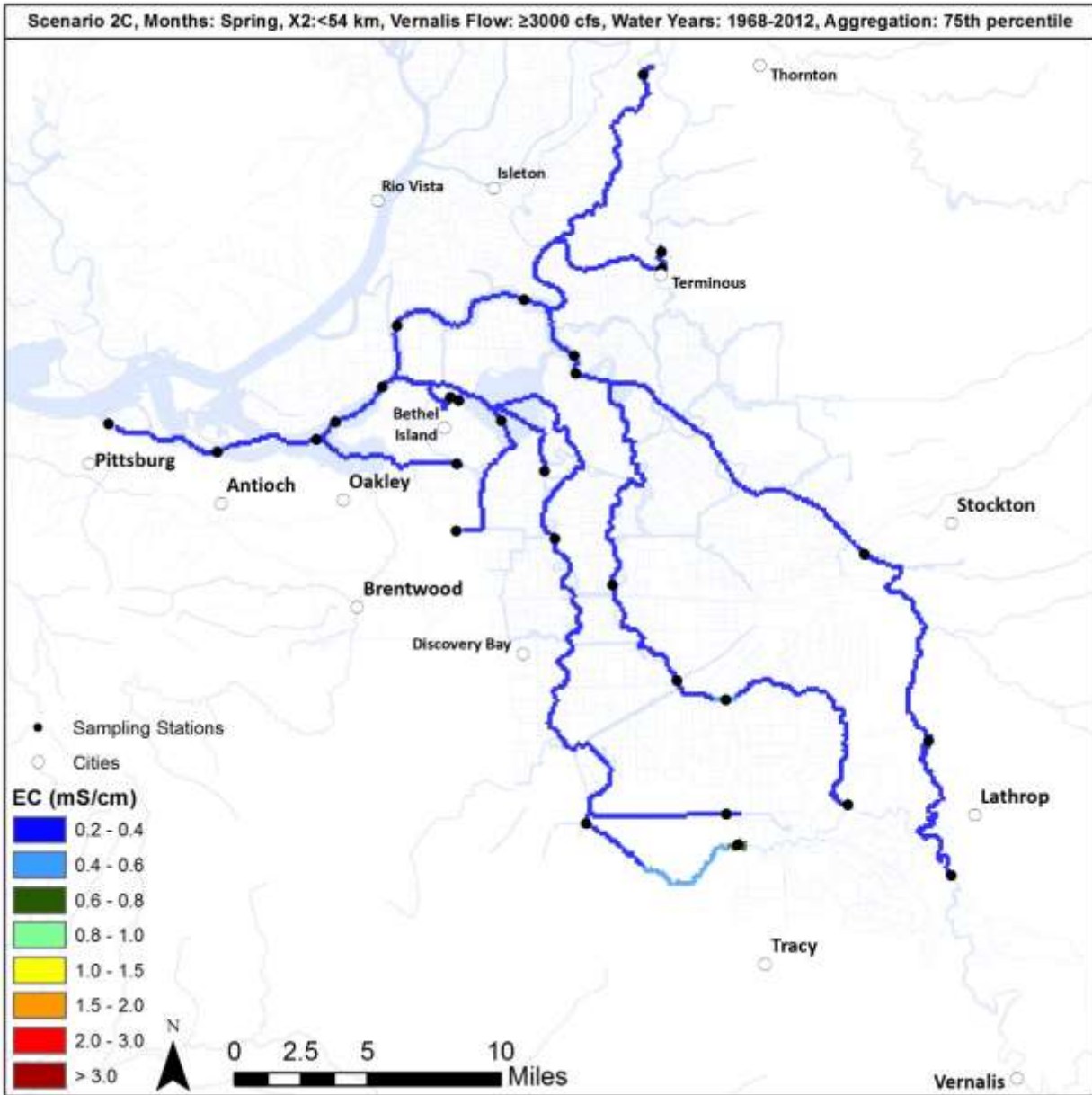


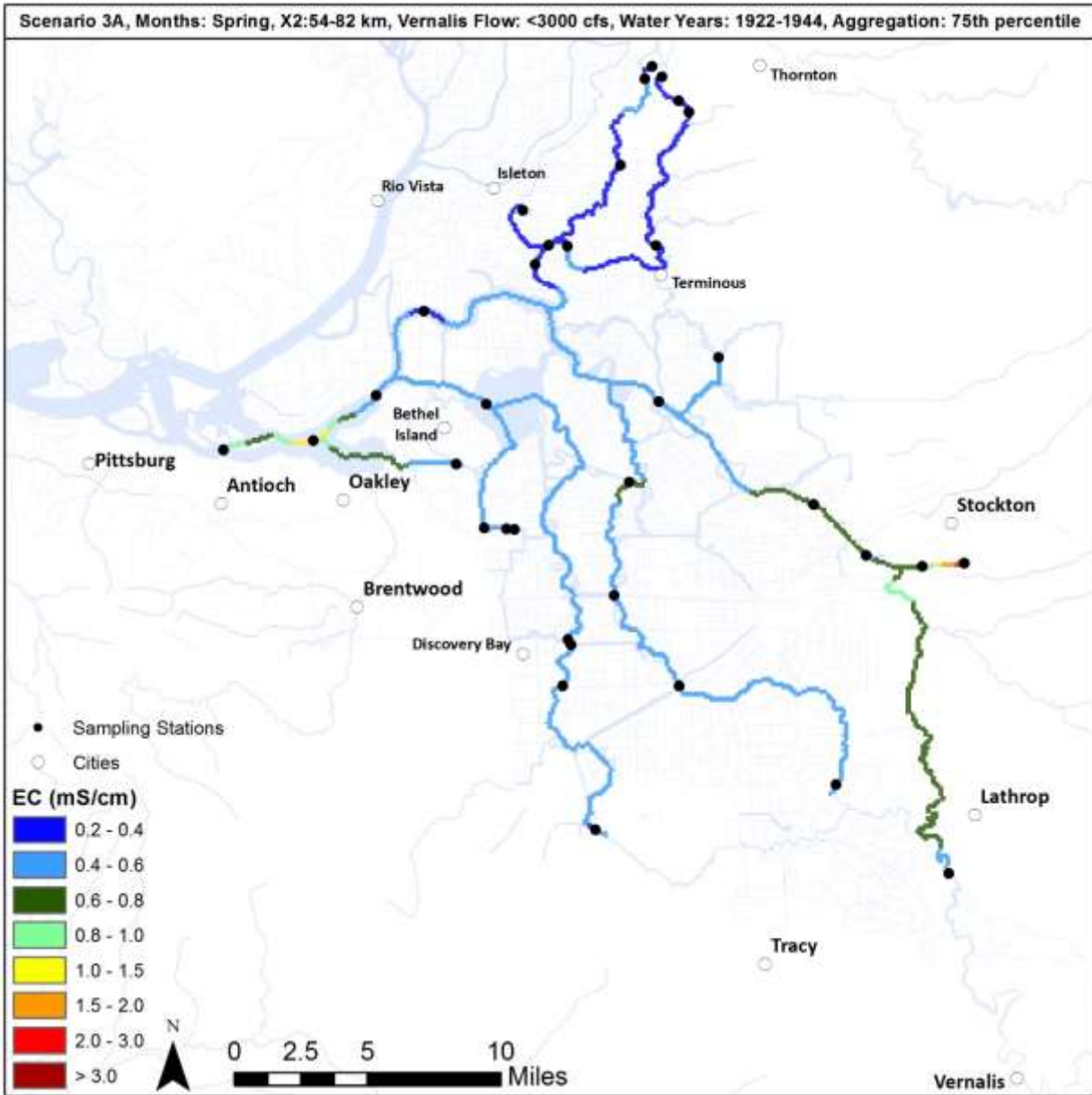


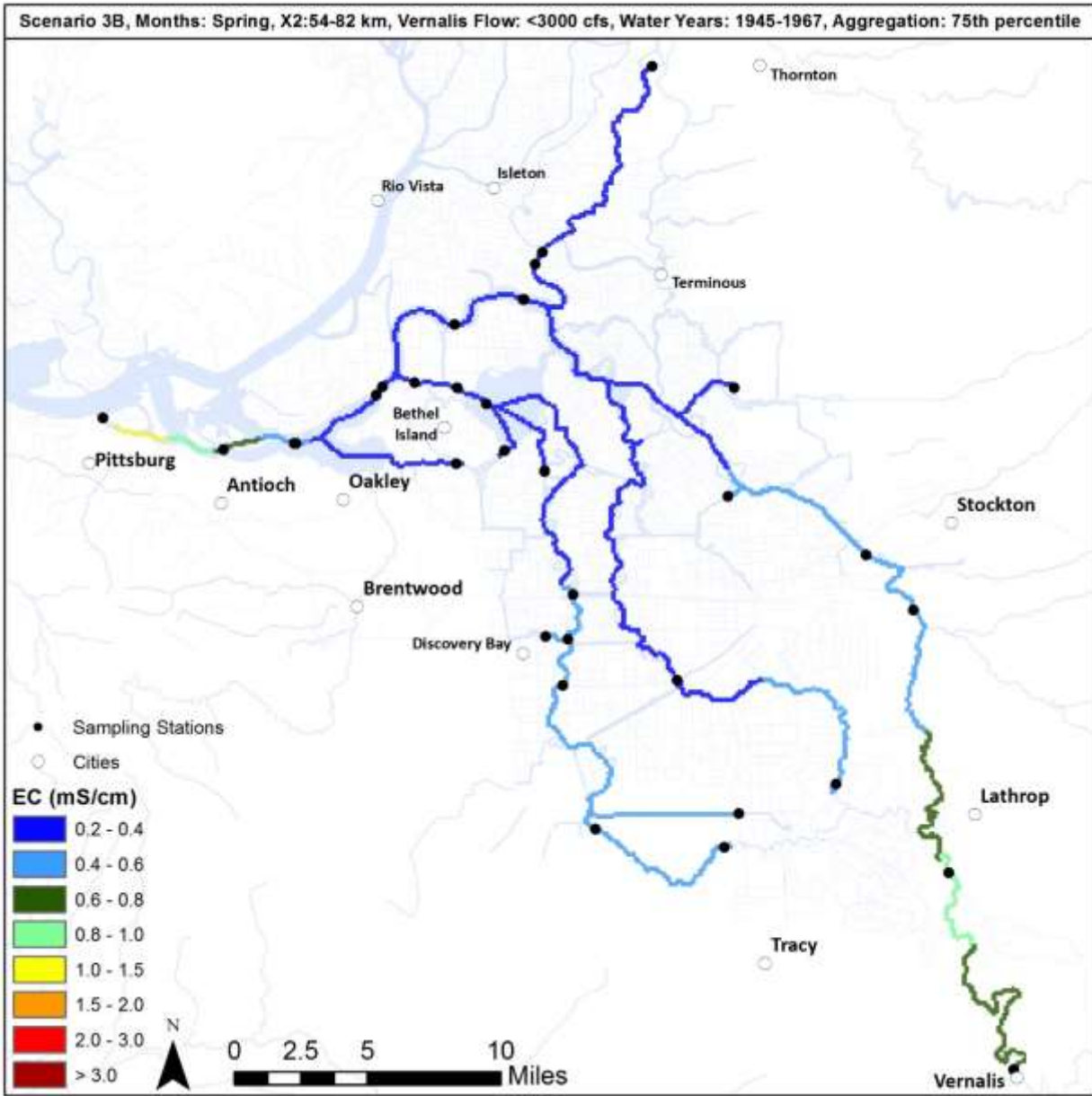
Appendix D. MAPS OF 75TH PERCENTILE SALINITY

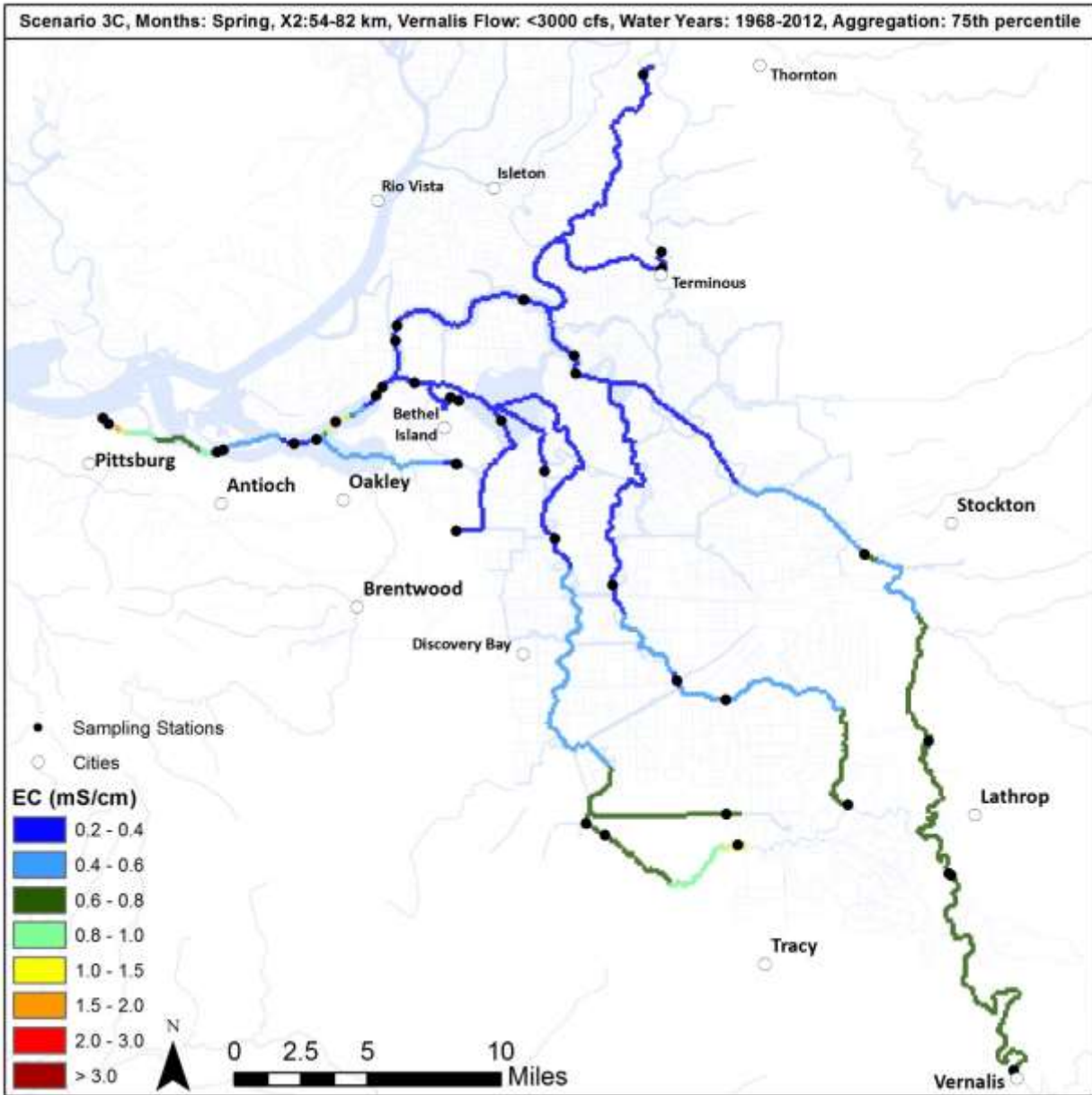


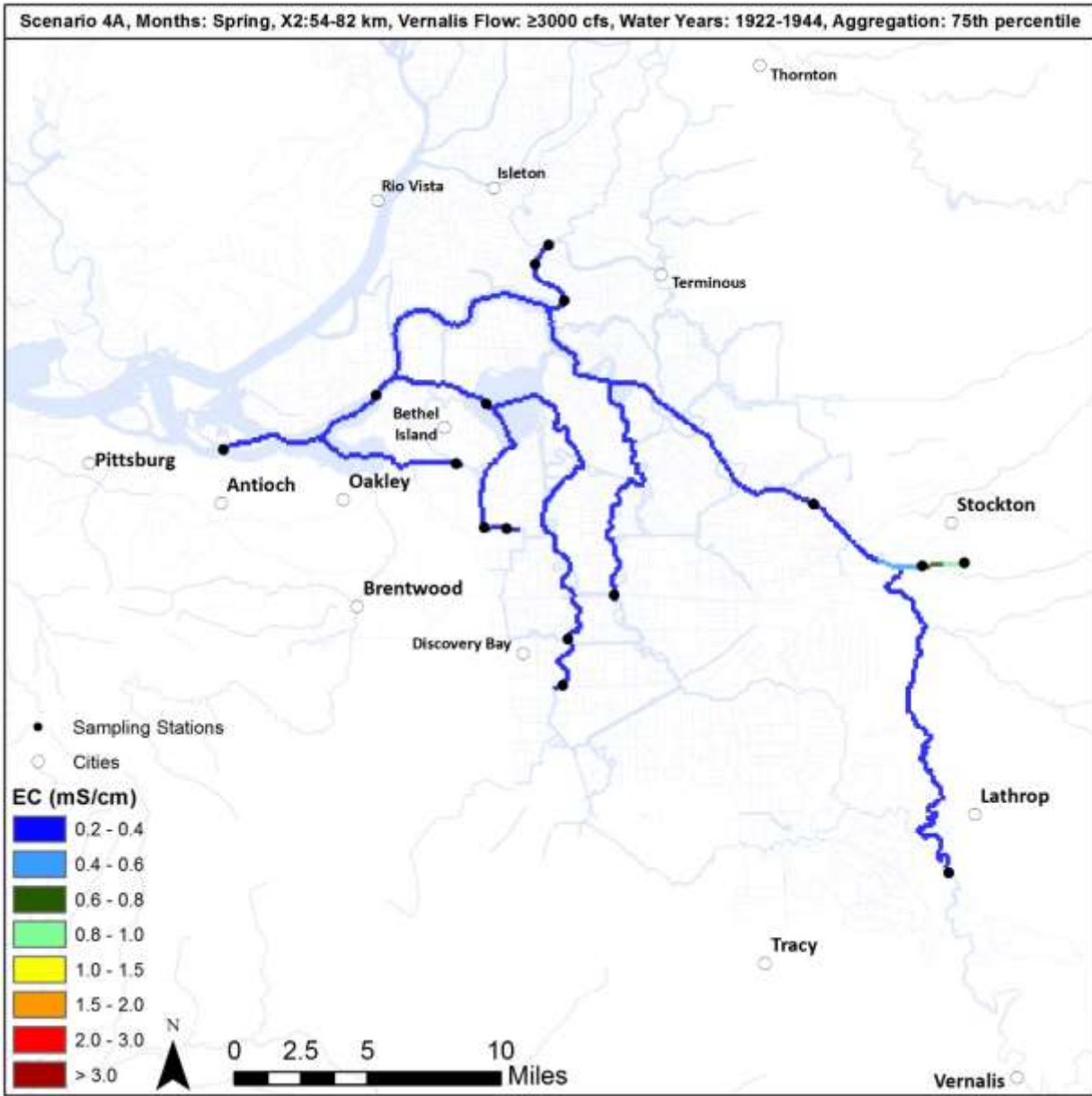


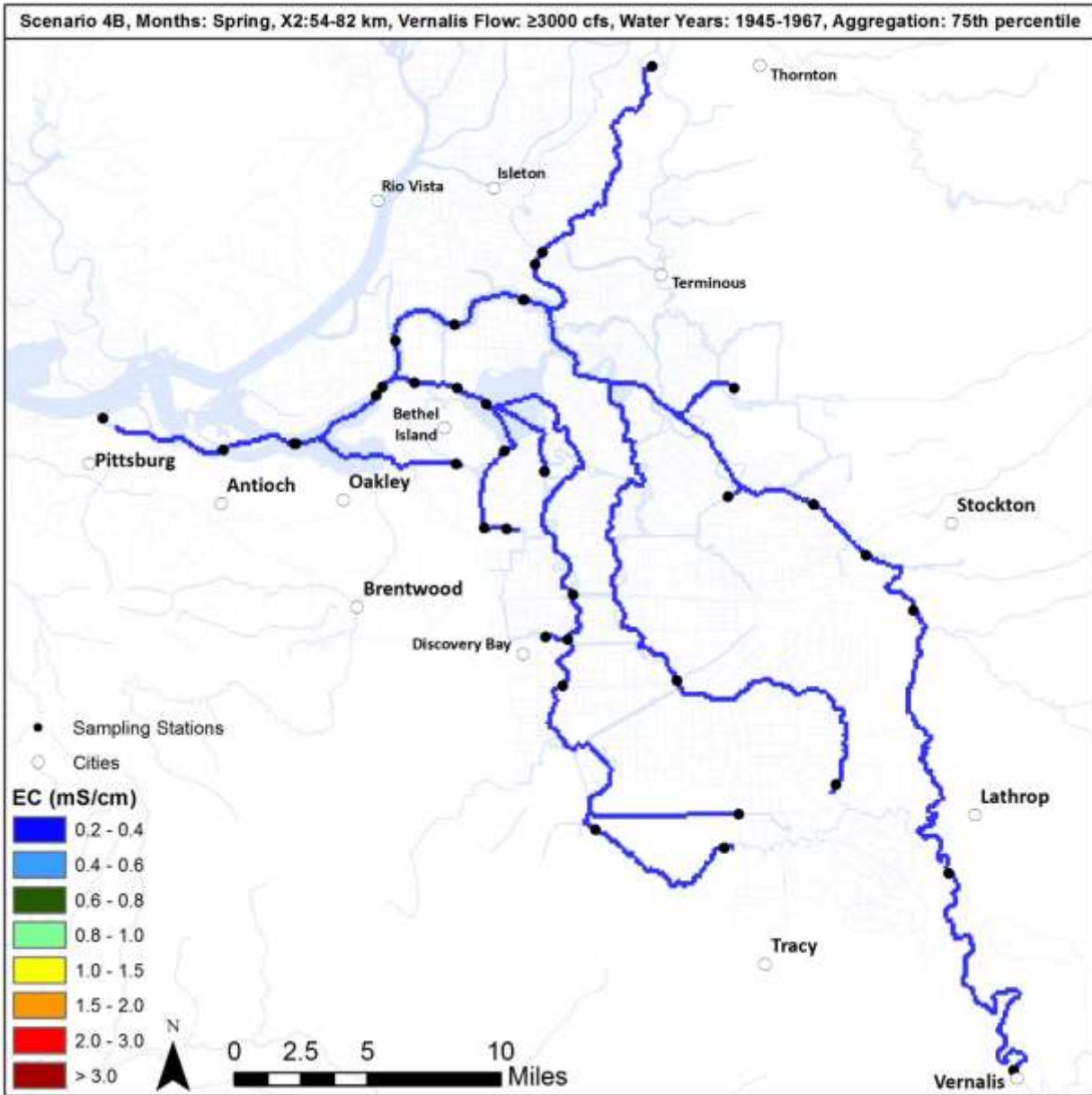


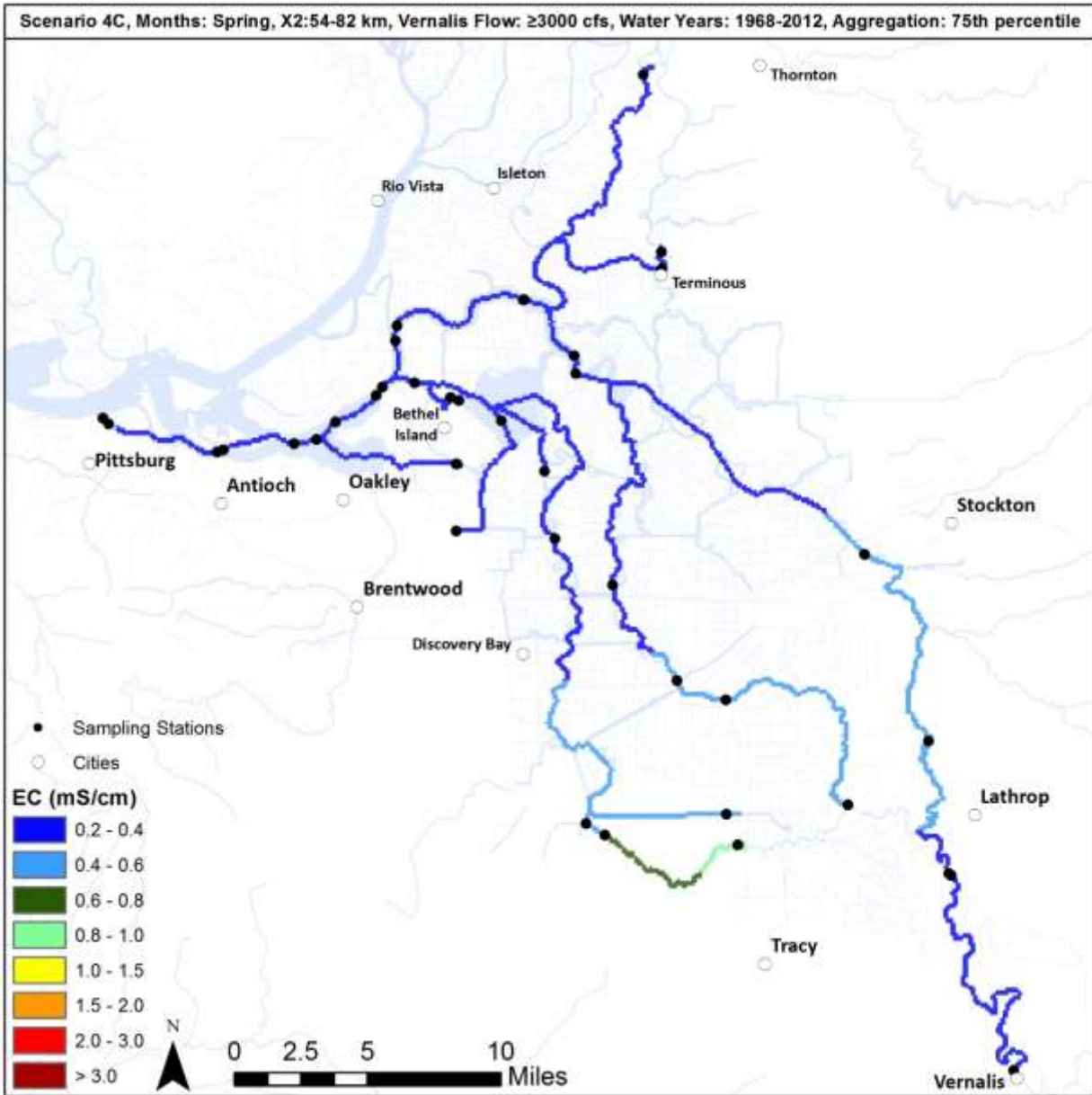


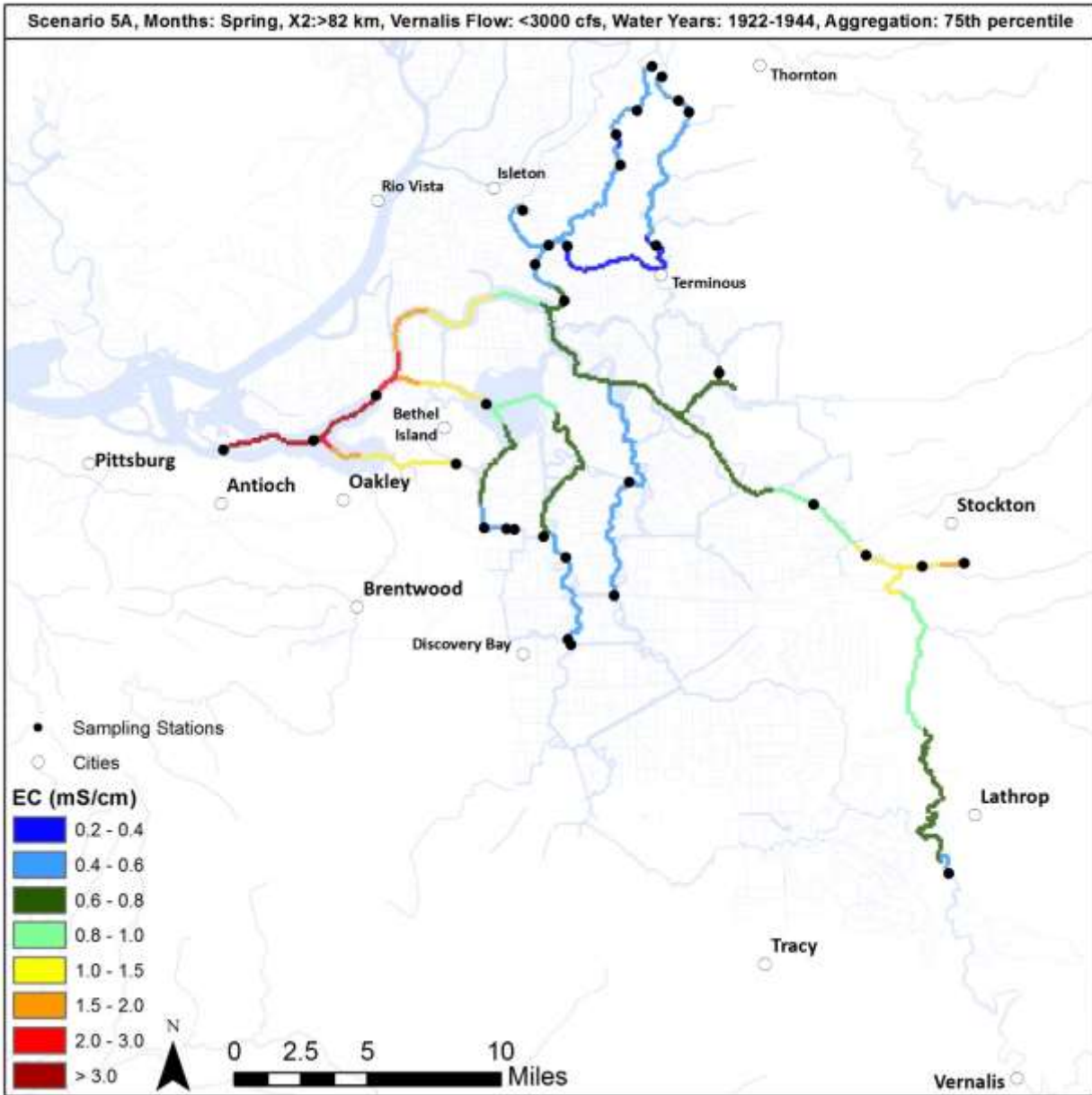


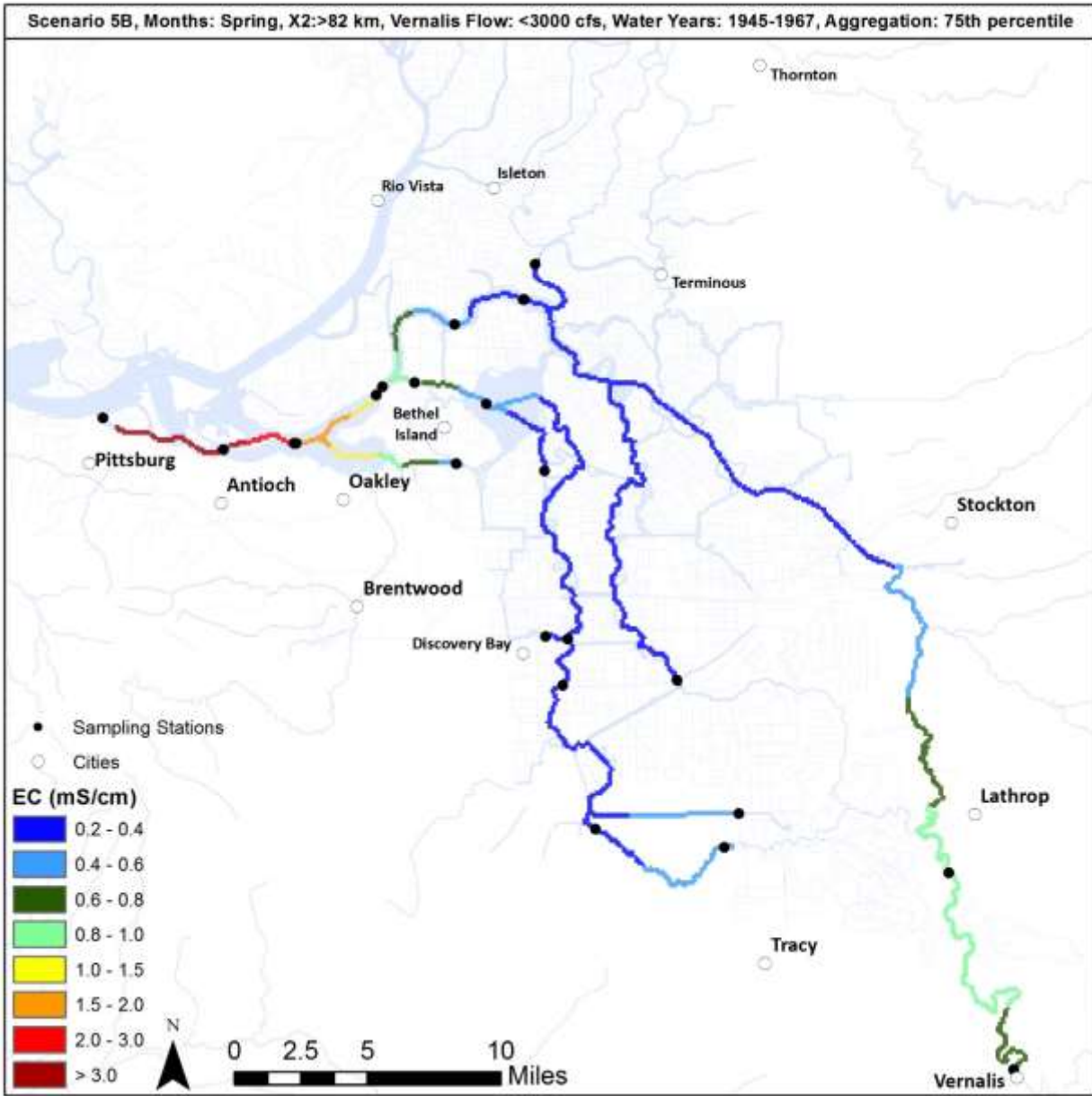


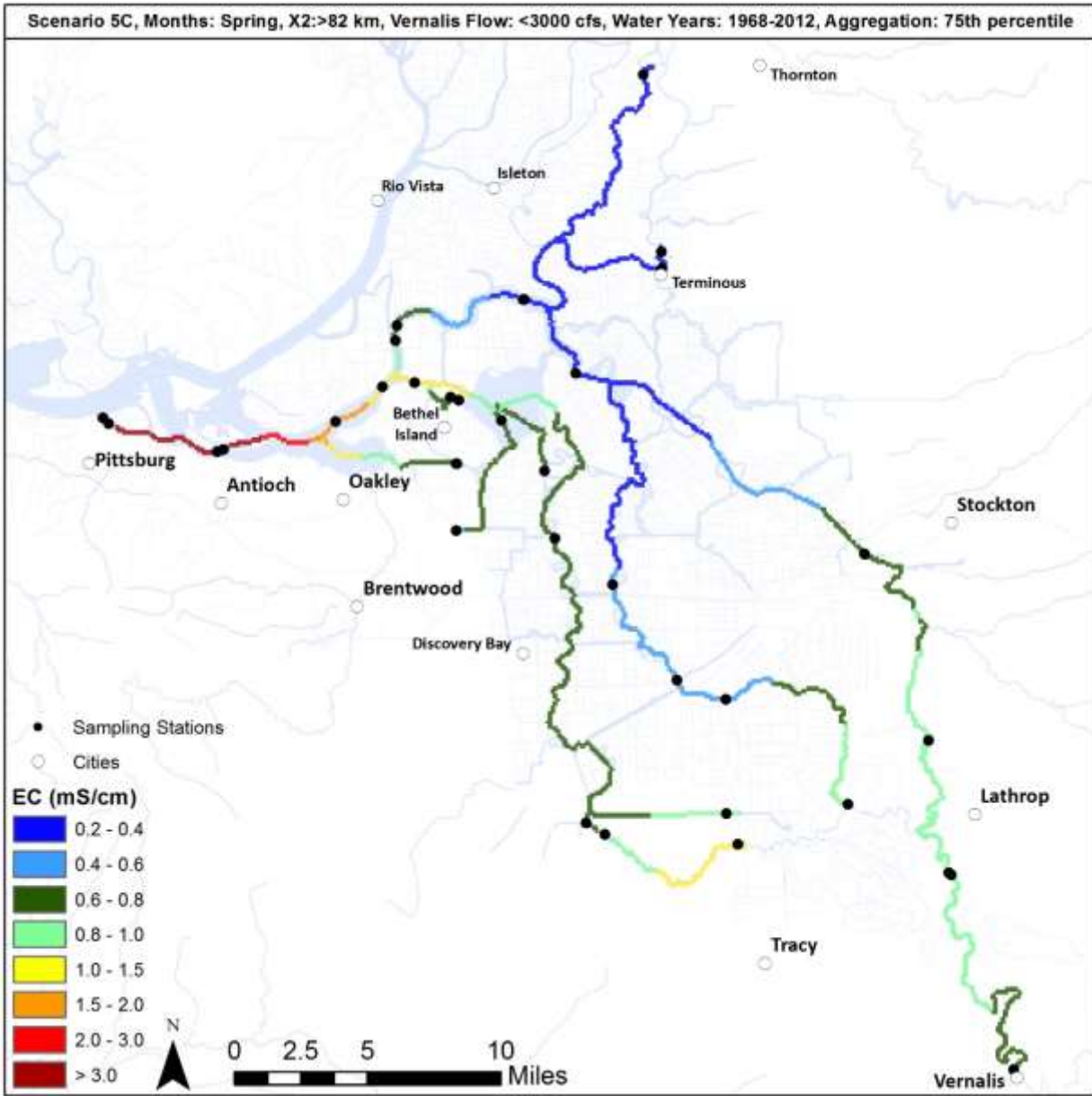


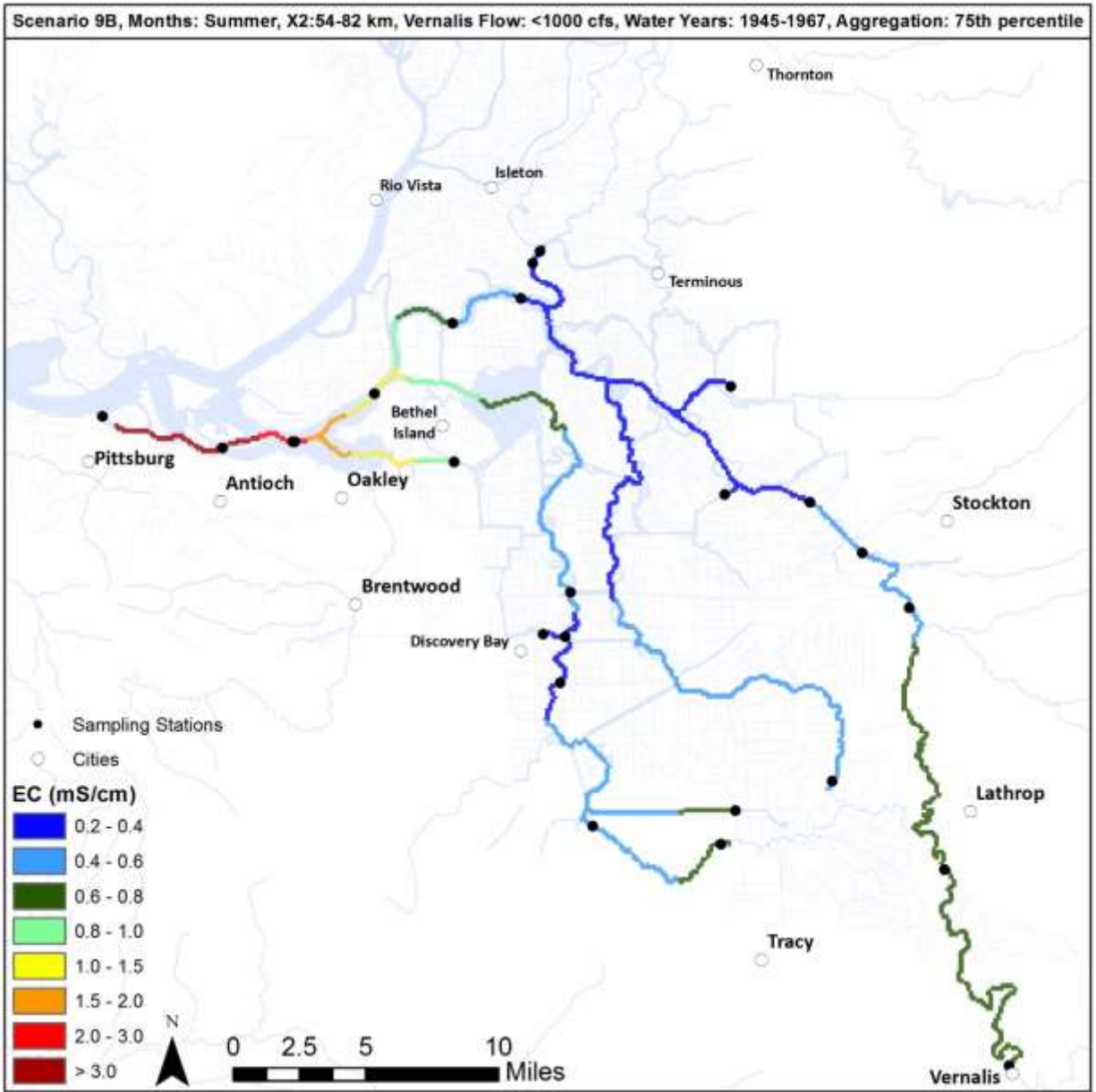


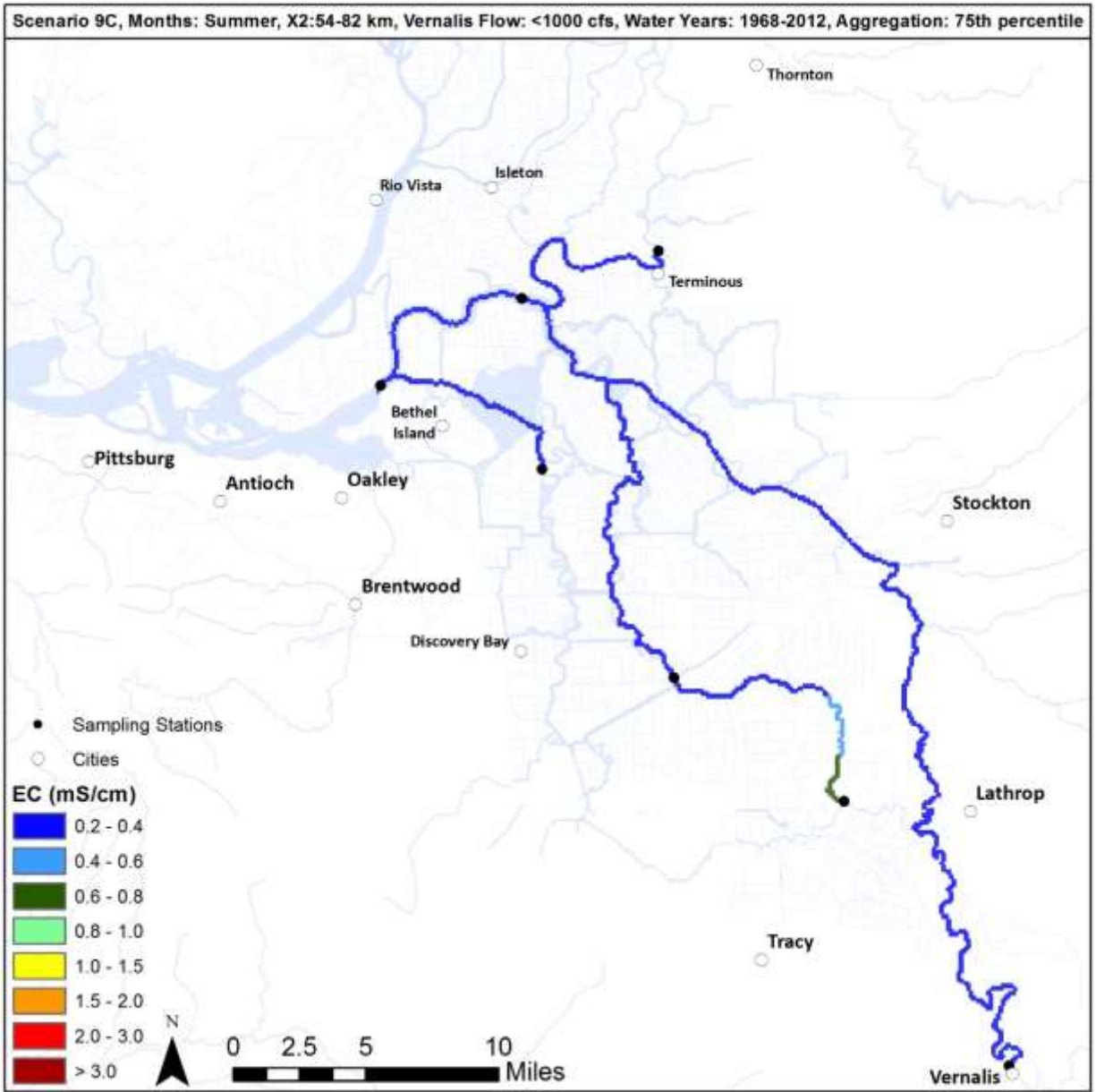


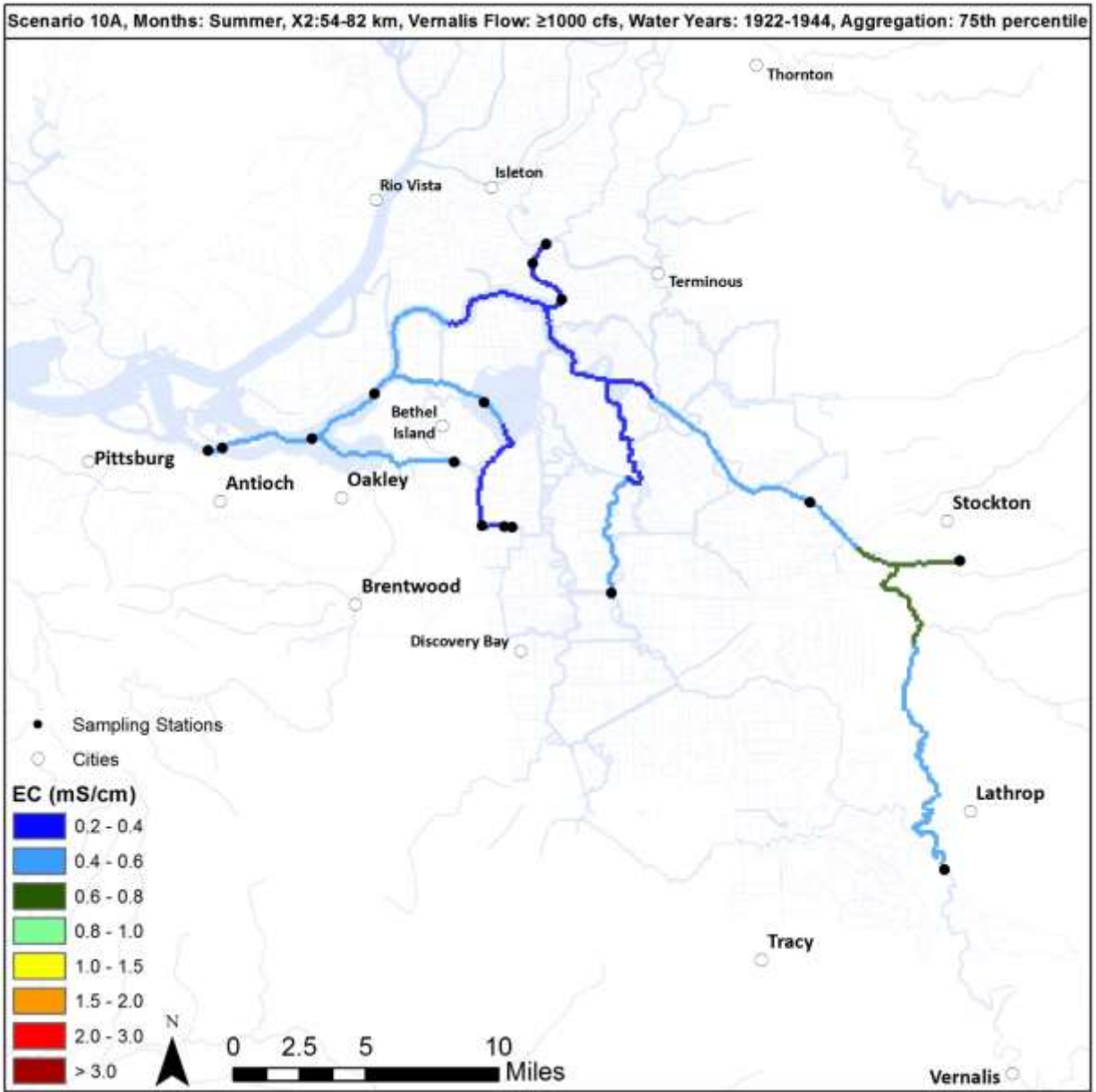


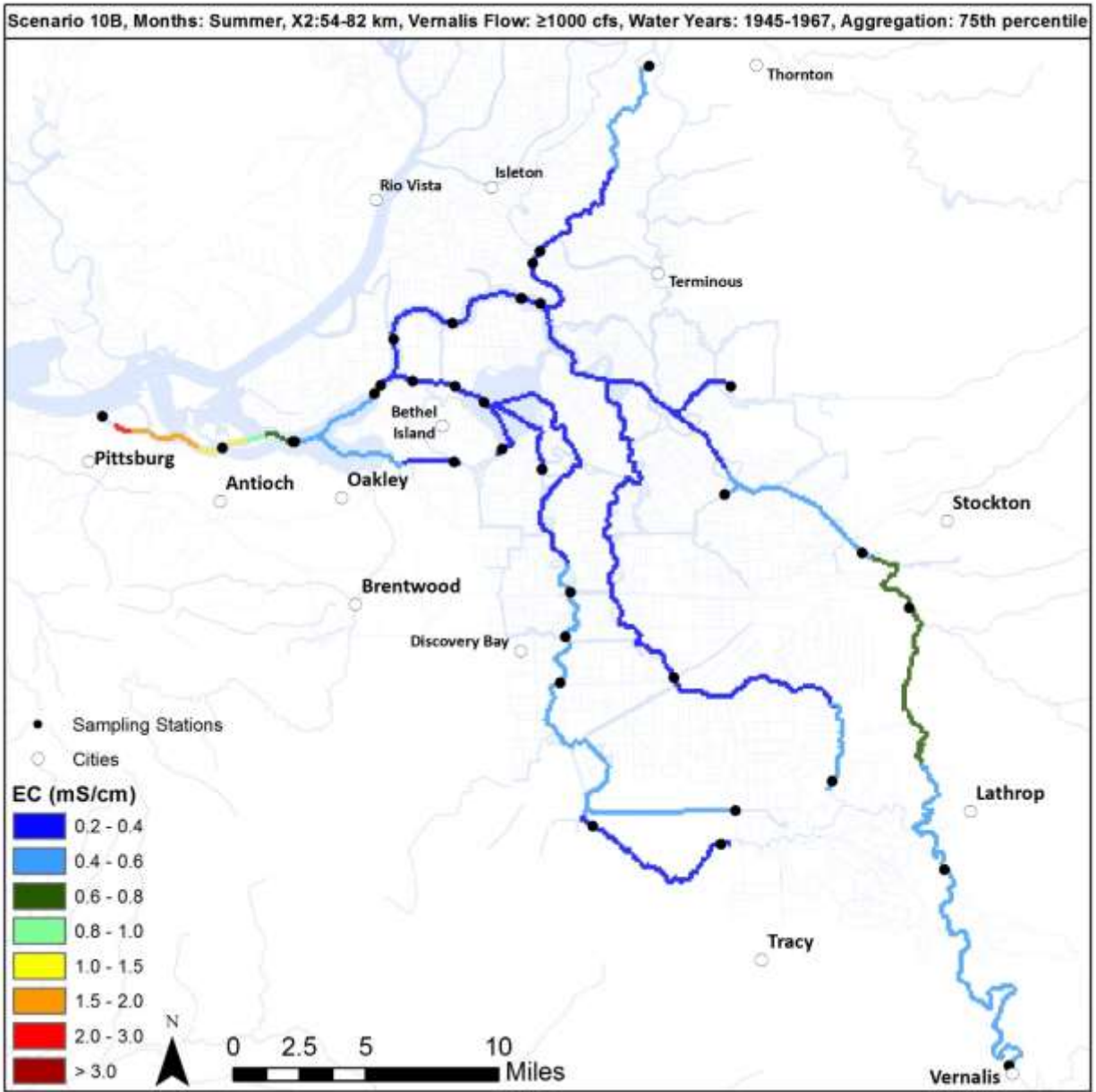


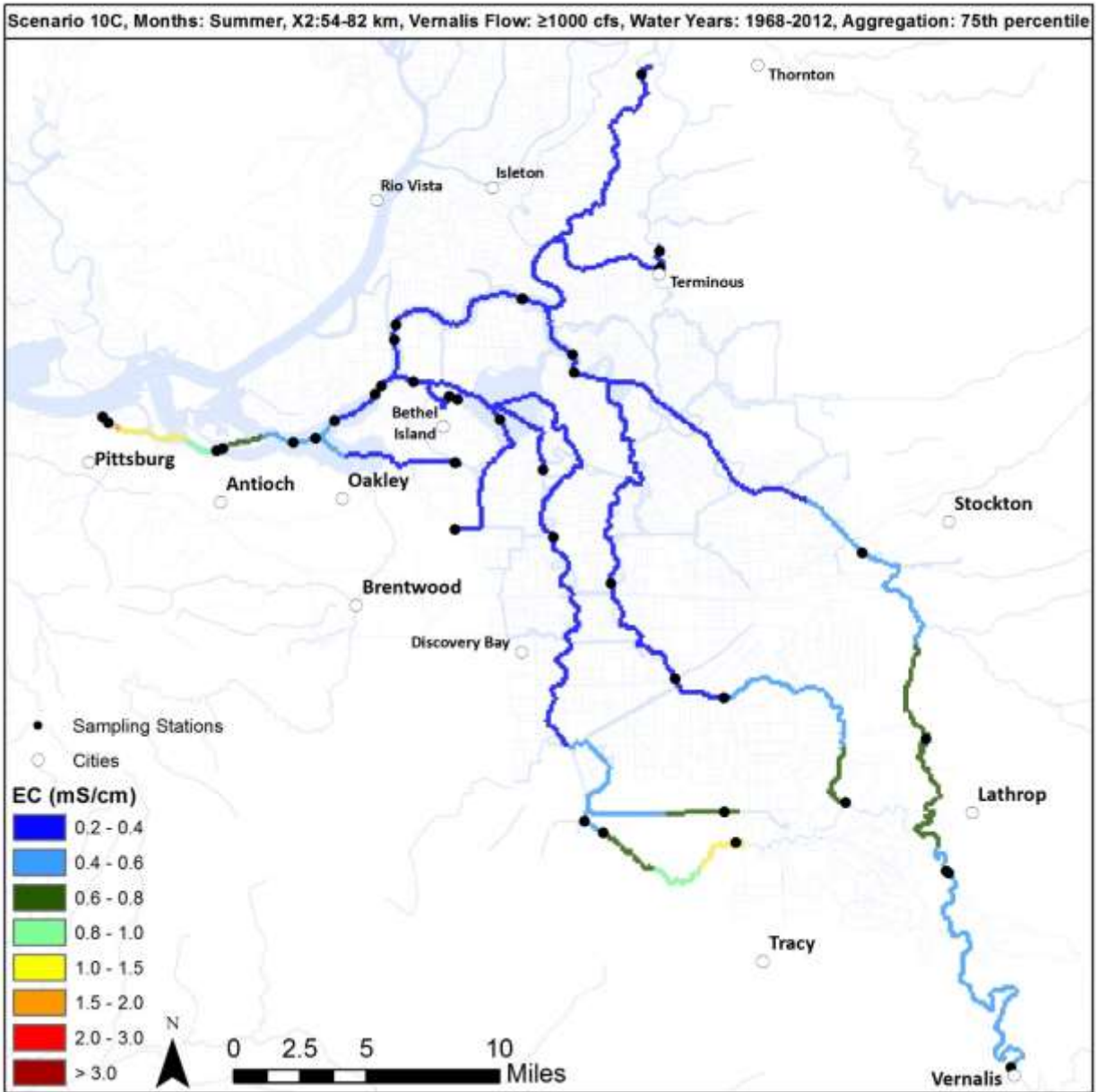


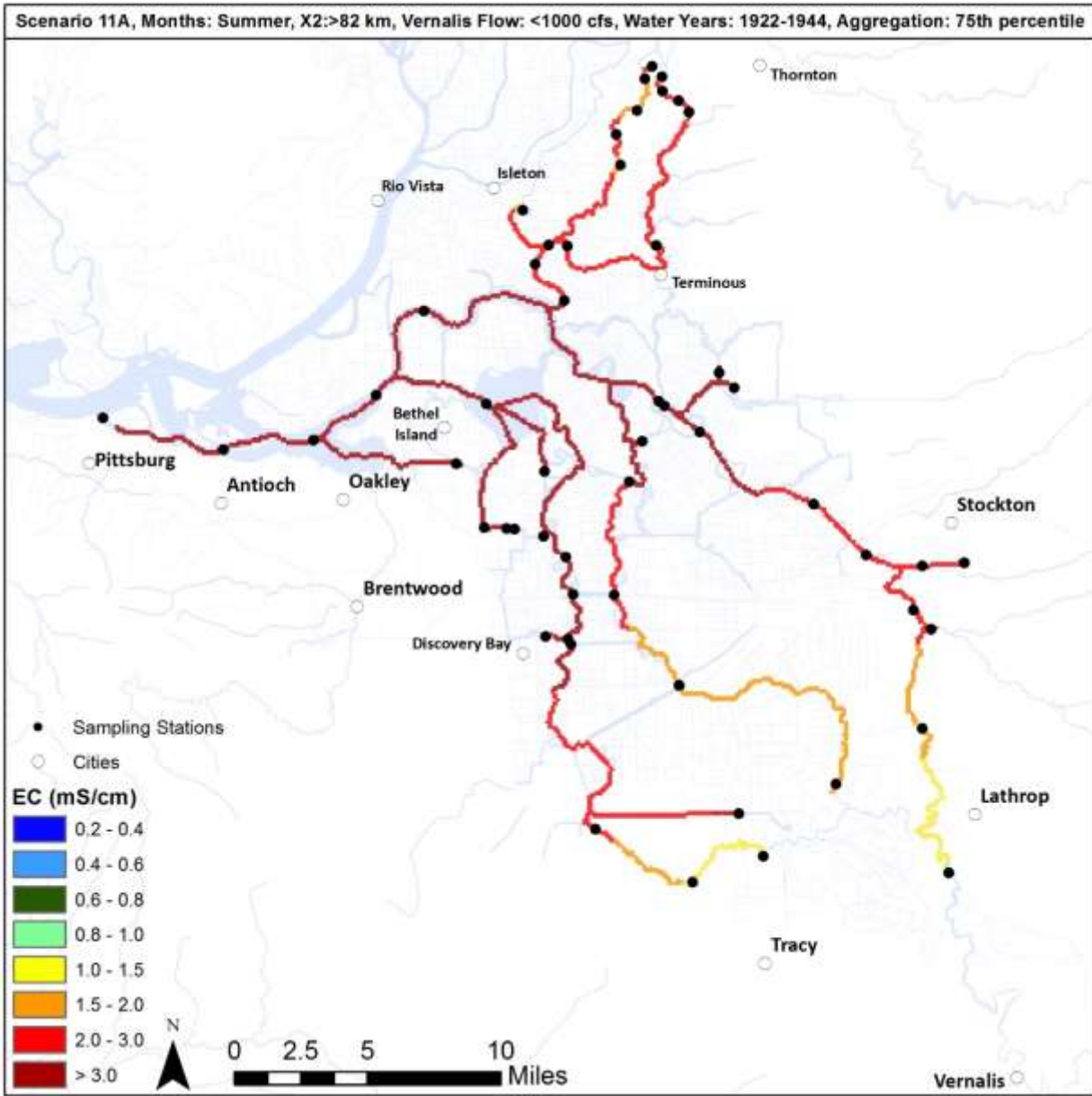


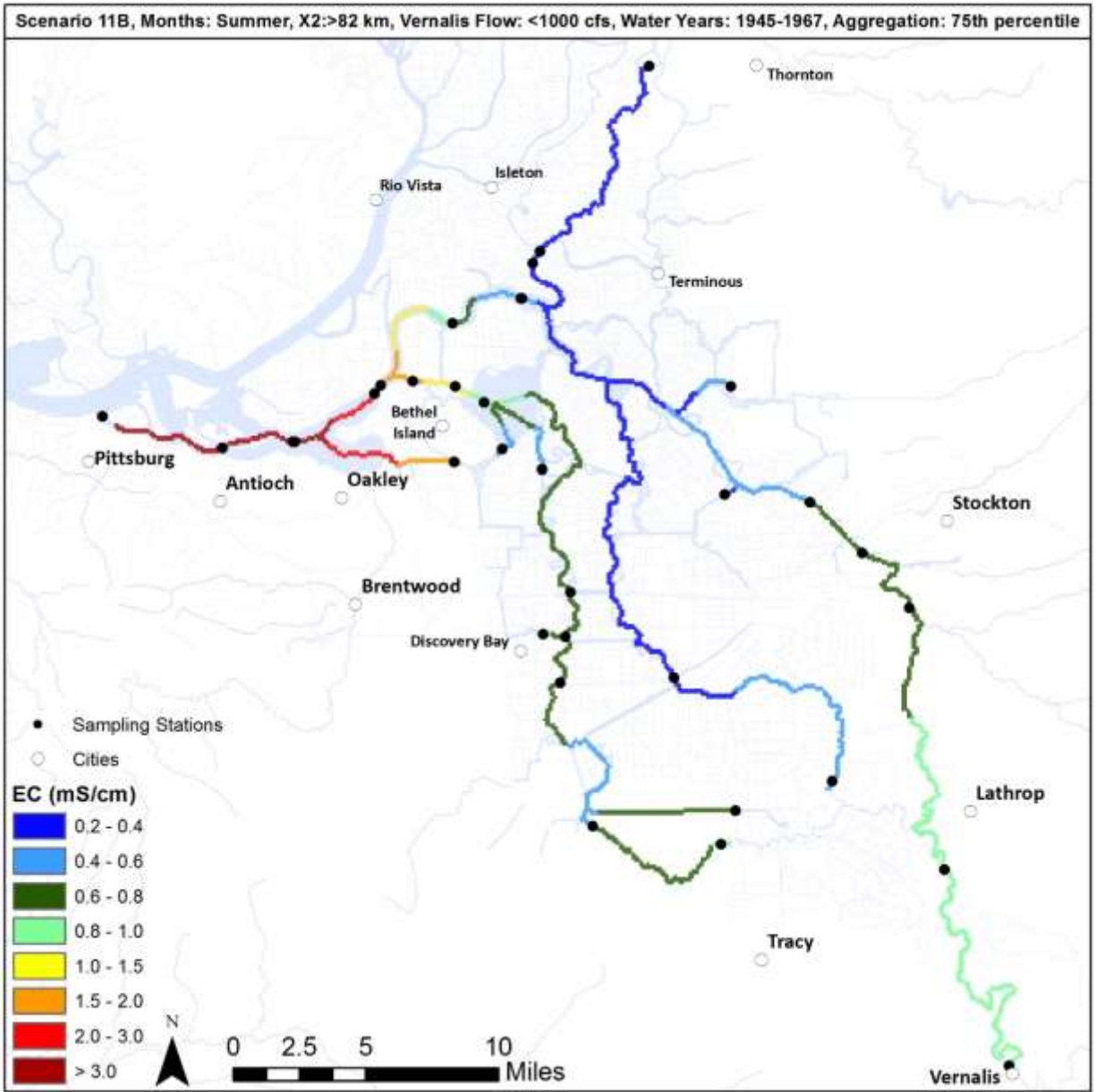


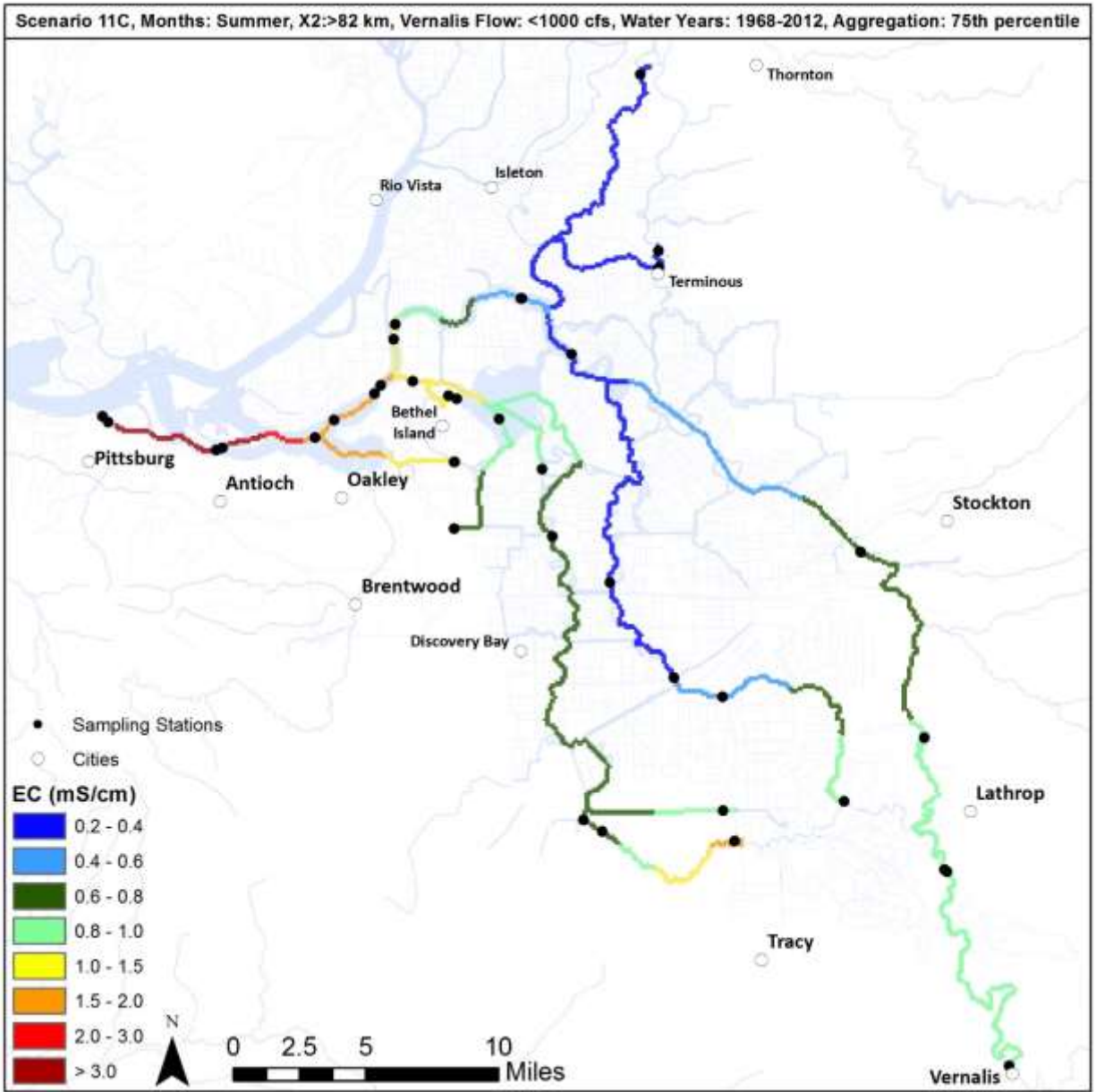


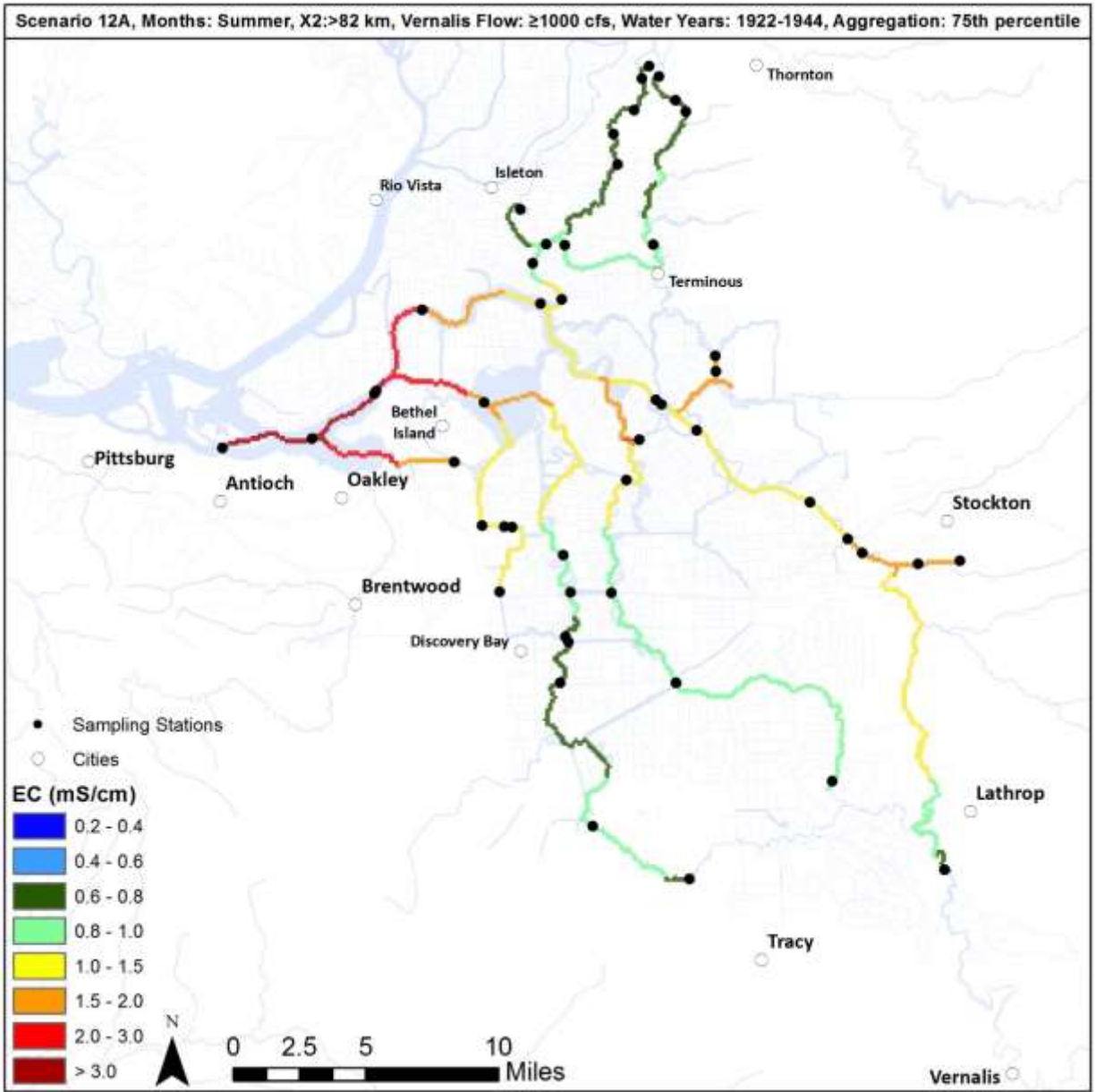


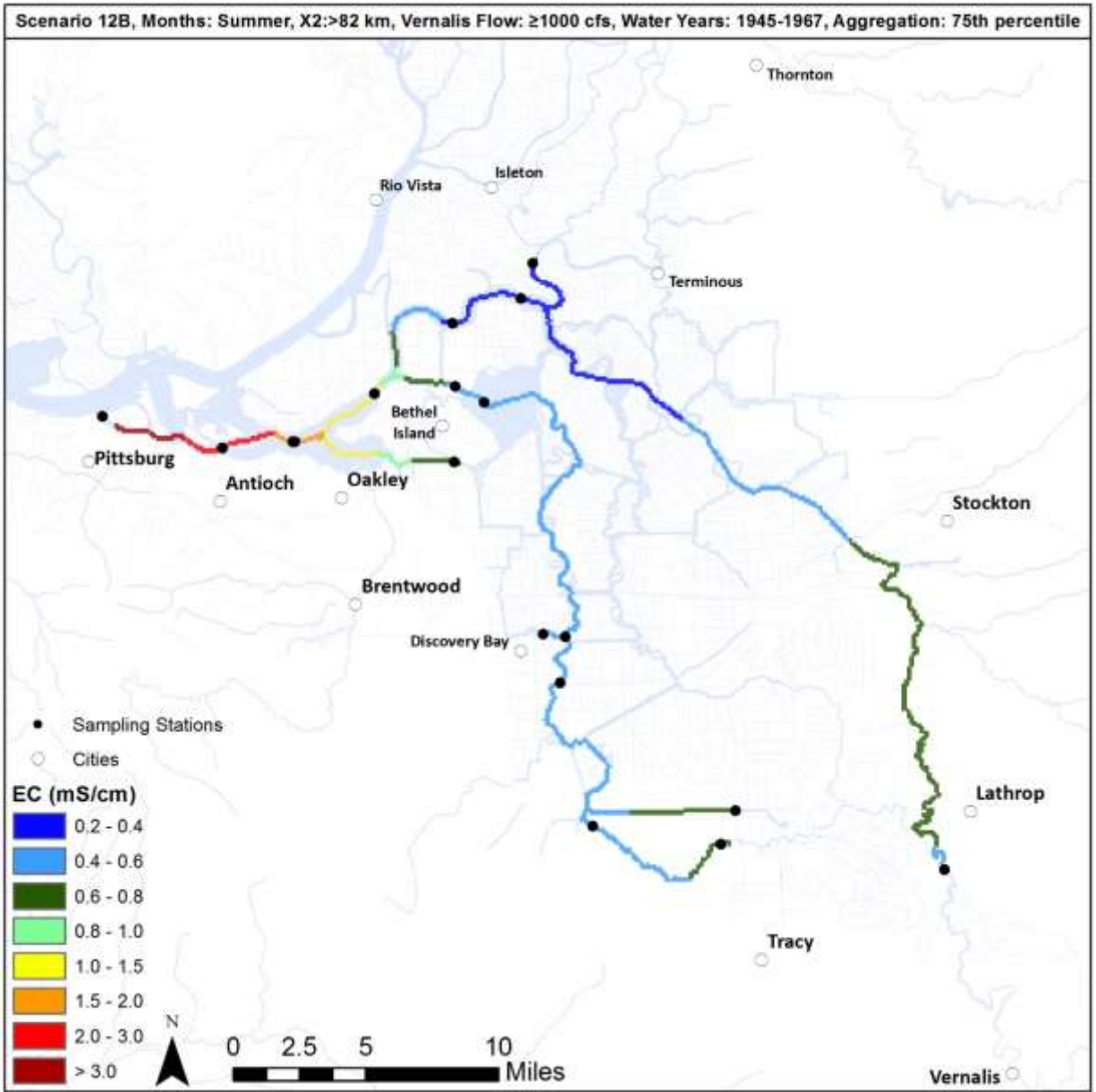


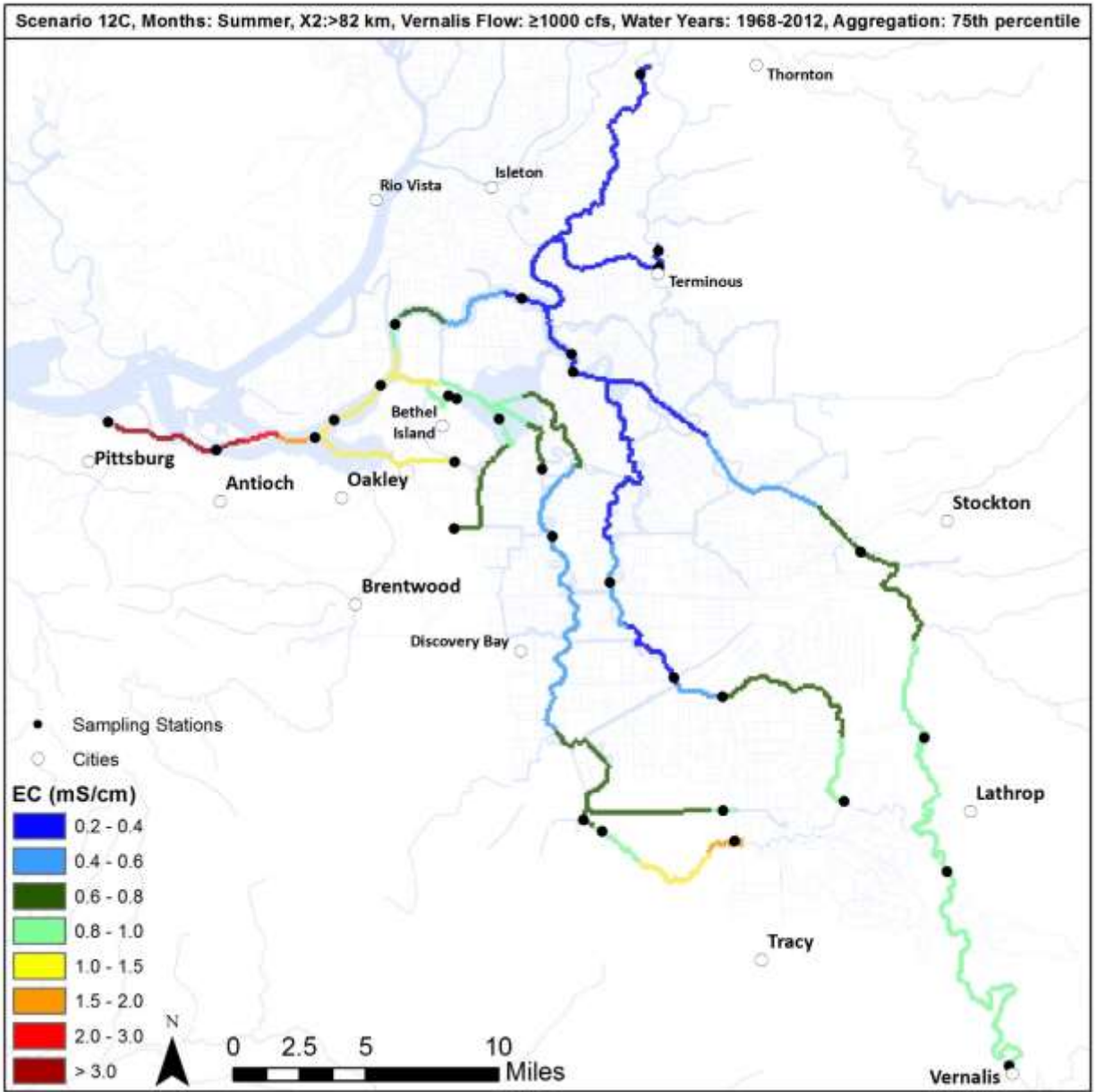












Appendix E. TREND PLOTS

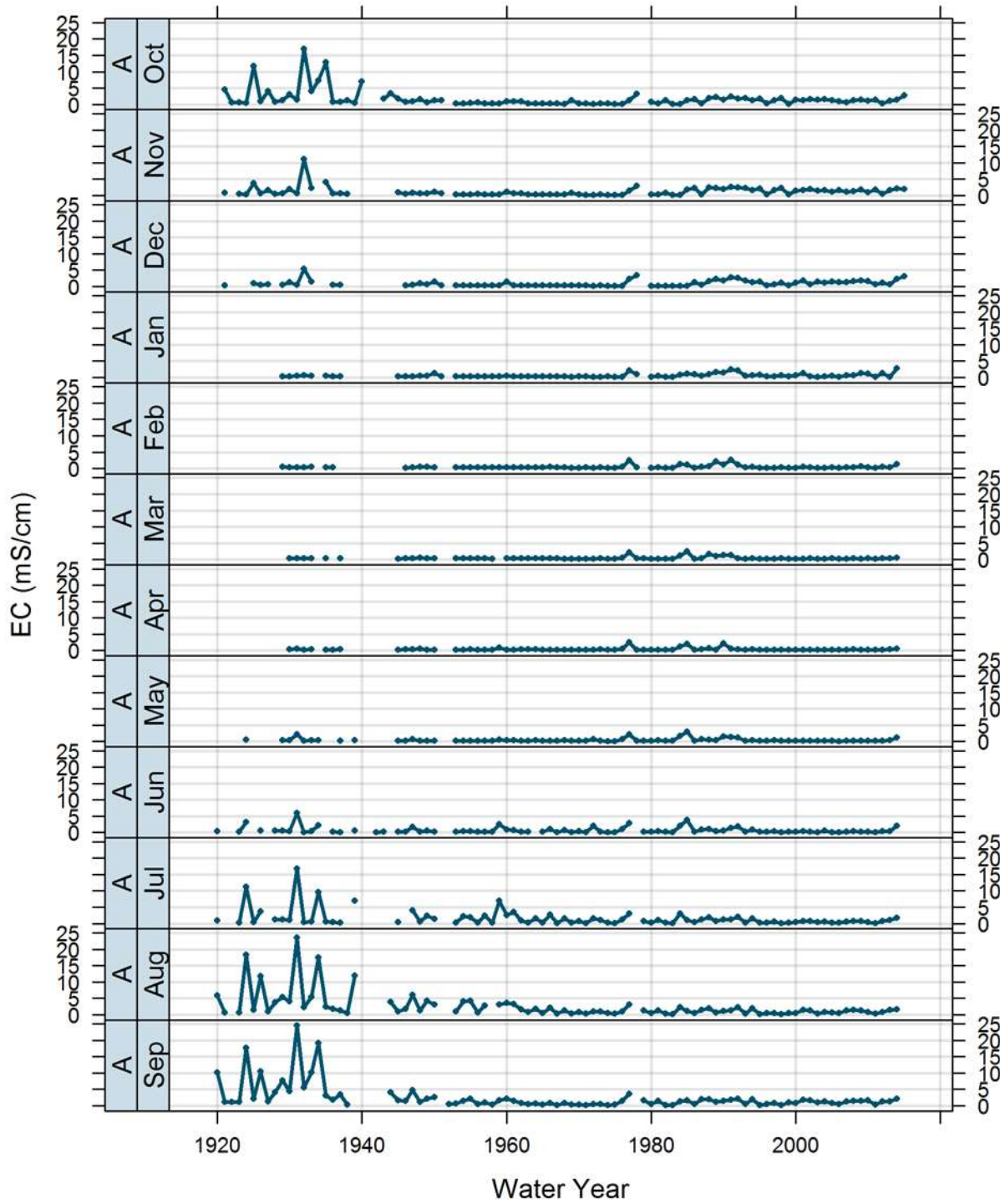


Figure E-1 Time series plots of group A by month. (Group-specific y-axis)

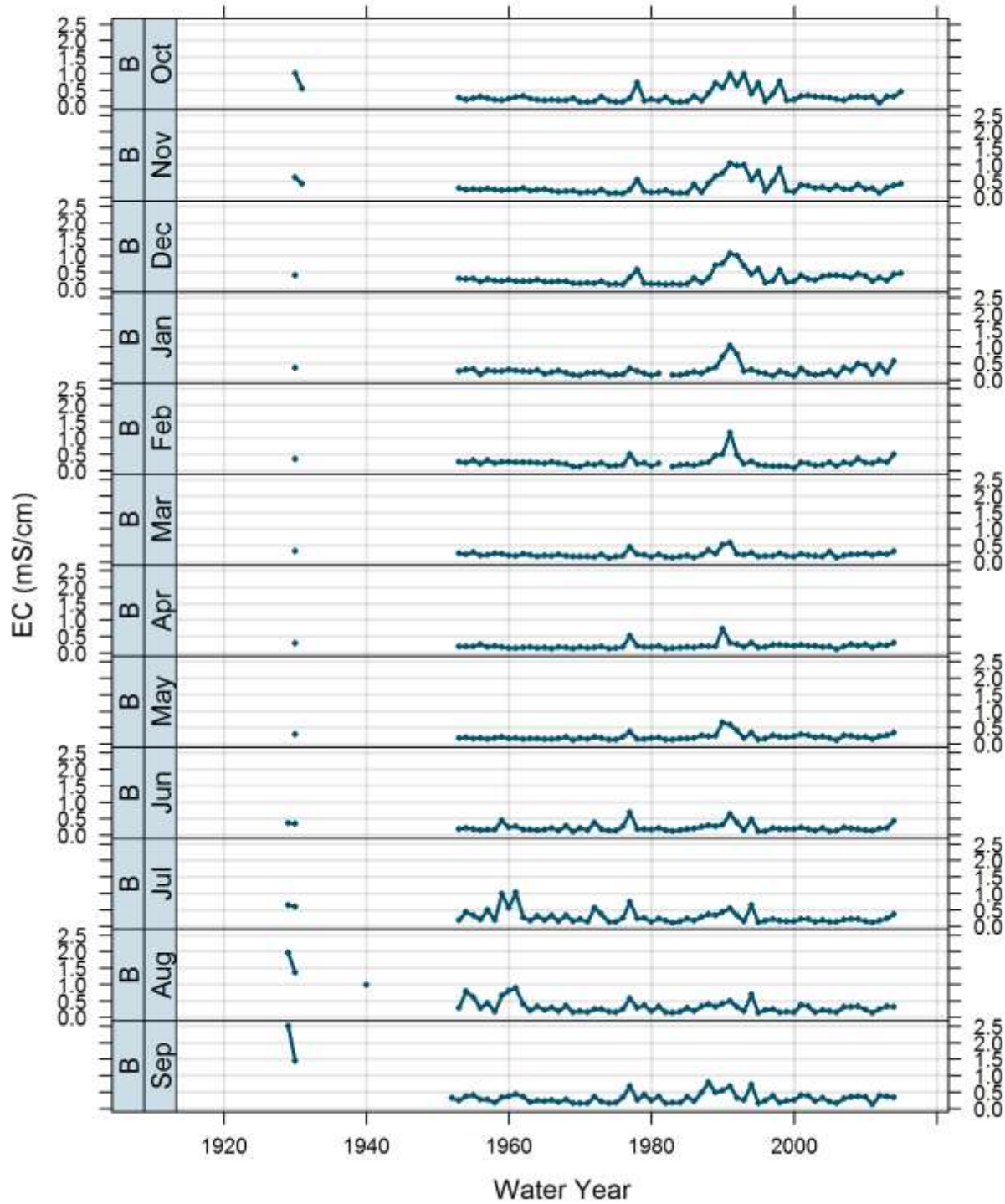


Figure E-2 Time series plots of group B by month. (Group-specific y-axis)

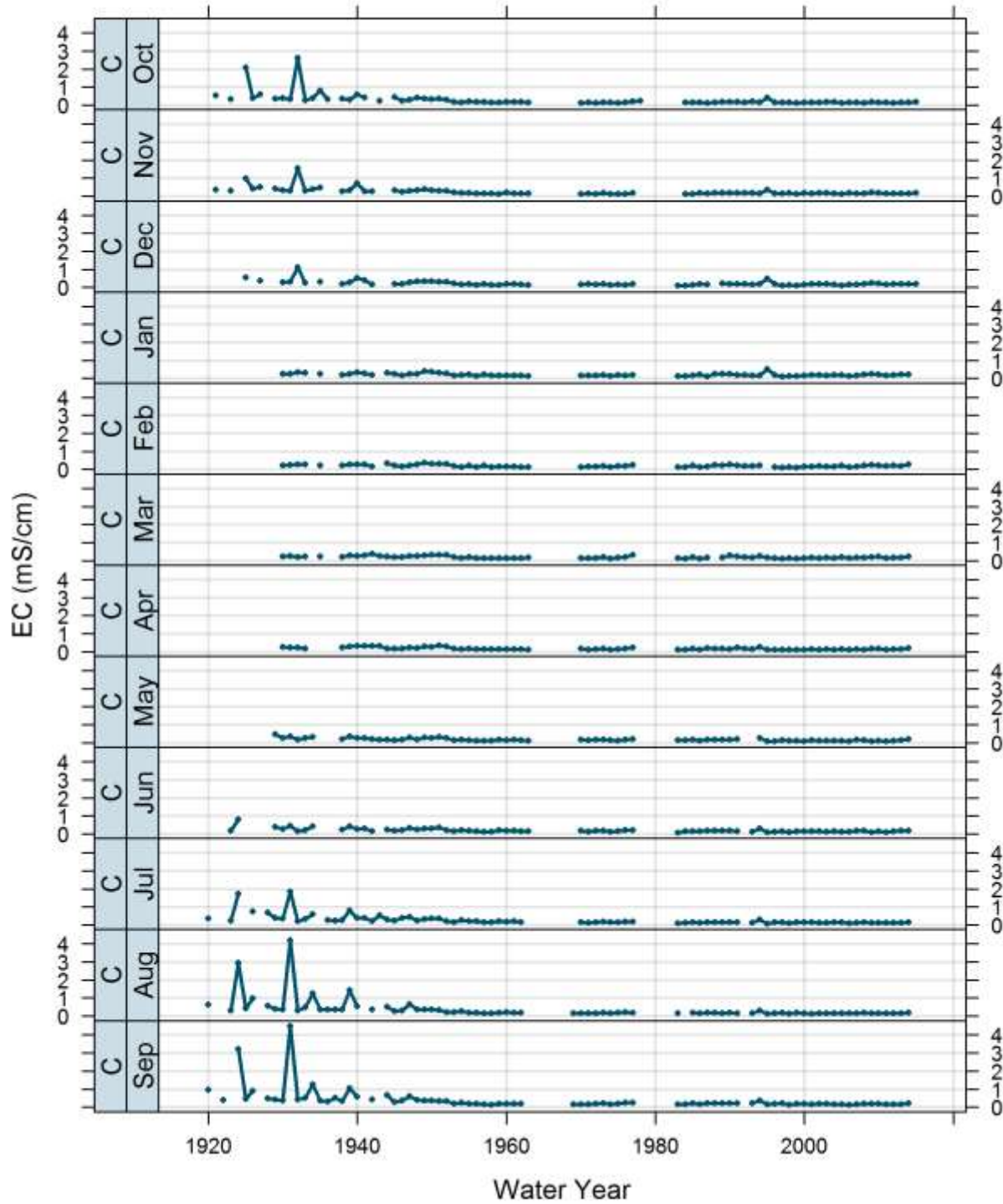


Figure E-3 Time series plots of group C by month. (Group-specific y-axis)

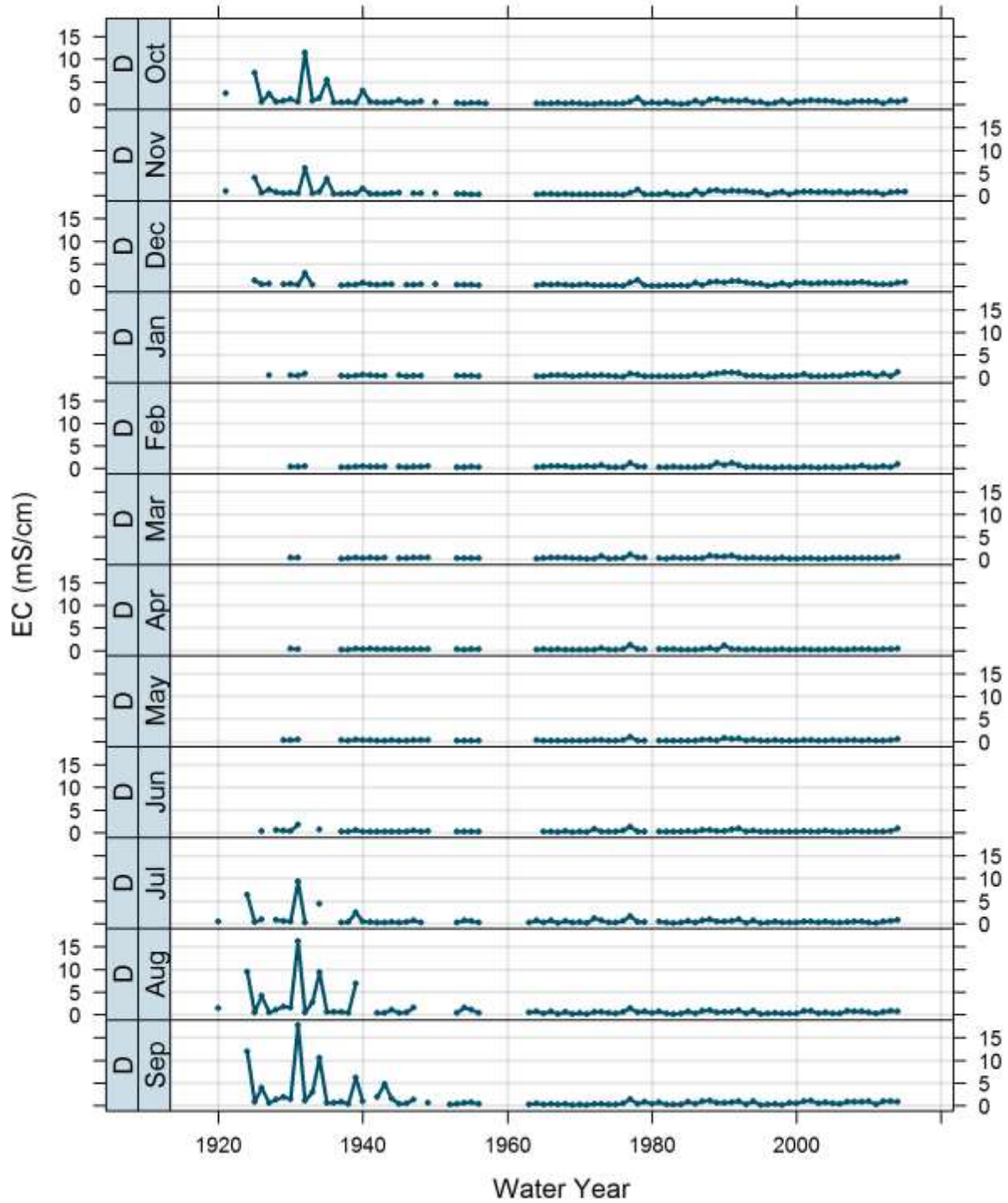


Figure E-4 Time series plots of group D by month. (Group-specific y-axis)

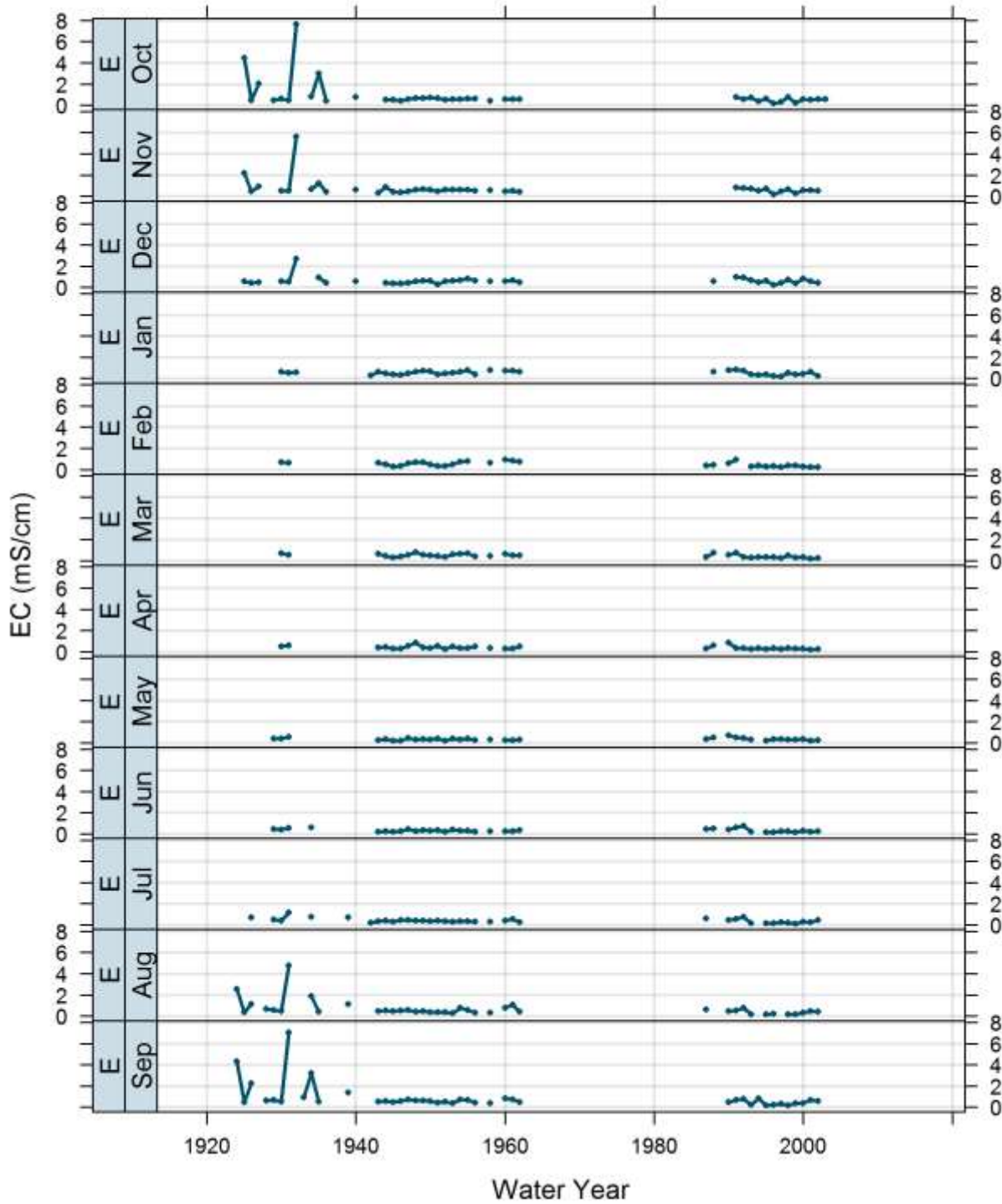


Figure E-5 Time series plots of group E by month. (Group-specific y-axis)

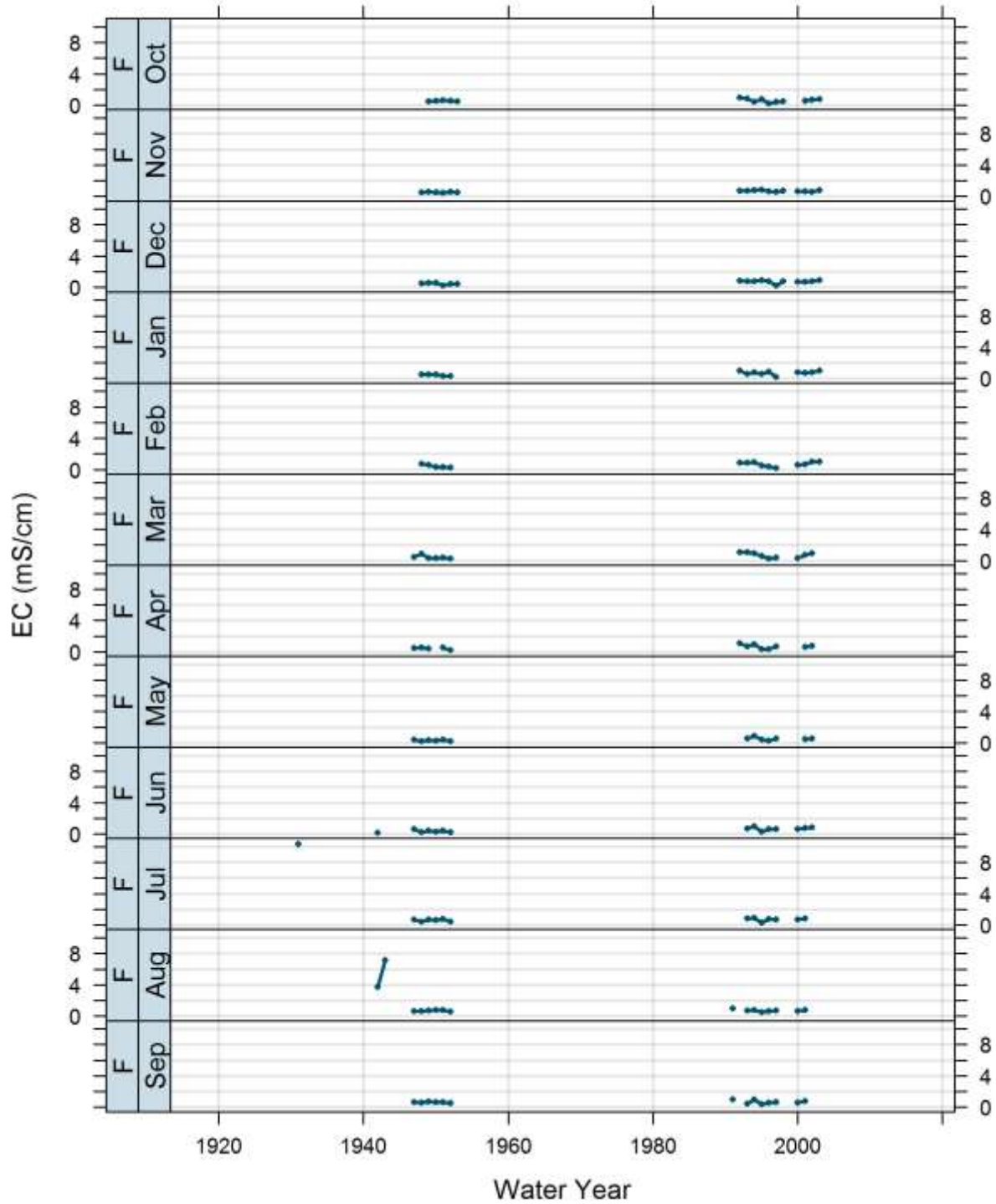


Figure E-6 Time series plots of group F by month. (Group-specific y-axis)

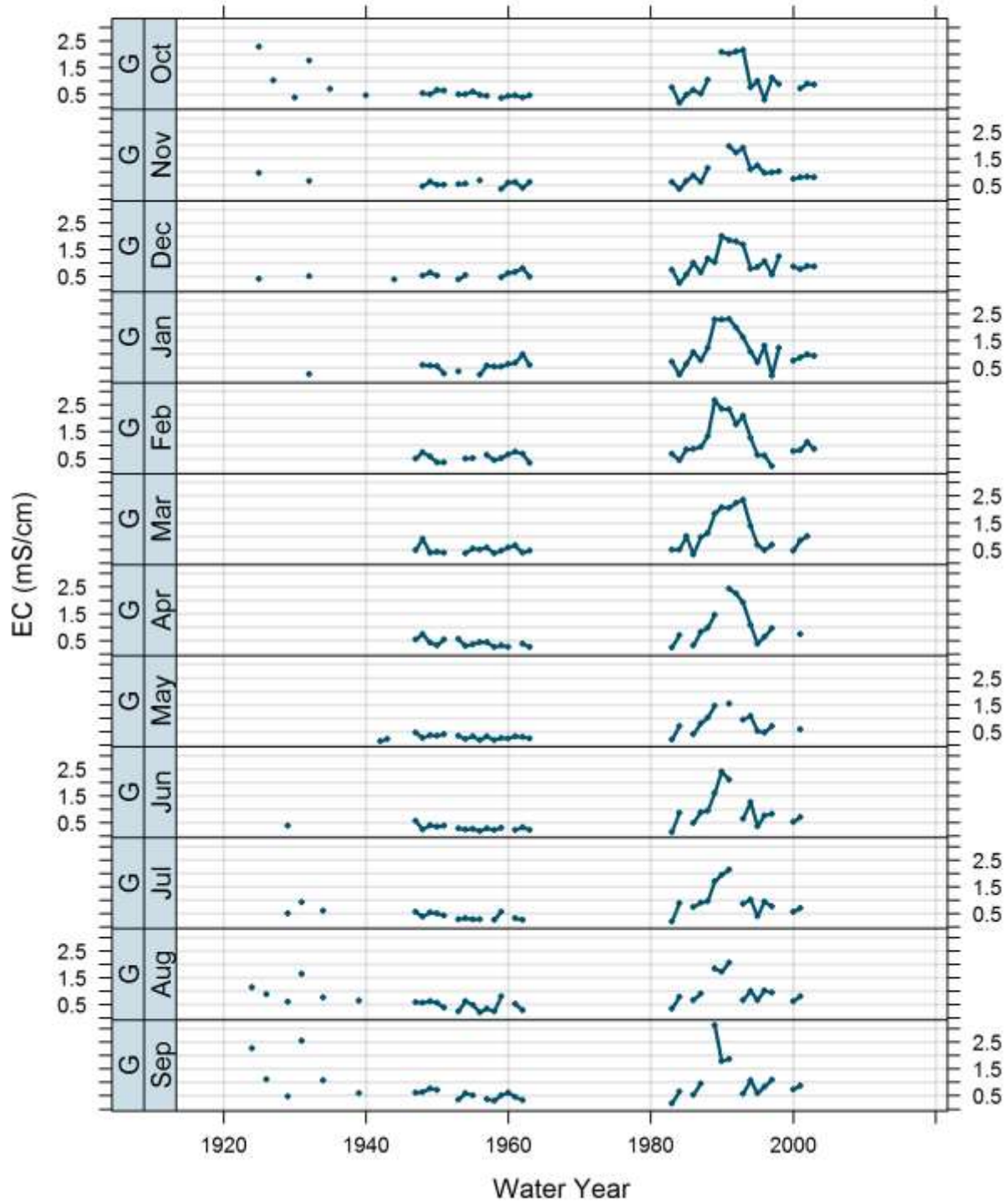


Figure E-7 Time series plots of group G by month. (Group-specific y-axis)

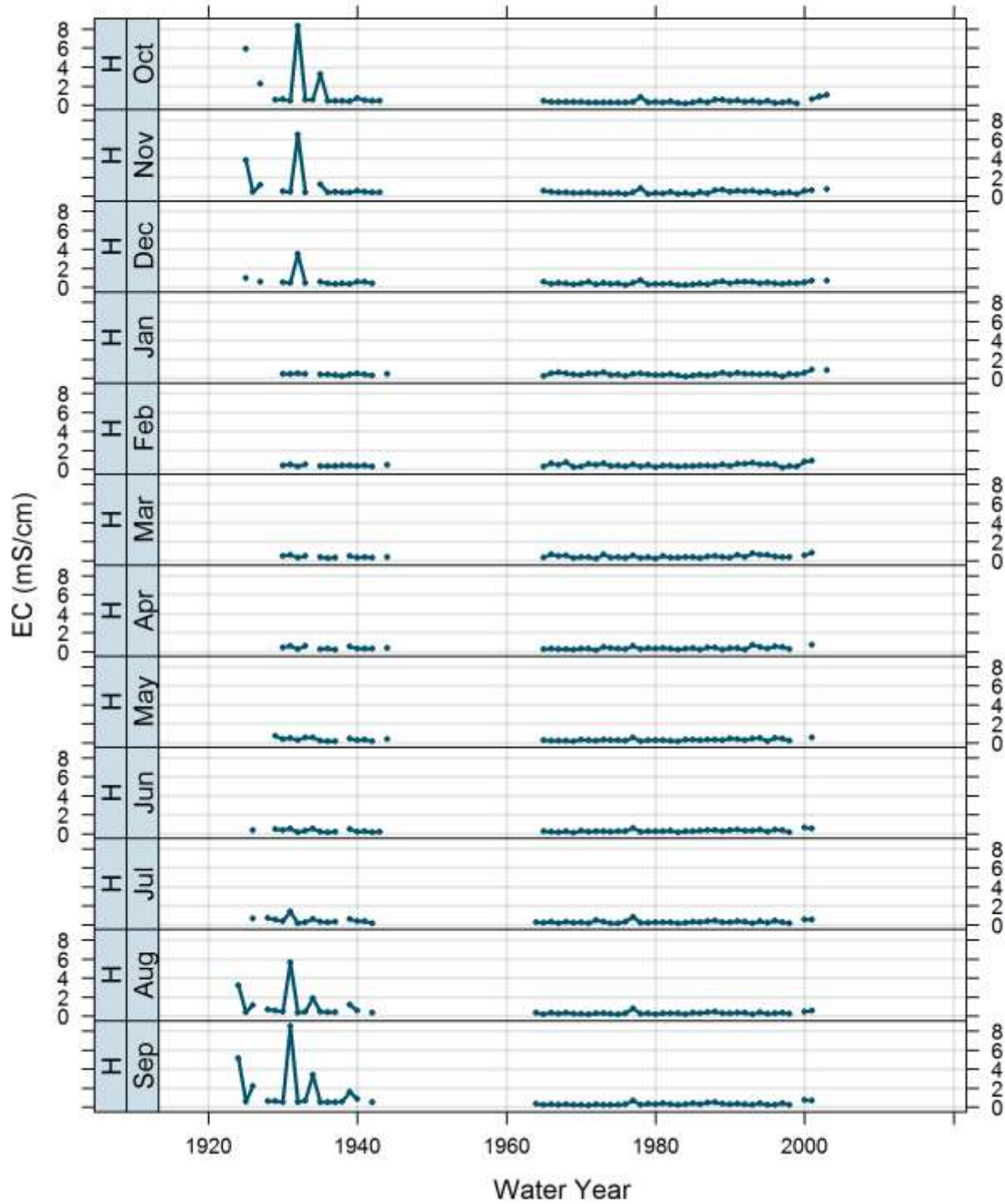


Figure E-8 Time series plots of group H by month. (Group-specific y-axis)

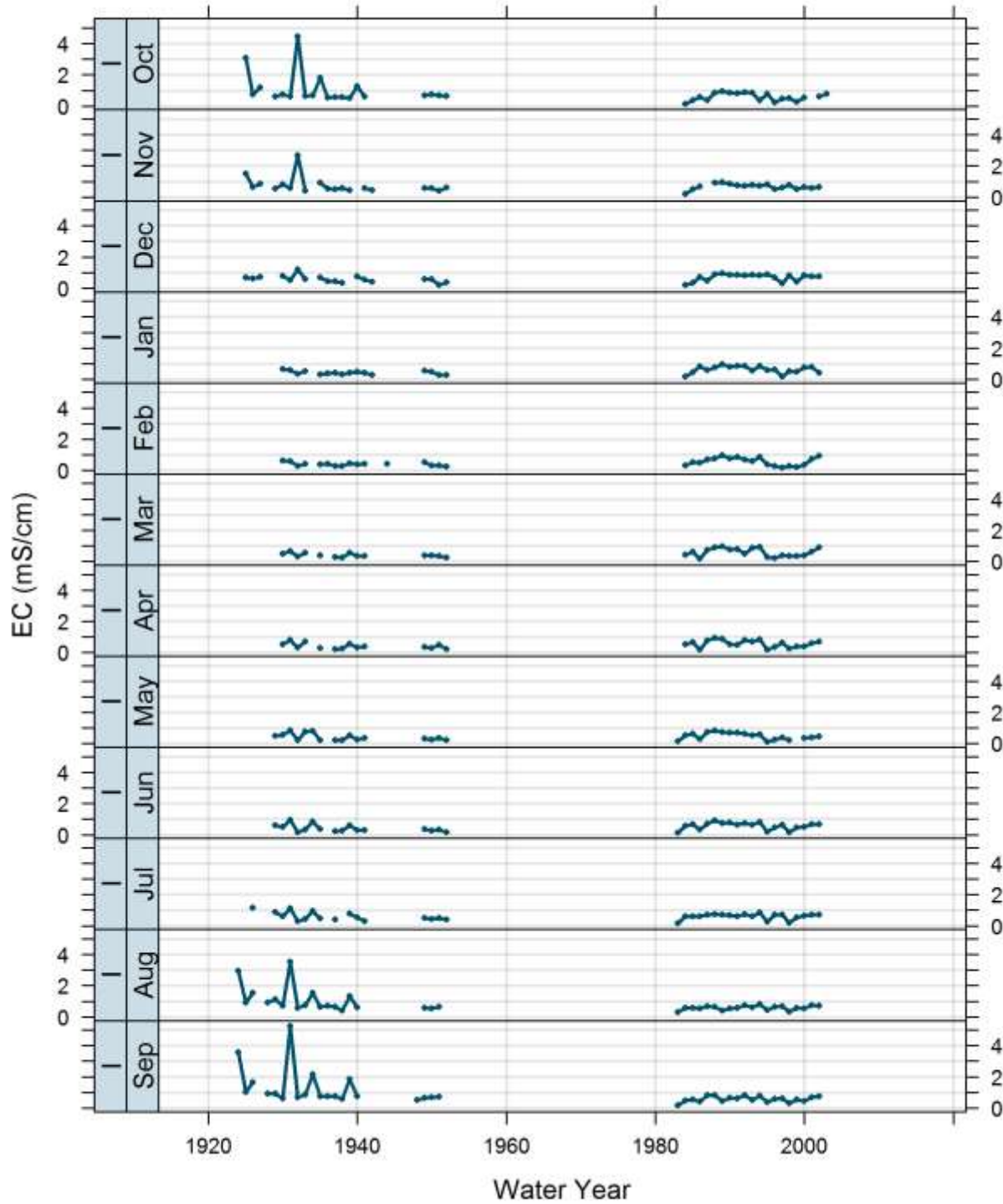


Figure E-9 Time series plots of group I by month. (Group-specific y-axis)

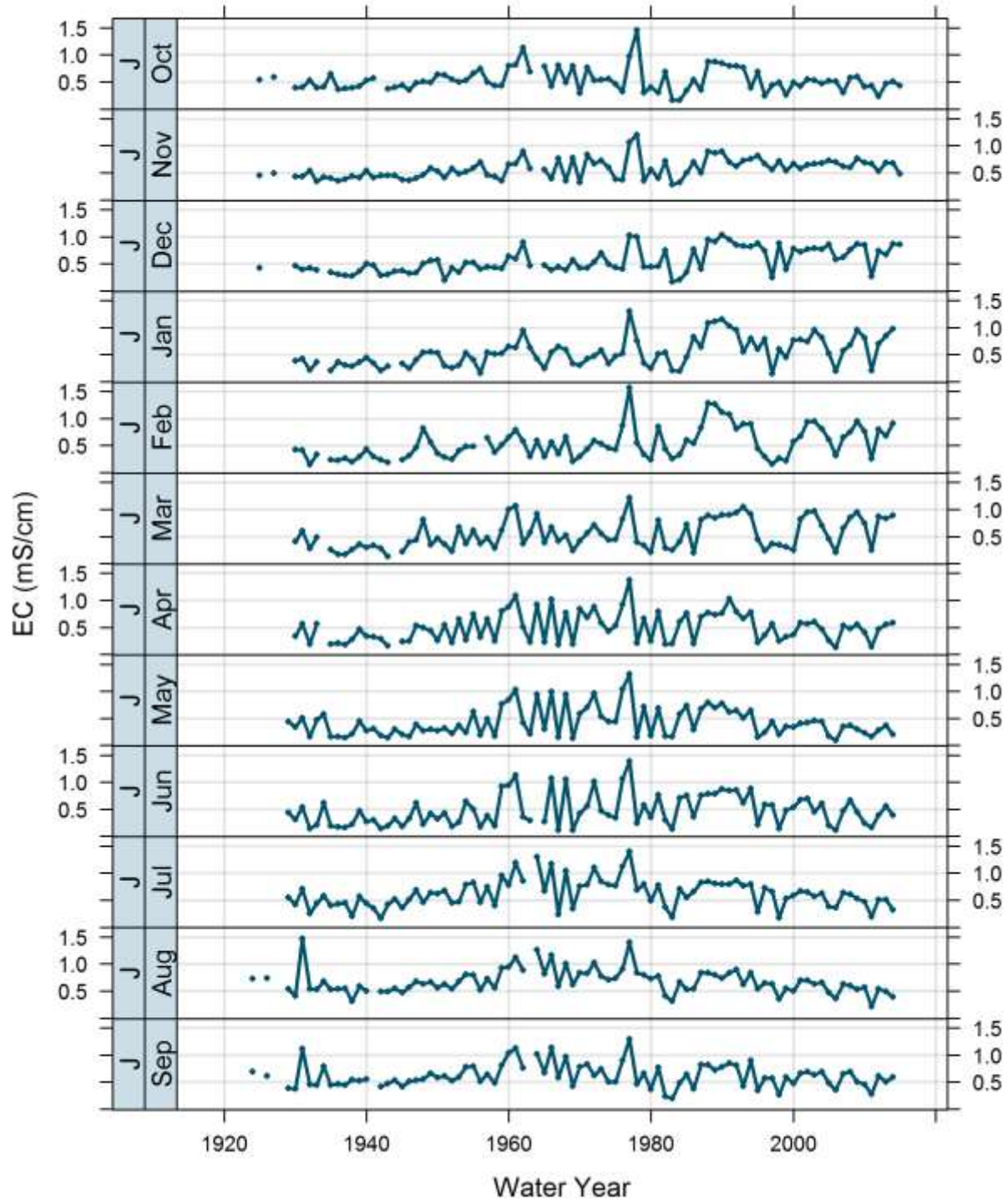


Figure E-10 Time series plots of group J by month. (Group-specific y-axis)

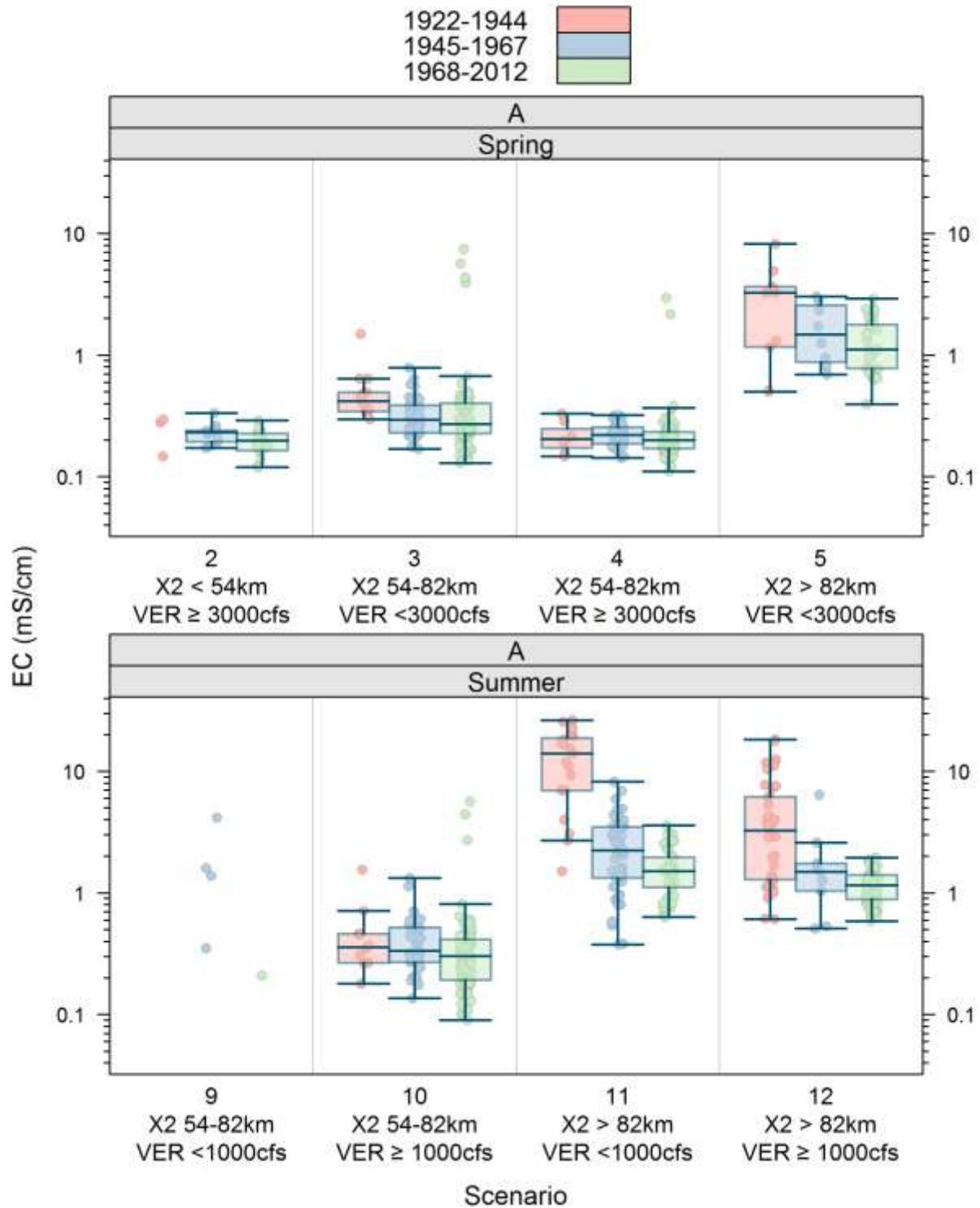


Figure E-11 **Box plots (when n > 5) and scatter plots of monthly average EC data for group A**

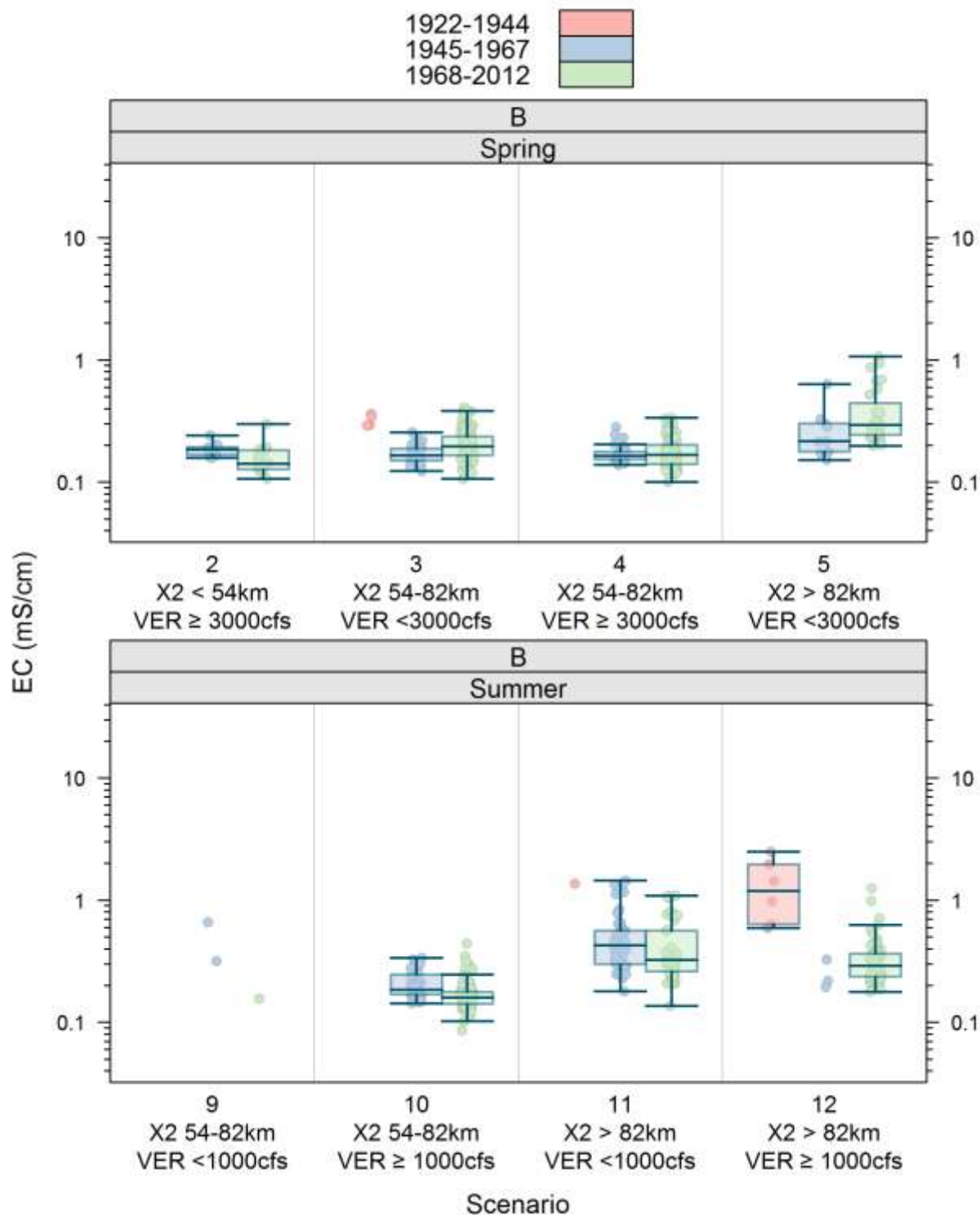


Figure E-12 Box plots (when n > 5) and scatter plots of monthly average EC data for group B

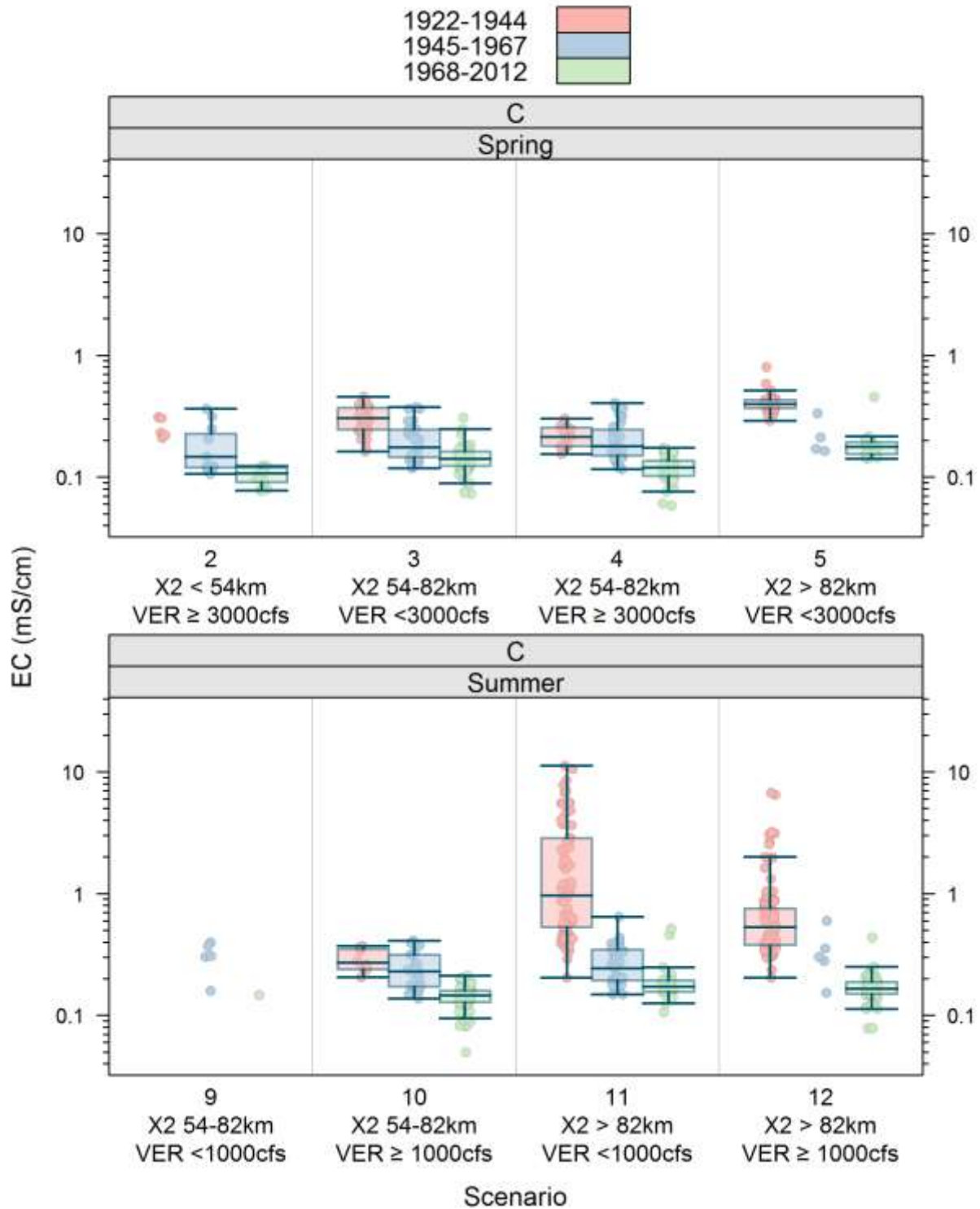


Figure E-13 Box plots (when n > 5) and scatter plots of monthly average EC data for group C

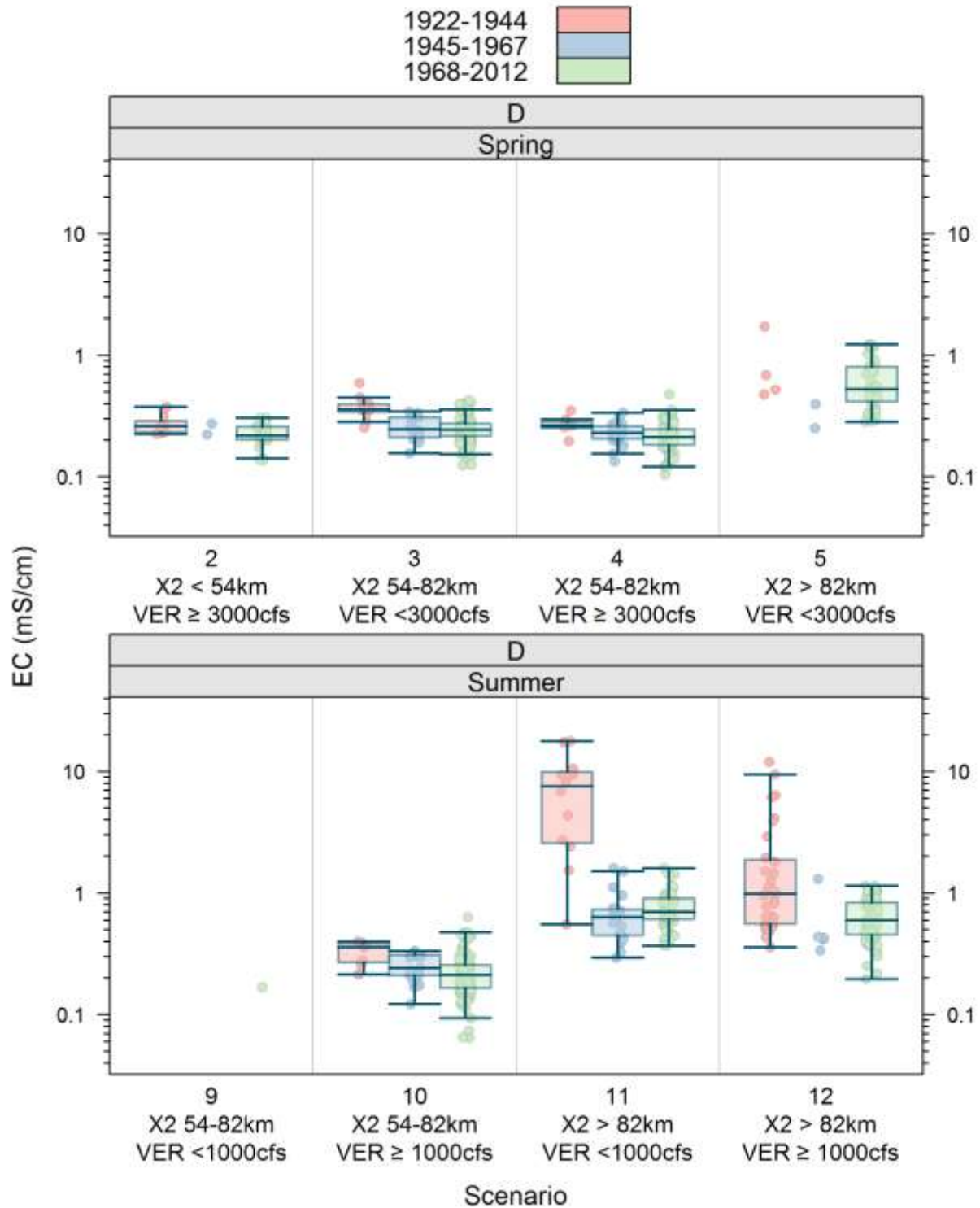


Figure E-14 Box plots (when n > 5) and scatter plots of monthly average EC data for group D

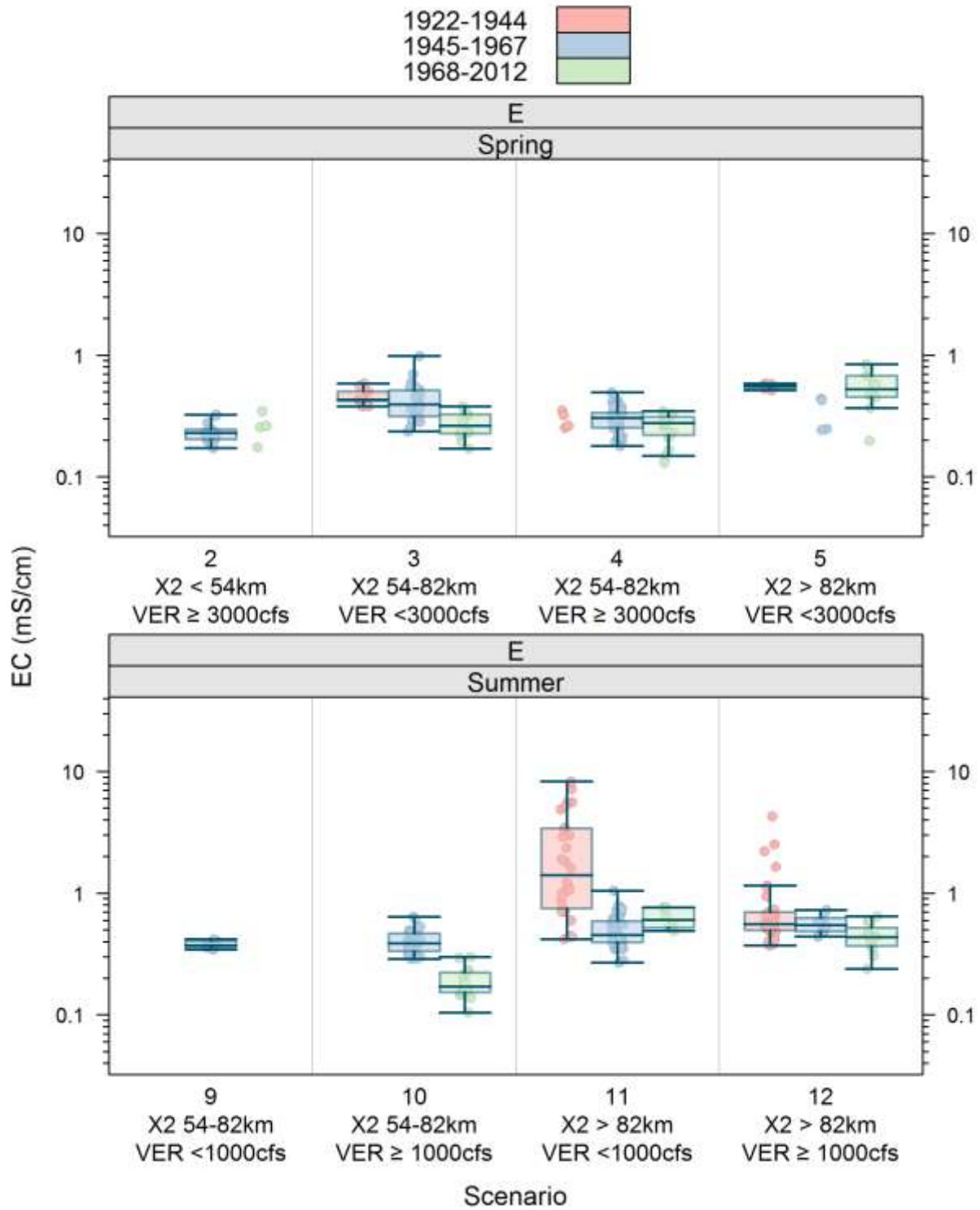


Figure E-15 **Box plots (when n > 5) and scatter plots of monthly average EC data for group E**

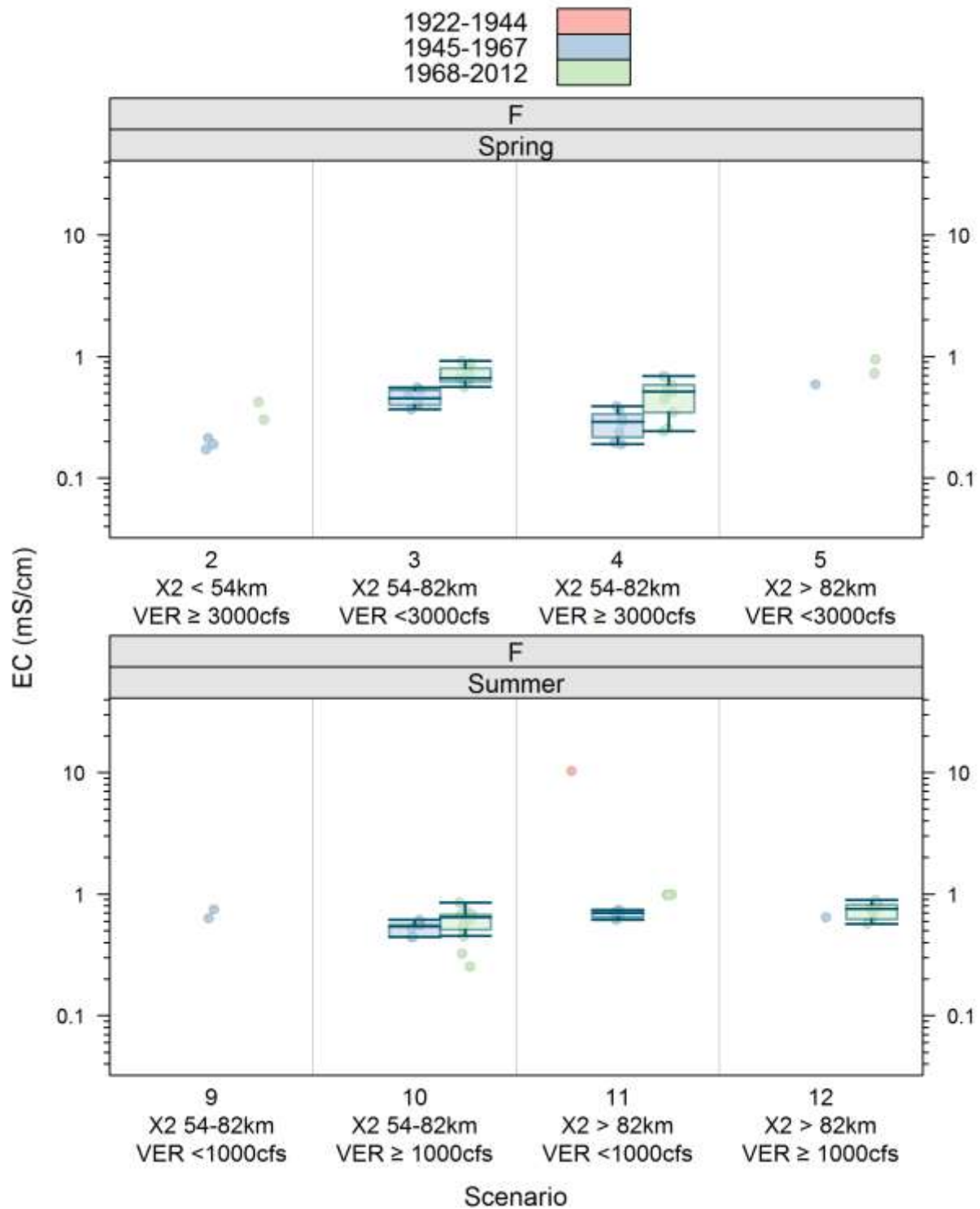


Figure E-16 Box plots (when n > 5) and scatter plots of monthly average EC data for group F

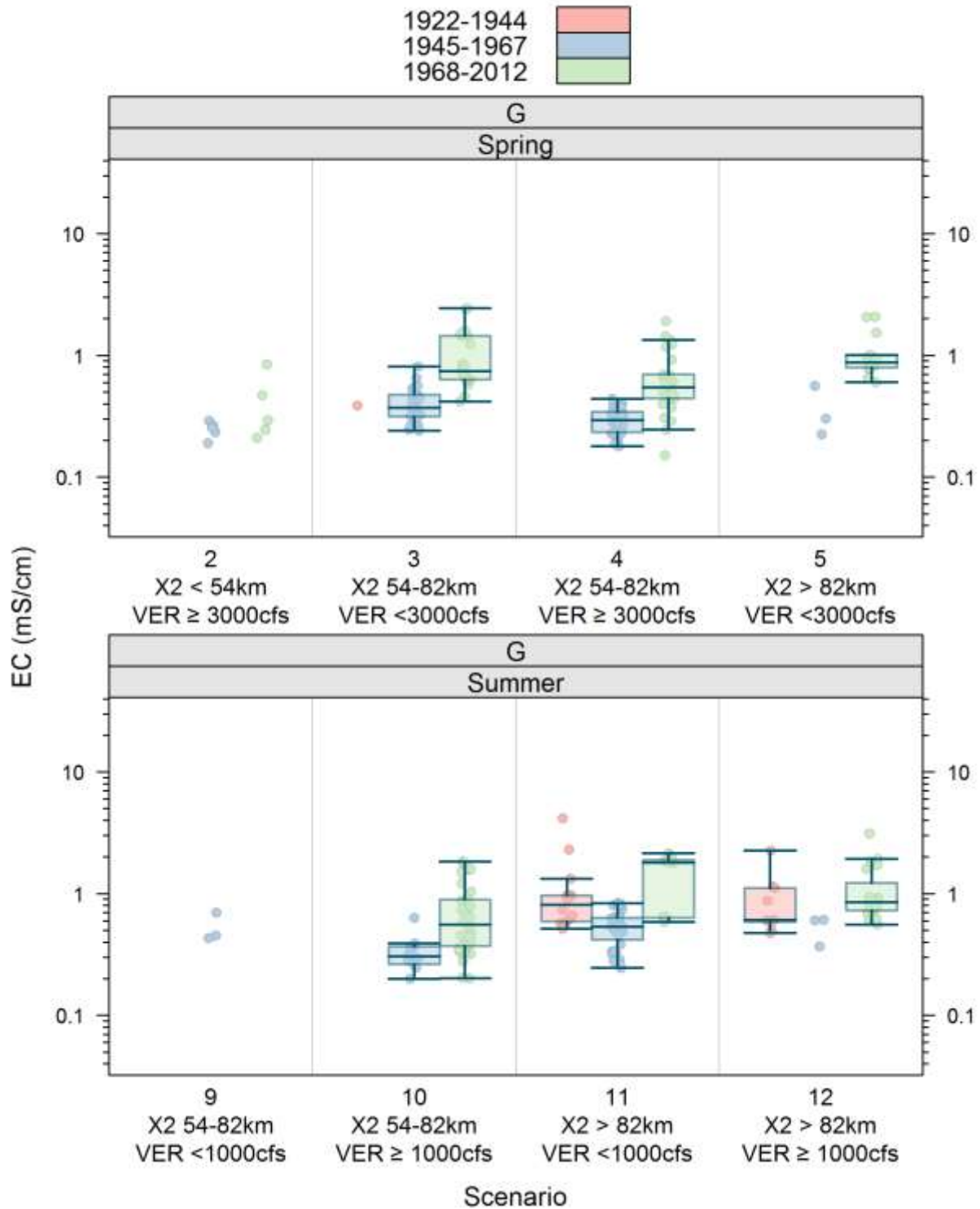


Figure E-17 Box plots (when n > 5) and scatter plots of monthly average EC data for group G

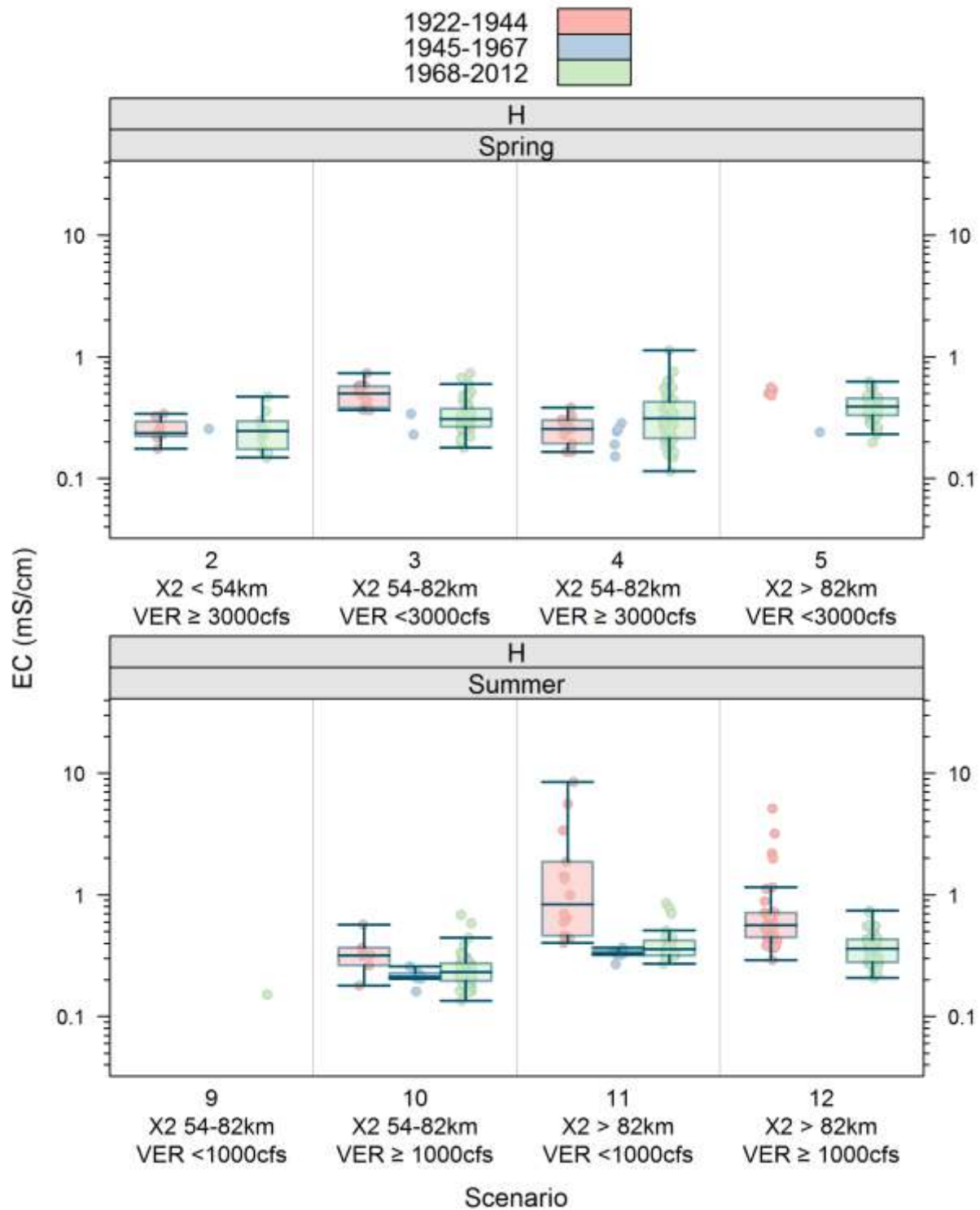


Figure E-18 Box plots (when n > 5) and scatter plots of monthly average EC data for group H

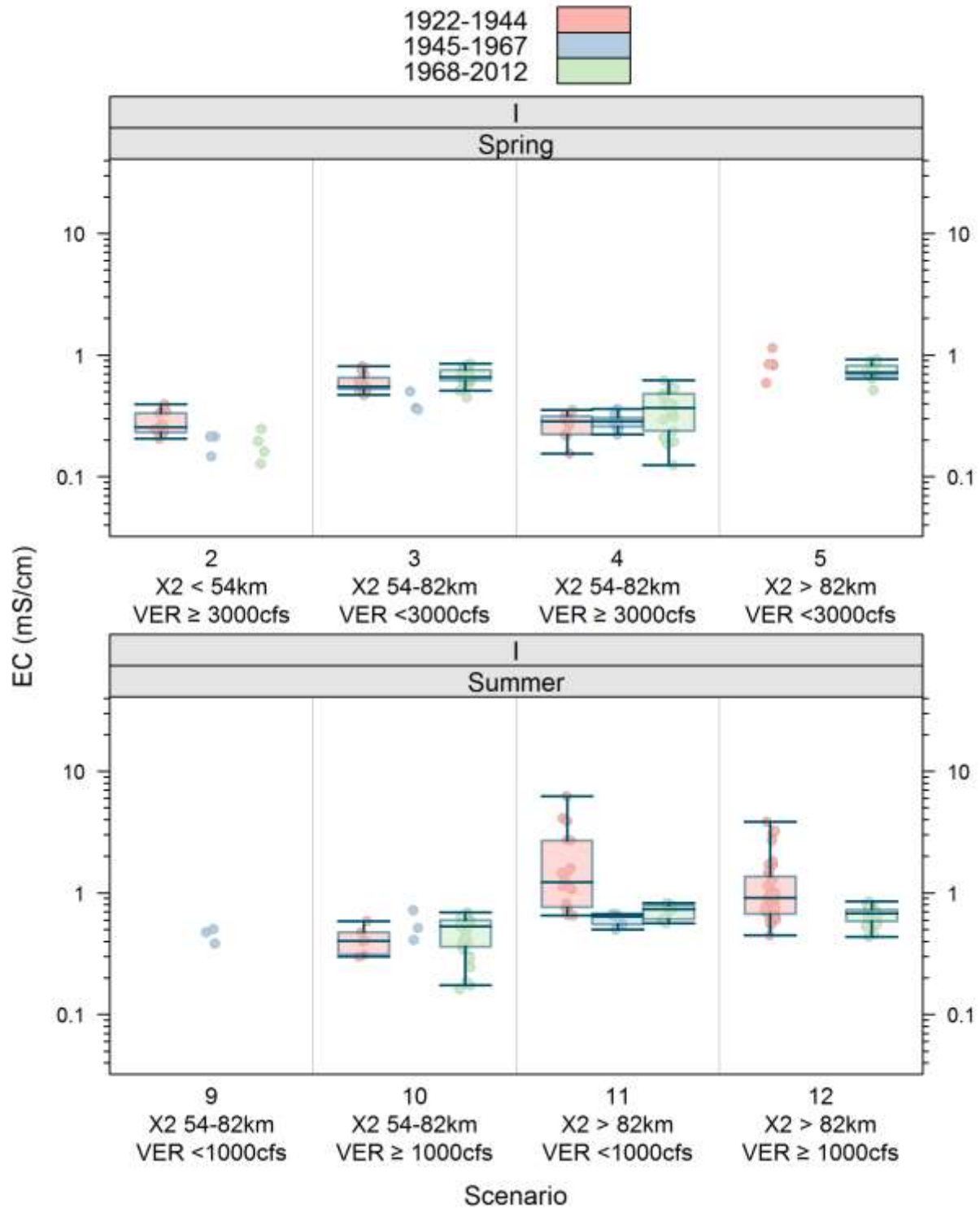


Figure E-19 Box plots (when n > 5) and scatter plots of monthly average EC data for group I

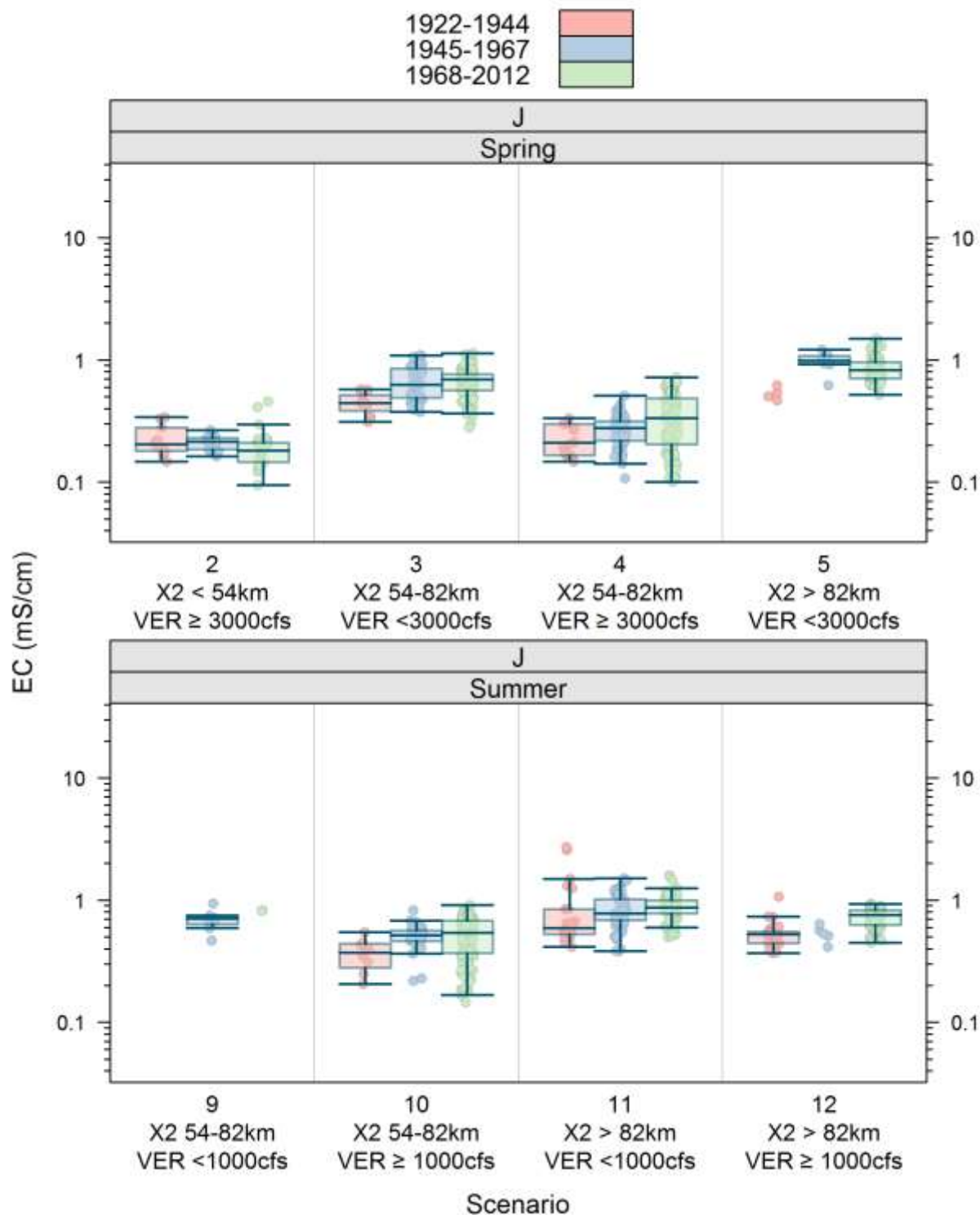


Figure E-20 Box plots (when n > 5) and scatter plots of monthly average EC data for group J